



National Library  
of Canada

Bibliothèque nationale  
du Canada

Canadian Theses Service

Service des thèses canadiennes

Ottawa, Canada  
K1A 0N4

## NOTICE

The quality of this microform is heavily dependent upon the quality of the original thesis submitted for microfilming. Every effort has been made to ensure the highest quality of reproduction possible.

If pages are missing, contact the university which granted the degree.

Some pages may have indistinct print especially if the original pages were typed with a poor typewriter ribbon or if the university sent us an inferior photocopy.

Reproduction in full or in part of this microform is governed by the Canadian Copyright Act, R.S.C. 1970, c. C-30, and subsequent amendments.

## AVIS

La qualité de cette microforme dépend grandement de la qualité de la thèse soumise au microfilmage. Nous avons tout fait pour assurer une qualité supérieure de reproduction.

S'il manque des pages, veuillez communiquer avec l'université qui a conféré le grade.

La qualité d'impression de certaines pages peut laisser à désirer, surtout si les pages originales ont été dactylographiées à l'aide d'un ruban usé ou si l'université nous a fait parvenir une photocopie de qualité inférieure.

La reproduction, même partielle, de cette microforme est soumise à la Loi canadienne sur le droit d'auteur, SRC 1970, c. C-30, et ses amendements subséquents.

**Developing Artificial Proteases and Nucleases: Catalytic  
Hydrolysis of Unactivated Amides, Nitriles and Phosphates**

**PART I**

Hydrolysis of Phosphate Esters promoted by Co(III) Complexes

**PART II**

Hydration of Nitriles Catalyzed by Co(III) Complexes

**PART III**

Hydrolysis of Amides promoted by Co(III) Complexes

by

Jung Hee Kim

*A thesis submitted to the Faculty of Graduate Studies and Research of  
McGill University in partial fulfillment of the requirements for the degree of  
Doctor of Philosophy*

February 1992  
Department of Chemistry  
McGill University  
Montreal, Quebec, Canada

© Jung Hee Kim, 1992



National Library  
of Canada

Bibliothèque nationale  
du Canada

Canadian Theses Service    Service des thèses canadiennes

Ottawa, Canada  
K1A 0N4

The author has granted an irrevocable non-exclusive licence allowing the National Library of Canada to reproduce, loan, distribute or sell copies of his/her thesis by any means and in any form or format, making this thesis available to interested persons.

The author retains ownership of the copyright in his/her thesis. Neither the thesis nor substantial extracts from it may be printed or otherwise reproduced without his/her permission.

L'auteur a accordé une licence irrévocable et non exclusive permettant à la Bibliothèque nationale du Canada de reproduire, prêter, distribuer ou vendre des copies de sa thèse de quelque manière et sous quelque forme que ce soit pour mettre des exemplaires de cette thèse à la disposition des personnes intéressées.

L'auteur conserve la propriété du droit d'auteur qui protège sa thèse. Ni la thèse ni des extraits substantiels de celle-ci ne doivent être imprimés ou autrement reproduits sans son autorisation.

ISBN 0-315-74802-8

Canada

To *H. S. Choi*

**PART I**

**HYDROLYSIS OF PHOSPHATE ESTERS PROMOTED BY  
COBALT(III) COMPLEXES**

**ABSTRACT**

Cis-diaqua cobalt complex  $[(L)Co(III)(OH_2)_2]^{3+}$  promoted hydrolyses of phosphate esters, nitriles and carboxy amides are examined (L represents 1,4,7,10-tetraazacyclododecane (cyclen) and its N-methylated derivatives).  $[(Cyclen)Co(OH_2)_2]^{3+}$  is more active than any other catalysts reported to date for hydrolyzing dimethyl phosphate, acetonitrile and formyl morpholine.

$[(Cyclen)Co(OH_2)_2]^{3+}$  efficiently hydrolyzes dimethyl phosphate under mild conditions ( $k = 3.7 \times 10^{-5} \text{ M}^{-1} \text{ sec}^{-1}$  at pD 6.3, 60 °C). This represents the first hydrolysis of dimethyl phosphate (P-O bond cleavage) at neutral pH. Mechanism for the cobalt complex promoted hydrolysis of dimethyl phosphate and its implication on the role of metal ions in ribozymes is discussed.

$[(Cyclen)Co(OH_2)_2]^{3+}$  catalyzes the hydration of nitriles to amides. Acetonitrile coordinated to the cobalt complex is hydrated  $10^9$  times more rapidly than the uncoordinated acetonitrile at pH 7 and 40 °C. Catalytic turnover for the hydration reaction is demonstrated for the first time with the Co(III) complex. Chelated benzamide, a key intermediate in the catalytic hydration of benzonitrile, is isolated and its crystal structure determined. Detailed kinetics and mechanistic analyses of the cobalt complex catalyzed hydration of acetonitrile including the equilibrium constant for complexation of acetonitrile to the cobalt complex ( $K = 0.6 \text{ M}^{-1}$ ) are reported. Synthetic utility of the catalyst including acrylamide production is discussed.

$[(Cyclen)Co(OH_2)_2]^{3+}$  efficiently hydrolyzes formyl morpholine under mild conditions ( $k = 7.97 \times 10^{-5} \text{ M}^{-1} \text{ sec}^{-1}$  at pD 6, 60 °C). The equilibrium constant for complexation of formyl morpholine to the cobalt complex is  $0.4 \text{ M}^{-1}$ . The equilibrium constant for complexation of amides to metal complexes had not been previously measured. The efficiency and mechanism of the cobalt complex for hydrolyzing amides are compared to those of carboxypeptidase A.

## RESUME

Les complexes de Cis-diaqua cobalt  $[(L)Co(III)(OH_2)_2]^{3+}$  où L représente 1,4,7,10-tetraazacyclododecane (cyclen) et ses dérivés N-méthylés permettant l'hydrolyse des esters de phosphate, des nitriles et des amides carboxyliques sont examinés.  $[(Cyclen)Co(OH_2)_2]^{3+}$  est plus actif que n'importe quel autre catalyseur connu jusqu'ici, pour l'hydrolyse du diméthyl phosphate, l'acétonitrile et le formyl morpholine.

$[(Cyclen)Co(OH_2)_2]^{3+}$  hydrolyse efficacement le diméthyl phosphate dans des conditions douces ( $k = 3.7 \times 10^{-5} M^{-1} sec^{-1}$  à pD 6.3, 60 °C). Ceci représente la première hydrolyse du diméthyl phosphate (clivage de la liaison P-O) à pH neutre. Le mécanisme de l'hydrolyse du diméthyl phosphate par le complexe de cobalt ainsi que l'implication du complexe comme ion métal dans les ribozymes sont discutés.

$[(Cyclen)Co(OH_2)_2]^{3+}$  catalyse l'hydratation du nitrile à l'amide. L'Acétonitrile lié au complexe de cobalt est hydraté  $10^9$  fois plus vite que celui qui n'est pas lié à pH 7 et 40 °C. Le turnover catalytique de la réaction d'hydratation a été mis en évidence pour la première fois pour le complexe Co(III). La benzamide chélatée, a été isolée et sa structure cristalline déterminée. Les analyses cinétiques et mécanistiques détaillées du complexe de cobalt catalysant l'hydratation de l'acétonitrile, ainsi que la constante d'équilibre de complexation entre l'acétonitrile et le complexe de cobalt ( $K = 0.6 M^{-1}$ ) sont rapportés. L'utilité synthétique du catalyseur incluant la production d'acrilamide est discutée.

$[(Cyclen)Co(OH_2)_2]^{3+}$  hydrolyse efficacement le formyl morpholine dans des conditions douces ( $k = 7.97 \times 10^{-5} M^{-1} sec^{-1}$  à pD 6, 60 °C). La constante d'équilibre de complexation entre le formyl morpholine et le complexe de cobalt est de  $0.4 M^{-1}$  et c'est la première fois que de telles constantes, entre amides et complexe de métal, sont mesurées. L'efficacité et le mécanisme de l'hydrolyse d'amide par le complexe de cobalt sont comparés à ceux propres au carboxypeptidase A.

## ACKNOWLEDGEMENTS

I wish to gratefully acknowledge

my research supervisor, Prof. Jik Chin, for his enlightening ideas and discussions throughout my studies at McGill. His enthusiasm and support are greatly appreciated.

I would like to thank all my colleagues in the Otto Maass Bldg:

Dr. Mariusz Banaszczyk, Daphne Wahnnon, James Connolly, Bryan Takasaki, Barry Linkletter, Dr. Andrew Moore, Dr. Stephen Kawai, Dr. Vrej Jubian, Karen Mrejen, Dr. Warren Chew, and Dr. Michael Wrinn for their friendship and discussions.

I would also like to thank:

Dr. Françoise Sauriol for her assistance in NMR experiments,  
Dr. Jim Britten for the X-ray structural determinations,  
Louis Cuccia for proofreading the manuscript, and  
G rard Derbesy for translation of the abstract.

I am deeply indebted to:

my parents for their love and prayers,  
my brothers for their encouragement and motivation, and  
my sisters for their friendship.

I would like to thank my friends:

J.W. Cheon, D. O. Jang, I. S. Yun, J. R. Yun and Prof. M. S. Song for their encouragement, patience, love, and belief in me.

## GLOSSARY OF SYMBOLS AND ABBREVIATIONS

A	adenine
5'-AMP	adenosine 5'-monophosphate
anal.	analysis
[15]aneN5	1,4,7,10,13-pentaazacyclopentadecane
ApA	adenyl (3'-5') adenosine
Ar	aromatic
$\beta$ -ala	$\beta$ -alanine
$\beta_{lg}$ , $\beta_{nu}$	Brønsted coefficients
BDNPP	bis(2,4-dinitrophenyl)phosphate
BNPP	bis(4-nitrophenyl)phosphate
bpy	2,2'-bipyridine
t-BuOH	<i>tert</i> -butyl alcohol
Bz	benzoyl
Bzl	benzyl
ca.	about
calcd.	calculated
c-AMP	adenosine 3',5'-cyclic monophosphate
cmcylen	1,4-dimethyl-1,4,7,10-tetraazacyclododecane
conc	concentrated
CPA	carboxypeptidase A
cyclen	1,4,7,10-tetraazacyclododecane
$\delta$	scale (NMR) dimensionless
d(ApA)	2'-deoxy adenyl (3'-5') 2'-deoxy adenosine
DIP	4,7-diphenylphenanthroline
DMF	N,N-dimethylformamide
DMP	dimethyl phosphate
DMSO	dimethyl sulfoxide
DNA	2'-deoxyribonucleic acid
DNPP	2,4-dinitrophenyl phosphate
dpa	2,2'-dipyridylamine
DSS	3-(trimethylsilyl)-1-propanesulfonic acid
$\epsilon$	extinction coefficient
E-coli	<i>Escherichia coli</i>

EDTA

ethylenediaminetetraacetic acid

eq

equation

equiv

equivalent(s)

et al.

and others

Et<sub>4</sub>cyclen

2,5,8,11-tetraethyl-1,4,7,10-tetraazacyclododecane

g

gram(s)

GAC / GBC

general acid catalysis / general base catalysis

GC

gas chromatography

h

hour(s)

HASB

hard-soft acid-base theory

HPLC

high pressure liquid chromatography

Hz

hertz

k<sub>H2O</sub>

water attack rate constant

k<sub>OH</sub>

hydroxide attack rate constant

L

ligand(s)

λ

wavelength

Me

methyl

MeOH

methanol

mcyclen

1-methyl-1,4,7,10-tetraazacyclododecane

min

minute(s)

M-OH

metal hydroxide

mol

mole(s)

MP

methyl phosphate

mp

melting point

N<sub>4</sub>

tetradentate amine ligand(s)

NMR

nuclear magnetic resonance

NPP

4-nitrophenyl phosphate

phen

1,10-phenanthroline

PHOS

inorganic phosphate

ppm

parts per million

R

correlation coefficient

R / R<sub>w</sub>

unweighted / weighted agreement factor

RNA

ribonucleic acids

s

second(s)

σ<sub>v</sub>

plane of symmetry

tetren

tetraethylenepentamine

tricyclen	1,7-dimethyl-1,4,7,10-tetraazacyclododecane
TMP	trimethyl phosphate
TMS	tetramethylsilane
tren	tris(2-aminoethyl)amine
trien	triethylenetetraamine
trpn	tris(3-aminopropyl)amine
Ts	p-toluenesulfonyl
U	uracil
UpU	uridyl (3'-5') uridine
UV/VIS	ultraviolet-visible
v	volume
w	weight

**TABLE of CONTENTS**

<b>Abstract</b>	.....j
<b>Résumé</b>	.....ii
<b>Acknowledgements</b>	.....iii
<b>Glossary of Symbols and Abbreviations</b>	.....iv
<b>Table of Contents</b>	.....vii

**PART I     HYDROLYSIS OF PHOSPHATE ESTERS PROMOTED BY  
Co(III) COMPLEXES**

**1     INTRODUCTION**

1.1	Biology of Phosphate Esters	.....1
1.2	Artificial Restriction Enzymes	.....2
1.3	Mechanism of Phosphate Ester Hydrolysis	.....6
	1.3.1 Phosphate monoesters	.....8
	1.3.2 Phosphate diesters	.....8
	1.3.3 Phosphate triesters	.....10
1.4	Metal promoted Hydrolysis of Phosphate Esters	
	1.4.1 Mechanism of metal catalysis	.....11
	1.4.2 Metal complex promoted phosphate diester hydrolysis	.....12
	1.4.3 Metal complex promoted phosphate monoester hydrolysis	.....15
1.5	Plan of Study	.....19

**2     RESULTS**

2.1	Synthesis of Ligands and Co(III) complexes	
	2.1.1 Synthesis of ligands and their Co(III) complexes	.....20
	2.1.2 Spectral data and acid dissociation constants of Co(III) complexes	.....22
2.2	Binding with Acetate, Phenyl Phosphonate, Inorganic Phosphate, and Dimethyl Phosphate	.....24
2.3	Relationships between Chelate Formation and the Basicity of Bidentate Ligands	.....30
2.4	Kinetics	

2.4.1	Co(III) complex promoted hydrolysis of phosphate esters with good leaving groups .....	31
2.4.2	Co(III) complex promoted hydrolysis of phosphate esters with poor leaving groups .....	33

### 3 DISCUSSION

3.1	Synthesis of Ligands and their Co(III) Complexes .....	39
3.2	Co(III) complex promoted Hydrolysis of Phosphate Esters with Good Leaving Groups	
3.2.1	Mechanism .....	41
3.2.2	Ligand effects on the reactivity .....	43
3.3	Co(III) complex promoted Hydrolysis of Phosphate Diesters with Poor Leaving Groups	
3.3.1	Hydrolysis of c-AMP .....	47
3.3.2	Hydrolysis of UpU and ApA .....	48
3.3.3	Hydrolysis of DMP .....	50

## PART II HYDRATION OF NITRILES CATALYZED BY Co(III) COMPLEXES

### 1 INTRODUCTION

1.1	Mechanism of Nitrile Hydration .....	57
1.2	Metal assisted Hydration of Nitriles	
1.2.1	Previous work .....	59
1.2.2	Hydration of nitriles vs hydrolysis of amides .....	62
1.3	Plan of Study .....	64

### 2 RESULTS

2.1	Kinetics	
2.1.1	Co(III) complex catalyzed hydration of acetonitrile .....	65
2.1.2	pD-rate profile .....	67

2.1.3	Dependence of acetonitrile hydration rate on the concentration of Co(III) complex .....	68
2.1.4	Dependence of acetonitrile hydration rate on the concentration of acetonitrile .....	68
2.1.5	Equilibrium binding constant for acetonitrile to cobalt complexes .....	70
2.1.6	Co(III) complex catalyzed formation of chelated amides .....	71
2.1.7	Equilibrium chelation of acetamide to Co(III) complexes .....	72
2.1.8	Hydration of acrylonitrile and other nitriles .....	73
2.2	Binding of Nitriles and Amides to Co(III) complexes	
2.2.1	Binding of acetonitrile and acetamide at pH < 3 .....	77
2.2.2	Binding of acetonitrile and acetamide at neutral pH .....	78
2.3	Crystal Structure of a Chelated Benzamide to [(tmcyclen)Co(OH <sub>2</sub> ) <sub>2</sub> ] <sup>3+</sup> .....	80

### 3 DISCUSSION

3.1	Binding of Acetonitrile and Acetamide to Co(III) complexes .....	81
3.2	Crystal Structure of [(tmcyclen)Co( $\eta^2$ -N,O-benzamide)] <sup>2+</sup> complex .....	83
3.3	Mechanism	
3.3.1	Hydration of acetonitrile catalyzed by [(cyclen)Co(OH <sub>2</sub> ) <sub>2</sub> ] <sup>3+</sup> .....	85
3.3.2	Regioselective hydration of acrylonitrile .....	91
3.4	Concluding Remarks .....	92

## PART III HYDROLYSIS OF AMIDES PROMOTED BY Co(III) COMPLEXES

### 1 INTRODUCTION

1.1	Artificial Peptidases .....	93
1.2	Mechanism of Amide Hydrolysis .....	97
1.3	Metal assisted Hydrolysis of Amides .....	98
1.4	Plan of Study .....	101

### 2. RESULTS

2.1	Kinetics .....	102
2.2	Binding of Amides to Co(III) complexes .....	105

### 3 DISCUSSION

3.1	Structural Requirements for the Catalysts	
3.1.1	Model studies based on ester hydrolysis	106
3.1.2	Amide hydrolysis	109
3.2	Equilibrium Binding of Amides to Cobalt complexes	110
3.3	Hydrolysis of Amides promoted by [(cyclen)Co(OH <sub>2</sub> ) <sub>2</sub> ] <sup>3+</sup>	
3.3.1	Mechanism	112
3.3.2	Reactivity	115

### PART IV EXPERIMENTAL ( PART I, PART II, PART III)

1	GENERAL	119
2	MATERIALS	120
3	SYNTHESIS	
3.1	Synthesis of Tetraamine Ligands	121
3.2	Preparation of Co(III) complexes	125
3.3	Preparation of [(tmcyclen)Co(η <sup>2</sup> -N,O-benzamide)] <sup>2+</sup> complex	127
3.4	Preparation of [(trpn)Co(η <sup>2</sup> -O,O-β-ala)] <sup>3+</sup> complex	129
4	TITRATION	131
5	KINETICS / BINDING STUDIES	
5.1	UV/VIS spectroscopy	131
	Hydrolysis of phosphate esters	
	Equilibrium binding constants of acetonitrile and acetamide	
	Hydration of acetonitrile	
5.2	<sup>1</sup> H NMR and <sup>31</sup> P NMR spectroscopy	132
	Binding of phosphate	
	Hydrolysis of nucleotides	
	Hydrolysis of DMP, nitriles and amides	
5.3	<sup>13</sup> C NMR spectroscopy	133
	Binding of acetate and carboxylates	
	Binding of acetonitrile and acetamide	
5.4	HPLC	134
	Contribution to Knowledge	135
	Appendix	138

## 1 INTRODUCTION

### 1.1 Biology of Phosphate Esters

There is hardly anything that goes on in living cells where esters of phosphoric acid are not involved at some stage.<sup>1</sup> Table I.1 shows phosphate esters of biological interest classified on the basis of substitution on the phosphoric or pyrophosphoric acid molecules.

**Table I.1** General classification of phosphate esters of biological interest

$\begin{array}{c} \text{O} \\    \\ \text{X}-\text{P}-\text{OH} \\   \\ \text{OH} \end{array}$	$\text{X} = \text{RO}$ $\text{X} = \text{RC}(\text{Z})\text{O}, \text{Z} = \text{C or O}$ $\text{X} = \text{RNH}$	sugar phosphates, glycerol phosphates, mononucleotides phosphoenolpyruvic acid, acetylphosphate creatine phosphate, arginine phosphate
$\begin{array}{c} \text{O} \quad \quad \text{O} \\    \quad \quad    \\ \text{X}-\text{P}-\text{O}-\text{P}-\text{OH} \\   \quad \quad   \\ \text{OH} \quad \quad \text{OH} \end{array}$	$\begin{array}{c} \text{O} \quad \quad \text{O} \quad \quad \text{O} \\    \quad \quad    \quad \quad    \\ \text{X}-\text{P}-\text{O}-\text{P}-\text{O}-\text{P}-\text{OH} \\   \quad \quad   \quad \quad   \\ \text{OH} \quad \quad \text{OH} \quad \quad \text{OH} \end{array}$	$\begin{array}{c} \text{O} \quad \quad \text{O} \\    \quad \quad    \\ \text{X}-\text{P}-\text{O}-\text{P}-\text{Y} \\   \quad \quad   \\ \text{OH} \quad \quad \text{OH} \end{array}$
$\text{X} = \text{nucleoside } 5', \text{ Y} = \text{RO}$		
nucleoside 5'-diphosphate thiamine pyrophosphate	adenosine 5'-triphosphate	nucleotide coenzyme
$\begin{array}{c} \text{O} \\    \\ \text{X}-\text{P}-\text{Y} \\   \\ \text{OH} \end{array}$	$\text{X} = \text{nucleoside } 5'$ $\text{Y} = \text{acyloxy group}$  $\text{X} = \text{RO}, \text{Y} = \text{R}'\text{O}$	acyl adenylates  nucleic acids, phospholipids, cell wall polymers

The first class of phosphate esters includes phosphorylated derivatives of carbohydrates, mononucleotides, phosphoproteins, and coenzymes required for the function of some vitamins. A number of high energy phosphate esters are mixed anhydrides such as phosphoenolpyruvic acid, or phosphoamidic acids such as creatine phosphate.

<sup>1</sup> Khorana, H. G. in *Some Recent Developments in the Chemistry of Phosphate Esters of Biological Interest*; John Wiley & Sons, Inc.: New York, London, 1961.

The second class of phosphate esters includes monoesters of pyrophosphoric acid such as nucleoside-5' diphosphates. Other examples are coenzyme B<sub>12</sub> and 5-O-phosphoryl- $\alpha$ -D-ribofuranose-1-pyrophosphate which is the biological precursor of ribonucleoside 5'-phosphate. Pyrophosphates such as isopentyl-, geranyl- and farnesyl pyrophosphate are found in the biosynthesis of a host of polyisoprenoid compounds (e.g. squalene). Monoesters of triphosphoric acid and diesters of pyrophosphoric acid are the principal biochemical energy reservoirs (e.g. ATP). They are also found in a variety of nucleotide coenzymes.

The last class of phosphate esters covers the widest variety of organochemical structures. Vitamin B<sub>12</sub> and its related compounds all contain a phosphodiester bridge. Genetic molecules such as RNA and DNA are polynucleotide chains that are joined by diester linkages. Phospholipids are the major class of cell membrane lipids. Lipids have a variety of biological roles as fuel molecules, highly concentrated energy stores, signal molecules, and as components of membranes.

The reasons for phosphates being so abundant and playing most important roles in biological systems are perhaps their ability for being ionized under all pH conditions and their stability towards hydrolysis.<sup>2</sup> Nature has chosen the phosphate diester linkage for the storage of genetic material because of its robust nature. Transformations of phosphodiester linkages are controlled only by specific enzymes that hydrolyze or form esters of phosphoric acids. There has been considerable research interest in understanding the ubiquitous hydrolysis reaction of phosphate esters.

## 1.2 Artificial Restriction Enzymes

Natural restriction endonucleases, which are essential in recombinant DNA technology, recognize specific base sequences of four to eight base pairs in double helical DNA and then cleave the DNA at those sites.<sup>3</sup> A potential advantage of artificial restriction enzymes over natural ones would be their ability to bind and cleave any desired nucleotide sequence. This could be invaluable for human genome sequencing or gene cloning experiments. Their application, in the long term, may lead to the development of precise agents that could control disease states at the level of DNA itself.<sup>4</sup>

---

<sup>2</sup> Westheimer, F. H. *Science*, **1987**, 235, 1173.

<sup>3</sup> a) Stryer, L. in *Biochemistry*; 3rd Ed.; Freeman and Co.: New York, 1988.

b) Dervan, P. B. *Science*, **1986**, 232, 464.

<sup>4</sup> Baum, R. M. *Chem. Eng. News*, **1988**, 66(1), 20.

An artificial restriction enzyme contains two structural domains, each with its own specific function: one binds a DNA sequence specifically, and the other cleaves DNA. Most studies have focused on probing the details of DNA recognition.<sup>4</sup> There has been considerable development of sequence specific DNA binding agents attached to Fenton-like molecules for nicking DNA.<sup>4,6-10</sup> Cu(II)(phenanthroline)<sub>2</sub> complex<sup>5</sup> has been attached covalently to a DNA binding protein or a deoxyoligonucleotide by Sigman (Fig. I.1).<sup>6</sup>

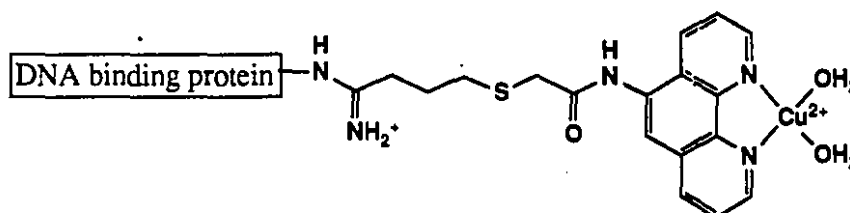


Figure I.1 DNA binding protein covalently linked to the phenanthroline-copper complex.

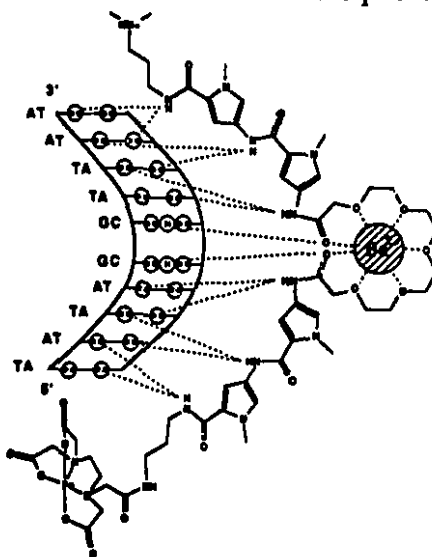


Figure I.2 Bis(netropsin)-3,6,9,12,15-pentaoxaheptadecanediamide-EDTA-Fe(II) complex in sequence specific DNA cleavage in the presence of Sr<sup>2+</sup> or Ba<sup>2+</sup>

Dervan has attached an Fe(II)(EDTA) complex to known DNA binding molecules, such as methidium, distamycin, netropsine, and oligonucleotides (Fig. I.2).<sup>7</sup> Barton has shown

5 Sigman, D. S. *Acc. Chem. Res.* 1986, 19, 180.

6 a) Chen, C. B.; Sigman, D. S. *Science*, 1987, 237, 1197. b) Chen, C. B.; Sigman, D. S. *J. Am. Chem. Soc.* 1988, 110, 6570.

7 a) Dervan, P. B. *Science*, 1986, 232, 464. and references therein. b) Strobel, S. A.; Dervan, P. B. *J. Am. Chem. Soc.* 1989, 111, 7286. c) Moser, H. E.; Dervan, P. B. *Science*, 1987, 238, 645.

that some metal complexes can be used as binding probes for DNA<sup>8</sup> as well as cleaving agents. Ru(III)(bpy)<sub>3</sub> binds to specific DNA conformations. When the ruthenium complex is attached to a DNA cleaving group, double stranded DNA is cleaved sequence specifically.<sup>9</sup> Triple helix formation by oligonucleotides holds high potential as a general recognition technology and even a modification motif for DNA.<sup>10</sup>

Despite great success in developing specific binding groups in the models described above, cleavage proceeds oxidatively. The metal cation generates a highly reactive, diffusible hydroxyl radical from dioxygen which oxidizes deoxyribose groups in DNA resulting in the cleavage of the sugar-phosphate backbone. In contrast, natural restriction enzymes hydrolyze DNA producing 3'- or 5'-phosphomonoester termini. Although some of these oxidative artificial restriction enzymes have been used as footprinting and affinity cleaving agents, hydrolytic cleavage of DNA or RNA has distinct advantages over its oxidative counterpart. Hydrolytic manipulation of nucleic acid polymers could generate fragments that are chemically competent for ligation to other oligonucleotides by routine enzymatic reactions and chemical methods. Dervan has reported chemical ligation of the double helical DNA by placing two DNA termini in juxtaposition with a guide sequence in a triple helix, which was accompanied by chemical activation of the terminal phosphates (Fig. I.3).<sup>11</sup> There has been considerable interest in developing catalysts for DNA or RNA hydrolysis and in probing the mechanism of metal catalyzed hydrolysis of phosphate diesters.

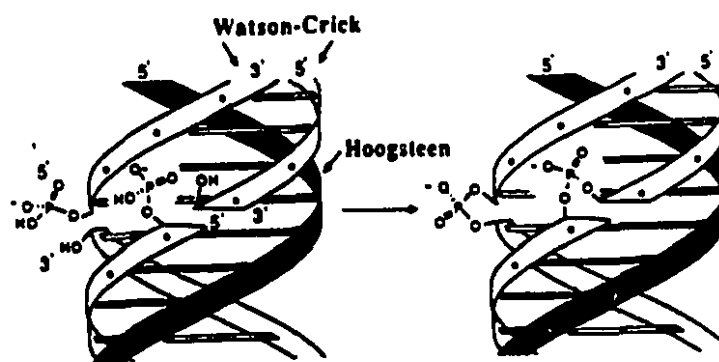


**Figure I.3** Ligation of a 3'-hydroxyl and an activated 5'-phosphate of two oligonucleotides through formation of an adjacent triple-helical complex.

8 Barton, J. K. *Science* 1986, 233, 727.

9 Basile, L. A.; Barton, J. K. *J. Am. Chem. Soc.* 1987, 109, 7548.

10 Povsic, T. J.; Dervan, P. B. *J. Am. Chem. Soc.* 1990, 112, 9428.

11 a) Luebke, K. J.; Dervan, P. B. *J. Am. Chem. Soc.* 1991, 113, 7447. b) Luebke, K. J.; Dervan, P. B. *J. Am. Chem. Soc.* 1989, 111, 8733.

Progress has been made in cleaving super-coiled DNA hydrolytically by using  $\text{Ru}(\text{DIP})_2\text{Macro}^{\text{n}+}$  with non-redox active Zn metal (Fig. I.4).<sup>12</sup> Although the process is not as efficient as the oxidative cleavage, there is an indication of hydrolytic cleavage. Sequence selective hydrolysis of super-coiled DNA was also achieved by Schultz's group using a hybrid nuclease consisting of a short oligonucleotide selectively fused to a relatively nonspecific phosphodiesterase, staphylococcal.<sup>13</sup> Recently, it has been shown that  $\text{Cu}(\text{II})(\text{bpy})(\text{OH}_2)_2$  attached to a deoxyoligonucleotide hydrolyzes the phosphate diester backbone of RNA at neutral pH (Fig.I.5).<sup>14</sup>

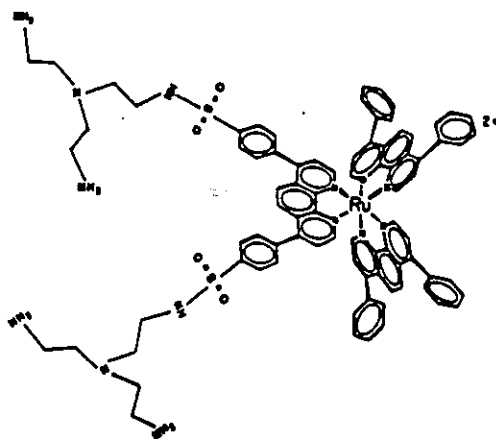


**Figure I.4**  $\text{Ru}(\text{DIP})_2\text{Macro}^{\text{n}+}$  in hydrolytic cleavage of plasmid pBR322 in the presence of Zn(II), Cd(II), and Pb(II).

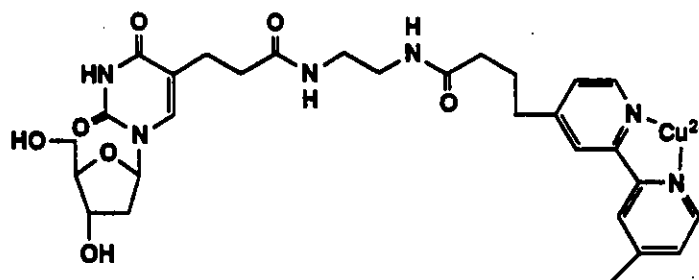


**Figure I.5**  $\text{Cu}(\text{bpy})$  nucleotide: hydrolysis of poly(A)<sub>18</sub>

12 Basile, L. A.; Raphael, A. L.; Barton, J. K. *J. Am. Chem. Soc.* **1987**, *109*, 7550.

13 a) Corey, D. R.; Pei, D.; Schultz, P. G. *J. Am. Chem. Soc.* **1989**, *111*, 8523. b) Pei, D.; Corey, D. R.; Schultz, P. G. *Proc. Natl. Acad. Sci. U. S. A.* **1990**, *87*, 9858.

14 Modak, A. S.; Gard, J. K.; Merriman, M. C.; Winkeler, K. A.; Bashkin, J. K.; Stern, M. K. *J. Am. Chem. Soc.* **1991**, *113*, 283.

The reactivity of super-coiled DNA is much greater than that of linear DNA. RNA phosphate diester bonds are also hydrolyzed much faster due to the 2'-hydroxyl group participation. It has been estimated that the half-life for the hydroxide catalyzed hydrolysis of phosphate diester bonds of DNA is 200 million years at neutral pH. There is still much to be realized in cleaving DNA hydrolytically with great efficiency.

Our research is focused on the development of metal complexes that can cleave unactivated phosphate diesters hydrolytically and the elucidation of these catalytic mechanisms.

### 1.3 Mechanism of Phosphate Ester Hydrolysis

Phosphate ester hydrolysis proceeds much slower than carboxylic ester hydrolysis (Table I.2). Despite considerable interest to organic and biochemists of phosphate diester hydrolysis, detailed mechanistic studies were limited to highly reactive substrates, or substrates that contain a neighboring group which participates in the hydrolysis reaction. A major difficulty in studying the hydrolysis of unactivated phosphate diesters is their stability.

**Table I.2** Rate constants for hydrolysis of phosphate esters (P-O bond cleavage) and carboxylic esters at pH 7, 25 °C.

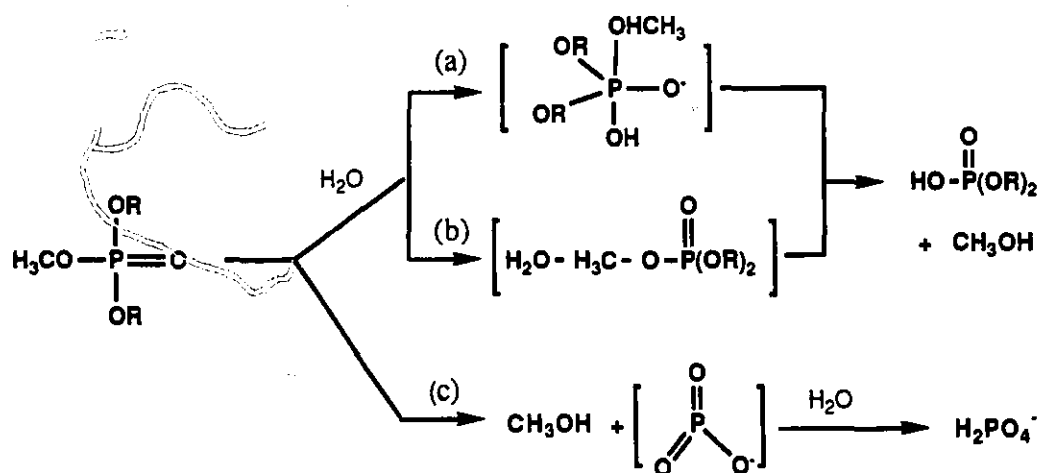
Ester	k (sec <sup>-1</sup> )	rel.rate
(CH <sub>3</sub> O) <sub>3</sub> PO <sup>a,c</sup>	1.6 x 10 <sup>-11</sup>	2.4 x 10 <sup>7</sup>
(CH <sub>3</sub> O) <sub>2</sub> PO <sub>2</sub> <sup>- a,c</sup>	6.8 x 10 <sup>-19</sup>	1
(CH <sub>3</sub> O)HPO <sub>3</sub> <sup>- a</sup>	2.6 x 10 <sup>-10</sup>	3.8 x 10 <sup>8</sup>
CH <sub>3</sub> CO <sub>2</sub> CH <sub>3</sub> <sup>b,c</sup>	1.5 x 10 <sup>-8</sup>	2.2 x 10 <sup>10</sup>

a) J. P. Guthrie, *J. Am. Chem. Soc.* **1977**, *99*, 3991.

b) J. P. Guthrie, *J. Am. Chem. Soc.* **1973**, *95*, 6999.

c) first-order rate constants were extrapolated from the hydroxide rate at pH 7.

Two major mechanisms have been suggested for the hydrolysis of phosphate esters and anhydrides.<sup>15,16</sup> In the associative mechanism, a nucleophile can attack either phosphorus or carbon (Scheme I.1, (a) and (b)). In the case of P-O bond cleavage, the coordination sphere increases from 4 to 5 forming a pentacoordinated trigonal bipyramidal intermediate in a mechanism similar to that for normal hydrolysis of carboxylic esters. In the dissociative mechanism, unimolecular cleavage of the P-O bond gives a metaphosphate intermediate where the coordination number of phosphorus decreases from 4 to 3 (Scheme I.1, (c)). This mechanism roughly parallels the acylium ion process for the hydrolysis of carboxylic acid esters.<sup>17</sup> In addition to these mechanisms, concerted, borderline, and merged mechanisms have also been proposed.<sup>18,19</sup>



**Scheme I.1** Possible paths for hydrolysis of phosphate esters

15 Westheimer, F. H. *Chem. Rev.* **1981**, 31, 313.

16 Guthrie, J. P. *Acc. Chem. Res.* **1983**, 16, 122.

17 a) Bruice, T. C.; Benkovic, S. In *Bioorganic Mechanisms*; W.A. Benjamin: New York, 1966; Vol. 2 b) Hines, J. S. in *Physical Organic Chemistry*, 2nd Ed.; McGraw Hill: New York, 1962.

18 Jencks, W. P.; Herschlag, D. H. *J. Am. Chem. Soc.* **1989**, 111, 7579.

19 Jencks, W. P. *Acc. Chem. Res.* **1980**, 13, 161.

### 1.3.1 Phosphate monoesters

The mechanism of monoester hydrolysis is complicated by the possible existence of three reactive species. Phosphate monoesters have two dissociable protons with  $pK_1 \sim 1$  and  $pK_2 \sim 6.5$ .



It has been proposed that both ionic species are hydrolyzed by unimolecular mechanisms involving the formation of a monomeric metaphosphate intermediate,<sup>20,21,22</sup> even though the formation of this intermediate has never been detected in aqueous solution. A bimolecular reaction with no metaphosphate intermediate has been proposed for substitution reactions of phosphorylated pyridine.<sup>18</sup> The driving force for the hydrolysis is the two negative charges on phosphate (dianion) (Scheme I.2.(a)) and internal or external proton transfer to the alkoxy or aryloxy leaving group (monoanion) (Scheme I.2.(b)). The formation of the kinetically equivalent zwitterionic intermediate following rapid pre-equilibrium (Scheme I.2.(b)-iii) was also suggested for monoanion hydrolysis.<sup>23</sup>

The relative reactivity of monoester mono- and dianions depends on the leaving group  $pK_a$ .<sup>23</sup> Linear free energy relationships between the hydrolysis rate and the  $pK_a$  of the leaving groups were obtained with slopes of -0.27 and -1.23 for hydrolysis of monoester monoanion and dianion, respectively. For monoesters with poor leaving groups ( $pK_a > 6$ ), the monoanionic form of monoester is hydrolyzed faster than the dianionic form, while for monoesters with good leaving groups ( $pK_a < 5$ ), the opposite reactivity holds.<sup>23</sup> At low pH, acid catalyzed and spontaneous hydrolysis of undissociated esters involving both C-O and P-O bond fission become important.<sup>20</sup>

### 1.3.2 Phosphate diesters

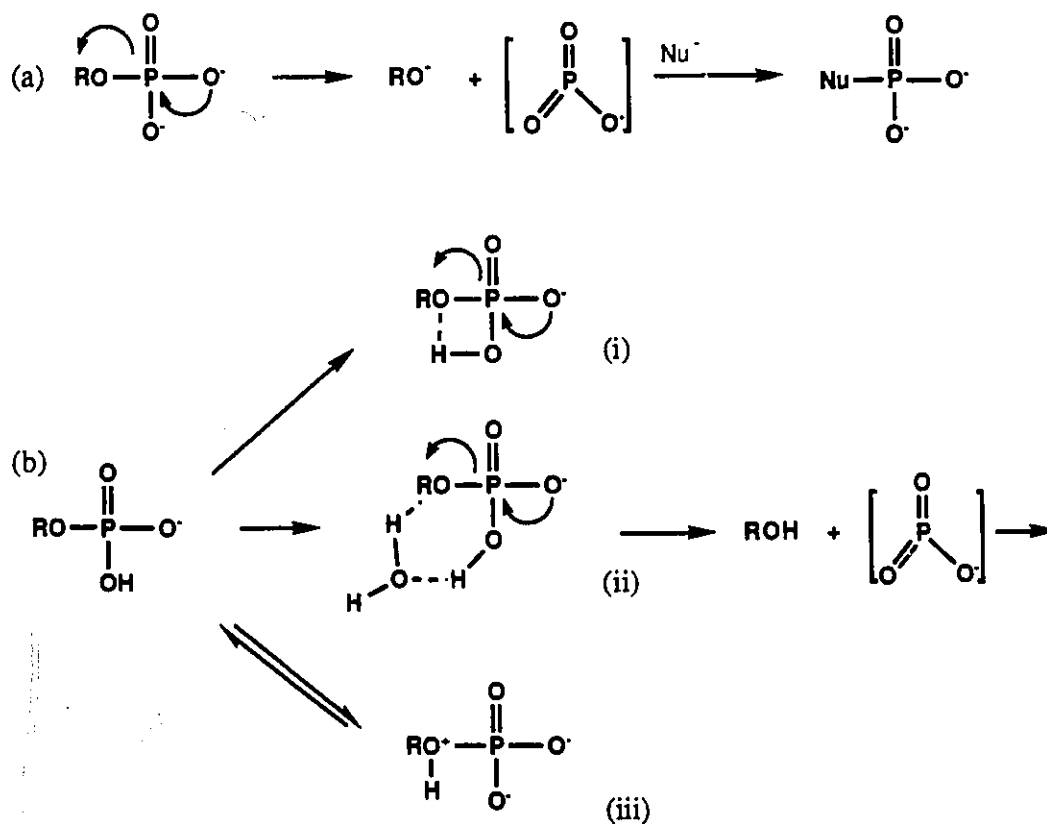
At  $pH > 2$ , the monoanionic form of phosphate diesters predominates in aqueous solution. The hydrolysis mechanism of diesters may be similar to that of monoester monoanions. However, the dependence of reactivity on the basicity of the leaving group is quite high ( $\beta_{lg} = -0.97$ ) for hydrolysis of diesters and rather small ( $\beta_{lg} = -0.27$ ) for that

20 a) Bunton, C. A. *Acc. Chem. Res.* 1970, 257. b) Cox, J. R.; Ramsay, O. B. *Chem. Rev.* 1964, 64, 317.

21 Bunton, C. A.; Liewellyn, D. R.; Oldham, K. G.; Vernon, C. A. *J. Am. Chem. Soc.* 1958, 3574.

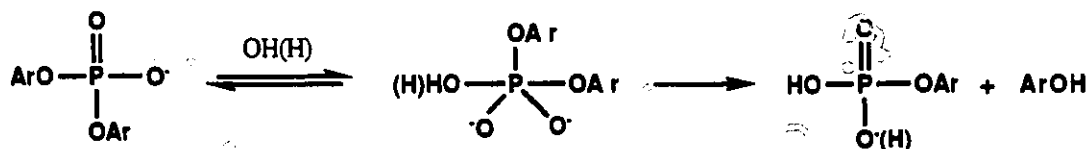
22 Freeman, S.; Freeman, J. M.; Knowles, J. R. *J. Am. Chem. Soc.* 1988, 110, 1268.

23 Kirby, A. J.; Varvoglis, A. G. *J. Am. Chem. Soc.* 1967, 89, 415. and references therein.



**Scheme I.2** Hydrolysis mechanism for phosphate monoesters: (a) monoester dianion, (b) monoester monoanion.

of monoester monoanions.<sup>24</sup> Monoester hydrolysis involves a special proton transfer mechanism and occurs by the dissociative pathway.<sup>15,16</sup> In contrast, hydrolysis of diesters proceeds with bimolecular nucleophilic attack (Scheme I.3).



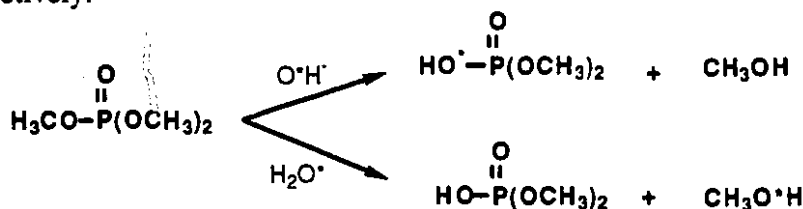
**Scheme I.3** Hydrolysis of phosphate diesters

According to the <sup>18</sup>O tracer experiments done with aryl phosphate diesters, hydrolysis involves P-O bond cleavage in acidic to weakly basic regions, while a considerable

proportion of C-O bond cleavage occurs in alkaline hydrolysis.<sup>24,25</sup> This probably reflects the diminishing electrostatic repulsion directed against the attacking negative ion, where phosphorus is more electronegative than the aryl or alkyl oxygen. These unfavorable electrostatic interactions, between an anionic nucleophile and the negatively charged phosphate anion, make phosphate diesters the least reactive of the series of phosphates.<sup>26</sup> Enhanced reactivity was observed for the five membered cyclic diesters or diesters with neighboring functional groups such as 2-hydroxyalkyl- or carboxyl groups which can be converted to a five membered ring diester by an intramolecular transesterification.<sup>27</sup> Due to the stability of diesters, most mechanistic studies have been based on activated esters. The alkaline hydrolysis of DMP and dibenzyl phosphate has been studied at 100 °C.<sup>20b,28</sup> The hydrolysis occurred through C-O bond cleavage under the experimental conditions used.

### 1.3.3 Phosphate triesters

Reactions of trialkyl phosphates are relatively simple. A nucleophile can attack either phosphorus or carbon. The position of attack is consistent with Pearson's HSAB theory (Scheme I.4).<sup>17a</sup> At phosphorus, hydroxide is a better nucleophile than water by a factor of  $10^8$ , while for attack on a saturated carbon, the corresponding factor is much smaller, ca.  $10^4$ . Thus, in triesters, where both carbon and phosphorus are vulnerable to nucleophilic attack, hydroxide ion and water will tend to be selective for phosphorus and carbon, respectively.<sup>29</sup>



**Scheme I.4** Hydrolysis mechanism for phosphate triesters

25 Bunton, C. A.; Farber, S. *J. Org. Chem.* **1969**, 34(4), 767.

26 a) Kirby, A. J.; Youna, M. *J. Chem. Soc. B* **1970**, 1165. b) Roos, A. M.; Toet, J. *J. Recl. Trav. Chim. Pays-Bas.* **1958**, 77, 946.

27 a) Westheimer, F. H. *Acc. Chem. Res.* **1968**, 1, 70. b) Kluger, R.; Taylor, S. D. *J. Am. Chem. Soc.* **1990**, 112, 6669. c) Steffens, J. T.; Siewers, I. J.; Benkovic, S. J. *Biochem.* **1975**, 14, 2431. d) Kirby, A. J.; Clark, V. M. *J. Am. Chem. Soc.* **1966**, 88, 3705. e) Kirby, A. J.; Abell, K. W. Y. *J. Chem. Soc., Perkin Trans. II*, **1983**, 1171. f) ref 17 a, and references therein.

28 a) Kumamoto, J.; Westheimer, F. H. *J. Am. Chem. Soc.* **1955**, 77, 2515. b) Bunton, C. A.; Mhala, M. M.; Oldham, K. G.; Vernon, C. A. *J. Chem. Soc.* **1960**, 3293. c) Haake, P. C.; Westheimer, F. H. *J. Am. Chem. Soc.* **1961**, 84, 1102.

29 Barnard, P. W. C.; Bunton, C. A.; Liewellyn, D. R.; Vernon, C. A.; Welch, V. A. *J. Chem. Soc.* **1961**, 1636.



phosphorus center has been observed in the hydrolysis of trimethyl phosphate (tmp) coordinated to a tripositive metal center.<sup>31</sup> The base hydrolysis of tmp was accelerated 400 fold upon coordination to the pentaamine-iridium moiety.<sup>31a</sup> This rate enhancement is minute compared to typical rate enhancement obtained with enzymes ( $10^{11}$  fold). Monodentate coordination of a phosphate ester alone is not adequate to explain the enormous rate enhancement observed in enzymatic systems.

Metal ions tend to lower the  $pK_a$  of coordinated ligands depending on the valence state of the metal and ligand. Metal hydroxide is a weaker nucleophile than free hydroxide.<sup>32</sup> In the metal hydroxide mechanism (B), the high effective concentration of metal hydroxide at neutral pH compensates for the reduced nucleophilicity due to metal binding. Metal hydroxides are efficient catalysts in hydrolyzing carboxylic esters with good leaving groups, but are not efficient in hydrolyzing unactivated esters such as methylacetate.<sup>33</sup>

The bifunctional mechanism (C), where the metal ion activates both substrate and nucleophile through the Lewis acid and the metal hydroxide mechanisms was proven to be the most efficient.<sup>34</sup> Although metal ions found in biological systems are usually divalent ions, most model studies have been done with substitutionally inert trivalent metal complexes such as Co(III), Ir(III), and Rh(III) to avoid mechanistic ambiguities that may be caused by labile divalent metal ions.<sup>35</sup>

#### 1.4.2 Metal complex promoted phosphate diester hydrolysis

Sargeson et al. have shown that a coordinated hydroxide is an efficient intramolecular nucleophile for cleaving 4-nitrophenol from bis(4-nitrophenyl) phosphate and 4-nitrophenylethylphosphate bound to trivalent Co and Ir complexes (Fig. 1.7 (b)).<sup>36</sup> The observed rate enhancement is over  $10^6$  fold as compared to that of free ester.

Other types of intramolecular nucleophiles such as amido ions can be better nucleophiles for hydrolyzing some esters coordinated to pentaamine Co(III) and Ir(III)

31 a) Hendry, P.; Sargeson, A. M. *Aust. J. Chem.* **1986**, *39*, 1177. b) *Ibid. J. Chem. Soc. Chem. Commun.* **1984**, 164. c) Dixon, N. E.; Jackson, W. G.; Marty, W.; Sargeson, A. M. *Inorg. Chem.* **1982**, *21*, 688.

32 Buckingham, D. A. in *Biological Aspects of Inorganic Chemistry*; Addison, A. W.; Cullen, W. R.; Dolphin, D.; James, B. R. Eds.; Wiley: New York, 1976, p 141.

33 Chin, J.; Zou, X. *J. Am. Chem. Soc.* **1984**, *106*, 3687.

34 Chin, J.; Banaszczyk, M. *J. Am. Chem. Soc.* **1989**, *111*, 2724.

35 a) Martell, A. E. in *Metal ions in Biological Systems*; Siegel, H. Ed.; Marcel Dekker Inc.: N. Y., **1973**, Vol. 2, ch. 5. b) Haight, Jr. *Coordination Chem. Rev.* **1987**, *79*, 293.

36 Hendry, P.; Sargeson, A. M. *J. Am. Chem. Soc.* **1989**, *111*, 2521.

complexes (Fig. I.7 (a)).<sup>37</sup> The  $pK_a$  of coordinated amine is ca. 16, whereas that of coordinated water is ca. 7, so that the efficiency of the nitrogen nucleophile can not be realized at neutral pH.

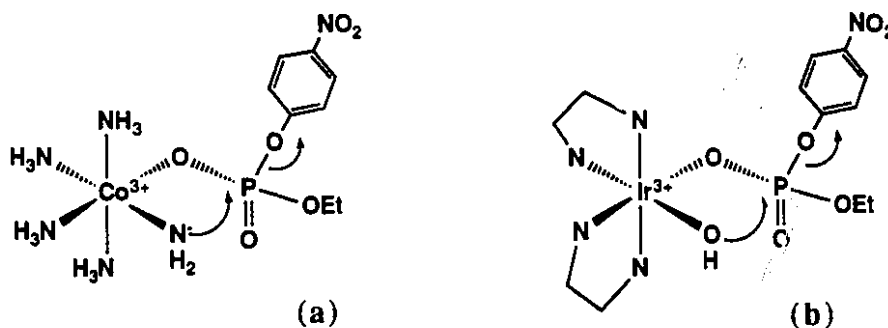
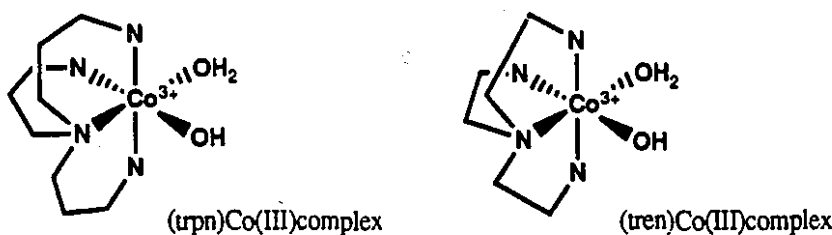


**Figure I.7** Hydrolysis of coordinated phosphate diesters by a nucleophilic attack of coordinated amido ion (a) and hydroxide (b).

Knowledge that this bifunctional mechanism including intramolecular catalysis is more efficient than others led to the design of catalysts with an optimum structure having two aqua ligands in close proximity. These requirements are fulfilled in cis-diaqua complexes.<sup>38</sup> It has been recently reported that large rate enhancement for the hydrolysis of phosphate esters with either good or poor leaving groups has been obtained with some cis-diaqua ( $N_4$ ) cobalt complexes ( $N_4$  represents tetradentate amine ligands) (Table I.3).<sup>39</sup>



37 Hendry, P.; Sargeson, A. M. *Inorg. Chem.* **1990**, *29*, 92.

38 a) Chin, J. *Acc. Chem. Res.* **1991**, *145*. b) Milburn, R. M.; Rawji, G.; Hediger, M. *Inorg. Chim. Acta.* **1983**, *79*, 247.

39 a) Chin, J.; Banaszczyk, M.; Jubian, V.; Zou, X. *J. Am. Chem. Soc.* **1989**, *111*, 186. b) Chin, J.; Banaszczyk, M.; Jubian, V. *J. Chem. Soc., Chem. Commun.* **1988**, 735.

**Table I.3** Observed pseudo first order rate constants( $\text{sec}^{-1}$ ) for hydrolysis of phosphate diesters promoted by  $(\text{N}_4)\text{Co}(\text{III})(\text{OH}_2)(\text{OH})$  at pH 7 and  $50^\circ\text{C}$ .

Catalyst	BNPP <sup>d</sup>	BDNPP <sup>d</sup>
$(\text{trpn})\text{Co}(\text{III})(\text{OH})(\text{OH}_2)^{\text{a}}$	$2.5 \times 10^{-2}$	$1.1 \times 10^{-1}$ <sup>b</sup>
$(\text{tren})\text{Co}(\text{III})(\text{OH})(\text{OH}_2)^{\text{a}}$	$8.1 \times 10^{-5}$	$1.6 \times 10^{-3}$
$\text{NaOH (1M)}^{\text{c}}$	$1.6 \times 10^{-11}$	$2.8 \times 10^{-9}$

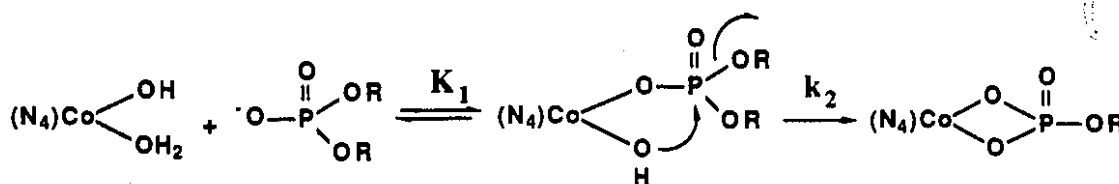
a)  $[\text{Co}]$  10 mM,  $[\text{substrate}]$   $5 \times 10^{-5}$  M    b) at  $25^\circ\text{C}$

c) second order rate constant was extrapolated to pH 7 ref:  
Bunton, C. A.; Farber, S. J. *Org. Chem.*, **34**, 767 (1969).

d) BNPP and BDNPP stands for bis(p-nitrophenyl) phosphate and bis(2,4-dinitrophenyl) phosphate, respectively.

The hydrolysis rate of the trpn complex bound BNPP is  $10^{10}$  fold greater than the hydroxide catalyzed rate at neutral pH. The proposed BNPP hydrolysis mechanism involves intramolecular metal hydroxide attack ( $k_2$ ) on a coordinated phosphate forming a strained four-membered ring cobalt-phosphate complex (Scheme I.5).

#### Scheme I.5



The reactivity of the cobalt complex is very sensitive to the tetraamine ligand structure.  $(\text{Trpn})\text{Co}(\text{III})(\text{OH}_2)_2$  is 300 times more reactive than its close structural analog,  $(\text{tren})\text{Co}(\text{III})(\text{OH}_2)_2$  in hydrolyzing BNPP, even though the equilibrium constants ( $K_1$ ) for binding of phosphate diester (DMP) to these complexes are comparable. Since the reaction mechanism involves the formation of a four-membered ring cobalt-phosphate complex,<sup>39</sup> the angle opposite to the bidentate phosphate plays an important role. X-ray structures of  $(\text{trpn})\text{Co}(\text{III})(\text{CO}_3)$  and  $(\text{tren})\text{Co}(\text{III})(\text{CO}_3)$  reveal that trpn is better able to stabilize the four-membered ring.<sup>40</sup> Both O-Co-O bond angles in  $(\text{trpn})\text{Co}(\text{III})(\text{CO}_3)$  ( $68^\circ$ ) and

40 a) Drouin, M. M. Sc. Thesis, McGill University, 1989. b) Schlemper, E. O.; Sen Gupta, P. K.; Dasgupta, T. P. *Acta Cryst. C* **39**, 1983, 1012.

(tren)Co(III)(CO<sub>3</sub>) (68°) are highly distorted from that found in a regular octahedral complex (90°). All the N-Co-N bond angles (87°) are rigidly held with tren, whereas the N-Co-N bond angle opposite to the O-Co-O bond angle in the trpn complex is free to expand to 100°. The bifunctional mechanism also applies to divalent metal ion promoted hydrolysis of triesters<sup>41</sup> and diesters.<sup>42,43,44</sup> Breslow et al. have shown that a Zn(N<sub>4</sub>) complex hydrolyzes a triester by this mechanism.<sup>42</sup> Diphenyl p-nitrophenyl phosphate, in the presence of the zinc catalyst, was hydrolyzed 10 times faster than the hydroxide catalyzed reaction (2nd order rate constant). This rate enhancement cannot be explained either by the metal hydroxide or the Lewis acid mechanism alone. Trogler et al have shown that Cu(II)(bpy)(OH<sub>2</sub>)<sub>2</sub> (bpy = 2,2-bipyridine) can hydrolyze p-nitrophenyl ethyl- and p-nitrophenyl diethyl phosphate to the corresponding monoester and diester, respectively, with a 10<sup>2</sup> to 10<sup>3</sup> fold rate enhancement over that in the absence of catalysts.<sup>43</sup>

Currently there is considerable interest in developing artificial DNases and artificial restriction enzymes. An efficient catalyst that can cleave unactivated phosphate esters such as DNA and dimethyl phosphate has not yet been reported.

### 1.4.3 Metal complex promoted monoester hydrolysis

There are two major mechanisms involved in hydrolysis of phosphate monoesters (Scheme I.6). Intramolecular metal hydroxide mechanism (a) has been considered to be more efficient than double Lewis acid activation mechanism (b) in hydrolyzing NPP coordinated to the cobalt complex.<sup>45,46</sup>

41 Morrow, J. R.; Trogler, W. C. *Inorg. Chem.* **1989**, *28*, 2330.

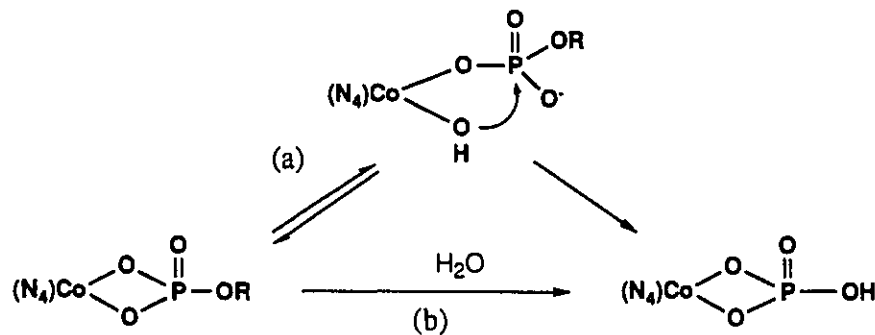
42 Gellman, S. H.; Petter, R.; Breslow, R. *J. Am. Chem. Soc.* **1986**, *108*, 2388.

43 Morrow, J. R.; Trogler, W. C. *Inorg. Chem.* **1988**, *27*, 3387.

44 a) De Rosch, M. A.; Trogler, W. C. *Inorg. Chem.* **1990**, *29*, 2409. b) Menger, F. M.; Gan, L. H.; Johnson, E.; Durst, D. H. *J. Am. Chem. Soc.* **1987**, *109*, 2800. c) Kenley, R. A.; Fleming, R. H.; Laine, R. M.; Tse, D.; Winterle, J. S. *Inorg. Chem.* **1984**, *23*, 1870.

45 a) Jones, D. R.; Lindoy, L. F.; Sargeson, A. M. *J. Am. Chem. Soc.* **1983**, *105*, 7327. b) *ibid.* *J. Am. Chem. Soc.* **1984**, *106*, 7907.

46 Chin, J.; Banaszczyk, M. *J. Am. Chem. Soc.* **1989**, *111*, 4103.



**Scheme 1.6** Mechanisms for the cobalt complex promoted hydrolysis of monoester: (a) intramolecular metal hydroxide and (b) double Lewis acid mechanism.

The hydrolysis of *p*-nitrophenyl phosphate bound to cobalt in both monomeric and dimeric ( $\mu$ -) forms has been studied (Fig. 1.8).<sup>45</sup>  $^{18}\text{O}$  labeling studies of the mononuclear complex have shown that the intramolecular hydroxide mechanism initially yields a five coordinated phosphorane, with a  $10^5$  fold rate enhancement over that in the absence of catalyst.

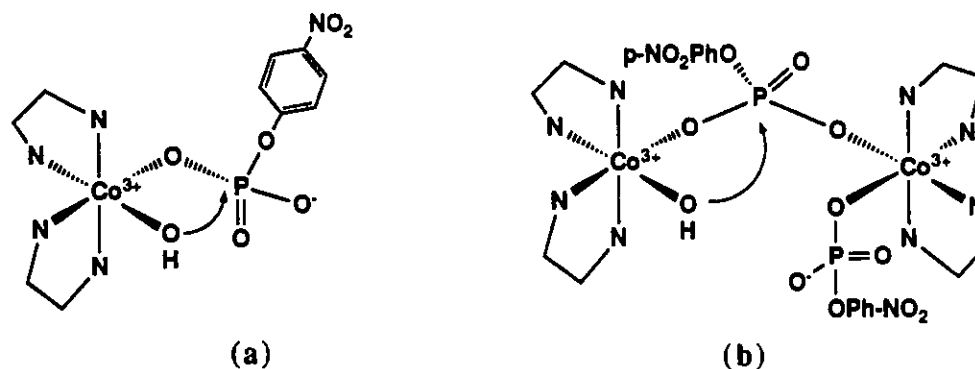


**Figure 1.8** Hydrolysis of the cobalt bound NPP: (a) monomeric, (b) dimeric form.

Hydrolysis of the dimeric species (Fig.1.8 (b)) showed a 26 fold increase in rate over that observed for the hydrolysis of the monomeric species (Fig. 1.8 (a)). Therefore, of the rate enhancement obtained in the hydrolysis of the phosphate monoester, about a 30 fold increase can be ascribed to a charge neutralization effect by each metal ion, while an intramolecular effect accounts for the remainder.

Two metal ion participation in hydrolysis of phosphate monoester is found in both enzymatic and model systems. The enzyme, purple acid phosphatase (PAPs) efficiently

hydrolyzes phosphate monoesters at pH 5.<sup>47</sup> Even though the precise mechanism and structure are not established, it is postulated that two iron ions in the active sites are bridged by inorganic phosphate. In an elegant model system, Chin and Banaszczyk<sup>46</sup> have shown that methyl phosphate is rapidly hydrolyzed by adding two equivalents of (trpn)Co(III)(OH)<sub>2</sub> with concomitant formation of a novel binuclear Co(III) complex (Fig.I.9 (b)). The proposed reaction mechanism for the trpn complex promoted hydrolysis of phosphate monoesters with poor leaving groups (e.g. methyl phosphate) involves initial formation of a stable cobalt complex, that is subsequently hydrolyzed upon further addition of the trpn complex.

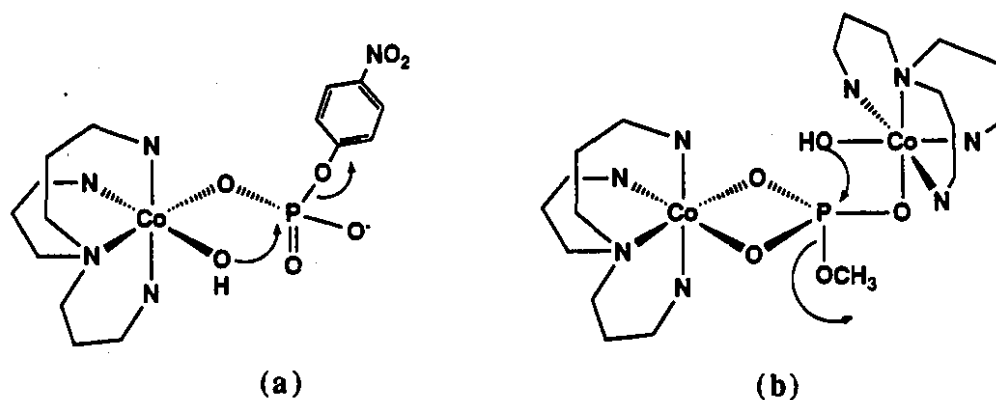


**Figure I.9** Hydrolysis of (a)BNPP and (b) MP promoted by the trpn complex.

There have been surprisingly few studies of divalent metal catalysis in the hydrolysis of phosphate monoesters.<sup>48</sup> The catalysis by metal ions in these reactions has been ascribed to screening negative charges and a template effect or assistance of leaving group departure.<sup>49</sup> Binding of a metal ion to the leaving group oxygen will enhance the metaphosphate-type mechanism (dissociative process), as observed in the hydrolysis of (O-imidazole-4-ylphenyl) phosphate upon addition of copper ion (Fig.I.10 (a)).<sup>50</sup> On the other hand, coordination to another oxygen will enhance the associative process. This is shown in Fig. I.10 (b) for the hydrolysis of 2-(1,10-phenanthroline) phosphate promoted by Cu(II) ion.<sup>51</sup>

47 Que, L., Jr.; Scarrow, R. C. In *Metal Clusters in Proteins*; Que, L., Jr., Ed.; ACS Symposium Series No.372; American Chemical Society; Washington, DC, 1988; 152.

48 a) Hay, R. W.; Basak, A. K.; Pujari, M. P.; Perotti, A. J. *Chem. Soc., Dalton Trans.* **1986**, 2029. b) Herschlag, D.; Jencks, w. P. *J. Am. Chem. Soc.* **1987**, 109, 4665.

49 a) Lloyd, G. J.; Cooperman, B. S. *J. Am. Chem. Soc.* **1971**, 93, 4883. b) Benkovic, S. J.; Schray, K. J. In *The Enzymes*; Boyer, P. D. Ed.; Academic: N. Y., 1973; Vol. 8, p 201.

50 Benkovic, S. J.; Dunikoski, L., Jr. *J. Am. Chem. Soc.* **1971**, 93, 1526.

51 Fife, T. H.; Pujari, M. P. *J. Am. Chem. Soc.* **1988**, 110, 7790.

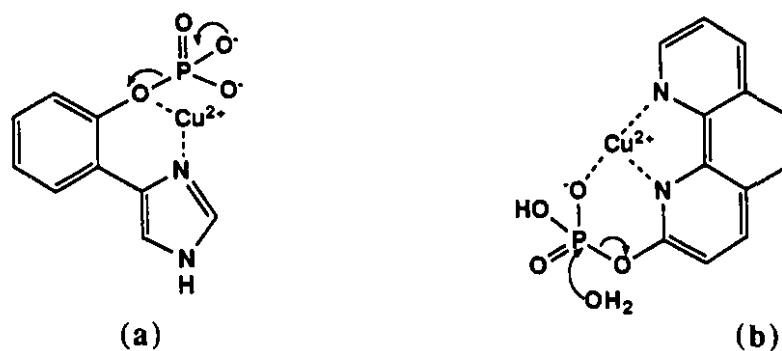


**Figure I.10** Cu(II) catalyzed hydrolysis of (a) (O-imidazole-4-ylphenyl) phosphate and (b) 2-(1,10-phenanthroline).

Hydrolysis of methyl phosphate with two equivalents of copper complex is not observed.  $\text{Cu(II)(dpa)(OH}_2)_2$  (dpa = 2,2'-dipyridylamine) is not active at hydrolyzing methyl phosphate. It is interesting that the hydrolysis of methyl phosphate proceeds by adding one equivalent of the dpa copper complex to the  $(\text{trpn})\text{Co(III)}(\eta^2\text{-O}_2\text{PO(OCH}_3))$  complex.<sup>52</sup>

## 1.5 Plan of Study

Hydrolysis of dimethyl phosphate in the absence of enzymes has never been detected at neutral pH. The half-life for the cleavage of dimethyl phosphate based on the water rate is estimated to be a billion years, at 25 °C. Numerous studies on the effect of simple metal complexes on hydrolysis of phosphate esters have been reported. Cobalt complexes, especially in the cis diaqua form, are among the most reactive for hydrolyzing highly activated diesters<sup>38a</sup> but they have been shown to be inactive for hydrolyzing DMP.<sup>53</sup> This is mainly due to the instability of the catalysts as well as their low efficiency. For example, (trpn)Co(III)(OH)(OH<sub>2</sub>), by far the most efficient catalyst for hydrolyzing BNPP<sup>39a</sup>, is not able to hydrolyze c-AMP while the less active (trien)Co(III)(OH)(OH<sub>2</sub>) hydrolyzes c-AMP.<sup>54</sup>

My research is focused on designing efficient yet stable catalysts that will allow us to study mechanistic details involved in the hydrolysis of unactivated phosphate esters. A series of cyclen derivatives will be prepared and tested as catalysts for the hydrolysis of several phosphate diesters including dimethyl phosphate. Detailed kinetic analyses will provide a mechanistic rationale for the observed hydrolysis reaction and will give valuable information in developing catalysts that can cleave DNA.

---

53 a) Farrell, F. J.; Kjellstrom, W. A.; Spiro, T. G. *Science*, **1969**, 164, 320. b) Schmidt, W.; Taube, H. *Inorg. Chem.* **1963**, 2, 698.

54 Chin, J.; Zou, X. *Can. J. Chem.* **1987**, 65, 1882.

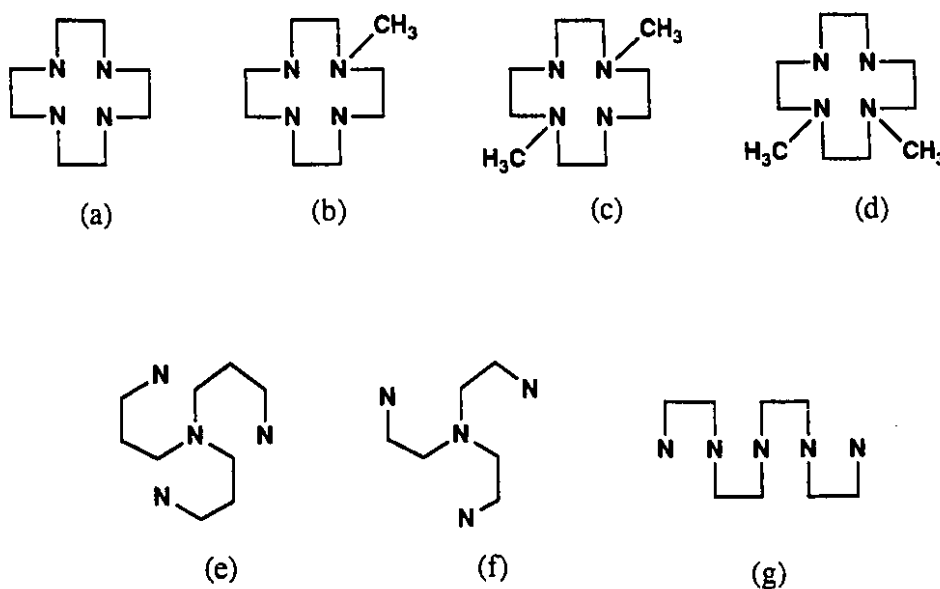
## 2 RESULTS

### 2.1 Synthesis of ligands and Co(III) complexes

#### 2.1.1 Synthesis of ligands and their Co(III) complexes

Tetraamine and pentaamine ligands used in this study are shown in Fig. I.11 with abbreviations.

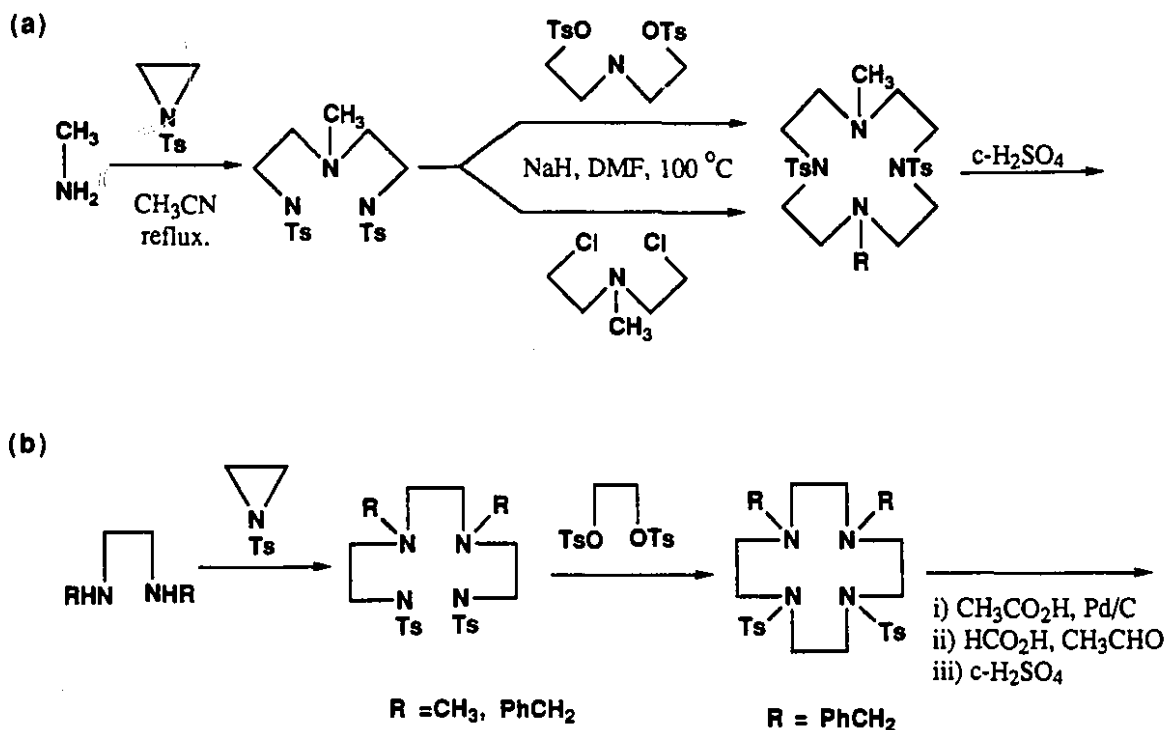
**Figure I.11** Tetra- and pentaamine ligands used in this study.



(a) 1,4,7,10-tetraazacyclododecane (**cyclen**) (b) 1-methyl-1,4,7,10-tetraazacyclododecane (**mcyclen**) (c) 1,7-dimethyl-1,4,7,10-tetraazacyclododecane (**tmcyclen**) (d) 1,4-dimethyl-1,4,7,10-tetraazacyclododecane (**cmcyclen**) (e) tris(3-aminopropyl)amine (**trpn**) (f) tris(2-aminoethyl)amine (**tren**) (g) tetraethylenepentamine (**tetren**)

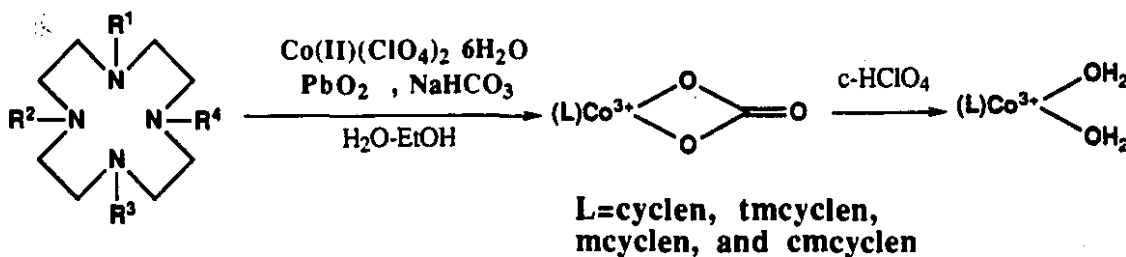
Cyclen and trpn were synthesized according to known procedures.<sup>55</sup> Tmcyclen, mcyclen, and cmcyclen were synthesized using N-tosylaziridine as a coupling reagent. Methyl groups were introduced before the cyclization for the synthesis of tmcyclen and mcyclen, while after the cyclization for the synthesis of cmcyclen. Tren and tetren are commercially available. The general synthetic scheme for the ligands is shown in Scheme I.7.

<sup>55</sup> a) Richiman, J. E.; Atkins, T. J. *J. Am. Chem. Soc.* **1974**, *96*, 2268. b) ref. 39.



**Scheme I.7** General synthetic scheme for (a) micyclen and tmcyclen (b) cmicyclen.

Cobalt carbonato complexes of tetraamine ligands were synthesized by known methods using  $\text{PbO}_2$  as an oxidizing agent.<sup>56</sup> The carbonato complex,  $\text{Co(III)(L)(CO}_3\text{)ClO}_4$ , was converted to the corresponding diaqua complex,  $\text{Co(III)(L)(OH}_2\text{)}_2\text{ClO}_4$ , using concentrated perchloric acid.  $^{13}\text{C}$  and  $^1\text{H}$  NMR spectroscopy were used for structure identification.



**Scheme I.8** Synthesis of the cobalt complexes of the tetradetate ligands.

A mixture of  $\alpha$ - and  $\beta$ -tren cobalt complex,  $(\text{tren})\text{Co(III)Cl}(\text{ClO}_4)_2$  was prepared according to literature procedures and then converted to  $\alpha$ - $(\text{tren})\text{Co}(\text{OH}_2)$  in aqueous solution (see Part IV).

### 2.1.2 Spectral data and acid dissociation constants of Co(III) complexes

In aqueous solution, a cis-diaqua cobalt complex exists in three different ionization states.

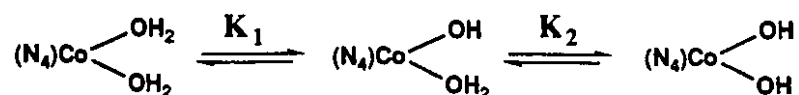


Table I.4 shows acid dissociation constants of cis-diaqua cobalt complexes used in this study, where  $K_1$  and  $K_2$  are represented by eq(1).

$$K_1 = \frac{[(\text{N}_4)\text{Co}(\text{OH}_2)(\text{OH})] [\text{H}]^+}{[(\text{N}_4)\text{Co}(\text{OH}_2)_2]} \quad K_2 = \frac{[(\text{N}_4)\text{Co}(\text{OH})_2] [\text{H}]^+}{[(\text{N}_4)\text{Co}(\text{OH}_2)(\text{OH})]} \quad \text{eq(1)}$$

Acid dissociation constants are comparable for the cobalt complexes of all cyclen derivatives.

**Table I.4** Acid dissociation constants for  $(\text{L})\text{Co(III)}(\text{OH}_2)_x$  complexes.

L	Found <sup>a)</sup>		Literature value <sup>b)</sup>	
	$\text{pK}_{a1}$	$\text{pK}_{a2}$	$\text{pK}_{a1}$	$\text{pK}_{a2}$
trpn	4.8	7.4	4.8	7.6
tren	5.2	7.9	5.5	8.0
cyclen	5.4	7.9	5.6	8.0
N-methylcyclen	4.9	7.6	-	-
trans -N,N'-dimethylcyclen	4.6	7.6	-	-
tetren	5.9		-	

a) Ionic strength was maintained with 0.1 N  $\text{NaClO}_4$

b) Chin, J., Banaszczyk, M., Jubian, V., Zou, X. *J. Am. Chem. Soc.*, **111**, 186 (1989).

Table I.5 shows spectral data of the cobalt carbonato- and diaqua-complexes, along with the literature values.

**Table I.5** Visible Absorption Spectral data of (L)Co(III)(CO)<sub>3</sub> and (L)Co(III)(OH<sub>2</sub>)<sub>2</sub> complexes at 25 °C.

(L)Co(III)(CO <sub>3</sub> )	$\lambda_{\max}$ ( $\epsilon_{\max}$ ) [nm (M <sup>-1</sup> cm <sup>-1</sup> )]			
	Found <sup>a)</sup>		Literature value	
trpn	532(124)	364(154)	532(125) <sup>b)</sup>	363(153) <sup>b)</sup>
tren	504(160)	354(96)	504(130) <sup>c)</sup>	354(110) <sup>c)</sup>
cyclen	526(270)	368(207)	529(280) <sup>d)</sup>	368(210) <sup>d)</sup>
N-methylcyclen	524(239)	368(188)	-	-
trans -N,N'-dimethylcyclen	544(297)	378(223)	-	-
<b>(L)Co(III)(OH<sub>2</sub>)<sub>2</sub></b>				
trpn	532(60)	372(90)	531(58) <sup>e)</sup>	371(85) <sup>e)</sup>
tren	504(116)	360(85)	505(108) <sup>c)</sup>	360(79) <sup>c)</sup>
cyclen	504(253)	356(193)	504(229) <sup>f)</sup>	358(162) <sup>f)</sup>
N-methylcyclen	518(285)	364(222)	-	-
trans -N,N'-dimethylcyclen	538(385)	372(318)	-	-
(tetreten) Co(III)(OH <sub>2</sub> )	486(105)	354(97)	472(122) <sup>g)</sup>	350(85) <sup>g)</sup>

a) Extinction coefficients were measured in H<sub>2</sub>O for carbonato complexes and in 0.1 N HClO<sub>4</sub> for diaqua complexes at 25°C.

b) Massoud S.S.; Milburn, R. M. *Inorg. Chem. Acta.*, **154**, 115 (1988).

c) Eldik, R.; Harris, G. M. *Inorg. Chem.*, **19**, 3684 (1980).

d) Hung, Y.; Martin, L.; Jakels, S.; Tait, A.; Busch, D. *J. Am. Chem. Soc.*, **99**, 4029 (1977).

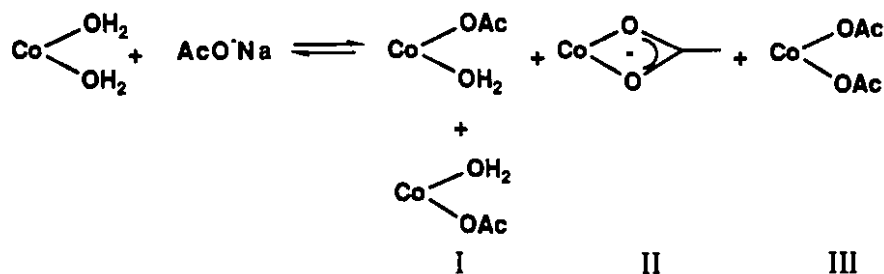
e) Banaszczyk, M. Ph.D. Thesis, McGill University (1989).

f) Moore, A. Ph.D Thesis, McGill University (1990).

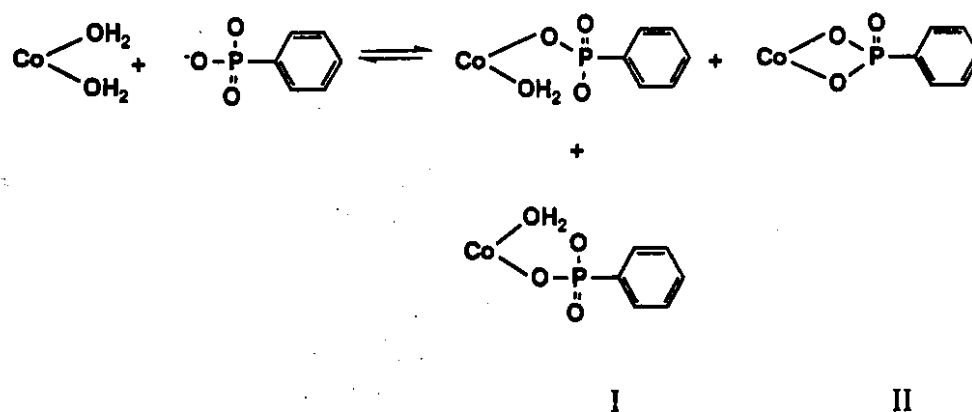
g) House, D. A. ; Garner, C. S., *Inorg. Chem.*, **2**, 272 (1967).

## 2.2 Binding with Acetate, Phenyl phosphonate, Inorganic phosphate, and Dimethyl phosphate

**Binding with acetate:** Binding studies were carried out by  $^{13}\text{C}$  NMR using  $^{13}\text{C}_1$  labelled acetate. Fig. I.12 shows the  $^{13}\text{C}$  NMR spectra of acetate coordinated to the cobalt cyclen, mcyclen, and tmcyclen complexes, respectively. NMR peaks were assigned by doing experiments with various concentration ratios of the cobalt complex and acetate. The peak at 178.5 ppm corresponds to free acetate, and peaks in the range of 186 to 192 ppm correspond to the cobalt bound acetates. Since the two aqua sites in the complex are non-equivalent ( $\sigma_v$ ), two isomers can exist for the cobalt complex-bound monodentate acetate. In the presence of high concentration ratio of acetate over cobalt complex (Figure I.12 (a) 1:1 ratio), there observed doubly bound monodentate acetate (III) as well as singly bound monodentate acetate (II). The peak appearing far downfield in each NMR spectrum (196 to 198 ppm) corresponds to a chelated acetate. The ratio of monodentate over bidentate acetate is approximately one for all three complexes studied.



**Binding with phenyl phosphonate:** Figure I.13 displays the  $^{31}\text{P}$  NMR spectra of phenyl phosphonate coordinated to the cobalt complexes of three cyclen derivatives.



Chemical shifts are reported with trimethyl phosphate as an external reference. Phenyl phosphonate produces each three new signals with the cyclen and the mcyclen complexes, and two new signals with the tmcyclen complex. The coordination modes of the phosphonate to cobalt complexes are similar to those for phosphates (will be discussed next). The two signals around 23 ppm (I) and the signal at 35 ppm (II) correspond to phenyl phosphonate bound as monodentates and a bidentate, respectively. A single peak at 35 ppm indicates a mononuclear chelate formation, otherwise the mcyclen complex would produce more than one peak in that region. The cyclen and the mcyclen complexes form the chelate with phenyl phosphonate, whereas the tmcyclen complex does not form the chelate.

**Binding with inorganic phosphate:** Figure I.14 displays  $^{31}\text{P}$  NMR spectra of inorganic phosphate coordinated to the cobalt complexes. Unlike phenyl phosphonate, inorganic phosphate has four available oxygens for coordination. The coordination modes of phosphate to cobalt complexes are quite well known.<sup>57</sup> Typically, phosphates with one, two, three, and four Co(III) phosphate oxygen bonds have  $^{31}\text{P}$  NMR chemical shifts at ca.  $\delta$  10, 20, 30, and 40 ppm respectively relative to the corresponding free phosphate. The signal at -2.7 ppm relative to the external reference TMP corresponds to free inorganic phosphate. Signals, each separated by ca. 10 ppm, correspond to the cobalt bound phosphates as mono-, bi-, tri-, and tetradentate respectively. When more than one oxygen is involved in binding, more than one cobalt complex may be involved.

The cyclen and the mcyclen complexes form a chelate as indicated by a single peak around 20 ppm. Signals appearing far downfield in each spectrum correspond to binuclear cobalt phosphato complexes. The cyclen and the tmcyclen complexes can have one isomer, while the mcyclen complex can have two isomers for this  $\mu^4$ -phosphato cobalt complex. According to the  $^{31}\text{P}$  NMR spectrum of the trpn complex and inorganic phosphate, the binuclear phosphato complex appears at 40 ppm when all four oxygens in the phosphate are used for binding.<sup>46</sup>

57 a) Haight, Jr. *Coordination Chem. Rev.* 1987, 79, 293. b) Jones, D. R.; Lindoy, L. F.; Sargeson, A. M.; Snow, M. R. *Inorg. Chem.* 1982, 21, 4155. c) ref. 45 b.

**Figure I.12**  $^{13}\text{C}$  NMR spectra of  $(\text{L})\text{Co}(\text{III})(\text{OH}_2)_2$  (0.05M) with 0.5 and 1 equivalents of  $\text{CH}_3\text{C}^*\text{OONa}$  at pD 4.6 and 25  $^\circ\text{C}$ .; L = a) cyclen, b) mtcyclen, c) tmcyclen:  $\nabla$  = free acetate.

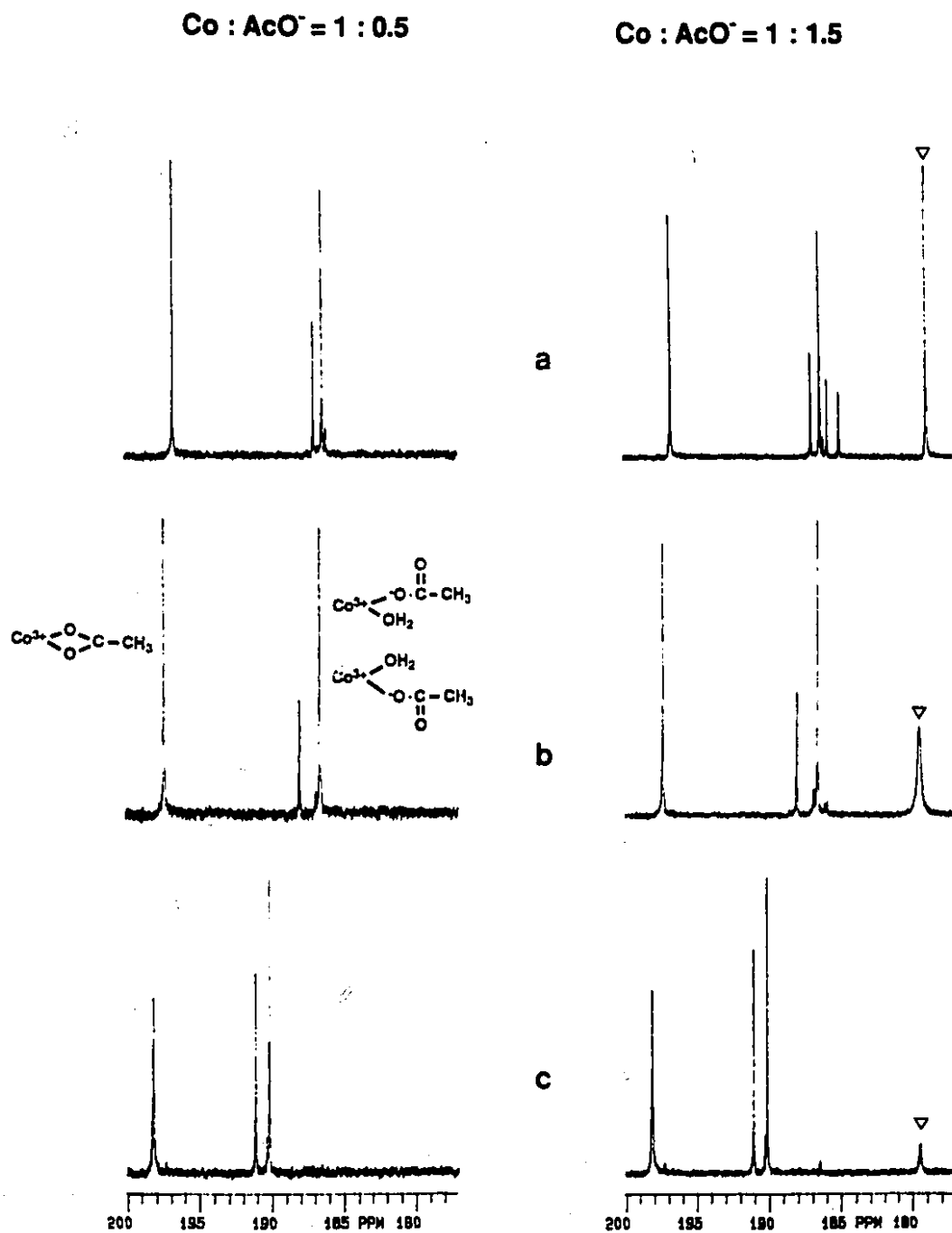


**Figure I.13**  $^{31}\text{P}$  NMR spectra of  $(\text{L})\text{Co}(\text{III})(\text{OH}_2)_2$  (0.05M) with one equivalent of phenyl phosphonate at pD 4.5, 25  $^\circ\text{C}$ . ; L =; a) cyclen, b) mcyclen, and c) tmcyclen:  $\nabla$  = free phenyl phosphonate.

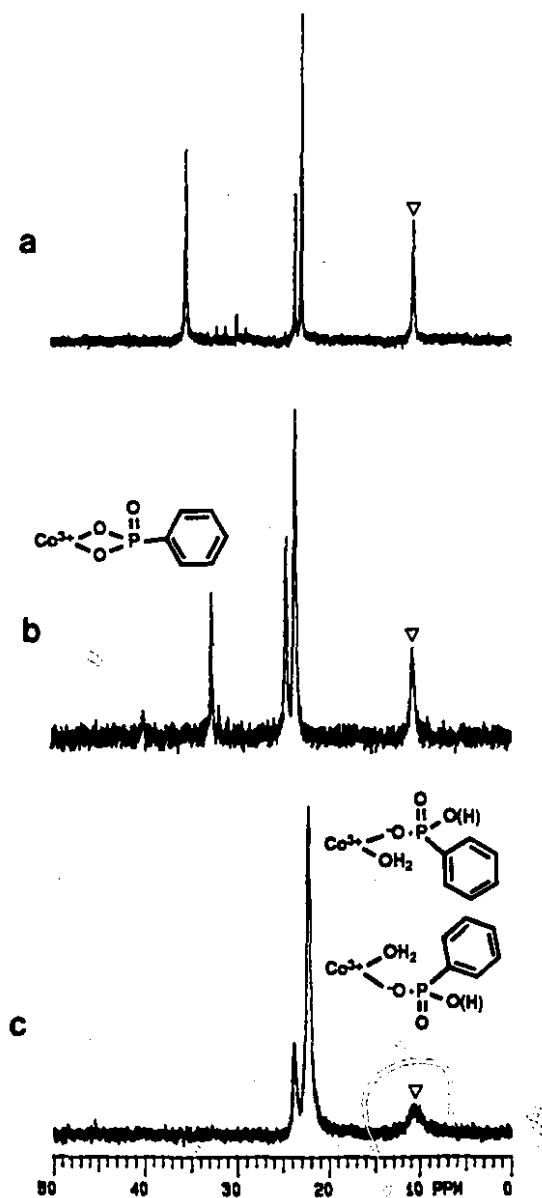
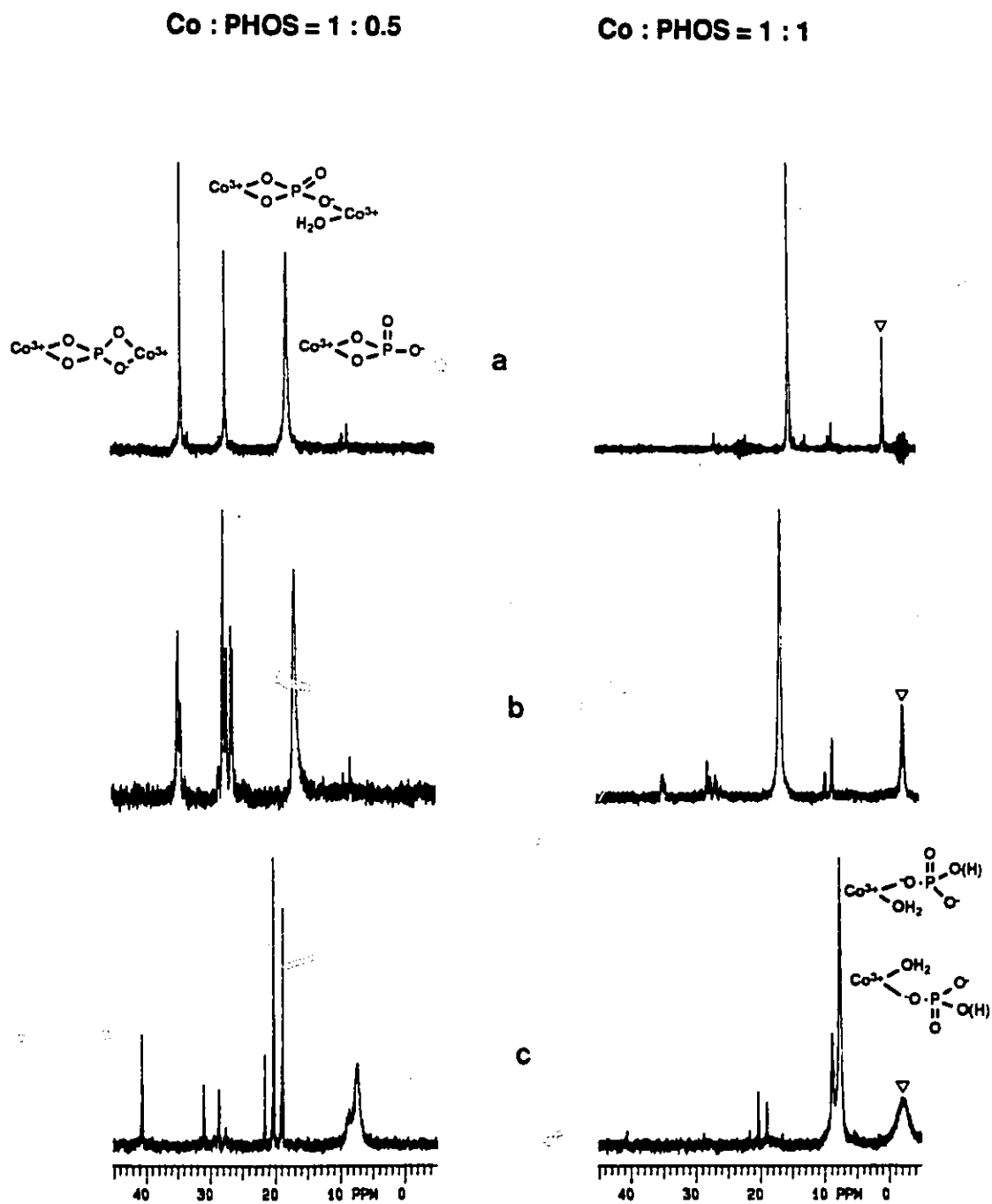


**Figure I.14**  $^{31}\text{P}$  NMR spectra of  $(\text{L})\text{Co}(\text{III})(\text{OH}_2)_2$  (0.05M) with 0.5 and 1 equivalents of inorganic phosphate at pD 6, 25 °C. ; L =; a) cyclen, b) mcyclen, c) tricyclen:  $\nabla$  = free inorganic phosphate.



**Binding with dimethyl phosphate:** Complexation of DMP to (cyclen)Co(III)(OH)<sub>2</sub> and (tetren)Co(III)(OH)<sub>2</sub> was observed by <sup>31</sup>P NMR (Fig.I.15). The concentration of DMP was varied from 50 mM to 0.1 M with 0.1 M of cobalt complexes. The cyclen complex produces two new signals at δ 6.48 and 6.97 ppm, which correspond to the two singly bound dimethyl phosphates. The tetren complex gives one major signal at 6.9 ppm with minor signals due to the presence of several isomers. Equilibrium binding constants (K) were obtained by converting the signal integration to concentration. Both cobalt complexes have approximately the same K value of 3 M<sup>-1</sup>.

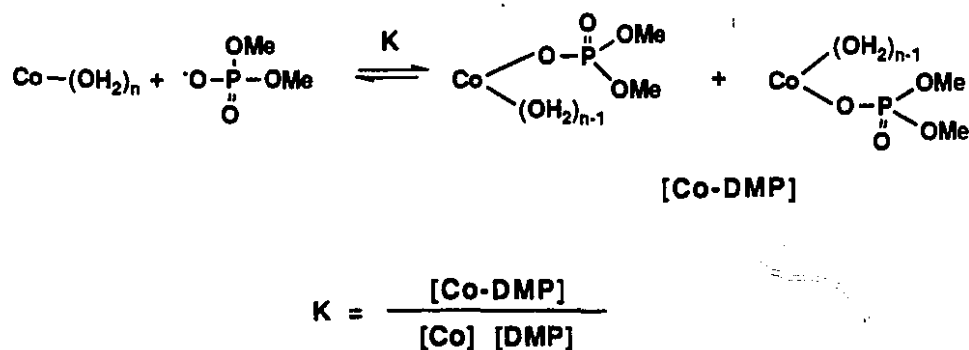
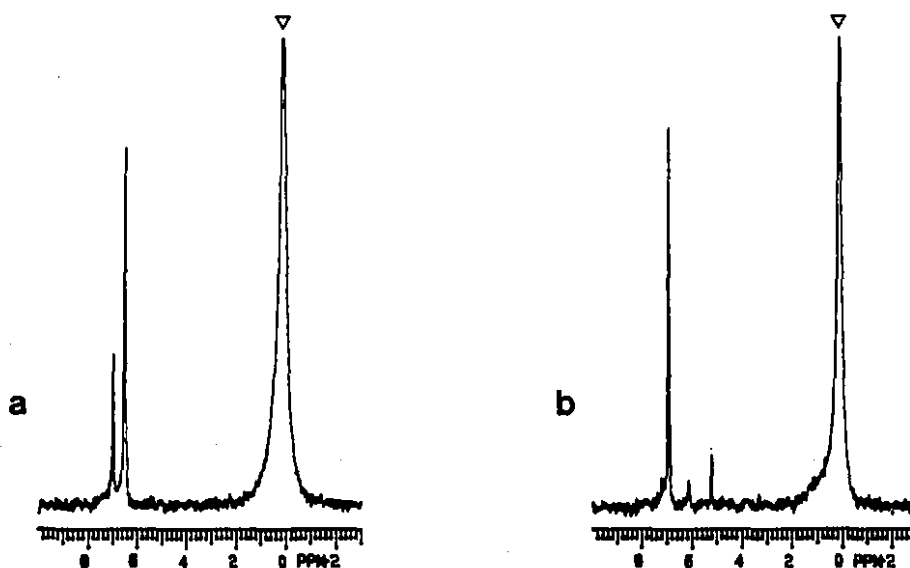
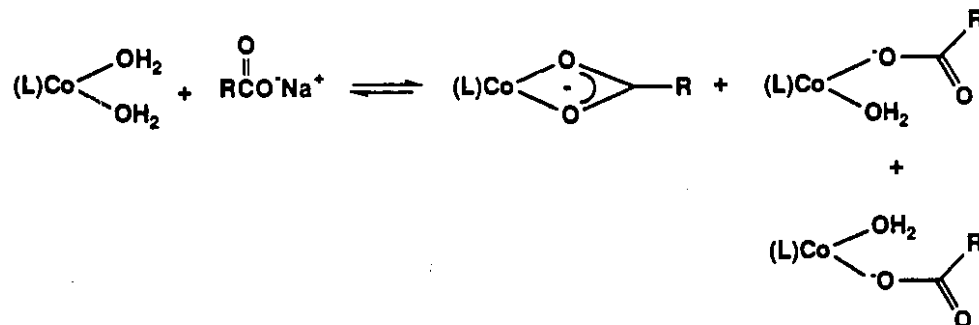


**Figure I.15** <sup>31</sup>P NMR of binding of DMP (0.1M) to the cyclen and the tetren complexes (0.1M) at pD 4 and 25 °C ; a) cyclen, b) tetren: ▽ = free DMP.



### 2.3 Relationships between Chelate Formation and the Basicity of Bidentate ligands.

Studies of equilibrium binding of carboxylates to  $(\text{trpn})\text{Co}(\text{III})(\text{OH}_2)_2$  and  $(\text{cyclen})\text{Co}(\text{III})(\text{OH}_2)_2$  were carried out by  $^{13}\text{C}$  NMR methods (Scheme I.9). Excess cobalt complex is used, so that the anion binds to the metal complex either in a monodentate fashion or as a chelate. Free carboxylate was not detected under the experimental conditions. The same peak interpretation as in the case of acetate binding studies (section 2.2) is applied to the analysis of the spectrum. The integration value is directly converted to the concentration of each species assuming that the relaxation time of carbonyl carbon is the same for a chelate and a monodentate carboxylate. The relative ratio of the chelate over the monodentate carboxylates is listed in Table I.6.



Scheme I.9 Equilibrium binding of carboxylates to the cis diaqua cobalt complexes.

Table I.6 Chelate formation of carboxylates with the trpn and the cyclen complexes (0.05 M).

carboxylic acids <sup>a)</sup>	pK <sub>a</sub>	[chelate]/[monodentate]	
		cyclen	trpn
Bromoacetic acid	2.86	0 <sup>b)</sup>	0.19
Formic acid	3.77	0	0.30
Benzoic acid	4.19	0.47	11.3
Acetic acid	4.76	1.12	28.4

a)  $^{13}\text{C}$  labeled carboxylates were used. [carboxylate] = 0.025 M, Temp = 23 °C.

b) the value 0 means that a chelate is not detected under the experimental conditions.

## 2.4 Kinetics

### 2.4.1 Co(III) complex-promoted hydrolysis of phosphate esters with good leaving groups

**Reactivity:** The rate constants for cobalt complex-promoted phosphate esters promoted by Co(III) complex are listed in Table I.7. The production of p-nitrophenolate and 2,4-dinitrophenolate was monitored by UV/VIS spectroscopy at 400 nm. One and two equivalents of the substituted phenol were released from the monoester and the diester, respectively. The anation reaction with inorganic phosphate was monitored by following the absorbance change due to formation of cobalt-phosphate complexes, at wavelengths that varied from 550 to 570 nm. The pseudo first order rate constants were obtained by fitting the data according to a first order kinetic equation ( $R > 0.98$ ). The rate constants reported represent an average value of at least three runs with standard deviations in the range of  $\pm 3\%$ . Ionic strength was not adjusted in these kinetic studies.

**Table I.7** Observed pseudo first order rate constants ( $\text{sec}^{-1}$ ) for (L)Co(III)(OH)(OH<sub>2</sub>) promoted hydrolysis of phosphate esters at pH 7.

L	BDNPP <sup>a)</sup>	BNPP <sup>a)</sup>	NPP <sup>a)</sup>	PHOS <sup>b)</sup>
cyclen	$9.2 \times 10^{-3}$	$3.3 \times 10^{-3}$	$1.2 \times 10^{-2}$	$7.7 \times 10^{-2}$
N-methylcyclen	$7.6 \times 10^{-3}$	$1.4 \times 10^{-3}$	$2.5 \times 10^{-3}$	$6.3 \times 10^{-2}$
<i>trans</i> -N,N'-dimethylcyclen	$4.5 \times 10^{-4}$	$1.2 \times 10^{-6}$	$3.3 \times 10^{-7}$	- <sup>c)</sup>

a) [Co] 5 mM, [Substrate]  $2.5 \times 10^{-5}$  M at 50 °C. b) at 25 °C, [Co] 5 mM, [PO<sub>4</sub>]  $5 \times 10^{-5}$  M

c) absorbance change is too small to be observed.

The cyclen complex is about two times more active in hydrolyzing BNPP than the mcyclen complex. The mcyclen complex shows a much lower reactivity compared to the cyclen or the mcyclen complexes in hydrolyzing BNPP.

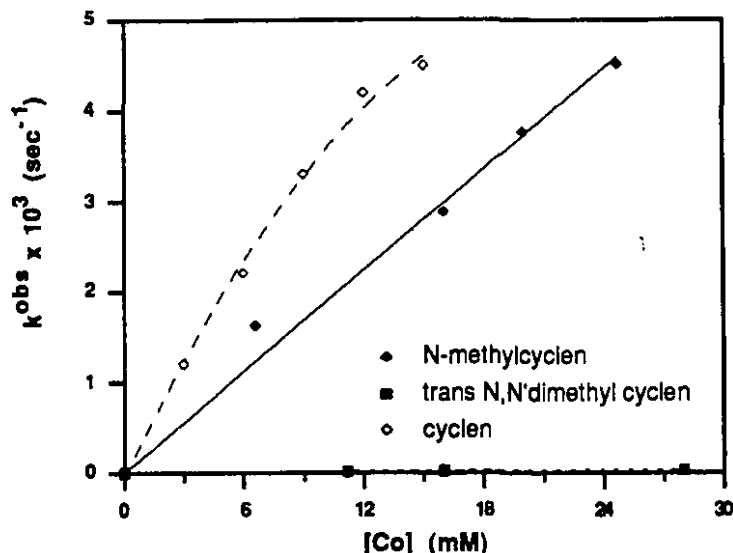
**Concentration dependence:** The observed pseudo first order rate constants of BNPP hydrolysis promoted by the cobalt complexes of three cyclen derivatives are listed in Table

I.8. The rate of hydrolysis of BNPP promoted by the cyclen complex levels off with increasing the catalyst concentration, while the hydrolysis rates promoted by both the mcyclen and tmcyclen complexes increase linearly. A plot of  $k^{\text{obs}}$  vs the catalyst concentration is shown in Fig. I.16.

**Table I.8** Dependence of the  $k^{\text{obs}}$  ( $\text{sec}^{-1}$ ) for BNPP ( $2.5 \times 10^{-5}$  M) hydrolysis on the concentration of  $[(\text{L})\text{Co}(\text{III})(\text{OH})(\text{OH}_2)]$  at pH 7, 50 °C.

Conc (mM)	cyclen	N-methyl-cyclen	<i>trans</i> -N,N'-dimethylcyclen
3.0	$1.2 \times 10^{-3}$	-	-
6.0	$2.2 \times 10^{-3}$	-	-
6.6	-	$1.62 \times 10^{-3}$	-
9.0	$3.3 \times 10^{-3}$	-	-
11.2	-	$2.53 \times 10^{-3}$	$2.0 \times 10^{-5}$
12.0	$4.2 \times 10^{-3}$	-	-
15.0	$4.5 \times 10^{-3}$	-	-
16.0	-	$2.88 \times 10^{-3}$	$2.5 \times 10^{-5}$
20.0	-	$3.76 \times 10^{-3}$	-
24.7	-	$4.52 \times 10^{-3}$	-
28.0	-	-	$3.4 \times 10^{-5}$

**Figure I.16** A plot of  $k^{\text{obs}}$  ( $\text{sec}^{-1}$ ) vs the catalyst concentration  $[(\text{L})\text{Co}(\text{III})(\text{OH})(\text{OH}_2)]$  (mM): L = cyclen, mcyclen, and tmcyclen.



#### 2.4.2 Co(III) complex promoted hydrolysis of phosphate esters with poor leaving groups

**Hydrolysis of c-AMP:** Hydrolyses of c-AMP and 2'-deoxy c-AMP promoted by the cyclen and the mcyclen complexes were monitored by  $^{31}\text{P}$  NMR spectroscopy (Fig. I.17). As the reaction proceeds, one equivalent of inorganic phosphate is produced, which binds tightly to the cobalt. The coordination modes of phosphate to cobalt complexes are well known and the binding of inorganic phosphate to the three cobalt complexes used has been studied previously (section 2.2). The NMR peak integration was used as a direct measure of the product concentration. The observed first order rate constants for the Co(III) complexes promoted hydrolysis of c-AMP and 2'-deoxy c-AMP are listed in Table I.9.

In the absence of the cobalt complex, no hydrolysis of c-AMP was observed at pH 7 (0.2 M phosphate buffer) and 100 °C even after one month. For both substrates, accumulation of monoesters has been observed, which indicates that the monoester hydrolysis is slower than initial hydrolysis of the corresponding diester. The mcyclen complex is slightly less active at hydrolyzing BNPP (Table I.7), while 10 times more efficient at hydrolyzing 2'-deoxy c-AMP than the cyclen complex. The reactivity difference between c-AMP and 2'-deoxy c-AMP is in the range of 2 to 5 fold.

**Table I.9** Second order rate constants ( $M^{-1} \text{ min}^{-1}$ ) for  $(L)\text{Co(III)(OH)(OH}_2)$  complex promoted hydrolysis of phosphate esters at pD 6, 50 °C.

L	c-AMP <sup>a)</sup>	5'-AMP <sup>b)</sup>	2'-deoxy c-AMP <sup>c)</sup>	
cyclen	$9.6 \times 10^{-2}$	$1.2 \times 10^{-4}$	$1.2 \times 10^{-2}$	$6.9 \times 10^{-4}$
N-methylcyclen	$8.5 \times 10^{-2}$	$1.3 \times 10^{-4}$	$4.3 \times 10^{-2}$	$5.4 \times 10^{-3}$

a) [Co] 0.066 M and [c-AMP] 0.033 M, rxn following the formation of 5'-AMP cobalt complex.

b) [Co] 0.1 M and [5'-AMP] 10 mM

c) [Co(cyclen)] 0.1 M, [Co(methylcyclen)] 0.2M, and [2'-deoxy-c-AMP] 10 mM, rate constants represent formation of monoester cobalt complex and formation of inorganic phosphato cobalt complex respectively.

**Hydrolysis of ApA:** Hydrolysis of UpU and ApA promoted by  $(\text{methylcyclen})\text{Co(III)(OH)}_2$  was monitored by  $^{31}\text{P}$  NMR following the formation of the inorganic phosphate-cobalt complexes (Fig. I.18). The  $^{31}\text{P}$  NMR spectrum of inorganic phosphate and the methylcyclen complex (1:10 ratio) is inserted within Figure I.18 for comparison. The hydrolysis of UpU was complete after five days under the experimental conditions used.

**Table I.10** Observed pseudo first order rate constants ( $\text{min}^{-1}$ ) for  $(\text{methylcyclen})\text{Co(III)(OH)}_2$  promoted hydrolysis of UpU and ApA at pD 6, 50 °C.<sup>a)</sup>

L	UpU	ApA
N-methylcyclen	$3.3 \times 10^{-4}$ <sup>b)</sup>	$1.8 \times 10^{-4}$
NaOH	-	$3 \times 10^{-10}$ <sup>c)</sup>

a) [Co] 0.2M, [substrate] 10 mM, rate constants obtained following the formation of inorganic phosphato-cobalt complex. b)  $1 \times 10^{-3} \text{ min}^{-1}$  was obtained for the hydrolysis of UpU by following the formation of monoester cobalt complex.

c) estimated hydroxide rate at pH 6 ref: Matsumoto, Y.; Komiyama, M. *J. Chem. Soc., Chem. Commun.* 1050 (1990).

**Figure I.17**  $^{31}\text{P}$  NMR spectra of hydrolysis of 2'-deoxy c-AMP (10 mM) promoted by the cyclen complex (0.1 M) at pD 6, 50 °C; a)  $t = 55$  min, b)  $t = 185$  min, and c)  $t =$  after 10 days.

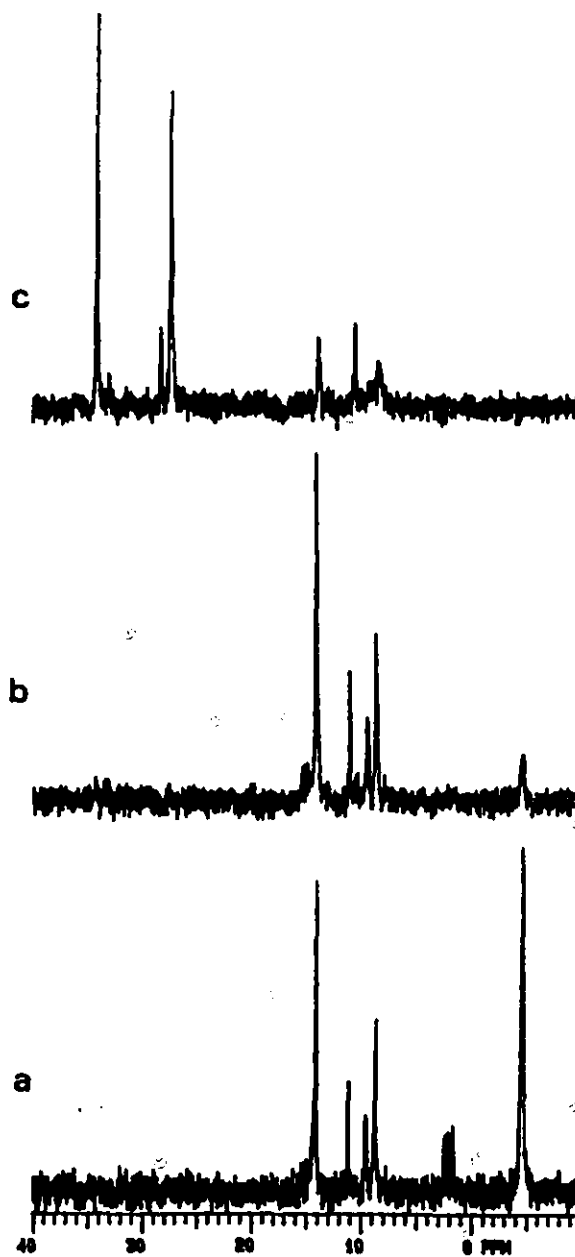
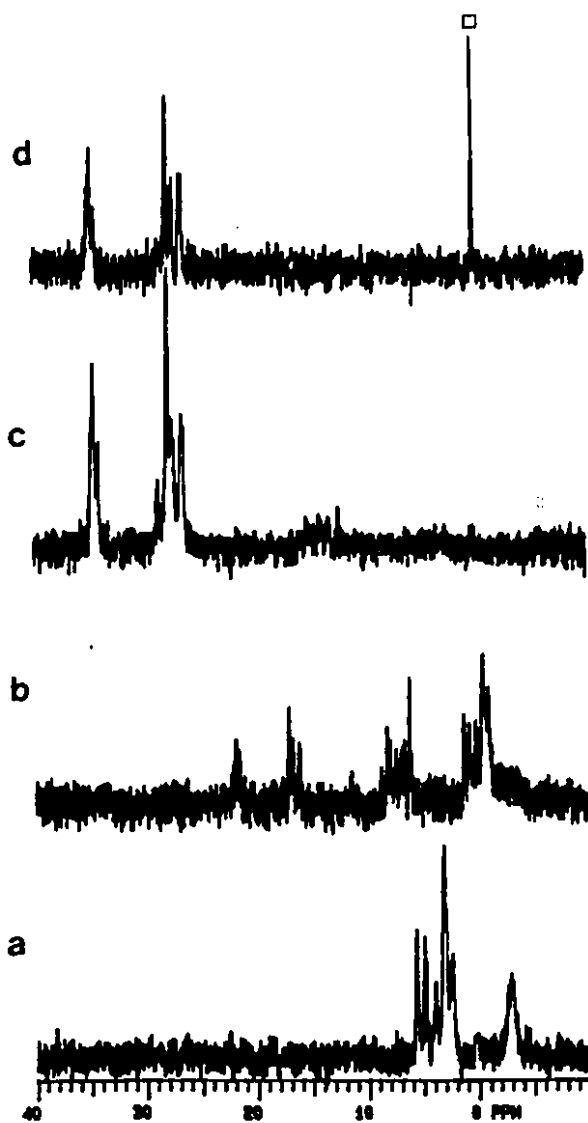


**Figure 1.18**  $^{31}\text{P}$  NMR spectra for (mcyclen)Co(III)(OH)(OH<sub>2</sub>) (0.2 M) promoted hydrolysis of UpU (10 mM) at pD 6 and 50 °C; a)  $t = 0$ , b)  $t = 11.5$  hr, c)  $t = 75$  hr, and d) the m cyclen complex with 0.1 equivalent of inorganic phosphate at pD 6: □ = TMP



**Hydrolysis of DMP:** Hydrolysis of DMP (0.5M) promoted by the cyclen complex (0.2M) was carried out at pD 5.5 to 6.3. Hydrolysis of DMP produces two equivalents of MeOH and inorganic phosphate without any observable build up of methyl phosphate during the reaction. The production of MeOH (3.42 ppm) was monitored by  $^1\text{H}$  NMR with the internal reference *t*-BuOH (1.22 ppm). The hydrolysis reaction was followed for up to 2 half lives (Fig. I.19). The data were fit according to a second order kinetic equation ( $R > 0.99$ ) and the second order rate constants for the hydrolysis of DMP are listed in Table I.11.

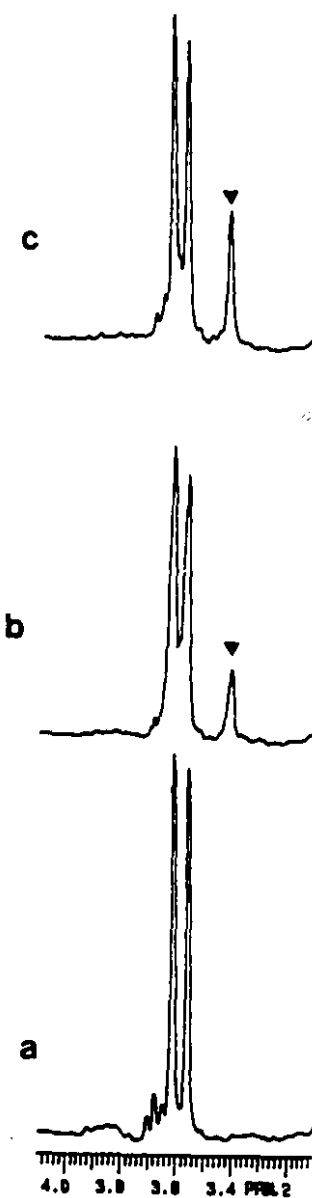
**Table I.11** Second order rate constants ( $\text{M}^{-1} \text{min}^{-1}$ ) for  $(\text{L})\text{Co}(\text{III})(\text{OH})(\text{OH}_2)$  complexes promoted hydrolysis of dimethyl phosphate (0.5 M).

L	pD	Temp.	k ( $\text{M}^{-1} \text{min}^{-1}$ )
cyclen	5.5	60 °C	$1.61 \times 10^{-5}$
	6.3	60 °C	$3.72 \times 10^{-5}$
	5.5	80 °C	$1.32 \times 10^{-4}$
tren	5.5	80 °C	$2.1 \times 10^{-5}$

a) [cyclen] 0.2 M, [DMP] 0.5 M b) [tren] 0.1 M, [DMP] 0.5 M

Under the same conditions (pD 5 and 6), (tren)Co(III)(OH<sub>2</sub>) (0.1M) and phosphate buffer (0.2M) did not hydrolyze DMP to any observable extent even when the reaction solution was heated at 100 °C for one month.

**Figure 1.19**  $^1\text{H}$  NMR of hydrolysis of dimethyl phosphate promoted by  $(\text{cyclen})\text{Co}(\text{OH}_2)_2$  at pD 5.5, 80 °C; a)  $t = 0$  hr, b)  $t = 4.8$  days, c)  $t = 20$  days:  $\blacktriangledown = \text{MeOH}$ .



### 3 DISCUSSION

#### 3.1 Synthesis of Ligands and their Co(III) complexes

**Synthesis of ligands:** There has been considerable interest in the synthesis of macrocyclic metal compounds because of the structural similarity between these synthetic compounds and several biologically important metal complexes.<sup>58</sup> Macrocyclic polyamines are generally synthesized by bimolecular cyclizations.<sup>59</sup> An increasing number of applications have been reported for these metal complexing ligands which contain additional functional groups. Substituents on nitrogen atoms are introduced before or after the cyclization step. A single substituent on one nitrogen atom is usually introduced by using a tritosyl protection-deprotection process.<sup>60</sup> Recently the synthesis of mono N-substituted derivatives of tetraazamacrocycles was achieved by using tris(dimethylamino) borane<sup>61</sup> or Cr(CO)<sub>6</sub>.<sup>62</sup> Three nitrogen atoms of tetraazamacrocycles are temporarily blocked keeping the fourth nitrogen atom free for the further selective alkylation reaction. These methods are quite efficient but require commercially available starting materials and they can not be used for the the synthesis of poly-substituted macrocycles.

For the synthesis of mono- and dimethylated cyclens, N-tosylaziridine is used as a key reagent to give N(4)-methyl N(1),N(7)-ditosyl diethylenetriamine for mcyclen and tmcyclen synthesis (Scheme I.7.a), or N(4),N(7) disubstituted N(1),N(10)-ditosyl triethylenetetraamine for cmcyclen synthesis (Scheme I.7.b). This method reduces a multistep protection-deprotection process into one step. The subsequent cyclization gives the desired product for mcyclen and tmcyclen. For the synthesis of cmcyclen, usual protection and deprotection method was used. Cyclization of N(4),N(7)-dimethyl, N(1),N(10)-ditosyl triethylenetetraamine with ditosyl ethyleneglycol was not successful. In contrast, N(4),N(7)-dibenzyl N(1),N(10) ditosyl triethylenetetraamine reacts with the cyclization counterpart yielding the cyclization product. For all three ligands, subsequent

58 a) Busch, D. H.; Farmery, K.; Goedken, V. L.; Katovic, V.; Melnyk, A. C.; Sperati, C. R.; Tokel, N. *Adv. Chem. Ser.*, **1971**, 100, 44. b) Moi, M. K.; Mears, C. F.; Denardo, S. J. *J. Am. Chem. Soc.* **1988**, 110, 6266.

59 a) ref 55 a, b) Izatt, R. M.; Christensen, J. J. in *Synthesis of Macrocycles*; Wiley Interscience: New York, 1987.

60 a) Heideger, M.; Kaden, T. A. *Helv. Chim. Acta* **1983**, 66, 861. b) Schiegg, A.; Kaden, T. A. *Helv. Chim. Acta* **1990**, 73, 716.

61 Bernard, H.; Yaouanc, J. J.; Clement, J. C.; Des Abbayes, H.; Handel, H. *Tetrahedron Lett.* **1991**, 32, 639.

62 Yaouanc, J. J.; Bris, N. L.; Clement, J. C.; Handel, H.; Des Abbayes, H. *J. Chem. Soc., Chem. Commun.* **1991**, 206.

detosylation of the cyclized products gives the desired mono- and dimethylated cyclens in high yields. Syntheses of the tetradentate ligands are described in detail in part IV.

**Configuration of cobalt complexes:** Due to the presence of four potentially chiral nitrogen atoms, a tetraamino macrocycle can give many configurational isomers even for a cis octahedral complex. However, most configurations can be safely ruled out on the basis of a strong repulsive interaction and angular strain. Configuration I ( $\sigma_v$ ) in Figure I.20 has been found by X-ray crystallography in the following cobalt complexes: (cyclen)Co(III)(CO<sub>3</sub>)ClO<sub>4</sub>·H<sub>2</sub>O<sup>63</sup>, (cyclen)Co(III)(NO<sub>2</sub>)<sub>2</sub>·Cl<sup>64</sup>, (tmcyclen)Co(CO<sub>3</sub>)ClO<sub>4</sub>·H<sub>2</sub>O<sup>65</sup>, and (Et<sub>4</sub>cyclen)Co(III)(serO) Br·ClO<sub>4</sub>·H<sub>2</sub>O<sup>66</sup>, and configuration II in Figure I.20 has been found in (tmcyclen)NiBr(H<sub>2</sub>O)·Br.<sup>67</sup> The stable configurations could also be predicted from MMX calculation.<sup>68</sup> According to this, the most stable isomer for the mcyclen complex is the one with the methyl group in the axial position (C<sub>1</sub>).

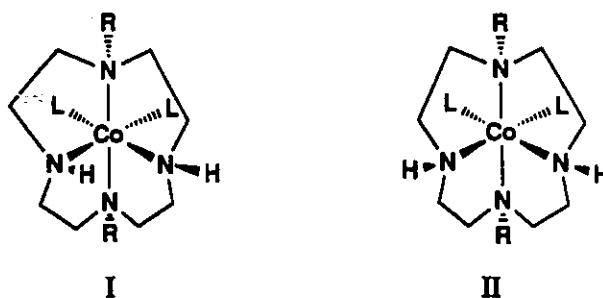


**Figure I.20** Two major isomers for the cobalt complexes of cyclen and its derivatives.

The two nitrogen protons trans to the water or carbonate ligand in the cobalt complexes of cyclen and its derivatives are not in equivalent environment because of different ion association and hydrogen bonding in solution.<sup>69</sup> The chemical shifts of these two protons are pH dependent. The signal of each proton is separable even though the proton exchange rates observed in DMSO-d<sub>6</sub> only differ by a factor of 3 within the range of 10<sup>7</sup> M<sup>-1</sup> sec<sup>-1</sup>.<sup>70</sup>

63 Loehlin, J. H.; Fleischer, E. B. *Acta Cryst.*, B 32, 1976, 3063.

64 Iitaka, Y.; Shina, M.; Kimura, E. *Inorg. Chem.* 1980, 19, 2886.

65 Giusti, J.; Chimichi, S.; Ciampolini, M. *Inorg. Chim. Acta.* 1984, 88, 51.

66 Tsuboyama, S.; Miki, S.; Chijimastu, T.; Tsuboyama, K.; Sakurai, T. *J. Chem. Soc., Dalton Trans.* 1989, 2359.

67 Ciampolini, M.; Micheloni, N.; Paoletti, P.; Dapporto, P.; Zanobini, F. *J. Chem. Soc., Dalton Trans.* 1984, 1357.

68 Houk, K. N.; Tucker, J. A.; Dorigo, A. E. *Acc. Chem. Res.* 1990, 23, 107.

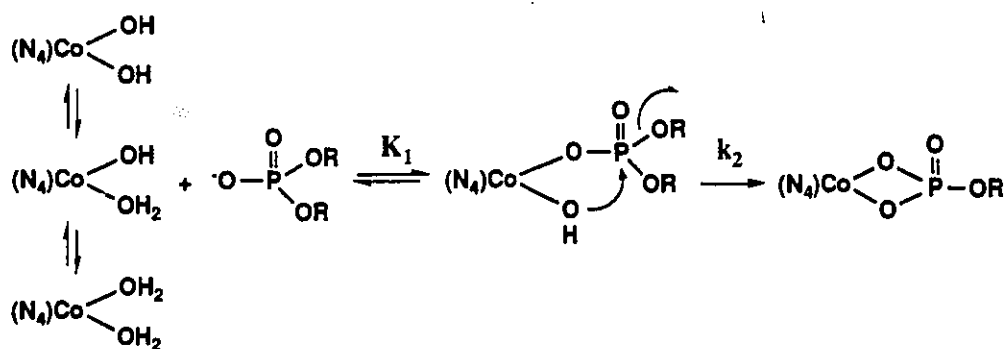
69 Nakazawa, H.; Sakaguchi, U.; Yoneda, H.; Morimoto, Y. *Inorg. Chem.* 1981, 20, 973.

70 Sosa, M. E.; Tobe, M. L. *J. Chem. Soc., Dalton Trans.* 1985, 475.

### 3.2 Co(III) complex promoted Hydrolysis of Phosphate Esters with Good Leaving Groups.

#### 3.2.1 Mechanism

The mechanism for (cyclen)Co(III)(OH)(OH<sub>2</sub>) promoted hydrolysis of BNPP is shown in Scheme I.10. The hydrolysis of the corresponding phosphate monoester(NPP) proceeds faster than that of the diester (BNPP) (Table I.7).



**Scheme I.10** Mechanism for the cyclen complex promoted hydrolysis of BNPP.

The hydrolysis mechanism is elucidated based on previous experimental observations<sup>39,71</sup>: (a) The bell shaped pH rate profile indicates that the aqua-hydroxy form of the complex is the most active species. (b) The mono aqua complex, (NH<sub>3</sub>)<sub>5</sub>Co(III)(OH<sub>2</sub>) does not hydrolyze BNPP. (c) A solvent isotope effect for the cyclen complex promoted hydrolysis of BNPP is not observed. A bifunctional role for the cobalt complex is proposed based on the above observations (a) and (b). If the Lewis acid or metal hydroxide mechanism alone took place, the hydrolysis rate would either decrease or increase with increasing pH. By the same token, the mono aqua cobalt complex would promote the hydrolysis of the diesters efficiently as the cis diaqua cobalt complex. Another possible mechanism, intramolecular general base catalysis, may be ruled out according to the observation (c). Lack of deuterium solvent isotope effects indicates that the metal hydroxide is a nucleophilic catalyst rather than a general base catalyst. In addition, the reactivity of the cobalt complexes was closely related to the ligand structure, especially the angle opposite to the four-membered ring intermediate (section 1.4.2). The efficiency of general base catalysis does not depend on small structural changes.<sup>72</sup> The relative rate enhancement in hydrolyzing BNPP

71 Chin, J.; Zou, X. *J. Am. Chem. Soc.* **1988**, *110*, 223.

72 Kirby, A. J. *Adv. Phys. Org. Chem.* **1980**, *17*, 183.

promoted by several cobalt complexes are listed in Table I.14. The cyclen complex is only 4 times less reactive than the trpn complex in hydrolyzing BNPP.

**Table I.14** second order rate constants ( $M^{-1}sec^{-1}$ ) for the hydrolysis of BNPP promoted by various catalysts at 50 °C (P-O bond cleavage).

catalysts	k ( $M^{-1}sec^{-1}$ )	rel. rate
None <sup>a</sup>	$5.5 \times 10^{-12}$	$2.2 \times 10^{-12}$
NaOH (1M) <sup>a</sup>	$1.6 \times 10^{-4}$	$6.6 \times 10^{-5}$
trien <sup>b</sup>	$5.7 \times 10^{-2}$	$2.3 \times 10^{-2}$
cyclen <sup>c</sup>	$6.6 \times 10^{-1}$	$2.6 \times 10^{-1}$
trpn <sup>d</sup>	2.5	1

a) water rate was divided by water conc. 55.5 M, ref; Kirby, A. J.; Younas, M. *J. Chem.Soc. (B)*, 510 (1970).

b) Zou, X. Ph. D. Thesis, McGill University (1987). c) this study.

d) Chin, J.; Banaszczyk, M.; Jubian, V.; Zou, X. *J. Am. Chem. Soc.* **111**, 186 (1989).

The rate determining step for the hydrolysis of BNPP is either intramolecular metal hydroxide attack on the coordinated BNPP or subsequent P-O bond cleavage. The binding step can not be the rate determining step since the anation rate ( $k_1$ ) is much greater than the actual hydrolysis rate ( $k_2$ ) (Table I.7). The mechanism for both the mcyclen and the tmcyclen complexes promoted hydrolysis of BNPP should be the same as that for the cyclen complex for the following reasons: (a) the structures of the cobalt complexes are closely related, (b) all three cobalt complexes form chelates with acetate and inorganic phosphate, and (c) the same bifunctional mechanism was proposed for both the cyclen and the tmcyclen complexes promoted hydration of acetonitrile (part II). The ligand effects on the reactivity of three cobalt complexes and the hydrolysis mechanism will be discussed in section 3.2.2. Other derivatives such as cmcyclen have been synthesized but their cobalt complexes are less efficient than the mcyclen complex and decompose during the reaction at 50 °C.

The cobalt complex promoted hydrolysis of the phosphate monoester (NPP) is slightly faster than that of the corresponding diester (BNPP) (Table I.7). The proposed mechanism for the hydrolysis of NPP involves a bifunctional activation by the cobalt complex.<sup>71</sup> Sargeson et al. proposed the same mechanism for the hydrolysis of the cobalt

bound phosphate monoester,  $(en)_2Co(III)(OH_2)(NPP)$ , based on the  $^{18}O$  isotope labelling experiments.<sup>45a</sup> The rate enhancement over that of the uncatalyzed hydrolysis is not as great as that of the corresponding diester hydrolysis. For example, the cyclen complex bound BNPP is cleaved  $10^{10}$  times more rapidly than the unbound diester, while the cyclen complex bound NPP is cleaved only  $10^6$  times faster than the free monoester. This may be due to an unfavorable electronic interaction between an anionic nucleophile and the two negative charges of the monoester oxygens. The mechanisms proposed for the rapid hydrolysis of phosphate monoesters as compared to those of diesters<sup>16-17,20-22</sup> are not applicable in the cobalt complex catalyzed hydrolysis of monoesters. In the present study, mechanistic details of the cobalt complex catalyzed hydrolysis of monoesters have not been investigated.

### 3.2.2 Ligand effects on the reactivity

A significant difference towards the hydrolysis of BNPP is observed by placing methyl groups on the macrocyclic nitrogens of cyclen. The mcyclen complex is almost as efficient as the cyclen complex in promoting BNPP hydrolysis, while the tmcyclen complex is 200 times less active than the cyclen complex (Table I.14). It is clear that the reactivity of the Co(III) complexes is highly sensitive to the ligand structure. These complexes are structurally related and have similar  $pK_a$ s for the metal bound water molecules yet hydrolyze BNPP at different rates. The ligand structure can affect the efficiency of the Co(III) catalysts.

**Table I.14** First order rate constants ( $\text{sec}^{-1}$ ) for the cobalt complex promoted hydrolysis of BNPP at 50 °C.<sup>a)</sup>

catalysts	BNPP	NPP <sup>b)</sup>
cyclen	1	1 (3.6)
mcyclen	0.42	0.2 (1.8)
tmcyclen	$3.6 \times 10^{-4}$	$2.8 \times 10^{-5}$ (0.3)

a) [Co] 5 mM, [phosphate]  $2.5 \times 10^{-5}$  mM, and pH 7.

b) values in brackets refer to the ratio of BNPP vs NPP hydrolysis rates.

**The relationship between the ligand structure and a chelate formation** The proposed mechanism for hydrolysis of phosphate diesters involves formation of a four-membered ring intermediate. Tetraamine cobalt complexes with bidentate ligands such as carbonate or acetate are often employed as an analog for this intermediate. There appears to be two major factors involved in chelate formation: (a) the basicity of the bidentate ligand and (b) the tetradentate ligand structure. A good relationship between the basicity of the bidentate ligand and the equilibrium binding constant for the chelate formation was found (section 2.3). Strongly basic ligands such as carbonate form chelates with a wide range of the tetraamine cobalt complexes including the tren complex.<sup>73</sup> As the basicity of the bidentate ligand increases, a higher ratio of the chelate over the monodentate is observed. With a weakly basic bidentate ligand of the same basicity, this chelate formation becomes dependent on the tetraamine ligand structure, especially the angle opposite to the four-membered ring intermediate. It is known that the trpn complex has a larger angle (N-Co-N) opposite to the chelate (O-C-O) than the cyclen complex in its carbonato complex. The ability to form a chelate with acetate or inorganic phosphate gives an indication of the catalyst efficiency in hydrolyzing phosphate and carboxylic esters. For example, the trpn and the cyclen complexes, which are able to form the chelated acetates, hydrolyze methyl acetate, whereas the tren complex neither forms the chelate nor hydrolyzes the same substrate.<sup>34</sup>

**Steric hindrance** The cobalt complexes of cyclen, mcyclen, and tmcyclen form the chelated acetates (Fig. I.13). A similar ratio of monodentate to bidentate acetate suggests that mono- and dimethylation on nitrogen atoms of cyclen do not alter the binding ability of their cobalt complexes to acetate. It also indicates that the three cobalt complexes have a similar opposite angle (N-Co-N) to the four-membered ring (O-C-O) intermediate. The three cobalt complexes also produce the chelated inorganic phosphates (Fig. I.15). The relatively small ratio of the bidentate over the monodentate phosphate with the tmcyclen complex is consistent with the low reactivity in hydrolyzing BNPP. However, a rather significant difference in the reactivity of the tmcyclen complex suggests that there must be another factor other than the angle involved.

Binding studies with phenyl phosphonate provide insight into structure and reactivity relationships. The phenyl group in phenyl phosphonate interacts with the axial methyl groups in the complex upon coordination (Fig. I.21). Both the cyclen and the mcyclen complexes form the chelated phenyl phosphonate, while the tmcyclen complex forms only the monodentate (Fig. I.13). Phenyl phosphonate is a better model compound

73 a) tren CO<sub>3</sub>: Leohlin, J. H.; Fleisher, E. B. *Acta Cryst. B*32, 1976, 3063.

for studying the efficiency of catalysts that hydrolyze diesters. Its structure represents actual phosphate substrates better than inorganic phosphate and it produces a relatively simple spectrum (Fig. I.13). It became clear that the methyl groups in the tmcyclen complex inhibit the formation of a four-membered ring intermediate during hydrolysis of phosphate diesters.

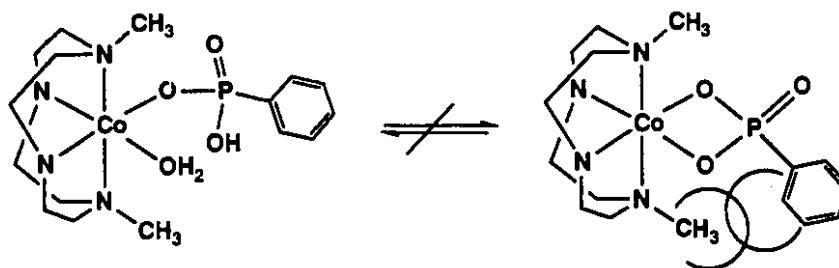


**Figure I.21** Binding of phenyl phosphonate to the tmcyclen cobalt complex.

**Dimerization:** A plot of hydrolysis rate for BNPP promoted by the cobalt complex vs the catalyst concentration (Fig. I.16) gives a linear slope for both the mcyclen and the tmcyclen complexes. In contrast, the rate dependence on that of the cyclen complex levels off at the high catalyst concentration.

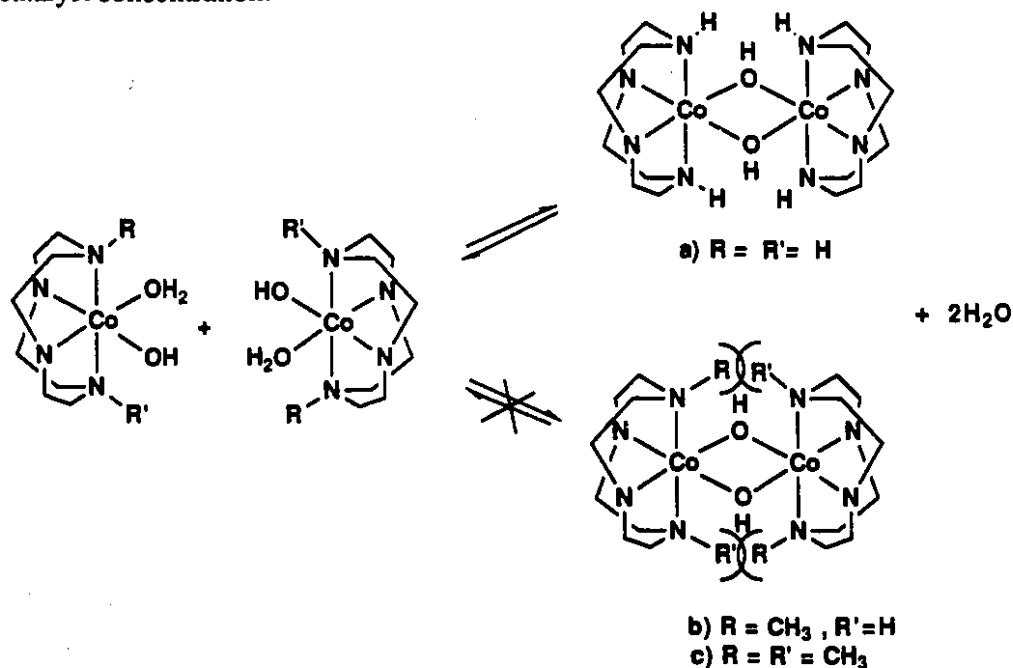


**Figure I.22** Dimerization of the aqua hydroxy cobalt complexes: (a) formation of an inactive hydroxy-bridged dimer with the cyclen complex and (b) and (c) unfavorable dimer formation with the tmcyclen and the mcyclen complexes.

This non-linear plot for the cyclen complex is attributable to the known dimerization reaction for cis diaqua cobalt complexes. The dimer form of the complex is not active since there is no free coordination sites available for the substrate binding to the metal complex. The mcyclen and the tmcyclen complexes do not dimerize because of unfavorable steric interaction brought by the methyl groups (Fig. 1.22).

### 3.3 Cobalt complex-promoted Hydrolysis of Phosphate Diesters with Poor Leaving Groups.

Metal complexes which are efficient at hydrolyzing esters with good leaving groups are not necessarily efficient at hydrolyzing esters with poor leaving groups.<sup>33,74</sup> Having succeeded in finding a stable cobalt complex that gives up to a  $10^{10}$  fold rate enhancement in the hydrolysis of BNPP, we tested it on phosphate diesters with poor leaving groups. Table I.15 shows the reactivity of some phosphate diesters with poor leaving groups at neutral pH.

**Table I.15** First order rate constants ( $\text{sec}^{-1}$ ) for hydrolysis of phosphate esters in water at 50 °C (P-O bond cleavage).

phosphate diester	k ( $\text{sec}^{-1}$ )	t <sub>1/2</sub> (yr)
BNPP <sup>a</sup>	$3.0 \times 10^{-10}$	$1.1 \times 10^2$
c-AMP <sup>b</sup>	$1.0 \times 10^{-14}$	$2.2 \times 10^6$
ApA <sup>c</sup>	$5 \times 10^{-12}$	$4.4 \times 10^3$
$(\text{CH}_3\text{O})_2\text{P}(\text{O})\text{O}^{\text{d}}$	$10^{-19}$	$2.2 \times 10^{11}$

a) Kirby, A. J.; Younas, M. *J. Chem. Soc. (B)*, 510 (1970).

b) estimated from the data reported by Gerlt, J. A., Westheimer, F. H.; Sturtevant, J. M. *J. Biol. Chem.* **250**, 5059 (1975).

c) the rate was estimated from the pH rate profile. ref; Matsumoto, Y.; Komiyama, M. *J. Chem. Soc. Chem. Commun.*, 1050 (1990).

d) extrapolated from the data reported by Kirby et al. see in the text. Guthrie also estimated this rate to be  $10^{-14} \text{sec}^{-1}$  at 25 °C: *J. Am. Chem. Soc.* **99**, 3991 (1977).

### 3.3.1 Hydrolysis of c-AMP

Cyclic nucleotides such as adenosine 3',5'-cyclic monophosphate (c-AMP), are key molecules that function as intramolecular hormones in both bacterial and animal cells.<sup>75</sup> The level of c-AMP in cells is regulated by specific phosphodiesterases which hydrolyze c-AMP to 5'-monophosphate (AMP). c-AMP phosphodiesterase is a metalloenzyme and requires divalent metal ions such as Mg(II) or Mn(II) for its optimal activity.<sup>73b</sup>

(Trien)Co(III)(OH)(OH<sub>2</sub>) was able to hydrolyze c-AMP under mild conditions (50 °C, pD 7).<sup>54</sup> Both the cyclen and the mcyclen complexes have proven to be more efficient than the trien complex in hydrolyzing BNPP.<sup>71</sup> The mcyclen and the cyclen complexes promote the hydrolysis of c-AMP with observed second order rate constants of  $8.5 \times 10^{-2}$  and  $9.6 \times 10^{-2} \text{ M}^{-1} \text{ min}^{-1}$ , respectively at pD 6 and 50 °C.

The mechanism for the hydrolysis of c-AMP promoted by the cobalt complexes should be the same as that for the hydrolysis of BNPP (Scheme I.10 and I.11). The resulting phosphate monoesters, 5'- or 3'-AMP are hydrolyzed more slowly than c-AMP in the presence of the cyclen or the mcyclen complex. c-AMP is hydrolyzed to either 3'- or 5'-AMP with similar enthalpies.<sup>76</sup> The accumulation of the monoesters during the hydrolysis reaction is due to a higher reactivity of the phosphate diester in c-AMP. The alkaline hydrolysis of the phosphate diester bond in c-AMP is known to be  $2 \times 10^4$  times faster than that of dimethyl phosphate.<sup>76a</sup>

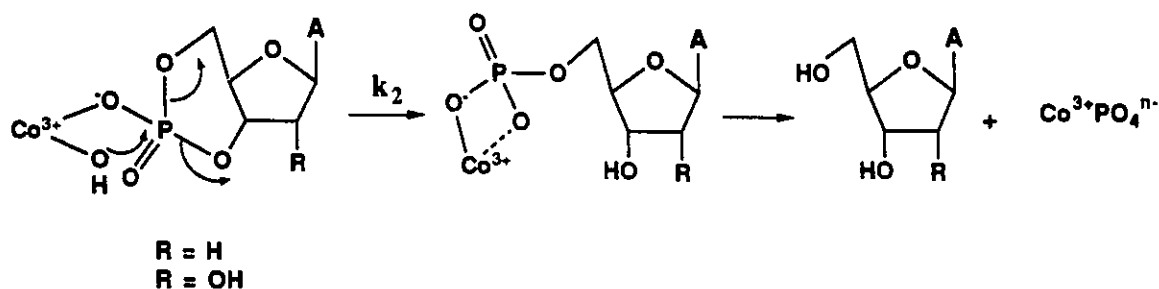
The half-life for the hydrolysis of the cobalt bound c-AMP can be calculated to be ca. 30 min ( $k_2 = 5.3 \times 10^{-4} \text{ sec}^{-1}$ ) from the second order rate constant and the equilibrium constant for binding of phosphate diester (DMP) to the cyclen complex ( $3 \text{ M}^{-1}$ ). The rate constant for the hydrolysis of c-AMP in water had been previously estimated to be  $1.0 \times 10^{-14} \text{ sec}^{-1}$  at 50 °C.<sup>54</sup> At least a  $10^{10}$  fold rate enhancement over the water rate was obtained in the hydrolysis of the cobalt bound c-AMP. However, the catalytic efficiency of these cobalt complexes is somewhat less than that of enzymes. Enzymes hydrolyze c-AMP in seconds. For example, the  $k_{\text{cat}}$  value for 3',5'-c-AMP phosphodiesterase catalyzed hydrolysis of c-AMP is  $4.9 \times 10^{-2} \text{ sec}^{-1}$  at pH 7.7 and 30 °C.<sup>77</sup> Nevertheless, these two cobalt complexes are the most efficient catalysts among metal complexes in hydrolyzing c-AMP. Also, the efficiency of the cyclen and the mcyclen complexes in hydrolyzing BNPP

75 a) Waterman, M.; Murdoch, G. H.; Evans, R. M.; Rosenfield, M. *Science*, **1985**, 229, 267. b) Robinson, G. L.; Butcher, R. W.; Sutherland, E. W. in *Cyclic AMP*; Academic Press: New York and London, 1971. c) ref 3 a.

76 a) Gerlt, J. A.; Westheimer, F. H.; Sturtevant, J. M. *J. Biol. Chem.* **1975**, 250, 5059. and references therein. b) Yu, J. H.; Sopchik, A. E.; Arif, A. M.; Bentrude, W. G. *J. Org. Chem.* **1990**, 55, 3444.

77 Nair, K. G. *Biochemistry* **1966**, 5, 150.

is maintained in hydrolyzing c-AMP, which is  $10^4$  times less reactive than BNPP under basic conditions.



**Scheme I.11** The cyclen and the mcyclen complexes promoted hydrolysis of (2'-deoxy-) c-AMP: only 5'-AMP production is shown.

The rate constant for the hydrolysis of 2'-deoxy c-AMP has not yet been reported but it should be less than that for the hydrolysis of c-AMP. Although the hydroxyl group does not participate directly in the hydrolysis of c-AMP, it can serve to enhance the reactivity of the adjacent 3'-hydroxyl group.<sup>78a</sup> The maximum inductive effect due to a 2'-hydroxyl group can not account for more than a 100 fold reactivity difference.<sup>78</sup> Interestingly, the mcyclen complex hydrolyzes 2'-deoxy c-AMP slightly more rapidly than the cyclen complex. This reverse reactivity is probably due to less dimer formation for the mcyclen complex.

### 3.3.2 Hydrolysis of UpU and ApA

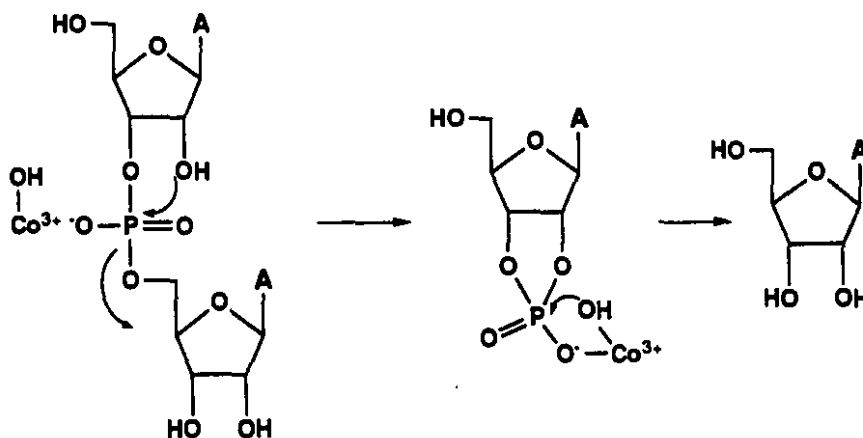
Ribonucleotides are much more vulnerable towards hydrolysis than deoxyribonucleotides. The higher reactivity of ribonucleotides is due to intramolecular nucleophilic attack by the 2'-hydroxyl group,<sup>79</sup> which is absent in the hydrolysis of deoxyribonucleotides. Although the subsequent hydrolysis of the resulting five-membered cyclic phosphate is rapid (the hydrolysis of ethylene phosphate is  $10^8$  times faster than that of dimethyl phosphate under basic conditions<sup>28c</sup>), the initial cyclization step is usually much faster than the subsequent hydrolysis, so the intermediate may be readily isolated.

It has been reported that the trien complex hydrolyzes ApA with a  $10^5$  fold rate

78 a) Haines, A. H. *Adv. Carbohydrate Chem. Biochem.* **1986**, 25, 4473. b) Deslongchamp, P. in *Stereoelectronic effects in Organic Chemistry*, 1st Ed.; Pergamon Press: Oxford, New York, 1983.

79 Breslow, R.; Huang, D. L. *Proc. Natn. Acad. Sci. U.S.A.* **1991**, 88, 4080.

enhancement over the hydroxide rate at pH 6.<sup>80</sup> The mcyclen complex is 10 times more active than the trien complex under the same conditions. Several mechanisms including a bifunctional mechanism are possible. Unlike in the cobalt complex promoted hydrolysis of BNPP, the cobalt complex most likely hydrolyzes ApA only by a Lewis acid mechanism (Scheme I.12). The cobalt bound hydroxide could act as a general base catalyst pulling off the proton from the 2'-hydroxyl group. This is unlikely since the effective molarity for the intramolecular general base catalysis (maximum 80 M) is low compared to that for intramolecular nucleophilic catalysis (maximum  $10^8$  M).<sup>72</sup> Lewis acid activation of phosphate diesters by metal ions has been proposed for the role of Mg(II) in the Hammerhead RNA self-cleavage reaction.<sup>81</sup> It has been shown that the substitution of sulfur for a nonbridging oxygen atom substantially reduces the affinity of a Mg(II) ion necessary for the efficient cleavage.<sup>81</sup> This suggests that the Mg(II) ion coordinates directly to the phosphate at the cleavage site. Based on this mechanism, it is not surprising that cis diaqua cobalt complexes such as trien and cyclen show almost the same reactivity in hydrolyzing ApA.



**Scheme I.12** The Co(III) complex promoted hydrolysis of ApA: a Lewis acid activation by the cobalt complex and intramolecular nucleophilic attack by the 2'-hydroxyl group.

<sup>80</sup> Matsumoto, Y.; Komiyama, M. *J. Chem. Soc., Chem. Commun.* 1990, 1050.

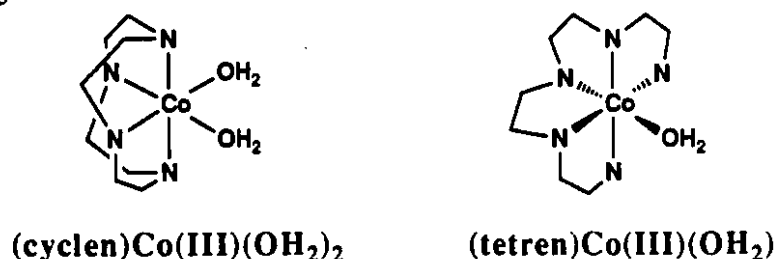
<sup>81</sup> Dahm, S. C.; Uhlenbeck, O. C. *Biochemistry* 1991, 30, 9464.

### 3.3.3 Hydrolysis of DMP

The half-life for the cleavage of dimethyl phosphate is estimated to be a billion years (Table I.15) and the reactivity of DNA is somewhat greater than that of DMP, so that hydrolysis of DNA or DMP<sup>53,82</sup> in the absence of enzymes has never been detected at neutral pH. With knowledge that the two cobalt complexes of cyclen and mtcyclen are the most stable and efficient for hydrolyzing c-AMP, we tested the catalysts for the hydrolysis of d(ApA) and DMP.

The cyclen complex is able to hydrolyze DMP producing 2 equivalents of methanol. Methyl phosphate does not accumulate to an observable extent during the hydrolysis. It is well known that cis diaqua cobalt complexes efficiently hydrolyze phosphate monoesters.<sup>46,53a</sup> The mtcyclen complex appears to be unstable under the experimental conditions used (60 to 80 °C). The second order rate constant for the cyclen complex-promoted hydrolysis of dimethyl phosphate is  $3.7 \times 10^{-5} \text{ M}^{-1} \text{ min}^{-1}$  at pD 6.3 and 60 °C. Since the equilibrium constant for complexation of DMP to the cyclen complex is  $3 \text{ M}^{-1}$ , the first order rate constant for the hydrolysis of the cobalt bound DMP is  $1.2 \times 10^{-5} \text{ min}^{-1}$ . The rate constant obtained under these experimental conditions should be comparable to that at pD 7 since the cyclen complex promoted hydrolysis of BNPP gives a bell shaped pH-rate profile with the maximum rate at pH 6.8.<sup>39a</sup> In contrast, the monoqua cobalt complex, (tren)Co(III)(OH) did not hydrolyze DMP to any observable extent.

Figure I. 23



The proposed mechanism for the cyclen complex promoted hydrolysis of DMP involves coordination of the diester to the metal complex followed by intramolecular metal hydroxide attack (Fig. I.24 a). Such a mechanism has been proposed for the hydrolysis of esters, nitriles, phosphate mono- and diesters.<sup>38a</sup> Three experimental observations that are consistent with the mechanism are: (a) DMP coordinates to the cyclen complex as a monodentate ligand and not as a bidentate ligand (Fig. I.15). (b) The monoqua complex,

82 Gerlt, J. A.; Westheimer, F. H. *J. Am. Chem. Soc.* 1973, 95, 8166.

(tetren)Co(III)(OH<sub>2</sub>) is not reactive at hydrolyzing DMP even though the equilibrium binding constant for DMP is comparable to that of the cyclen complex. (c) There is no solvent isotope effect for the cyclen promoted hydrolysis of bis(p-nitrophenyl) phosphate (BNPP). Based on the above observations, several mechanisms may be ruled out. Oxidative cleavage<sup>5</sup> of dimethyl phosphate can be ruled out on the basis that two equivalents of methanol are produced upon cleavage of the diester. A double Lewis acid mechanism (Fig. I.24 b) is unlikely since the diester coordinates to the cyclen complex as a monodentate ligand. Lack of any deuterium solvent isotope effect suggests that the metal hydroxide is not a general base catalyst (Fig. I.24 c).

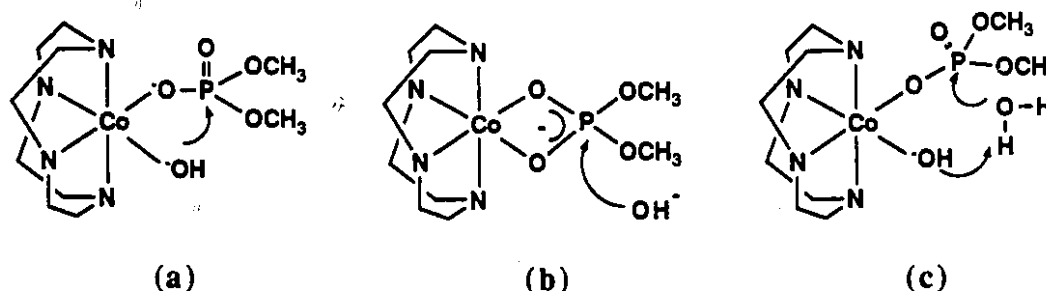


**Figure I.24** Three possible mechanisms for the cyclen complex promoted hydrolysis of dimethyl phosphate (P-O bond cleavage).

Uncatalyzed hydrolysis of activated esters occurs through P-O bond cleavage,<sup>24</sup> while the hydrolysis of DMP results in both P-O and C-O bond cleavage. Westheimer et al. have shown that the hydroxide catalyzed hydrolysis of DMP occurs exclusively through C-O bond cleavage.<sup>28c</sup> The reactivity of DMP has been studied in the form of complete pH-rate profiles by Guthrie.<sup>83</sup> However, due to the lack of experimental data, it was not clear whether the hydrolysis of dimethyl phosphate in neutral water proceeds with P-O bond cleavage or C-O bond cleavage.<sup>28c</sup> It has been proposed that a bifunctional mechanism is the most efficient in hydrolyzing activated phosphate diesters through P-O bond cleavage.<sup>38a</sup> It would be interesting to know if these metal complexes also accelerate C-O bond cleavage. Figure I.25 shows possible mechanisms for C-O bond cleavage similar to those proposed for P-O bond cleavage (Fig. I.24).

<sup>83</sup> Guthrie, J. P. *J. Am. Chem. Soc.* 1977, 99, 3991.



used (pH 6, 80 °C), the hydrolysis of the glycosidic bond occurs much faster than that of the phosphate diester bond of 2'-deoxy adenosine and d(ApA).\*\*

**Estimation of the water rate for the hydrolysis of DMP:** The hydrolysis rate for dimethyl phosphate (P-O bond cleavage) in neutral pH has never been measured because of its stability. However it can be estimated as follows: A good linear free energy relationship between the hydroxide catalyzed rate constant for phosphate diester hydrolysis at 25 °C and the pK<sub>a</sub> of the conjugate acid of the leaving group was found.<sup>39a</sup> Both alkyl and aryl phosphate diesters were shown to fit on the same plot with equation 3.1.

$$\log k = 0.69 - 0.76 \text{ pK}_a \quad (\text{eq 3.1})$$

Similarly Kirby and Younas<sup>24</sup> has been that there is a linear free energy relationship between the water rate for diaryl phosphate hydrolysis at 100 °C and the pK<sub>a</sub> of the conjugate acid of the leaving group (eq 3.2).

$$\log k = 1.57 - 0.97 \text{ pK}_a \quad (\text{eq 3.2})$$

According to the <sup>18</sup>O tracer experiments, hydrolysis involves P-O bond cleavage in the acidic to neutral pH range. The calculated rate constant for the P-O bond cleavage in DMP is then  $3.4 \times 10^{-14} \text{ sec}^{-1}$  (pK<sub>a</sub> of methanol 15.5) at 100 °C.

The water rate for DMP had been previously estimated to be  $2 \times 10^{-14} \text{ sec}^{-1}$  at 25 °C<sup>83</sup> and  $5 \times 10^{-14} \text{ sec}^{-1}$  at 50 °C.<sup>86</sup> Guthrie's estimate<sup>83</sup> was based on the rate of DMP hydrolysis at 100 °C between pH 1 and 5, where the water rate is insignificant. Cech and Herschlag<sup>86</sup> estimated the water rate for DMP hydrolysis based on the hydroxide rate for DMP hydrolysis and β<sub>nuc</sub> for 2,4-dinitrophenyl methyl phosphate.<sup>24,87</sup> According to the reactivity-selectivity principle, β<sub>nuc</sub> for DMP hydrolysis is expected to be greater than that for 2,4-dinitrophenyl methyl phosphate. Indeed, the ratio of the water rate to the hydroxide rate for the hydrolysis of BDNPP is much greater than that for the hydrolysis of DMP.<sup>88</sup> Therefore, Cech and Herschlag's estimate should be an upper limit.

\*\* preliminary experimental results: the production of adenine and 2'-deoxy adenosine from 2'-deoxy adenosine and d(ApA) respectively was monitored by HPLC (see experimental).

86 Herschlag, D.; Cech, T. R. *Nature*, 1990, 344, 405.

87 Kirby, A. J.; Younas, M. J. *Chem. Soc. B*, 1970, 1165.

88 water rates were estimated from ref 24 and the hydroxide rate for BDNPP and DMP from ref.25 and 84 respectively.

Kirby et al.<sup>24</sup> showed that the activation entropy for the solvent catalyzed hydrolysis of bis-2,4-dinitrophenyl phosphate (BDNPP) is - 25.5 eu. Assuming the activation entropy for the hydrolysis of DMP is the same as that for the hydrolysis of BDNPP, the activation enthalpy for DMP hydrolysis is 35.5 kcal / mole. The water rate for DMP hydrolysis calculated from the activation parameters is  $1.5 \times 10^{-19} \text{ sec}^{-1}$  and  $9.5 \times 10^{-17} \text{ sec}^{-1}$  at 25 °C and 60 °C, respectively. The rate of hydrolysis of dimethyl phosphate bound to the cyclen complex is some  $10^{10}$  times greater than the water rate for free DMP hydrolysis.

**Comparison to Ribozymes:** The ability of RNA to act as a biological catalyst has become well established in the last few years.<sup>89</sup> The examples of such ribozymes fall into two categories.<sup>90</sup> Self-splicing and self-cleaving RNAs exemplify intramolecular catalysis. In addition, RNA also acts as a catalyst on other molecules, cutting and joining them without itself being changed in the process. An intriguing feature of the self splicing RNA from *Tetrahymena thermophila* is that the 2'-hydroxyl group is not directly involved in the hydrolysis reaction.<sup>86</sup>

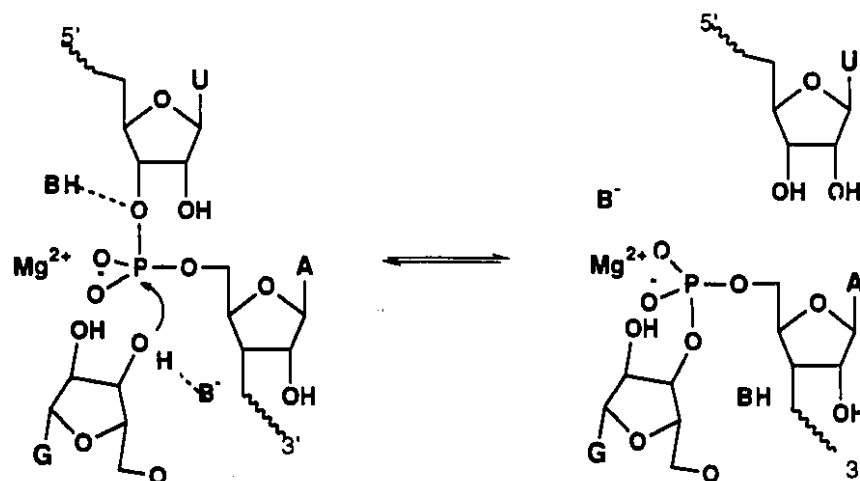


**Figure I.26** Model for the initial step of pre-rRNA self splicing involving nucleophilic attack by the 3'-hydroxyl group of guanosine on the phosphorus atom at the 5' splice site.

The 3'-hydroxyl group of G414, the terminal guanosine of the IVS RNA, or that of a free guanosine added to the 5' end of the downstream RNA fragment during cleavage is the

89 a) Cech, T. R.; Zaug, A. J.; Grabowski, P. J. *Cell*, 1981, 27, 487. b) Bass, B. L.; Cech, T. R. *Nature* 1984, 308, 820. c) Cech, T. R. *Angew. Chem. Int. Ed. Engl.* 1990, 29, 759 and references there in.

90. Cech, T. R. *Science* 1987, 236, 1532.

acting nucleophile for the ribozyme catalyzed reactions.<sup>91</sup> These reactions proceed through several consecutive transesterification reactions in the presence of Mg(II). The initial step of pre-rRNA self-splicing involves nucleophilic attack by the 3'-hydroxyl group of guanosine on the phosphorus atom at the 5' splice site. Figure I.26 shows the proposed mechanism for this transesterification reaction.<sup>90</sup> Coordination of Mg<sup>2+</sup> to the phosphate would enhance the electrophilicity of phosphorus atom and could stabilize the trigonal bipyramidal transition state. However, the hypotheses of acid (BH) and base (B<sup>-</sup>) catalysis and coordination of Mg ion to the phosphate are untested. In addition to its interaction with the phosphate, it was also suggested that the metal ion could activate the 3'-hydroxyl as a nucleophile by enabling the oxyanion to exist at a pH far below pH 12.5, the normal pK<sub>a</sub> of the hydroxyl group.<sup>90</sup>

Recently Cech and Herschlag<sup>86</sup> showed that DNA bound to an RNA enzyme derived from the self-splicing intervening sequence of *Tetrahymena thermophila* is hydrolyzed sequence specifically with a half-life of about 0.05 days at 50 °C. Dimethyl phosphate bound to (cyclen)Co(III)(OH)<sub>2</sub> is hydrolyzed with a half-life of 40 days at 60 °C.

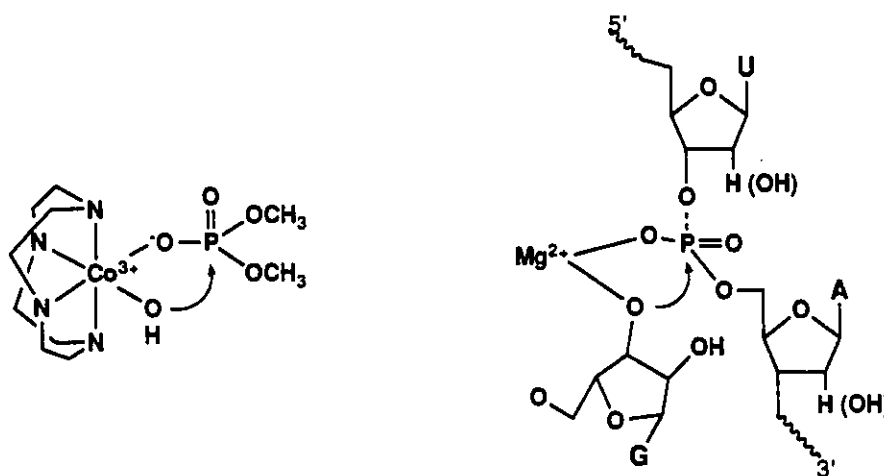


**Figure I.27** Alternative mechanism for the role of Mg(II) ion in the hydrolysis of DNA or RNA by the 3' hydroxyl group of guanosine similar to the bifunctional role of the cyclen complex for hydrolyzing dimethyl phosphate.

Based on a linear free energy relationship (eq 3.2), the water rate for DNA hydrolysis should be somewhat greater ( $>10^2$ ) than that for dimethyl phosphate hydrolysis since the hydroxyl group in methanol (pK<sub>a</sub> of 15.5) is less acidic than the 3'- or 5'-hydroxyl groups

<sup>91</sup> Zaug, A. J.; Been, M. D.; Cech, T. R. *Science* 1986, 324, 429.

of nucleosides ( $pK_a$  of ca. 12.4).<sup>92</sup> The mechanistic role of  $Mg^{2+}$  in ribozymes for catalyzing transesterification of DNA molecules may be related to the mechanistic role of the cyclen complex for hydrolyzing dimethyl phosphate (Fig. 1.27). The metal ion activates the phosphate as well as the 3'-hydroxyl group of guanosine at the same time in the bifunctional mechanism. Although the reactivity of the cyclen complex is somewhat less than that of natural enzymes,<sup>82</sup> it is remarkable that a simple metal complex like the cyclen complex has comparable reactivity as a ribozyme for hydrolyzing unactivated phosphate diesters such as dimethyl phosphate. This is the first example of the cleavage of unactivated phosphate diesters at neutral pH.

---

<sup>92</sup> Saenger, W. in *Principles of Nucleic Acid Structure*; Springer-Verlag: New York, Berlin, Heidelberg, and Tokyo, 1984, p108.

**PART II    HYDRATION OF NITRILES CATALYZED BY COBALT(III)  
COMPLEXES**

## 1 INTRODUCTION

There are many examples of metal ion promoted or catalyzed hydrolysis reactions of phosphate esters, carboxylic esters, and amides.<sup>1</sup> In comparison to hydrolysis of amides, nitrile hydration has received less attention since nitriles are not as biologically interesting as amides and also nitriles are more resistant towards hydrolysis than the corresponding amides. For example, the hydroxide catalyzed hydrolysis rate of acetonitrile<sup>2</sup> and acetamide<sup>3</sup> are  $1.6 \times 10^{-6} \text{ M}^{-1} \text{ sec}^{-1}$  and  $7.4 \times 10^{-5} \text{ M}^{-1} \text{ sec}^{-1}$ , respectively.

Acrylamide polymers are major industrial chemicals used in paper and surfactant production, wastewater treatment, and oil recovery.<sup>4</sup> Carboxamides including acrylamide are generally prepared by hydration of the corresponding nitriles with strong acid or base catalysts.<sup>5</sup> These reactions are slow and appreciable hydrolysis of the product carboxamide to the carboxylic acid as well as hydrolysis of other functional groups present occurs faster than nitrile hydration.<sup>5</sup> Difficulties<sup>4</sup> involved in the conventional sulfuric acid promoted hydration of acrylonitrile have led to an intensive research effort to develop catalysts for regioselective hydration of nitriles to amides.<sup>4,5,7</sup>

Although numerous catalysts have been developed involving metal ions or complexes for hydration of nitriles, the catalytic mechanisms are not fully understood. In order to design a simple but more efficient catalyst for hydration of nitriles, it is important to study the mechanistic details involved in the reaction.

### 1.1 Mechanism of Nitrile Hydration

Hydrolysis of nitriles proceeds through amides to yield the corresponding carboxylic acids and amines under both basic and acidic conditions. The mechanism of base catalyzed nitrile hydration<sup>5</sup> is shown in Scheme II.1(a). The initial hydration of

1 a) Bruice, T. C.; Benkovic, S. J. in *Bioorganic Mechanisms*; Benjamin: New York, 1966, Vol. 1 and Vol. 2. b) Hay, R. W.; Morris, P. J. *Metal Ions Biol. Systems* 1976, 5, 173.

2 Buckingham, D. A.; Keene, F. R. Sargeson, A. M. *J. Am. Chem. Soc.* 1973, 95, 5649.

3 Yamana, T.; Mizukami, Y.; Tsuji, A.; Yasuda, Y.; Masuda, K. *Chem. Pharm. Bull.* 1972, 20, 881.

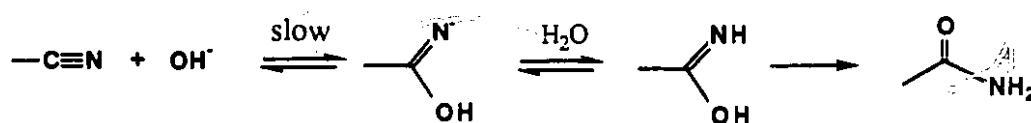
4 Matsuda, F. *Chemtech.* 1977, 7, 306 and ref therein.

5 a) Compagnon, P. L.; Miocque, M. *Ann. Chim.* 1970, 5, 11. b) Schaefer, F. G. in *The Chemistry of the Cyano Group*, Rappoport, Z. Ed.; Interscience: London, New York, 1970. p. 256.

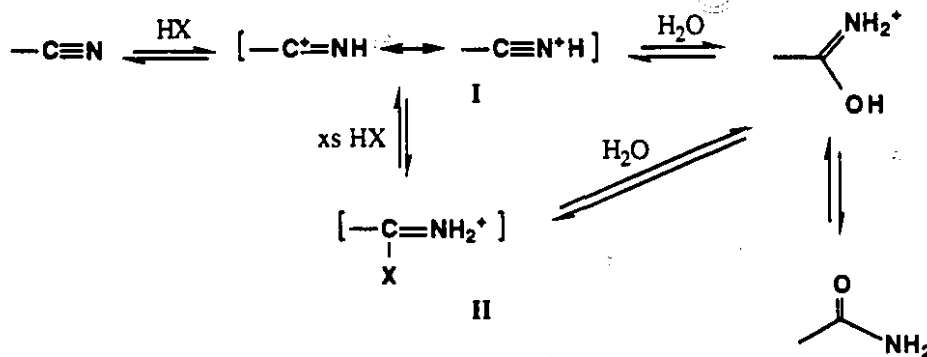
6 a) Wainwright, M. S.; Onuoha, N.I.; *Chem. Eng. Commun.* 1984, 29, 1. b) Nozaki, F.; Sodesawa, T.; Yamamoto, T. *J. Catal.* 1983, 84, 267. c) Villain, G.; Klack, P.; Gaset, A. *Tetrahedron Lett.* 1980, 21, 2901. d) Villain, G.; Gaset, A.; Klack, P. *J. Mol. Catal.* 1981, 12, 103.

7 Jensen, C. M.; Trogler, W. C. *J. Am. Chem. Soc.* 1986, 108, 723 and references therein.

nitriles is, in general, slower than hydrolysis of the corresponding amides. For example, propionitrile is about 10 times less reactive than propionamide under basic conditions.<sup>8</sup> In some cases, hydrolysis of nitriles is faster than that of the corresponding amides. The reverse reactivity is often observed with nitriles and the corresponding amides with electronegative substituents.<sup>9</sup> The rate of nitrile hydration is more dependent on the substituent than it is for amide hydrolysis, as Hammett  $\rho$  values of 2.31 and 1.06 suggested for base catalyzed hydration of benzonitrile and for the hydrolysis of benzamide, respectively.<sup>9</sup> For example, the hydration of 2-cyano-1,10-phenanthroline is 15 times as fast as the hydrolysis of 2-carboxamido-1,10-phenanthroline under basic conditions.<sup>10</sup>



(a) base catalyzed hydration of nitriles.



(b) acid catalyzed hydration of nitriles

**Scheme II.1** Hydrolysis of nitriles under basic and acidic conditions.

The mechanism of acid catalyzed hydration of nitriles<sup>5</sup> is shown in Scheme II.1(b). Under acidic conditions, the rate of nitrile hydration substantially exceeds the rate of subsequent hydrolysis of the product amide. In concentrated hydrogen halide solution, the nitrile is, to

8 Winkler, C. A.; Rabinovitch, B. S. *Can. J. Chem.* 1942, 19, 20(B),185.

9 Hammett, L. P. in *Physical Organic Chemistry*, 1st Ed.; McGraw Hill: New York, 1940.

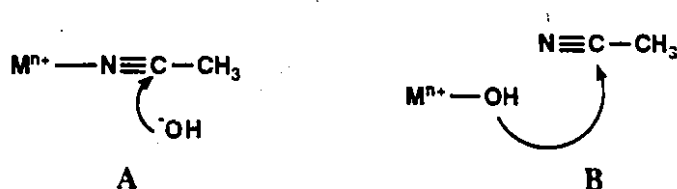
10 Breslow, R.; Fairweather, R.; Keana, J. *J. Am. Chem. Soc.* 1967, 89, 2135.

some extent, converted to the protonated imidyl halide, II, which is more electrophilic than I (Scheme II.1 (b)).

## 1.2 Metal Assisted Hydration of Nitriles

### 1.2.1 Previous work

There are two routes of activation that a metal can provide in hydrolysis reactions.



First, metal ion can act as a Lewis acid (A). Simple nitriles directly coordinated to Co(III)<sup>2</sup>, Rh(III)<sup>11</sup>, Ru(III)<sup>12</sup> and Ir(III)<sup>11</sup> complexes can be easily hydrated to their corresponding amido complexes at ambient temperature (Fig. II.1). Metal polarized substrates are more susceptible to nucleophilic attack. Acetonitrile coordinated to pentaammine cobalt(III)<sup>2</sup> and ruthenium(III)<sup>12</sup> is hydrolyzed 10<sup>6</sup> and 10<sup>8</sup> fold faster than the free nitrile, respectively.

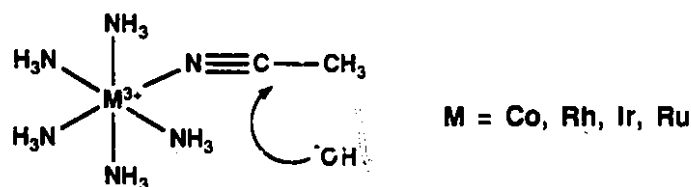


**Figure II.1** Hydration of the coordinated acetonitrile: Lewis acid activation by metal ion.

Second, greater rate enhancement can be obtained for hydrolysis at neutral pH when a metal hydroxide rather than free hydroxide is involved. Although metal hydroxide is not as good a nucleophile as hydroxide itself, it is a much better nucleophile than water.<sup>13,14</sup> The ability of metal ions to enhance deprotonation of water would ensure that at neutral pH metal hydroxide concentration is much higher than that of free hydroxide (10<sup>-7</sup> M). Numerous studies indicate that the metal hydroxide almost retains a nucleophilicity of free

11 Curtis, N. J.; Sargeson, A. M. *J. Am. Chem. Soc.* 1984, 106, 625.

12 Zanella, A. W.; Ford, P. C. *J. Chem. Soc., Chem. Commun.* 1974, 795.

13 Martin, R. B. *J. Inorg. Nucl. Chem.* 1975, 38, 511.

14 Woolley, P. J. *Chem. Soc., Faraday Trans. 2*, 1977, 318.

hydroxide, despite a  $10^{-7}$  fold lowering of Brønsted basicity.<sup>15,16</sup> The increased concentration of metal hydroxide more than offsets the lower nucleophilicity of metal hydroxide relative to hydroxide. A rather smooth relationship between  $k_{\text{MOH}}$  and  $\text{p}K_{\text{a}}$  of the aqua complex holds for a wide range of reactions. The slopes (Brønsted coefficient) for hydration reactions of different hydroxide-containing nucleophiles with  $\text{CO}_2$  and acetaldehyde were found to be 0.18 and 0.4, respectively.<sup>14,17</sup>

$\text{Cu(II)}$ ,  $\text{Ni(II)}$  and  $\text{Zn(II)}$  have all been shown to catalyze hydration of nitriles when the nitrile is covalently linked to metal coordinating functionalities.<sup>10,18</sup> Hence, 2-cyanopyridine<sup>18a</sup> and 2-cyano-1,10-phenanthroline<sup>10</sup> are rapidly hydrated to their corresponding amides under mild conditions. Cyanomethyl substituted tetraaza-cyclotetradecane is hydrolyzed in the presence of  $\text{Cu(II)}$  or  $\text{Ni(II)}$ .<sup>18b</sup> Hydration of nitriles catalyzed by metal(II) hydroxide shows a  $10^7$  to  $10^9$  fold rate enhancement over the hydroxide rate as well as no further hydrolysis to their corresponding carboxylic acids. Intramolecular attack by the coordinated hydroxide on the pendant non-coordinating nitrile in *cis*-[(en)<sub>2</sub>Co(III)(OH)NH<sub>2</sub>CH<sub>2</sub>CN-Hg(II)] showed a  $10^{12}$  fold rate enhancement as compared with the uncoordinated case at pH 7.<sup>19</sup> It is well known that an intramolecular reaction can show large rate enhancements over that for an intermolecular process due to the gain in translational entropy.<sup>20</sup>

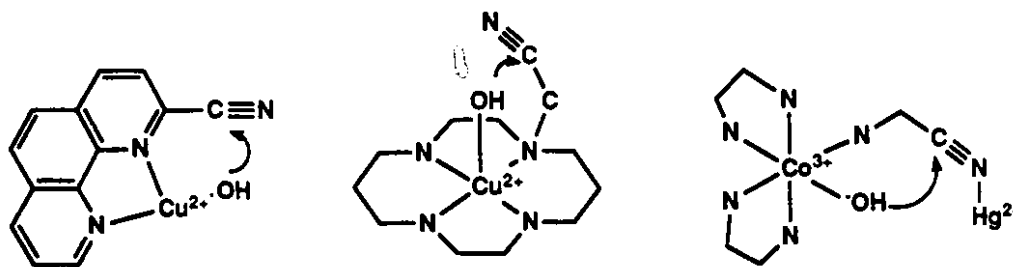


**Figure II.2** Hydration of nitriles: metal hydroxide mechanism.

The two mechanisms described above suggest that if both mechanisms are combined, the rate enhancement would be greater than if each mechanism were operating

15 Buckingham, D. A. in *Biological Aspects of Inorganic Chemistry*; Addison, A. W.; Cullen, W R.; Dolphin, D.; James, B. R. Eds.; Wiley : New York, 1976, p141.

16 a) Chin, J.; Zou, X. *J. Am. Chem. Soc.* **1984**, 106,3687. b) Suh, J.; Han, H. *Bioorg. Chem.* **1984**, 12, 177.

17 Chatte, E.; Dasgupta, T. P.; Harris, G. M. *J. Am. Chem. Soc.* **1973**, 95, 4169.

18 a) Barnard, P. F. *J. Chem. Soc. (A)*, **1969**, 2140. b) Schibler, W.; Kaden, T. A. *J. Chem. Soc., Chem. Commun.* **1981**, 603.

19 Buckingham, D. A.; Morris, P. Sargeson, A. M.; Zanella, A. *J. Am. Chem. Soc.* **1977**, 99, 1910.

20 Jencks, W. P. in *Adv. Enzymol. Relat. Areas Mol. Biol.* **1975**, 43, 219.

alone. This double activation by metal ion has been tested by Sargeson et al. in a binuclear dicobalt complex.<sup>21</sup>

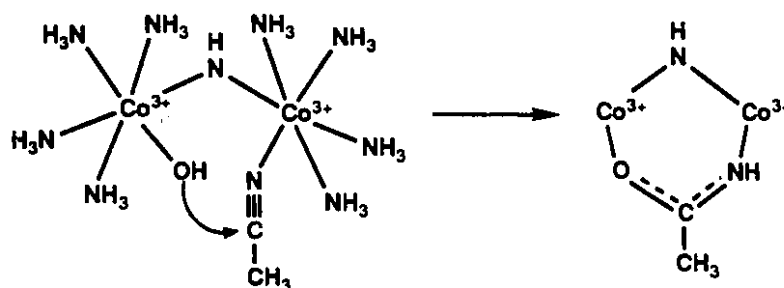
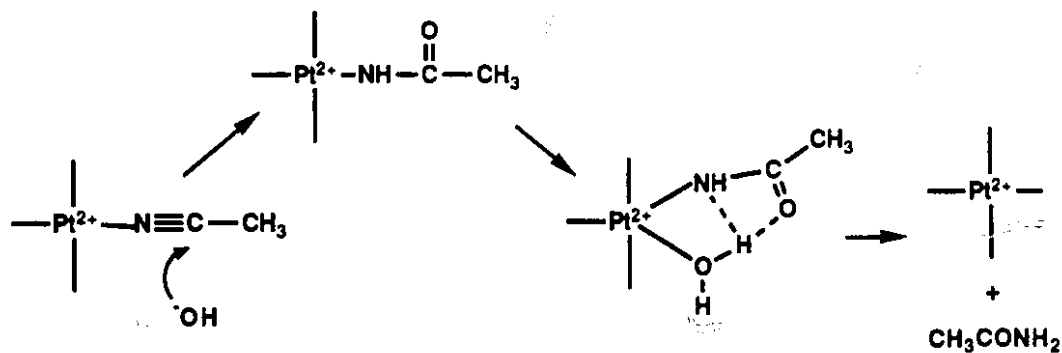


**Figure II.3** Intramolecular hydration of coordinated acetonitrile in the binuclear  $\mu$ -amido-octaammine dicobalt(III) complex.

Intramolecular attack of the cobalt bound water at acetonitrile directly coordinated to the other cobalt yields a stable  $\mu$ -amido-cobalt complex under acidic conditions ( $\text{pH} < 2$ ). A rate enhancement extrapolated to  $\text{pH} 7$  is more than  $10^{15}$  fold over that for the uncoordinated substrate, yet competing dimerization of the catalyst would predominate at neutral  $\text{pH}$ .

Despite large increases in the rate of nitrile hydration, no catalytic turnover was observed with substitutionally inert  $\text{Co(III)}$ ,  $\text{Rh(III)}$ ,  $\text{Ru(III)}$  and  $\text{Ir(III)}$  complexes due to the formation of a thermodynamically stable amido metal complex. Trogler et al. have shown that  $\text{Pt(II)}$  complexes can catalyze the hydration of simple nitriles such as acetonitrile and acrylonitrile under basic reflux conditions.<sup>7</sup>



**Scheme II.2**

Catalytic hydration of acetonitrile catalyzed by  $\text{Pt(II)H(H}_2\text{O)(phosphine)}_2$

The proposed catalytic mechanism involves external hydroxide attack followed by proton transfer from solvating water to the coordinated N-carboxamido group to give the hydration product (Scheme II.2). The Pt complexes are efficient catalysts for hydration of saturated nitriles, but they are not selective catalysts for the hydration of acrylonitrile. Coordination of the C-C double bond to the metal complex makes hydration of the double bond feasible resulting in several side products.<sup>7</sup>

There are three aspects to consider in developing a perfect catalyst: reactivity, selectivity, and catalytic turnover. The metal catalysts described above are far from perfect in these respects.

### 1.2.2 Hydration of nitriles vs hydrolysis of amides

In the sodium hydroxide solution, the rate of hydration of 2-cyano-1,10-phenanthroline is only 15 times faster than that of the corresponding amide to carboxylates.<sup>10</sup> However, the Ni(II) promoted hydration of the same nitrile is accelerated by a factor of  $10^5$  over the hydrolysis of the corresponding amide.<sup>10</sup> The rates of alkaline hydrolysis of the pentaammine cobalt (III) complexes of acetonitrile<sup>2</sup> and DMF<sup>22</sup> are  $10^6$  and  $10^4$  fold greater than those of the uncoordinated cases respectively. The hydroxide catalyzed hydrolysis reaction of acetonitrile is  $10^2$  times slower than that of DMF. The reverse reactivities of amide and nitrile hydration in the presence of a metal complex over the uncatalyzed reaction may be due to a different hydrolysis mechanism or different binding properties of the substrates to the metal. Coordination modes of nitriles and amides will be described in this section, and the hydrolysis mechanism of amides and its comparison with that of nitriles will be discussed in part III.

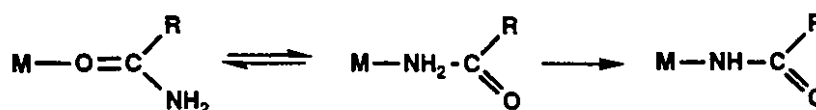
Nitrile binding occurs through the nitrogen with most trivalent metals except low valent transition metal ions such as Pt(II) and Cu(I), where the metal binds through the CN triple bond.<sup>23</sup> Coordination to the metal through the nitrile nitrogen increases the polarity of the CN bond making it more susceptible to nucleophilic attack. Trivalent metal ions are stronger Lewis acids than divalent metal ions.

Amides are potential ambidentate ligands for metal ions. Both N- and O-bonded linkage isomers of the pentaammine Co(III) and Cr(III) complexes of formamide and

22 Buckingham, D. A.; Harrowford, J. M.; Sargeson, A. M. *J. Am. Chem. Soc.* 1974, 96, 1726.

23 Cotton, F. A.; Wilkinson, G. in *Advanced Inorganic Chemistry*; 5th Ed.; John Wiley & Sons: New York, 1988.

acetamide are known.<sup>24,25</sup> It was demonstrated that an O-bonded isomer is formed initially under mild conditions (kinetic control) and subsequently rearranges with release of a proton to the N-bonded isomer.<sup>26</sup>



Coordination of amides to the metal ion occurs through amide oxygen since the basicity of the carbonyl oxygen in free amide is greater than that of the free amide nitrogen ( $\text{pK}_a$ , -1 vs -8).<sup>27</sup> Addition of a positive charge to amide oxygen polarizes the carbonyl bond which makes the carbonyl carbon more susceptible to nucleophilic attack. Although metal binding through nitrogen of neutral amides is much weaker than through oxygen, substitution of N bound hydrogen by a metal ion would create a stronger bond. It has been shown that the  $\text{pK}_a$  of an amide NH is lowered by 11 to 12 units upon coordination to trivalent metals such as Ru, Co, Rh, and Ir.<sup>2,24,28</sup> With divalent metals such as Cu, Zn, and Ni, this effect is somewhat reduced to 3 to 7  $\text{pK}_a$  units.<sup>23</sup> This  $\text{pK}_a$  lowering effect plays an important role in metal mediated hydrolysis of amides since it is known that coordination of amide nitrogen to metal ions actually inhibits amide hydrolysis. These aspects will be further discussed in part III.

24 Balahura, R. J.; Jordan, R. B. *J. Am. Chem. Soc.* 1970, 92, 1533.

25 Guadado, P.; Lawrance, G. A.; Eldik, R. V. *Inorg. Chem.* 1989, 28, 976.

26 Angel, R. L.; Fairlie, D. P.; Jackson, W. G. *Inorg. Chem.* 1990, 29, 20.

27 Siegel, H.; Martin, R. B. *Chem. Rev.* 1982, 82, 385.

28 Pinnell, D.; Wright, G. B.; Jordan, R. B. *J. Am. Chem. Soc.* 1972, 94, 6104.

### 1.3 Plan of Study

Recently it has been shown that cis-diaqua cobalt complexes of trpn and cyclen are highly efficient at catalyzing the hydrolysis of unactivated esters such as methyl acetate.<sup>29</sup> Hydrolysis of amides and nitriles pose an even greater challenge than the hydrolysis of esters, since amide and nitriles are thousands of times more stable than esters. There are many examples of metal ion promoted or catalyzed reactions of amides and nitriles. Most studies have involved substrates which are directly coordinated or connected through the ligand to the metal ion and no catalytic turnover has been observed in the model systems.

My research plan is to study the mechanism of nitrile hydration catalyzed by the cobalt complexes of cyclen and its derivatives. We are also interested in testing their efficiency on a variety of nitriles such as acrylonitrile for synthetic applications. Detailed mechanistic and binding studies will give valuable information concerning the development of catalysts that hydrolyze amides.

---

<sup>29</sup> Chin, J.; Banaszczyk, M. *J. Am. Chem. Soc.* **1989**, *111*, 2724.

## 2 RESULTS

### 2.1 Kinetics

#### 2.1.1 Co(III) complex catalyzed hydration of acetonitrile

The rate constants for various Co(III) complexes catalyzed hydration of acetonitrile are listed in Table II.1.

**Table II.1** First order rate constants for the hydration of acetonitrile in the presence of Co(III) complexes at pH 7.

Catalysts	k (sec <sup>-1</sup> )	rel.rate
(trpn)Co(III)(OH <sub>2</sub> )(OH) <sup>a,b</sup>	6 x 10 <sup>-3</sup>	2 x 10 <sup>4</sup>
(cyclen)Co(III)(OH <sub>2</sub> )(OH) <sup>b</sup>	3.2 x 10 <sup>-4</sup>	10 <sup>3</sup>
(tren)Co(III)(OH <sub>2</sub> )(OH) <sup>b</sup>	2.1 x 10 <sup>-5</sup>	6 x 10 <sup>2</sup>
(NH <sub>3</sub> ) <sub>5</sub> Co(III)(NCCH <sub>3</sub> ) <sup>c</sup>	3.4 x 10 <sup>-7</sup>	1
NaOH <sup>d</sup>	1.6 x 10 <sup>-13</sup>	5 x 10 <sup>-7</sup>

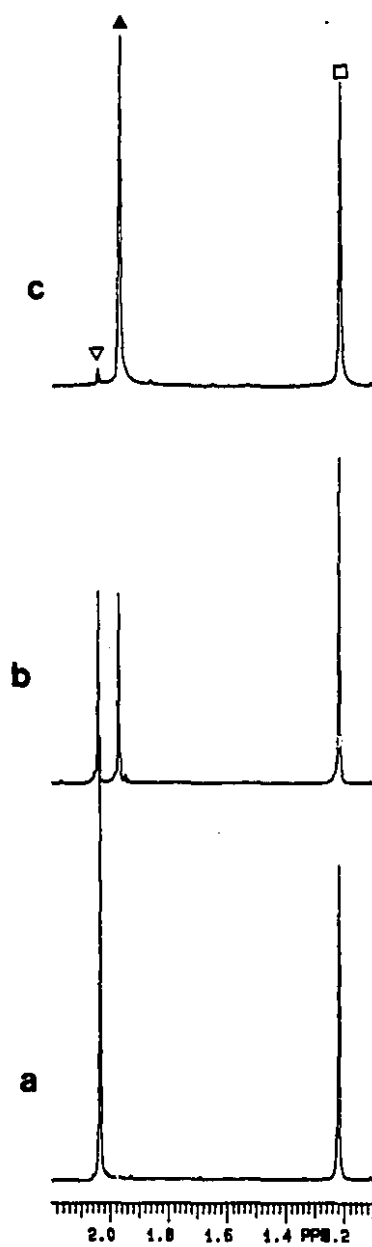
a) ligand deligation occurs after giving 3 turnovers. b) pseudo-first order rate constant at [Co] 10 mM, [CH<sub>3</sub>CN] 0.5 M, and pD 7 and 40 °C. c) at pH 7, 25°C ref:

D.A. Buckingham, F. R. Keene, and A.M. Sargeson, *J. Am. Chem. Soc.*, **95**,5649 (1973)

d) 25 °C, calculated from the second order rate constant, ref: as same as above

At neutral pH, (cyclen)Co(III)(OH)(OH<sub>2</sub>) (10 mM) gives a 10<sup>9</sup> fold rate acceleration over the hydroxide rate. The trpn complex is slightly more reactive than the cyclen complex in hydrating nitriles, but ligand deligation is taking place during the reaction. Product amide formation was monitored by <sup>1</sup>H NMR (Fig. II.4) and peak integration was used as a direct measure of product concentration. The data were fit according to a first order kinetic equation (R > 0.98). All the data reported represent an average value of at least three runs. The kinetic runs were reproducible within 5 % error.

**Figure II.4**  $^1\text{H}$  NMR spectrum of hydration of acetonitrile catalyzed by (cyclen)Co(III)(OH)(OH<sub>2</sub>) at pD 7, 40 °C ; a) t = 0, b) t = 5.5 hr, c) t = 23 hr:  $\square$  = t-BuOH(reference),  $\blacktriangle$  = acetamide, and  $\nabla$  = acetonitrile.



### 2.1.2 pD-Rate profile

The pD-rate profile for the cyclen complex catalyzed hydration of acetonitrile is shown in Fig. II.5. The observed pseudo first order rate constant for the amide production is given by eq 2.1.

$$k_{\text{obs}} = k [\text{RCN}] \frac{K_1 [\text{H}^+]}{K_1 K_2 + K_1 [\text{H}^+] + [\text{H}^+]^2} \dots\dots\dots \text{eq 2.1}$$

where  $k$  is the second order rate constant for (cyclen)Co(III)(OH)(OH<sub>2</sub>) catalyzed hydration of CH<sub>3</sub>CN and  $K_1$  and  $K_2$  are the first and second acid dissociation constants of the cobalt bound water molecules. The data (Table II.2) were fit according to eq 2.1 with an iterative non linear least squares curve fitting program\* ( $K_1 = 5.5$ ,  $K_2 = 7.2$ , and  $k = 3.8 \times 10^{-4} \text{ M}^{-1} \text{ sec}^{-1}$ ). The data points are averages from at least two kinetic runs.

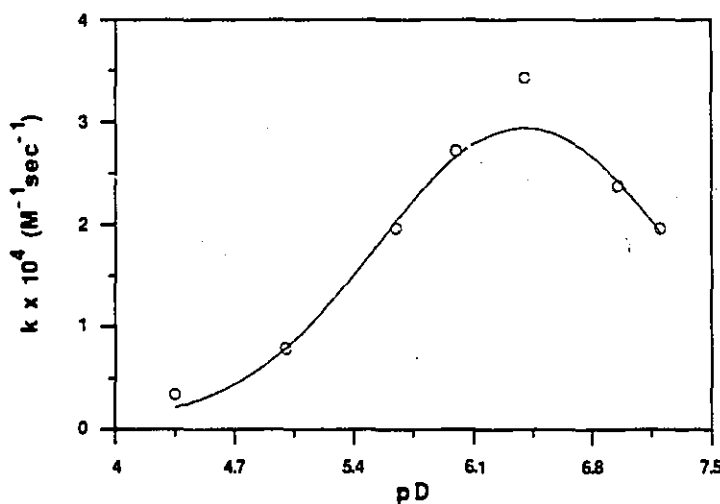
**Table II.2** Observed second order rate constants for the hydration of acetonitrile catalyzed by the cyclen complex at different pD, 40 °C.

pD	$k \times 10^4 (\text{M}^{-1} \text{sec}^{-1})$	pD	$k \times 10^4 (\text{M}^{-1} \text{sec}^{-1})$
4.35	0.34	6.40	3.43
5.00	0.79	6.95	2.38
5.65	1.97	7.20	1.97
6.00	2.72	7.95	1.14

a) [Co] 10 mM, [CH<sub>3</sub>CN] 0.1 M, and at 40°C

\* *Kaleidograph*, version 2.0.2, developed by Abelbeck software.

**Figure II.5** pD-rate profile for the hydration of acetonitrile (0.1M) catalyzed by (cyclen)Co(III)(OH)<sub>2</sub> (10 mM) at 40 °C.



### 2.1.3 Dependence of acetonitrile hydration rate on the concentration of Co(III) complex

The rate of acetonitrile hydration shows a first order dependence on the catalyst concentration under the experimental conditions used. A plot of the rate vs concentration of the cobalt complex (Fig. II.6) gives a straight line up to 10 mM concentration of the cyclen complex.

### 2.1.4 Dependence of acetonitrile hydration rate on the concentration of acetonitrile

The hydration of acetonitrile catalyzed by (cyclen)Co(III)(OH)(OH<sub>2</sub>) is initially first order with respect to the nitrile concentration and becomes independent at high nitrile concentrations. (Fig. II.7). The observed pseudo zero order kinetics for turnover of the cyclen complex in the presence of excess nitrile confirms the catalytic reaction. A maximum rate constant of  $4 \times 10^{-4} \text{ sec}^{-1}$  was obtained from the Eadie-Hofstee plot ( $v = V_{\text{max}} - K_m v / [\text{nitrile}]$ ).<sup>30</sup>

30 a) Fersht, A. in *Enzyme Structure and Mechanism*, 2nd Ed.; W. H. Freeman and Company: New York, 1985. b) Moore, J.; Pearson, R. G. in *Kinetics and Mechanism*, 3rd Ed.; Wiley: New York, 1981.

Figure II.6 Dependence of the rate of acetonitrile (0.2 M) hydration catalyzed by (cyclen)Co(III)(OH)(OH<sub>2</sub>) on the catalyst concentration [Co], at pD 7 and 40 °C.

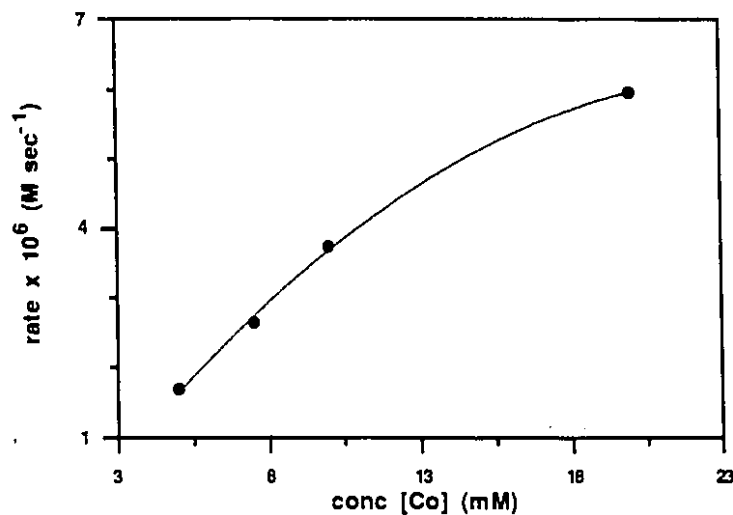
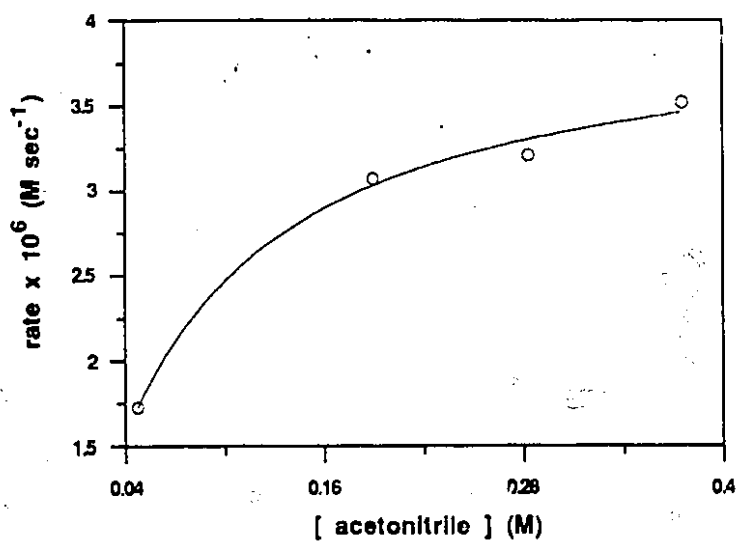


Figure II.7 Dependence of the rate of acetonitrile hydration catalyzed by (cyclen)Co(III)(OH)(OH<sub>2</sub>) on the concentration of acetonitrile at [Co] 10 mM, pD 7, and 40 °C.



### 2.1.5 Equilibrium binding constant of acetonitrile to cobalt complexes

The equilibrium binding of acetonitrile to (cyclen)Co(III)(OH)<sub>2</sub> was monitored at 460 nm under pseudo first order conditions at pD 2 (Fig II.8). Absorbance changes are due to binding of acetonitrile to the cyclen complex since the subsequent hydration is slow under the experimental conditions. Figure II-14 shows the <sup>13</sup>C NMR spectrum obtained from acetonitrile and the cobalt complex at pD 2 showing that there is no diadduct formation.

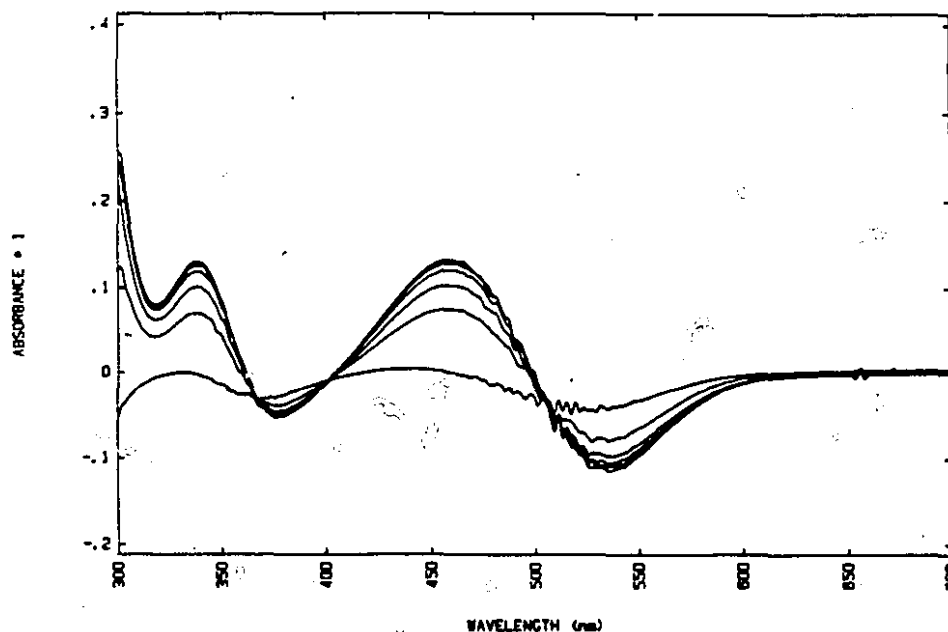


The rate for the attainment of equilibrium is given by eq 2.2.<sup>31</sup>

$$\text{Rate} = (k_1 [\text{CH}_3\text{CN}] + k_{-1}) [\text{Co}] = k_1^{\text{obs}} [\text{Co}] \quad \text{..... eq 2.2}$$

where  $k_1[\text{CH}_3\text{CN}]$  and  $k_{-1}$  are the forward and reverse first order rate constants.

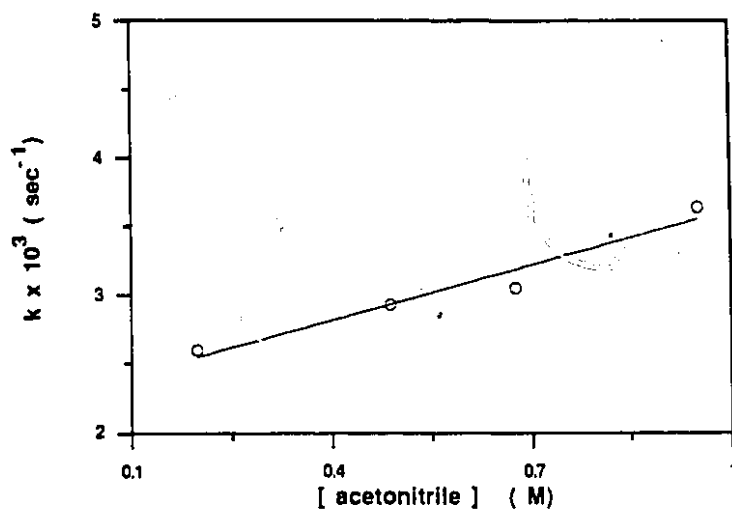
**Figure II.5** UV/VIS spectrum for acetonitrile (0.5 M) binding to (cyclen)Co(III)(OH)<sub>2</sub> (10 mM) at pD 2, 40 °C ; plot every 50 sec, ref: catalyst solution.



<sup>31</sup> Wilkins, R. G. in *The Study of Kinetics and Mechanism of Reactions of Transition Metal Complexes*; Allyn and Bacon, Inc.: Boston, 1974.

A plot of pseudo first order rate constants,  $k_1^{\text{obs}}$  for the approach to equilibrium vs acetonitrile concentration is shown in Fig II.9. The data were fit according to eq 2 with a linear least squares analysis of the plot ( $R > 0.97$ ). The slope ( $k_1$ ) and the intercept ( $k_{-1}$ ) are  $1.33 \times 10^{-3} \text{ M}^{-1} \text{ sec}^{-1}$  and  $2.28 \times 10^{-3} \text{ sec}^{-1}$ , respectively.  $K_{\text{eq}} (k_1 / k_{-1})$  for binding of acetonitrile to  $(\text{cyclen})\text{Co(III)}(\text{OH})_2$  is then  $0.58 \text{ M}^{-1}$  at pD 2 and 25 °C.

**Figure II.9** Plot of  $k_{\text{obs}} (\text{sec}^{-1})$  vs  $[\text{CH}_3\text{CN}] (\text{M})$  at  $(\text{cyclen})\text{Co(III)}(\text{OH})(\text{OH})_2$  (10 mM), pD 7 and 25 °C.



### 2.1.6 Co(III) complex catalyzed formation of chelated amides.

The rate constants for the accumulation of intermediate II by the cyclen and the uncyclen complexes were obtained under pseudo first order conditions. The reactions were followed by UV/VIS spectroscopy at 500 and 600 nm, respectively.

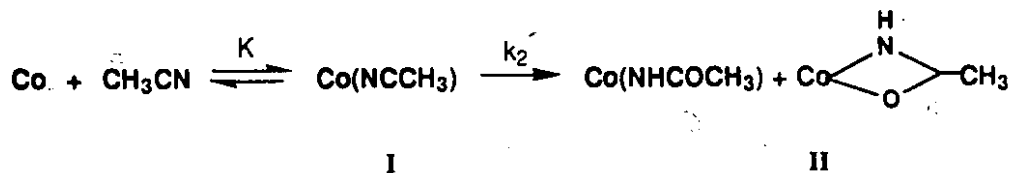
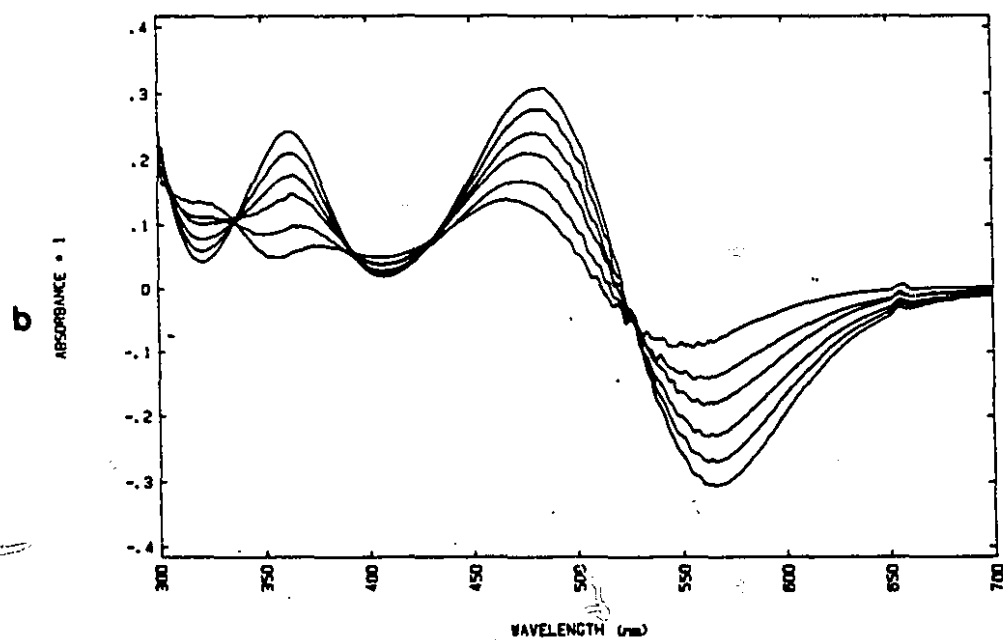
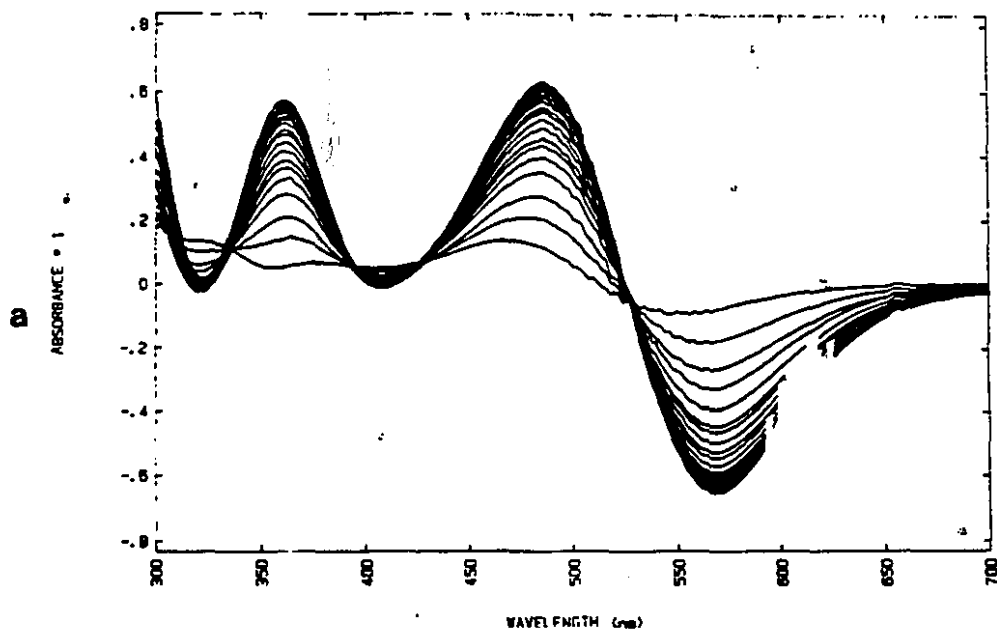


Figure II.10 (a) shows the change in the UV/VIS spectrum during hydration at pD 7. The spectra, which were recorded for the first 180 sec, suggest that the initial nitrile binding is rapid (Fig. II.10, b).

**Figure II.10** UV/VIS spectra for the hydration of acetonitrile (0.5 M) catalyzed by (cyclen)Co(III)(OH)(OH<sub>2</sub>) (10 mM) at pD 7, 40 °C ; a) plot every 70 sec for 1500 sec, b) replot of (a) for first 180 sec ref : catalyst solution.



The absorbance change is due to the formation of a chelated acetamide produced as a result of the hydration reaction. The chelated acetamide to the tmcyclen complex was isolated by reacting acetonitrile with the tmcyclen complex. The UV/VIS spectrum of the species produced from the hydration reaction is identical to that of the isolated chelate. The pseudo first order rate constants for the accumulation of the acetamido complex are shown in Table II.3. The rate constants increase as the concentration of acetonitrile increases.

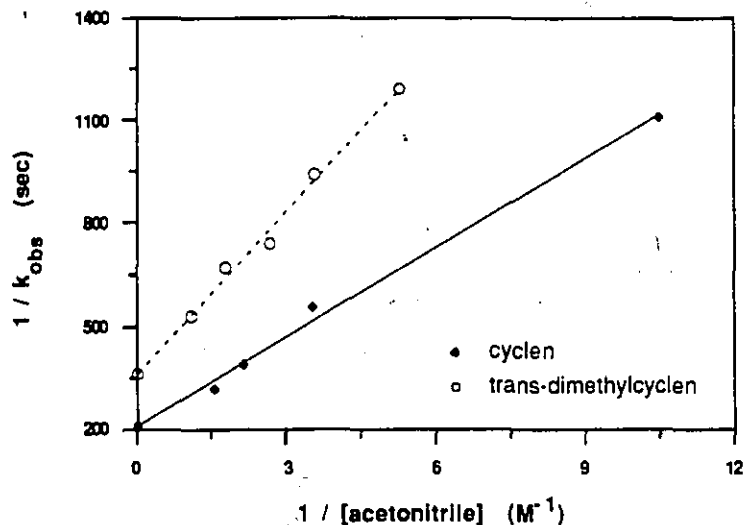
**Table II.3** Observed pseudo-first order rate constants ( $k^{\text{obs}} \times 10^3 \text{ sec}^{-1}$ ) for the accumulation of intermediate II,  $[(L)\text{Co}(\text{NHCOCH}_3)]^{2+}$  at  $[\text{Co}]$  10 mM, pD 7 and 40 °C <sup>a</sup>.

$[\text{CH}_3\text{CN}]$ (M)	cyclen	tmcyclen <sup>b</sup>
0.09	0.90	-
0.19	-	0.84
0.28	1.79	1.06
0.38	-	1.25
0.47	2.56	-
0.56	-	1.48
0.65	3.12	-
0.91	-	1.9

a)  $[\text{cyclenCo}]$  10 mM, rxn followed at 500 nm

b) rate constants were obtained by multiplying a factor of 2 to the rate constants obtained when  $[\text{Co}]$  5 mM used ( the rate increases linearly with increasing  $[\text{Co}]$ ) the reaction was followed at 600 nm.

Figure II.11 The plot of  $(k^{\text{obs}})^{-1}$  (sec) vs  $[\text{CH}_3\text{CN}]^{-1}$  ( $\text{M}^{-1}$ ).

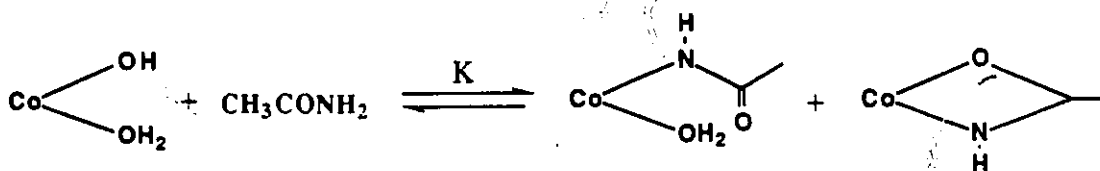


The data were fit according to eq 2.3 and analyzed by using a linear least squares method ( $R > 0.99$ ).

$$\text{Rate} = \frac{K k_2 [\text{CH}_3\text{CN}] [\text{Co}]}{1 + K [\text{CH}_3\text{CN}]} = k_2^{\text{obs}} [\text{Co}] \quad \text{.....eq 2.3}$$

where  $k_2^{\text{obs}} = (K \times k_2 [\text{CH}_3\text{CN}]) / (1 + K[\text{CH}_3\text{CN}])$ . A plot of  $(k_2^{\text{obs}})^{-1}$  vs  $[\text{CH}_3\text{CN}]^{-1}$  gives an intercept  $k_2^{-1}$  and a slope  $(K \times k_2)^{-1}$ . The first order rate constants  $k_2$  ( $4.69 \times 10^{-4} \text{ sec}^{-1}$  and  $2.75 \times 10^{-3} \text{ sec}^{-1}$ ) and the equilibrium binding constants  $K_{\text{eq}}$  ( $2.5 \text{ M}^{-1}$  and  $2.3 \text{ M}^{-1}$ ) for the cyclen and the tmcyclen complexes were obtained at pD 7 and  $40^\circ\text{C}$ .

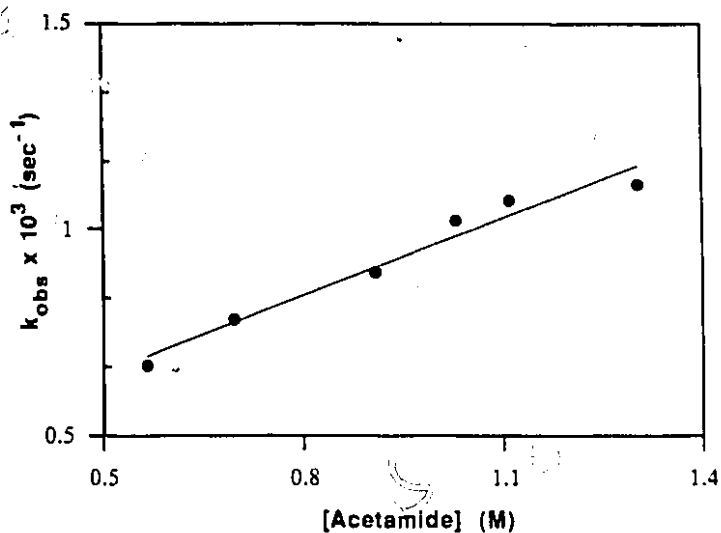
### 2.1.7 Equilibrium chelation of acetamide to Co(III) complex



The equilibrium constant for binding of acetamide to the cyclen aqua-hydroxy complex was measured in the same way used as for acetonitrile (section 2.1.5). The formation of a bidentate amide was followed at 560 nm by varying the acetamide

concentration. The data were analyzed according to eq 2.2 by using a linear least squares method. From the plot of  $k^{\text{obs}}$  vs [amide] (Fig. II.12), the equilibrium constant for acetamide binding to the aqua hydroxy cyclen complex is obtained as  $2 \text{ M}^{-1}$  ( $k_1 = 6.28 \times 10^{-4} \text{ M}^{-1} \text{ sec}^{-1}$ ,  $k_{-1} = 3.35 \times 10^{-4} \text{ sec}^{-1}$  at  $[\text{Co}] = 5 \text{ mM}$ , pD 7 and  $40 \text{ }^\circ\text{C}$ ). The intensity ratio of bidentate vs monodentate species is more than 7:1, according to the  $^{13}\text{C}$  NMR spectrum taken in the presence of excess acetamide.

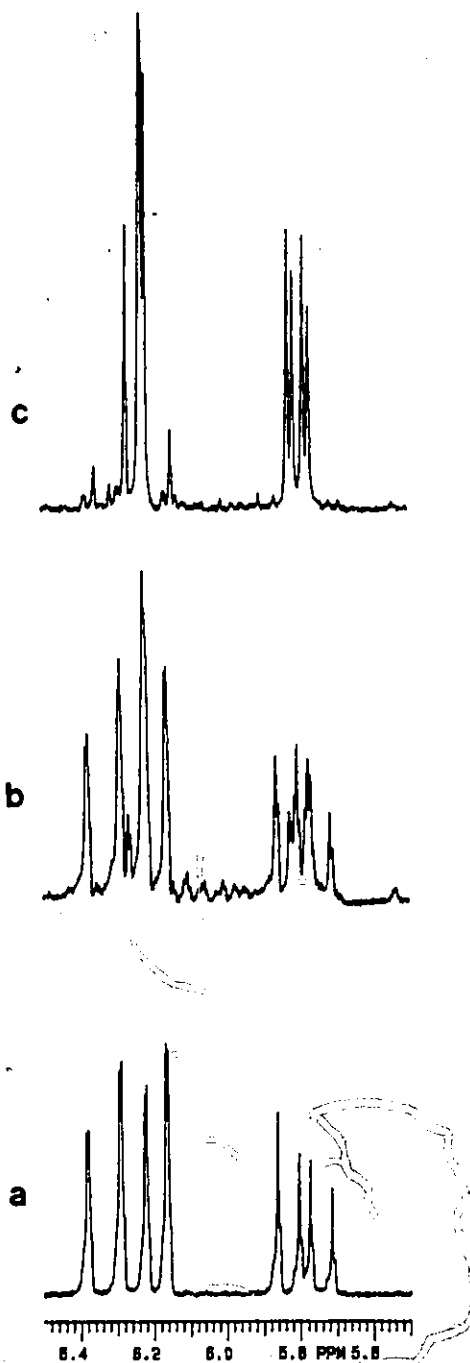
**Figure II.12** Plot of  $k^{\text{obs}}(\text{sec}^{-1})$  vs [Acetamide] (M) at  $[\text{Co}] 5 \text{ mM}$ , pD 7,  $40 \text{ }^\circ\text{C}$ .



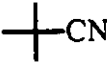
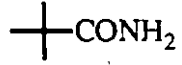
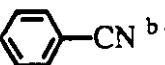
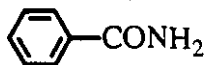
### 2.1.8 Hydration of acrylonitrile and other nitriles

(Cyclen)Co(III)(OH)(OH<sub>2</sub>) catalyzed hydration of acrylonitrile to acrylamide was followed by  $^1\text{H}$  NMR (Fig.II.13). There was no indication of side product formation. The presence of  $\beta$ -cyanoethanol, the double bond hydration product, was examined by GC. The cyclen complex is also an efficient catalyst for hydrating hindered nitriles. Trimethyl acetonitrile and benzonitrile are efficiently hydrated to their corresponding amides (Table.II.4).

**Figure II.13**  $^1\text{H}$  NMR spectrum of hydration of acrylonitrile catalyzed by  $(\text{cyclen})\text{Co}(\text{III})(\text{OH})(\text{OH}_2)$  at pD 6.8,  $40^\circ\text{C}$ ; a)  $t = 0$ , b)  $t = 3.5$  hr, and c)  $t = 20$  hr.



**Table II.4** The efficient hydration of various nitriles catalyzed by (cyclen)Co(III)(OH)(OH<sub>2</sub>) at pD 7.0 and 80 °C.

nitrile	product	time
CH <sub>3</sub> CN	CH <sub>3</sub> CONH <sub>2</sub>	35 min
		120 min
 <sup>b</sup>		40 min

a) [cyclenCo] 10 mM, [nitrile] 100mM

b) slightly miscible with water and upon cooling product benzamide is precipitated out.

## 2.2 Binding of Nitriles and Amides

### 2.2.1. Binding of acetonitrile and acetamide to Co(III) complexes at pH<3

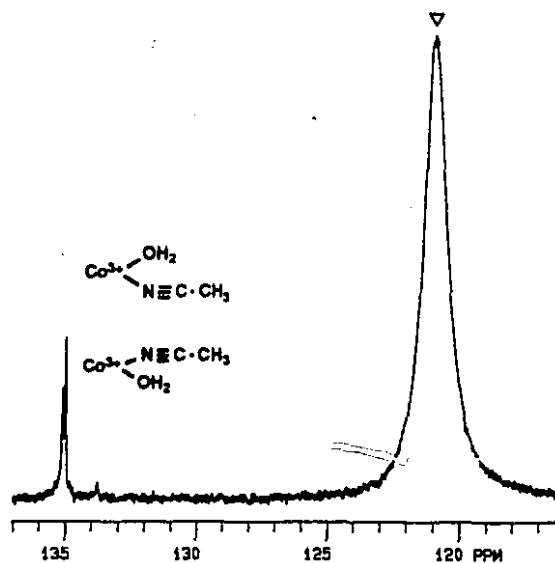
Binding studies of <sup>13</sup>C<sub>1</sub> labelled acetonitrile to the cyclen complex were carried out at low pH to avoid the hydration reaction. Two signals (134.9 and 135.0 ppm) in <sup>13</sup>C NMR are observed under the experimental conditions. These peaks correspond to the nitrile carbons bound to the cobalt in a monodentate fashion. It is known that two equatorial sites of the cyclen complex are different due to an asymmetric positioning (syn, anti) of the two secondary amine protons trans to them ( $\sigma_v$ ).<sup>32,33</sup> The chemical shift of syn and anti protons are different enough to give separate signals because of asymmetric hydrogen bonding. Both the mcyclen and the mcyclen complexes display the same binding patterns with acetonitrile. Binding of acetamide to the cobalt complexes can not be studied by using <sup>13</sup>C NMR spectroscopy. Even at high concentration of acetamide (0.2M), signals were not detectable within the <sup>13</sup>C NMR detection limit.

32 Nakazawa, H.; Sakaguchi, U.; Yoneda, H.; Morimoto, Y. *Inorg. Chem.* **1981**, *20*, 973.

33 Sosa, M. E.; Tobe, M. L. *J. Chem. Soc., Dalton Trans.* **1985**, 475.

Figure II.14

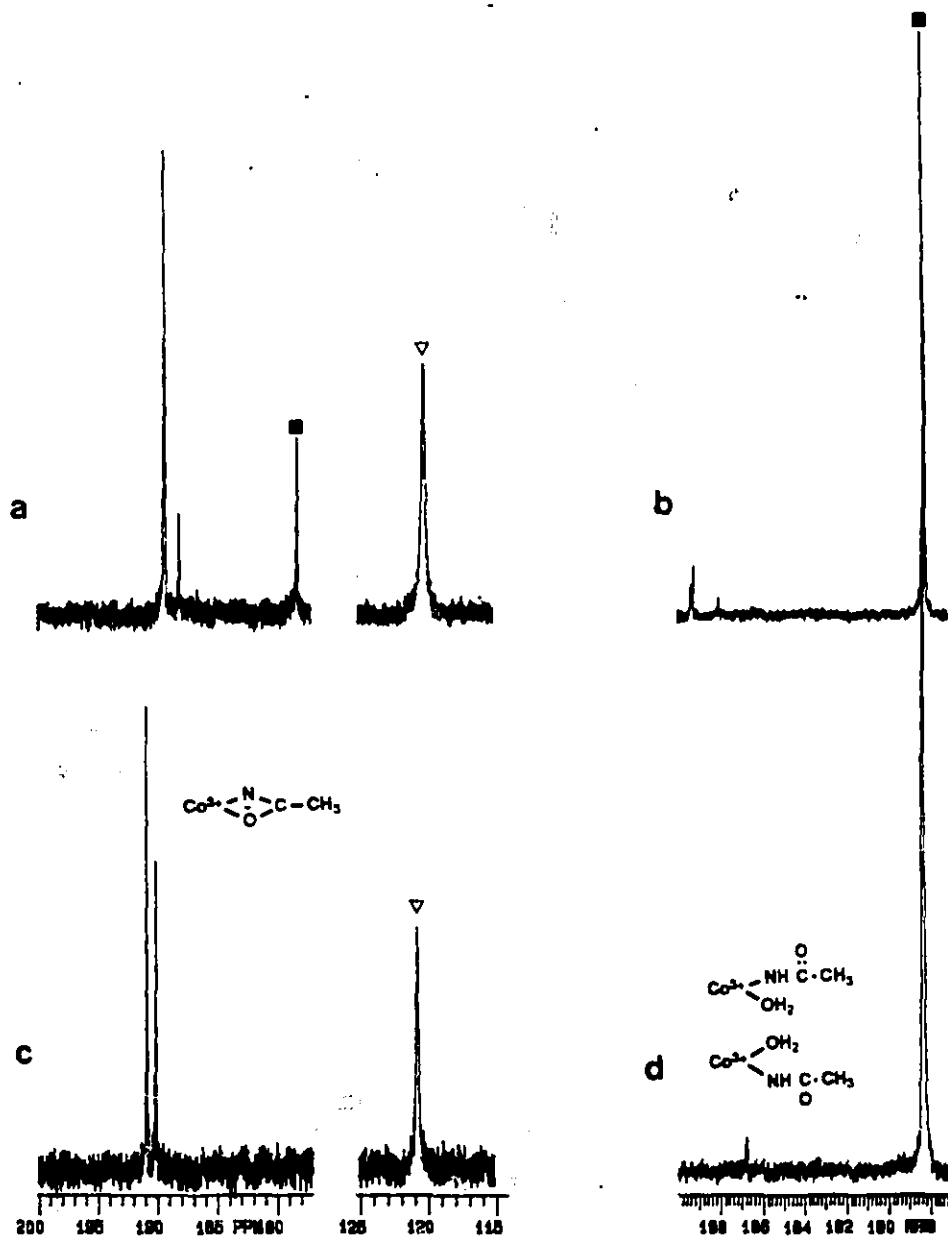
$^{13}\text{C}$  NMR of  $\text{CH}_3\text{C}^*\text{N}$  (0.05M) and  $(\text{cyclen})\text{Co(III)(OH}_2)_2$  (0.05M), at pH 2 and 25 °C:  $\nabla$  = free acetonitrile.



### 2.2.2 Binding of acetamide and acetonitrile to Co(III) complexes at neutral pH

Acetonitrile, initially bound to the cyclen complex, undergoes rapid hydration producing several intermediates and eventually free amide (Fig.II.15-a). Both acetonitrile and acetamide in the presence of the cyclen complex each produce three new signals at 188.0, 189.2, and 189.3 ppm. The peak at 178.0 ppm in Figure II.15 corresponds to the free acetamide. Binding of acetonitrile to the tmcyclen complex gives two new signals at 190.2 and 190.8 ppm (Fig. II.15-c), while binding of acetamide to the tmcyclen complex produces only one signal at 186.8 ppm (Fig.II.15-d).

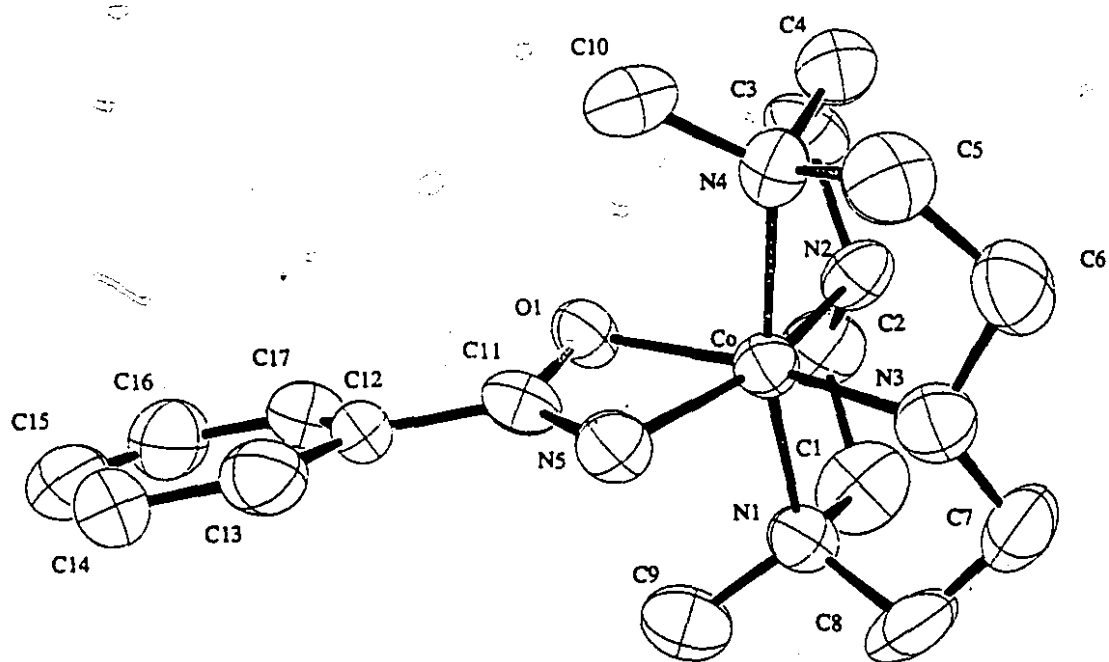
**Figure II.15**  $^{13}\text{C}$  NMR spectra of (cyclen)Co(III)(OH)(OH<sub>2</sub>) with a) 1:1 CH<sub>3</sub>C<sup>\*</sup>N (50 mM), b) 1:2 CH<sub>3</sub>C<sup>\*</sup>ONH<sub>2</sub> (50 mM); (tmcyclen)Co(III)(OH)(OH<sub>2</sub>) with c) 1:1 CH<sub>3</sub>C<sup>\*</sup>N (20 mM), d) 1:2 CH<sub>3</sub>C<sup>\*</sup>ONH<sub>2</sub> (50mM), at 25 °C, pD 6.4.:  
 $\nabla$  = free acetonitrile and  $\blacksquare$  = free acetarhide.



### 2.3 Crystal Structure of a Chelated Benzamide to $[(\text{tmcyclen})\text{Co}(\text{OH}_2)_2]^{3+}$

The crystal structure of  $[(\eta^2\text{-N,O-benzamide})(\text{tmcyclen})\text{Co}(\text{III})](\text{ClO}_4)_2 \cdot 2\text{H}_2\text{O}$  is shown in Figure II.16. The bond angles, bond distances, and other parameters are listed in Appendix A.

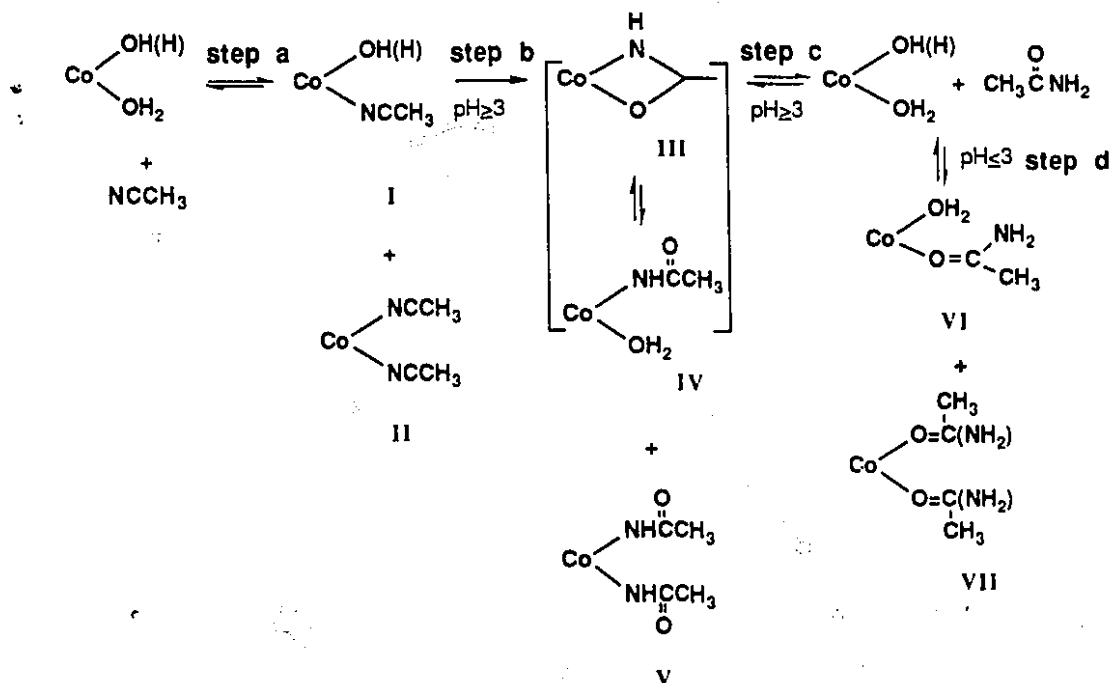
**Figure II.16** Perspective ORTEP drawing of the  $[(\eta^2\text{-N,O-benzamide})(\text{tmcyclen})\text{Co}(\text{III})](\text{ClO}_4)_2 \cdot 2\text{H}_2\text{O}$ . Nonhydrogen atoms are represented by thermal vibration ellipsoids drawn to encompass 50 % of electron density; hydrogen atoms are omitted for clarity.



### 3 DISCUSSION

#### 3.1 Binding of Acetonitrile and Acetamide to Co(III) complexes

Scheme II.3 shows possible intermediates produced from the coordination of acetonitrile and acetamide to the diaqua cobalt complex. Species, I, III, IV and VI each have two conformational isomers due to nonequivalent environment of the two cobalt bound water molecules.<sup>32,33</sup>



**Scheme II.3** Binding of acetonitrile and acetamide to the cobalt complex and the possible coordination species.

$^{13}\text{C}$  NMR can be a useful tool to identify the coordination products to metal ions since coordination to the metal causes large chemical shift changes for the nitrile carbon or the amide carbonyl carbon. Binding of acetonitrile and acetamide to the cobalt complexes of cyclen and tmcyclen will be discussed in this section.

The equilibrium binding of acetonitrile to the cyclen and the tmcyclen complexes was carried out at  $\text{pD} 2$  free from the subsequent hydration reaction (step a in Scheme II.3): Complexation of acetonitrile to the cyclen complex produces a characteristic absorbance change in UV/VIS spectroscopy and the cobalt bound nitriles were detected by

$^{13}\text{C}$  NMR (Fig. II.11). Two new signals, appearing downfield relatively to free acetonitrile by ca. 13 ppm, correspond to two singly bound acetonitriles.  $[(\text{tren})\text{Co}(\text{III})(\text{NCCH}_3)_2]$  has been synthesized but chemical shifts of coordinated acetonitrile have never been reported due to rapid solvolysis.<sup>34</sup> Under the same conditions (pD 2), complexation of acetamide to the cobalt complexes was not observed (step d in Scheme II.3) due to, in part, low detection limit of  $^{13}\text{C}$  NMR. There is no difference in the  $^{13}\text{C}$  NMR spectrum between the two cobalt complexes in complexation of acetonitrile and acetamide under the experimental conditions used (pD 2).

Complexation of acetonitrile to the cobalt complexes at neutral pH is accompanied by the hydration reaction (step b in Scheme II.3). Acetonitrile in the presence of the cyclen complex produces four new signals including that of free acetamide in  $^{13}\text{C}$  NMR. The same signals are observed separately by starting with acetamide. Complexation of acetamide to the cyclen complex produces three new peaks identical to those obtained from the reaction with acetonitrile. It is known that binding of amides to cobalt complexes is followed by deprotonation of the amide NH proton and it shifts the equilibrium in favour of formation of the thermodynamically stable amido metal complexes. Several amide bound pentaammine metal(III) complexes have been synthesized and characterized.<sup>23</sup> The singly bound amides to cobalt complexes usually have  $^{13}\text{C}$  NMR chemical shifts at 5 to 10 ppm downfield relative to their corresponding free amide in  $\text{DMSO-d}_6$ . The chemical shifts of the observed signals from complexation of acetonitrile and acetamide to the cyclen complex in  $\text{D}_2\text{O}$  are approximately in about the same range as that for a singly bound amide anion in  $\text{DMSO-d}_6$ .

Complexation of acetonitrile to the tmcyclen complex under the experimental conditions used (pD 7) gives two signals at 190.2 and 190.8 ppm. In contrast to the cyclen complex, there is no indication of acetamide production. This is consistent with the observed experimental data showing no catalytic turnover for the tmcyclen complex mediated hydration. Interestingly, complexation of acetamide to the tmcyclen complex produces only one new signal upfield to those found from the reaction with acetonitrile. This signal at 186.8 ppm must be due to the singly bound amide. The signals appearing at 190.2 and 190.8 ppm from the tmcyclen complex promoted acetonitrile hydration (Fig. II.15-c) should correspond to the species that are more delocalized than the cobalt bound monodentate acetamide anion. They can not be due to a doubly bound amide since the corresponding signal would be shifted upfield with respect to that of singly bound

<sup>34</sup> Curtis, N. J.; Lawrance, G. A. *J. Chem. Soc., Dalton Trans.* 1985, 1923.

monodentate amides.<sup>35</sup> It is well accepted that the linkage isomerization of the O- to the N bonded amide occurs intramolecularly through formation of a  $\eta^2$ -N,O-amido metal(III) complex at the transition state.<sup>25,36</sup> This, along with <sup>13</sup>C NMR data, suggests that it might be possible to trap a chelated amide with an appropriate metal complex. The signals at 190.2 and 190.8 ppm (Fig.II.15-c) can be assigned to the N,O chelated acetamides. Signals obtained from the cyclen complex with acetonitrile and acetamide at 189.2 and 189.3 ppm can then be assigned to a chelate and the signal at 188.0 ppm to a singly bound amide (Fig.II.15-a).

The reason why the tmcyclen complex forms a chelate with acetonitrile but not with acetamide could be explained as follows: Linear molecules such as acetonitrile react with the tmcyclen complex and a chelate is formed after the hydration reaction. To form a chelate from the product amide, initially bound acetamide through the nitrogen lone pair has to be deprotonated and rotate to be in the  $\sigma_v$  plane. This type of rotation appears to be restricted in the tmcyclen complex due to the interaction between the hydrogen atom on the deprotonated amide nitrogen and the two methyl group on the ligand. For comparison, the tmcyclen complex readily forms a chelate with acetate (part I). The reverse conformational change is required for the dissociation of the chelated acetamide from the cobalt complex. There appears to exist only a small rotational barrier for the formation and dissociation of a chelated amide to the cyclen complex.

### 3.2 Crystal Structure of $[(\eta^2\text{-N,O-benzamide})(\text{tmcyclen})\text{Co(III)}]^{2+}$ complex

Chelated amides are quantitatively formed by reacting the tmcyclen complex with nitriles. A purple multifaceted crystal was obtained by reacting the tmcyclen complex with benzonitrile. Although the X-ray structure of four-membered ring chelates of carbonate<sup>37</sup>, acetate<sup>38</sup>, and phosphate<sup>39</sup> are known, this is the first time the X-ray structure of an amide chelated to the metal complex has been obtained.

35 Banaszczyk, M. Ph. D. Thesis, McGill University 1989.

36 Curtis, N. J.; Dixon, N. E.; Sargeson, A. M. *J. Am. Chem. Soc.* 1983, 105, 5347.

37 Niederhoffer, E. C.; Martell, A. E.; Rudolf, P.; Clearfield, A. *Inorg. Chem.* 1982, 21, 3734.

38 a) Banaszczyk, M. Ph. D. Thesis, McGill University 1989. b) this study, see experimental section 3.4.

39 Anderson, B.; Milburn, R. M.; Sargeson, A. M. *J. Am. Chem. Soc.* 1977, 99, 2654.

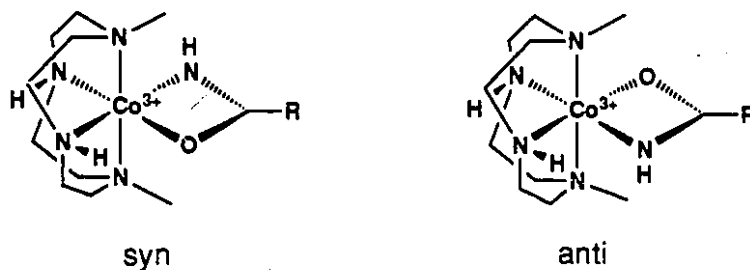


**Figure II.17** Two possible isomers for the chelated acetamide to the tmcyclen complex.

The  $\eta^2$  benzamide metal(III) complex could have at least two possible isomers. While maintaining its symmetry ( $\sigma_v$ ), the amide NH can face or anti-face the ligand NH in the mirror plane. Interestingly, the isolated complex produces only one carbonyl carbon signal in the  $^{13}\text{C}$  NMR obtained in a nonpolar solvent such as dichloromethane, whereas it shows two signals in polar solvents such as  $\text{D}_2\text{O}$  or  $\text{DMSO-d}_6$  (part IV). Studies on  $(\text{cyclen})\text{Co(III)Cl}_2$  showed that extensive exchange takes place between the solvent  $\text{D}_2\text{O}$  and protons on the nitrogen trans to the coordinated water.<sup>32</sup> The calculated R-factors of the two isomers differ by about 0.5.<sup>40</sup> Upon crystallization, the equilibrium shifts in favor of the anti isomer.

Compared to the conformation of other  $\eta^2$ -cobalt complexes, the N-C-O bond angle [68.2(3) $^\circ$ ] in the chelated amide is similar to the O-C-O angle in  $(\eta^2\text{-CO}_3)\text{Co(III)(tmcyclen)}$  [68.6(2) $^\circ$ ]<sup>41</sup> and in  $(\eta^2\text{-CO}_3)\text{Co(III)(trpn)}$  [67.38 $^\circ$ ].<sup>42</sup> The bond length of Co(III) to amide N in the chelate is much shorter (1.895 Å) than those found in pentaammine  $\eta^1$ -acetamido<sup>43</sup> or  $\mu^1$ -acetamido cobalt complexes (1.91(8)-1.92(2) Å).<sup>21</sup> The amide C-O bond length is 1.28(1) Å which is somewhat longer than those of an isolated carbonyl group (1.23 Å) and the  $\eta^1$ -complex (1.26(12) Å), and close to that of the  $\mu^1$ -complex. Overall, the amide bond in the  $\eta^2$ -cobalt complex is more delocalized than in the  $\eta^1$ -complex, but about the same as in the  $\mu^1$ -complex.

In conclusion,  $^{13}\text{C}$  NMR binding studies with labeled substrates and X-ray crystallography data provided useful information for the elucidation of the catalytic mechanism of nitrile hydration as well as for structure identification.

40 Stout, G. H.; Jensen, L. H. in *X-ray Structure Determination*, 2nd Ed.; Wiley: New York, 1989 pp 229-230. R represents the correctness of fit with the model used.  $R = \text{Residual Index}$  defined as  $R = \sum |\Delta F| / \sum |F_o|$ , where  $|\Delta F| = |F_o| - |F_c|$ ,  $|F_o|$  is the scaled observed structure amplitude,  $|F_c|$  is the calculated structure amplitude.

41 Giusti, J.; Chimichi, S.; Ciampolini, M. *Inorg. Chim. Acta* 1984, 88, 51.

42 38 a)

43 Schneider, M. L.; Ferguson, G.; Balahura, R. J. *Can. J. Chem.* 1973, 51, 2180.

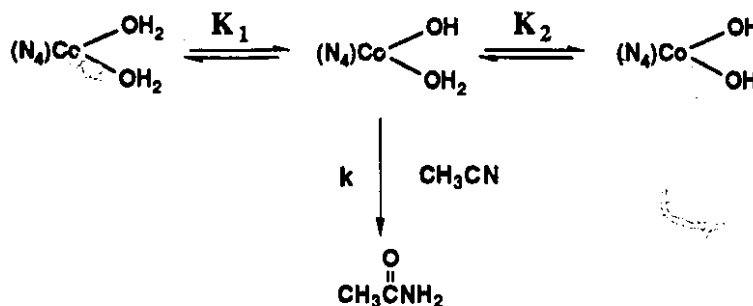
### 3.3 Mechanism

#### 3.3.1 Hydration of acetonitrile catalyzed by [(cyclen)Co(OH)<sub>2</sub>]<sup>3+</sup>

(Cyclen)Co(III)(OH)(OH<sub>2</sub>) is the most efficient catalyst for hydration of nitriles to the corresponding amides (Table II.1). It has been shown that the trpn complex forms the four membered ring intermediates with phosphates<sup>44</sup> and acetates<sup>45</sup> more readily than the cyclen complex. The trpn complex catalyzes the hydration of acetonitrile faster than the cyclen complex, but it starts to decompose after initial reaction due to amide promoted deligation of the tetraamine ligand. Amide promoted deligation of Co(III)-amine complexes is a known phenomenon.<sup>46</sup> Deligation does not take place with the cyclen complex, apparently because the cyclic tetraamine ligand binds very tightly to the cobalt ion.

The mechanism proposed for the nitrile hydration based on the pH-rate profile is shown in Scheme II.4.

Scheme II.4



The bell shaped pH profile suggest that the cobalt aqua-hydroxy form is the active species that catalyzes the hydration of acetonitrile. The pH-rate profile data can be fit to the expression shown in eq 3.1.

44Chin, J.; Banaszczyk, M.; Jubian, V.; Zou, X. *J. Am. Chem. Soc.* 1989, 111, 186.

45 see part I . section 2.3

46 a) ref 12 ,b) Tobe, M. L. in *Advanced in Inorganic and Bioorganic Mechanisms*; Sykes, A. G. Ed.; Academic Press: London, 1983, Vol. 2, p. 1.

$$\text{Rate} = k [\text{Co}(\text{OH})(\text{OH}_2)] [\text{RCN}] \quad \text{.....eq 3.1}$$

where  $k$  is the second order rate constant for nitrile hydration catalyzed by the aqua-hydroxy species. The cobalt complex exists in three different protonation states and the acid dissociation constants  $K_1$  and  $K_2$  are given by eq 3.2.

$$K_1 = \frac{[\text{Co}(\text{OH})(\text{OH}_2)] [\text{H}^+]}{[\text{Co}(\text{OH}_2)_2]} \quad K_2 = \frac{[\text{Co}(\text{OH})_2] [\text{H}^+]}{[\text{Co}(\text{OH})(\text{OH}_2)]} \quad \text{.....eq 3.2}$$

The total concentration of the cobalt complex,  $[\text{Co}]_{\text{tot}}$ , can be expressed by eq 3.3.

$$[\text{Co}]_{\text{tot}} = [\text{Co}(\text{OH}_2)_2] + [\text{Co}(\text{OH})(\text{OH}_2)] + [\text{Co}(\text{OH})_2] \quad \text{.....eq 3.3}$$

By substituting eq 3.2 into eq 3.3,  $[\text{Co}]_{\text{tot}}$  can be expressed as a function of the concentration of the aqua-hydroxy species.

$$[\text{Co}]_{\text{tot}} = [\text{Co}(\text{OH})(\text{OH}_2)] \frac{K_1 K_2 + K_1 [\text{H}^+] + [\text{H}^+]^2}{K_1 [\text{H}^+]} \quad \text{.....eq 3.4}$$

By substituting eq 3.4 into eq 3.1, the rate can be expressed as a function of the total catalyst concentration.

$$\text{Rate} = k \frac{K_1 [\text{H}^+] [\text{Co}]_{\text{tot}} [\text{RCN}]}{K_1 K_2 + K_1 [\text{H}^+] + [\text{H}^+]^2} \quad \text{.....eq 3.5}$$

Therefore, the pseudo first order rate constant,  $k_{\text{obs}}$ , is expressed in eq. 3.6.

$$\text{Rate} = k_{\text{obs}} [\text{Co}]_{\text{tot}}$$

$$k_{\text{obs}} = k [\text{RCN}] \frac{K_1 [\text{H}^+]}{K_1 K_2 + K_1 [\text{H}^+] + [\text{H}^+]^2} \quad \text{.....eq 3.6}$$

As proposed for the metal complex promoted hydrolysis of phosphate esters\*, there can be three possible mechanisms involved in the cyclen complex catalyzed hydration of acetonitrile.

---

\* see part I

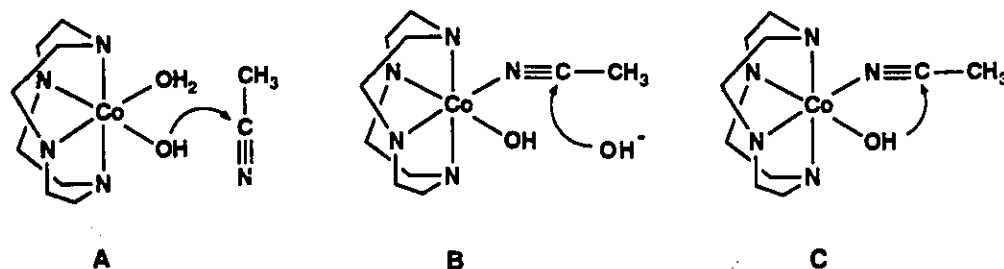


**Figure II.18** Three possible mechanisms for the cobalt complex catalyzed hydration of acetonitrile.

The first mechanism (A) involves intermolecular hydroxide attack which can be easily ruled out according to Table II.1. If mechanism A is correct, all complexes compared should give the same rate for nitrile hydration since the basicities of metal hydroxides are about the same. The second mechanism (B) involves coordination of acetonitrile followed by intermolecular hydroxide attack. The third mechanism (C) involves coordination of acetonitrile followed by intramolecular hydroxide attack. The pseudo first order rate constant for the hydration of  $[(\text{NH}_3)_5\text{Co}(\text{III})\text{NCCH}_3]$  in water to give the acetamide bound cobalt complex is  $3.4 \times 10^{-7} \text{ sec}^{-1}$  at pH 7.0 and 25 °C.<sup>2</sup> If the second mechanism is correct, the expected maximum rate of product formation for the cyclen complex (0.01M) catalyzed hydration of acetonitrile (0.5M) is  $3.4 \times 10^{-9} \text{ M sec}^{-1}$ . This is too slow to account for the observed rate of product formation ( $3.2 \times 10^{-6} \text{ M sec}^{-1}$ ). Furthermore, hydroxide catalyzed hydration of  $[(\text{NH}_3)_5\text{Co}(\text{III})\text{NCCH}_3]$  is accompanied by proton exchange for the methyl group.<sup>2</sup> For the acetonitrile complexes of pentaammine Co(III), Rh(III), and Ir(III), 35% of the protium label was lost to solvent during the hydrolysis in 0.5M NaOD solution.<sup>11</sup> In sharp contrast, the cyclen complex catalyzed hydration of acetonitrile does not show any proton exchange for the methyl group. The third mechanism C is consistent with the observed rate enhancement as well as the lack of any proton exchange for the methyl group. Above all, the strongest evidence for mechanism C is the formation of a chelated amide during the hydrolysis. As discussed in the previous section 3.1, the tmcyclen complex forms the chelated acetamide reacting with acetonitrile, but not with acetamide. This is due to unfavorable interconversion of the singly bound acetamide caused by two methyl groups (Fig. II.19).

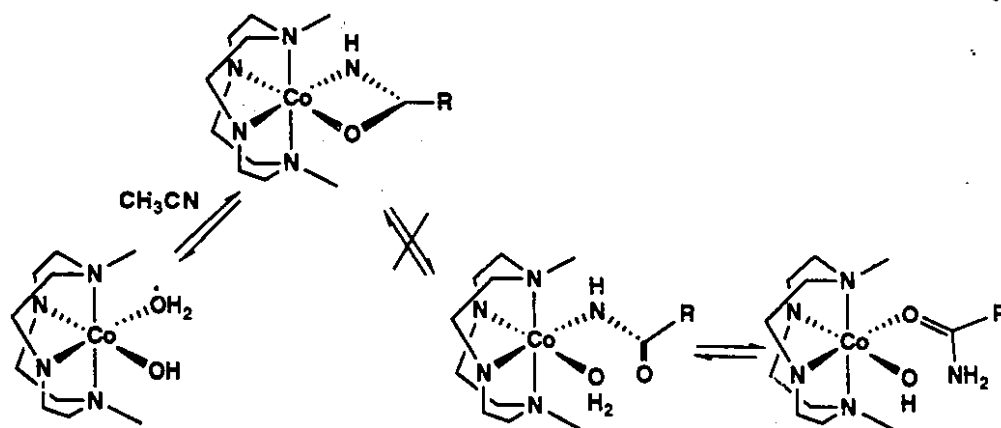


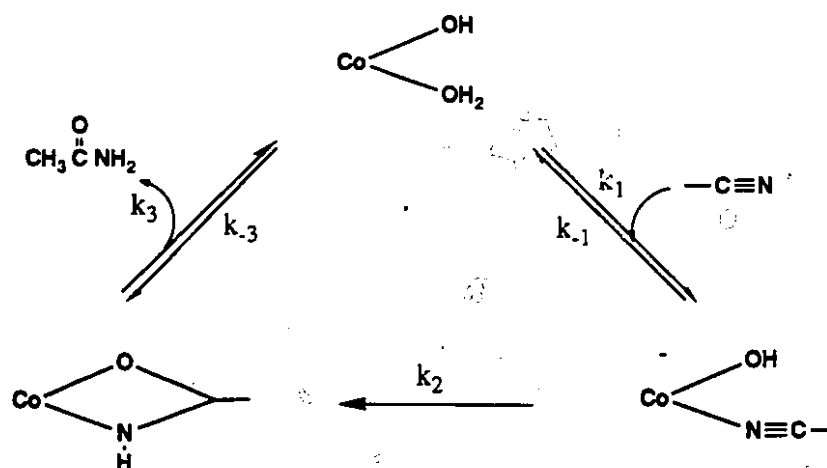
**Figure II.19** Restricted interconversion of a chelated amide to a monodentate amide.

Both mechanisms **A** and **B** lead to the initial formation of a singly coordinated acetamide, whereas mechanism **C** leads directly to the chelated acetamide. Since chelated acetamide can not be formed from singly coordinated acetamide, mechanisms **A** and **B** must be incorrect. The tricyclic complex should hydrate nitriles by the same mechanism as the cyclen complex since they have comparable reactivities for the chelated amide formation (section 2.1.6). We therefore propose that mechanism **C** is correct. Related mechanisms involving intramolecular metal hydroxide attack on the metal coordinated substrates have been proposed for Co(III) complex promoted hydrolysis of phosphate mono-, di-, and tri-esters as well as for carboxylate esters.<sup>47</sup>

It was mentioned that hydration of nitriles by various metal(III) complexes is stoichiometric rather than catalytic because the catalyst forms a stable amide metal complex. However, hydration of nitriles mediated by the cyclen complex is catalytic. A catalytic mechanism consistent with all of our experimental observations is given in Scheme II.5. The catalytic mechanism involves (a) equilibrium coordination of acetonitrile to the cobalt complex ( $k_1 / k_{-1}$ ) followed by (b) conversion of the cobalt bound nitrile to the chelated amide ( $k_2$ ) and (c) expulsion of the amide from the cobalt complex ( $k_3$ ). The first step ( $k_1, k_{-1}$ ) is faster than the second step ( $k_2$ ) which in turn is faster than the third step ( $k_3, k_{-3}$ ). As shown below, all of the rate constants in Scheme II.5 can be measured.

<sup>47</sup> Chin, *J. Acc. Chem. Res.* 1991, 24, 145.

**Scheme II.5** Catalytic cycle for the hydration of acetonitrile by (cyclen)Co(III)(OH)(OH<sub>2</sub>) at pD 7.



The first step of the catalytic cycle involves coordination of acetonitrile to the cobalt complex. The first and second  $pK_a$  values of the two cobalt bound water molecules in the cyclen complex are 5.4 and 7.9. Hydration of nitriles takes place at a pH in between the two  $pK_a$  values indicating that the active form of the catalyst is the aqua hydroxy form (section 2.1.2). At pD 2, complexation of acetonitrile to the cyclen cobalt complex was monitored by UV/VIS methods free from the hydration reaction.

The rate of exchange of the cobalt bound water molecules in the cyclen complex increases with increasing pH. Hence the rate of complexation and dissociation of acetonitrile also increases with increasing pH. A plot of  $k_1^{obs}$  vs  $[CH_3CN]$  gives a straight line with a slope that corresponds to  $k_1$  and an intercept that corresponds to  $k_{-1}$  (section 2.1.5). The equilibrium constant for the complexation of acetonitrile to the cyclen complex is  $0.6 \text{ M}^{-1}$ . This shows that, mole per mole, acetonitrile has a higher affinity than water for the cobalt complex even though acetonitrile is over ten orders of magnitude less basic than water.<sup>48</sup>

Complexation of acetonitrile to the cyclen complex could also be detected by <sup>13</sup>C NMR. Addition of acetonitrile to a solution of the cyclen complex at pD 2 gives rise to three nitrile carbon signals, which correspond to free and two singly bound acetonitriles (section 2.2.1). Under the experimental conditions, either of the two, but not both

<sup>48</sup> Deno, N. C.; Gaugler, R. W.; Wisotsky, M. J. *J. Org. Chem.* 1966, 31, 1967.

coordinated water molecules in the cyclen complex can be replaced by acetonitrile (section 3.1).

The second step of the catalytic cycle involves intramolecular nucleophilic attack of coordinated hydroxide on the coordinated nitrile. The acetonitrile hydration catalyzed by the cyclen complex was monitored by  $^{13}\text{C}$  and  $^1\text{H}$  NMR. It was shown that the concentration of the chelated amide accumulates to saturation before any free amide can be detected. The rate determining step must be the release of the amide from the chelate. Conversion of free acetonitrile to the chelated amide was monitored by UV/VIS methods (section 2.1.6). From a plot of  $k_2^{\text{obs}}$  vs  $[\text{CH}_3\text{CN}]$ ,  $K = 2.5 \text{ M}^{-1}$  and  $k_2 = 4.7 \times 10^{-3} \text{ sec}^{-1}$  were obtained. It appears that acetonitrile binds more tightly to the aqua hydroxy form of the cyclen complex than to the diaqua form. It should also be noted that the aqua hydroxy form undergoes ligand exchange more rapidly than the diaqua form.

Formation of chelated acetamide from the tmcyclen complex and acetonitrile can also be monitored by UV/VIS methods and analyzed by using eq 2.3 (section 2.1.6). Both  $K$  ( $2.3 \text{ M}^{-1}$ ) and  $k_2$  ( $2.8 \times 10^{-3} \text{ sec}^{-1}$ ) values for the tmcyclen complex are comparable to those for the cyclen complex. This is consistent with the proposed bifunctional mechanism since they have comparable reactivities for the chelated amide formation.

The last step of the catalytic cycle involves protonation followed by dissociation of the cobalt bound acetamide to yield the free amide. At high concentration of acetonitrile, the rate of formation of the free amide as detected by  $^1\text{H}$  NMR is zero order with respect to the acetonitrile concentration. This is because the cobalt complex has been saturated in the chelated form. The maximum rate (Fig. II.7) is then given by  $k_3[\text{Co}]_{\text{tot}}$  where  $[\text{Co}]_{\text{tot}}$  is the total cobalt complex concentration. An Eadie-Hofstee plot of the steady state data gives a  $k_3$  of  $4.0 \times 10^{-4} \text{ sec}^{-1}$ . The rate constants for the complexation of acetamide,  $k_3$  and  $k_{-3}$ , were also obtained by monitoring the equilibrium chelation of acetamide to the cyclen complex at neutral pH by UV/VIS methods (section 2.1.7). An intercept,  $k_3$  ( $3.3 \times 10^{-4} \text{ sec}^{-1}$ ) and a slope,  $k_{-3}$  ( $6.3 \times 10^{-4} \text{ M}^{-1} \text{ sec}^{-1}$ ) were obtained from a plot of  $k_3^{\text{obs}}$  vs  $[\text{acetamide}]$ . The  $k_3$  values obtained from the above two methods are in good agreement although the one obtained from the equilibration experiment should be more accurate. The equilibrium constant for the chelation of acetamide to the cyclen complex at neutral pH is  $1.9 \text{ M}^{-1}$ .

Overall, the observed rate constant,  $k_3$  ( $4 \times 10^{-4} \text{ sec}^{-1}$ ) for the hydration of the cobalt bound acetonitrile at pH 7 and  $40^\circ\text{C}$  corresponds to a  $10^9$  fold rate enhancement over the hydroxide rate ( $1.6 \times 10^{-13} \text{ sec}^{-1}$ ) at neutral pH and  $25^\circ\text{C}$ .

### 3.3.2 Regioselective hydration of acrylonitrile to acrylamide

Acrylamide results from the hydration of the CN bond of acrylonitrile. Numerous studies have been done to develop catalysts which give only acrylamide since unlike saturated nitriles, acrylonitrile may undergo hydration at both C-C and C-N multiple bonds.<sup>49</sup> Most catalysts including metal ions (Co(III), Fe(II)/Fe(III), Pt(II), Ni(II)) or metal oxides (Cu(II), Ni(II), Co(II)), give a mixture of  $\beta$ -cyanoethanol (ethylene-cyanohydrin) and  $\beta$ -dicyanoethyl ether as well as acrylamide. These results can be predicted by considering the mechanism involved in the hydration process. For example, *trans*-Pt(II)H(OH)(PMe<sub>3</sub>)<sub>2</sub>, which hydrates acetonitrile to acetamide efficiently, displays low regioselectivity towards acrylonitrile hydration.<sup>7</sup> The reaction mechanism in the Pt complex catalyzed hydration involves the external hydroxide as a nucleophile, so that the coordinated olefin as well as the nitrile CN bond becomes the target for a nucleophilic attack.

It was proposed\* that the intramolecular hydroxide attack on the coordinated nitrile is the important step during the hydration of acetonitrile catalyzed by the cyclen complex. It was also demonstrated that the rate of external metal hydroxide attack on the nitrile carbon is much faster than the rate of proton exchange on the  $\alpha$ -carbon.<sup>2</sup> If the same mechanism is applied to hydration of acrylonitrile, the rate of the nitrile C-N bond hydration would be greater than that of the olefin C-C bond hydration.

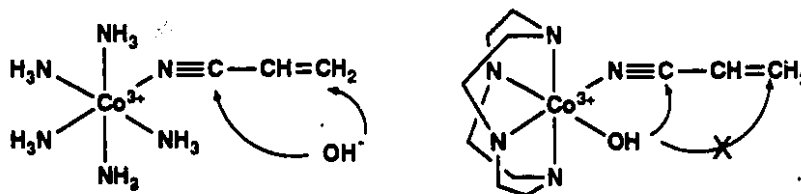


**Figure II.20** Intramolecular metal hydroxide attack vs intermolecular hydroxide attack on acrylonitrile.

Experiments were carried out under the same conditions used as for acetonitrile hydration (10mM cobalt complex, 0.1M acrylonitrile, pD 7 and 40 °C). Acrylamide production was monitored by <sup>1</sup>H NMR and there was no indication for formation of side

49 in *The Chemistry of Acrylonitrile*; American Cyanamid Company Petrochemicals Department; American Cyanamid; New York, 1957.

\* this study

products.\*\* (Cyclen)Co(III)(OH)(OH<sub>2</sub>) shows high regioselectivity for the acrylamide production. Detailed kinetic studies have not been carried out since this high regioselectivity can only be explained through the bifunctional mechanism as proposed for the acetonitrile hydration.

(Cyclen)Co(III)(OH)(OH<sub>2</sub>) can also be used in organic synthesis. The advantages over other catalysts are: a) its high reactivity and selectivity, b) catalytic turnover, c) requirement of relatively mild reaction conditions (room temperature to 80 °C and neutral pH), and d) versatility in the solvent selection. For example, benzonitrile, which is only slightly miscible with water, is completely hydrated to the corresponding amide (Table II.4).

### 3.4 Concluding Remarks

The three most important criteria in developing a perfect catalyst are reactivity, selectivity, and turnover number. Unlike enzymes, simple catalysts are far from being perfect. Nevertheless, the cyclen complex is an excellent catalyst for the hydrolysis of nitriles. The catalytic mechanism involving intramolecular metal hydroxide attack on the Co(III) complex coordinated nitrile allows for unprecedented reactivity and selectivity. Furthermore, rapid dissociation of the product from the metal complex allows for the catalytic turnover to take place for the first time using a Co(III) complex.

---

\*\* confirmed by GC.

**PART III    HYDROLYSIS OF AMIDES PROMOTED BY COBALT(III)  
COMPLEXES**

# 1 INTRODUCTION

## 1.1 Artificial Peptidases

Proteins play a key role in virtually all biological processes.<sup>1</sup> Nearly all catalysts in biological systems are proteins called enzymes that determine the pattern of chemical transformations in cells. They mediate a wide range of other functions, such as transport and storage, coordinated motions, mechanical supports, immune protection, excitability, integration of metabolism, and the control of growth and differentiation. Proteins are synthesized from the basic twenty amino acids, which are joined by peptide linkages (amide bond). They perform the above functions through their specific sequence and structure, then they are degraded by enzymes.

The ability of proteolytic enzymes and chemical reagents to selectively cleave peptides and proteins at a defined sequence have greatly facilitated the sequence analysis of large or blocked proteins, functional analysis of protein domains, and structural analysis of receptors.<sup>2</sup> Only a limited number of selective peptide cleaving agents exist, in contrast to the wide array of selective nucleases available for analyzing and manipulating nucleic acid structure. The development of site specific peptidases for any defined sequence would greatly facilitate the mapping of protein structural domains, and may lead to the generation of new therapeutic agents which might selectively hydrolyze protein coats of viruses, cancer cells, or other physiological targets.<sup>3</sup>

There have been enormous research efforts in developing catalysts that cleave amides and esters for the above purposes, and also for understanding of the catalytic mechanism in general. With the aid of rapidly developing techniques, such as site directed mutagenesis, X-ray crystallography, and chemical and enzymatic kinetic analysis, enzyme structure-reactivity relationships are being revealed.<sup>4</sup> Studies of several hundred proteolytic enzymes from all types of organisms have shown that there are two major types of catalytic mechanisms. Some peptidases such as CPA, thermolysine, and angiotensin converting enzyme are activated by metal ions, while other peptidases such as chymotrypsin, papain, and pepsin have serine, thiol, and carboxylic functionalities in the active site of the enzymes, respectively.

---

1 a) Stryer, L. in *Biochemistry*, 3rd Ed.; W. H. Freeman : New York, 1988. b) Bruice, T. C.; Benkovic, S. in *Bioorganic Mechanisms*; W. A. Benjamin: New York, 1966; Vol. 2.

2 Hoyerr, D.; Cho, H.; Schultz, P. G. *J. Am. Chem. Soc.* **1990**, 112, 3249.

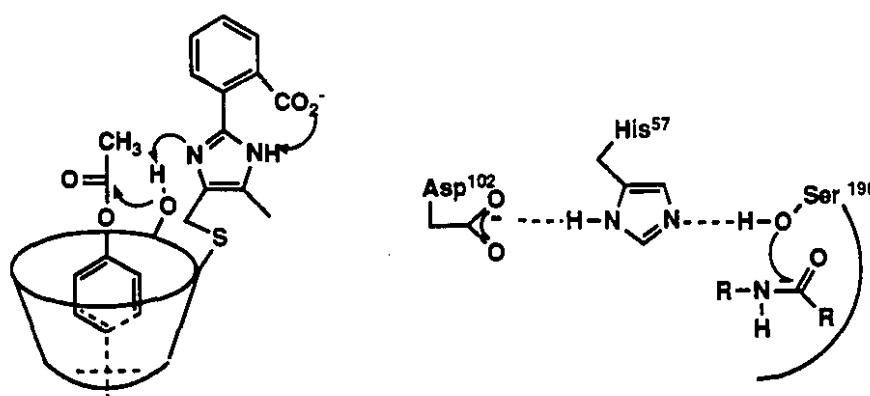
3 Schultz, P.G.; Lerner, R. A.; Benkovic, S. *J. Chem. Eng. News* **1990**, 68(22),26.

4 a) Gardel, S. J.; Craik, C. S.; Hilvert, D.; Urdea, M. S.; Rutter, W. J. *Nature (London)*, **1985**, 317, 551. b)

c) Breslow, R.; Chin, J.; Hilvert, D.; Trainer, G. *Proc. Natl. Acad. Sci. U. S. A.* **1983**, 80, 4585.

The basic strategy for developing artificial proteases is to incorporate these functional groups into one system, which usually includes specific binding groups.<sup>5</sup> Modified cyclodextrin designed by Bender et al. is a classical example of a representative model system where a covalently attached imidazole-benzoate and a secondary hydroxyl group mimic the triad function of chymotrypsin; while cyclodextrin provides a specific binding pocket.<sup>5</sup> It was later revealed that the reaction mechanism involved nucleophilic attack by 2'-hydroxyl group in the cyclodextrin, rather than a charge transfer mechanism.<sup>6</sup> The idea of developing an artificial enzyme was fully reflected, however.

Figure III.1



Other model systems which mimic enzyme esterases have been continuously developed and provide valuable information concerning molecular recognition as well as catalytic functions.<sup>7</sup> However an efficient artificial peptidase has never been reported. This is partly due to the stability of amide bonds and partly due to the lack of a sensitive detection method to monitor the slow process. A recently reported rate constant of  $3 \times 10^{-9} \text{ sec}^{-1}$  for the uncatalyzed hydrolysis of a peptide, corresponding to a half life of approximately 7 years, puts the difficulty of this reaction into perspective.<sup>8</sup>

There has been a new approach to cleave peptides by using catalytic antibodies.<sup>9</sup> A chemical potential of the immune system was underscored in 1986, when the research groups of Schultz and Lerner showed that antibodies raised to tetrahedral, negatively charged phosphate and phosphonate transition state analogs could selectively catalyze

5 D'Souza, V. T.; Bender, M. L. *Acc. Chem. Res.* 1987, 20, 146.

6 a) Breslow, R.; Chung, S. *Tetrahedron Lett.* 1989, 30, 4353. b) Zimmerman, S. C. *Tetrahedron Lett.* 1989, 30, 4357.

7 a) Lehn, J. M. *Science* 1985, 227, 849. b) Peterson, I. *Science News* 1987, 132, 90.

c) Rebeck, J. Jr. *Angew. Chem. Int. Ed. Engl.* 1990, 29, 245.

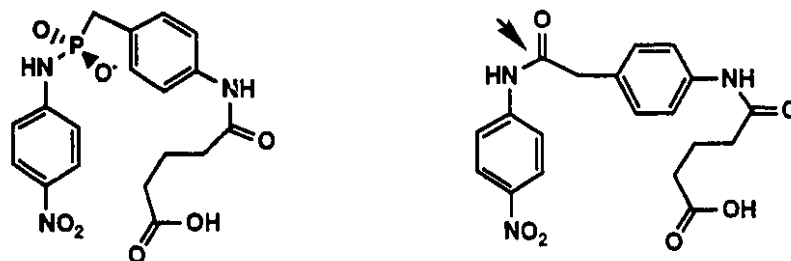
d) Tecilla, p.; Hamilton, A. D. *J. Chem. Soc., Chem. Commun.* 1990, 1232.

8 Kahne, D.; Still, W. C. *J. Am. Chem. Soc.* 1988, 110, 7529.

9 Lerner, R. A.; Benkovic, S. J.; Schultz, P. G. *Science*, 1991, 252, 659. and references therein

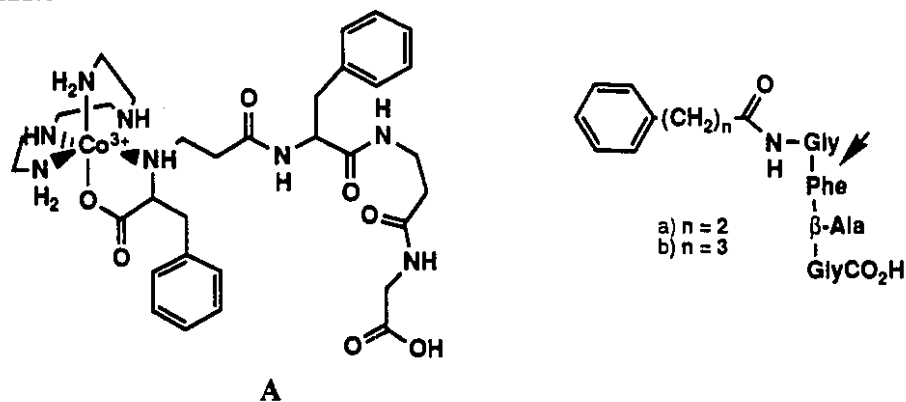
hydrolysis of carbonates and esters, respectively. Since then, antibodies have been generated that catalyze a wide array of chemical reactions including energetically demanding peptide hydrolysis. For example, monoclonal antibodies generated against a phosphoramidate, catalyzed the hydrolysis of the corresponding amide substrates with a rate acceleration of  $2.5 \times 10^5$  relative to background hydrolysis (Fig. III.2).<sup>10</sup>

Figure III.2



Also with antibodies raised against hapten A (Fig. III.3), cleavage was observed for substrates with the trien complex of metal ions such as Zn(II), Ga(III), Fe(III), and Cu(II).<sup>11</sup>

Figure III.3



General strategies for the development of catalytic antibodies include a) the use of antibodies to stabilize negatively or positively charged transition states (Fig. II.2), b) the use of antibodies as entropic traps, and c) the generation of antibodies with catalytic groups and cofactors in their binding sites (Fig. II.2). Although catalytic antibodies have been shown to hydrolyze peptides with great efficiency (typical rate enhancements are in the range of  $10^3$  to  $10^6$  compared to that of the uncatalyzed reaction), their reactivity depends on the

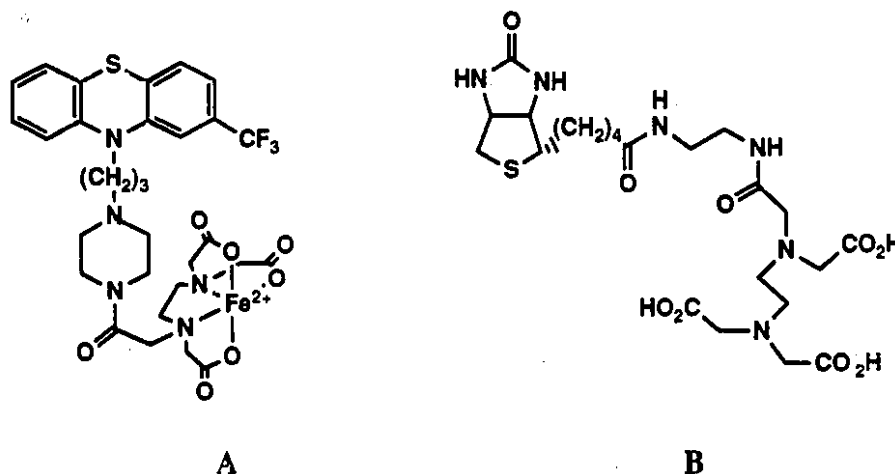
<sup>10</sup> Janda, K. D.; Schloeder, D.; Benkovic, S. J.; Lerner, R. A. *Science*, 1988, 241, 1188.

<sup>11</sup> Iverson, B. L.; Lerner, R. A. *Science*, 1989, 243, 1184.

diversity of immune response when they were generated. The rate enhancement obtained from amide hydrolysis (Fig. III.2) results, only in part, from differential stabilization of the transition state by the antibody. Other factors such as acid or base catalysis or ground state destabilization are also involved in the catalysis. Generation of an antibody combining site with these additional catalytic interactions could simply be the result of immunological diversity.

Concerning the sequence specificity of protein cleavage, a few agents have been developed.<sup>2,12</sup> Schepartz's group has shown that EDTA, which is covalently tethered to calmodulin antagonist trifluoperazine (TFP), cleaves calmodulin to produce six major fragments in the presence of Fe(II), Ca(II), and oxygen (Fig. III.4-A)<sup>12a</sup> Similarly, Schultz has shown that biotin-EDTA Cu(II) chelate cleaves streptavidin in close proximity to the biotin binding site, also in the presence of oxygen (Fig. III.B).<sup>12c</sup>

Figure III.4



These somewhat efficient protein cleaving agents may achieve sequence specific cleavage, but their catalysis is based on the oxidative cleavage of the protein backbone, while natural enzymes cleave peptides hydrolytically.

Therefore, there is a need for developing a simple, yet efficient catalyst that can cleave amides hydrolytically and the detailed mechanistic studies based on these model systems will give valuable information on understanding the catalytic mechanism of peptidases.

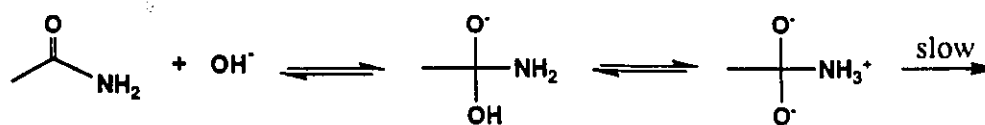
12 a) Cuenoud, B.; Schepartz, A. *J. Am. Chem. Soc.* **1990**, *112*, 3247. b) Rana, T. M.; Mears, C. F. *J. Am. Chem. Soc.* **1990**, *112*, 2457. c) Hoyerr, D.; Cho, H.; Schultz, P. G. *J. Am. Chem. Soc.* **1990**, *112*, 3249.

## 1.2 Mechanism of Amide Hydrolysis

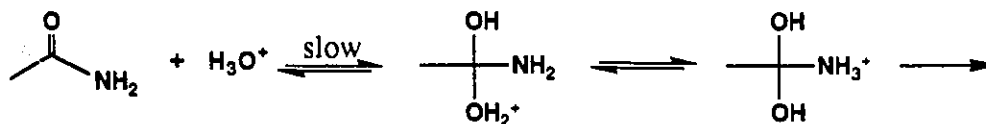
The hydrolysis of amides can occur under both acidic and basic conditions and requires vigorous conditions.<sup>13</sup> Because of this, most studies on amide hydrolysis have been focused on model systems involving activated amides such as p-nitroanilide and activated acyl amides or intramolecular catalysis.<sup>14</sup>

Base catalyzed hydrolysis of unactivated amides, such as acetamide, involves addition of hydroxide to the amide forming a tetrahedral intermediate followed by proton transfer to give an anionic zwitterion and the rate determining expulsion of the amine leaving group.<sup>15</sup>

Scheme III.1



(a) base catalyzed hydrolysis of unactivated amide



(b) acid catalyzed hydrolysis of unactivated amide

Since amide hydrolysis involves a poor leaving group (formally  $\text{RNH}^-$ ), the amide nitrogen must be protonated either prior to, or in concert with C-N bond cleavage. This is why intramolecular catalysis of 4-hydroxybutyramide is more efficient at neutral pH than at high pH by ca. 800 fold.<sup>16</sup> The breakdown of the tetrahedral intermediate may also be subject to GAC under neutral conditions. It has previously been demonstrated that both external

13 a) Carey, F. A.; Sunberg, R. J. in *Advanced Organic Chemistry, Part A*, 3rd Ed.; Plenum Press: New York, 1984. b) Dugas, H. in *Bioorganic Chemistry; A Chemical Approach to Enzyme Action*, 2nd Ed.; Springer-Verlag: N. Y., 1989.

14 a) O'Connor, C. Q. *Rev. Chem. Soc.* **1970**, *24*, 553.

b) Pollack, R. M.; Bender, M. L. *J. Am. Chem. Soc.* **1970**, *92*, 7190.

c) Kershner, L. D.; Schowen, R. L. *J. Am. Chem. Soc.* **1971**, *93*, 2014.

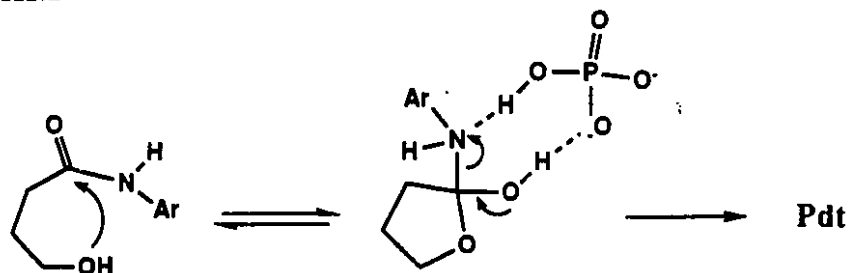
b) Kirby, A. J.; Lancaster, P. W. *J. Chem. Soc., Perkin Trans. II*, **1972**, 1206.

15 a) Kirby, A. J.; Ferscht, A. *Prog. Bioorg. Chem.* **1971**, *1*, 1. b) Drake, D.; Schowen, R. L.; Jayaraman, H. *J. Am. Chem. Soc.* **1973**, *95*, 454. c) Kluger, R.; Chin, J. *J. Am. Chem. Soc.* **1982**, *104*, 4154. d) Slebocka-Tilk, H.; Bennet, A. J.; Keillor, J. W.; Brown, R. S.; Guthrie, J. P.; Jodhan, A. *J. Am. Chem. Soc.* **1990**, *112*, 8507.

16 Bruce, T. C.; Marquardt, F. H. *J. Am. Chem. Soc.* **1962**, *66*, 365.

and intramolecular GAC greatly facilitate amide hydrolysis.<sup>17</sup> Interestingly, bifunctional buffers, such as phosphate and carbonate, are often found to be efficient catalysts in hydrolyzing amides.<sup>15a</sup> They accelerate hydrolysis through protonation of the leaving group nitrogen and deprotonation of the hydroxyl function as shown in Scheme III.2. In contrast, imidazole buffer does not induce any rate acceleration suggesting that the buffer structure plays an important role in hydrolysis reactions.

**Scheme III.2**



Catalysis by protons at low pH results in rapid C-N bond cleavage, where the rate determining step becomes the formation of the tetrahedral intermediate.<sup>18</sup>

### 1.3 Metal assisted Hydrolysis of Amides

There have been extensive studies on the metal ion catalyzed hydrolysis of esters and amides since Kroll's discovery of the hydrolysis of amino acid esters catalyzed by Cu.<sup>19</sup> Many studies have involved substitutionally inert Co(III) complexes in order to avoid the mechanistic ambiguities that may be caused by labile divalent metal complexes. There are at least two mechanisms observed in both enzymatic<sup>20</sup> and model systems<sup>21</sup> in hydrolyzing amide bonds by using metal ions. The first mechanism involves the metal ion acting as a Lewis acid while the second mechanism involves a metal hydroxide. In the case of stoichiometric Co(III) promoted amide hydrolysis in aqueous solution, both mechanisms

17 a) Chin, J.; Breslow, R. *Tetrahedron Lett.* **1982**, 4221. b) Venkatasubban, K. S.; Schowen, R. L. *J. Org. Chem.* **1984**, 49, 653.

18 Challis, B. C.; Challis, J. A. in *The Chemistry of Amides*; Interscience; Zabicky, J. Ed.; Interscience: London, N. Y., 1970; p 814

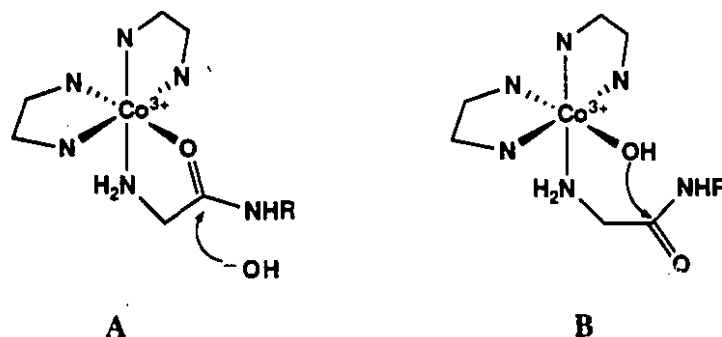
19 Kroll, H. *J. Am. Chem. Soc.* **1952**, 74, 2036.

20 a) Lipscomb, W. N. *Acc. Chem. Res.* **1982**, 15, 232. b) Mathews, B. W. *ibid.* **1988**, 21, 333.

21 a) Collman, J. P.; Buckingham, D. A. *J. Am. Chem. Soc.* **1963**, 85, 3039. b) Buckingham, D. A.; Foster, D. M.; Sargeson, A. M. *ibid.* **1970**, 92, 6151. c) Buckingham, D. A.; Davis, C. E.; Foster, D. M.; Sargeson, A. M. *ibid.* **1970**, 92, 5571. d) Brehm, C. J.; Buckingham, D. A.; Keene, F. R.; *J. Am. Chem. Soc.* **1979**, 101, 1409. e) Sutton, P. A.; Buckingham, D. A. *Acc. Chem. Res.* **1987**, 20, 357. and references therein. f) Schepartz, A.; Breslow, R. *ibid.* **1987**, 109, 1814. g) Groves, J. T.; Baron, L. A. *ibid.* **1989**, 111, 5442. h) Groves, J. T.; Chambers, R. R., Jr. *J. Am. Chem. Soc.* **1984**, 106, 630.

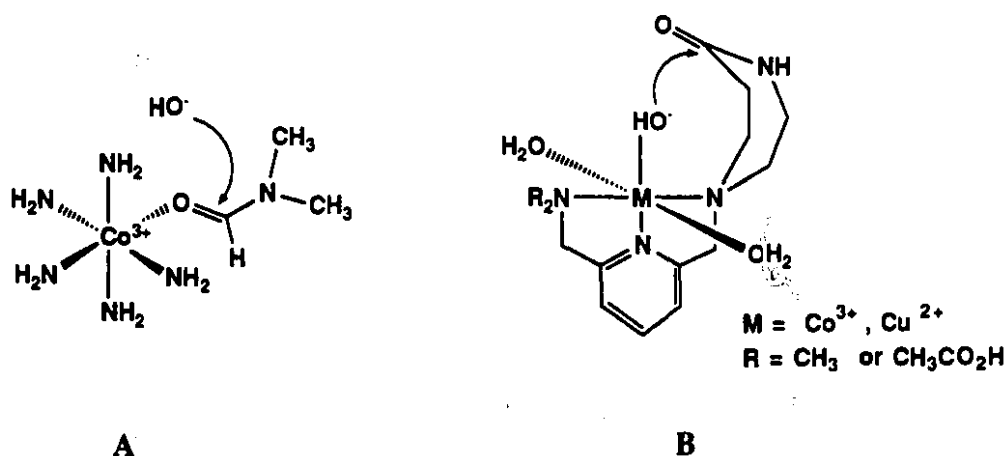
significantly increase the amide hydrolysis.<sup>21e</sup> It has been shown that in hydrolyzing glycine amide tethered to the cobalt via the amine group, intramolecular metal hydroxide attack (**B** in Fig. III.5) is  $10^2$  times faster than hydroxide attack on the chelated amide (**A** in Fig. III.5).<sup>21c,e</sup> In this system the carbonyl activation and the metal hydroxide alternative can be distinguished by oxygen isotope labeling experiments.

Figure III.5



These two types of metal activation have also been examined separately. Sargeson et al. have shown that the cobalt bound amide in  $\text{Co(III)(NH}_3)_5(\text{DMF})$  is hydrolyzed  $10^4$  times faster than free amide under basic conditions, where only the Lewis acid mechanism can take place (Fig. III.6-A).<sup>22</sup> One of the CPA models designed by Groves displayed  $10^7$  to  $10^8$  fold rate enhancements compared to the hydroxide at neutral pH, where only the metal hydroxide mechanism is possible due to geometrical constraints of the metal hydroxide (Fig. III.6-B).<sup>21g,h</sup>

Figure III.6

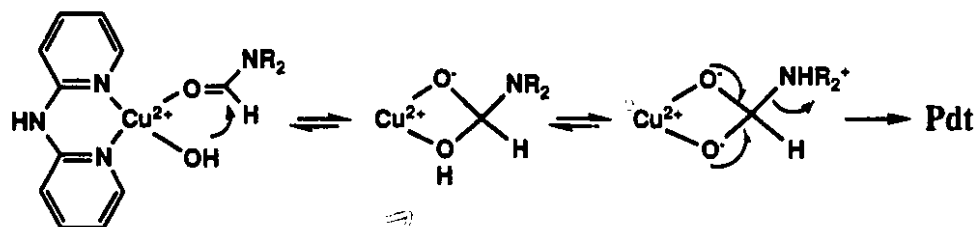


Whether the mechanism involves Lewis acid or metal hydroxide participation, there are certain things in common. Most studies have been done on activated amides or unactivated

amides either covalently attached through a chelated ligand or carefully designed not to bind through the amide nitrogen.

Recently, Chin et al. have shown that a simple copper complex can hydrolyze free unactivated amides such as DMF under reflux conditions.<sup>23</sup> The proposed mechanism includes features from both mechanisms: simultaneous carbonyl activation and intramolecular metal hydroxide attack. The rate acceleration has been ascribed to the chelation of the tetrahedral intermediate to  $(\text{dpa})\text{Cu}(\text{II})(\text{OH})_2$  by increasing concentration of reactive species (Scheme III.3). This result suggests that the bifunctional mechanism predominates over each mechanism alone and it is likely the role of metal ions in metalloenzymes such as CPA.<sup>24</sup> Interestingly, a considerably lower reactivity was observed for the mono aqua complex,  $\text{Cu}(\text{II})(\text{terp})(\text{OH})_2$  promoted hydrolysis of the same amides.

**Scheme III.3**



<sup>23</sup> Chin, J.; Jubian, V.; Mrejen, K. *J. Chem. Soc., Chem. Commun.* 1990, 1326.

<sup>24</sup> Christianson, D. W.; Lipscomb, W. N. *Acc. Chem. Res.* 1989, 22, 62.

## 1.4 Plan of Study

There is a great deal of interest in developing catalysts that hydrolyze amide efficiently and numerous reports exist for metal ion promoted hydrolysis of amides. Model systems include either highly activated amides or amides covalently linked to metal binding functionalities. Recently, it has been shown that a simple copper complex,  $(\text{dpa})\text{Cu}(\text{II})(\text{OH})(\text{OH}_2)$  ( $\text{dpa} = 2,2'$ -dipyridylamine) hydrolyzes free amides such as DMF at 100 °C. Studies on the nitrile hydration catalyzed by cobalt complexes suggest that  $\text{Co}(\text{III})$  complexes would give greater rate enhancements than  $\text{Cu}(\text{II})$  complexes. In addition, the substitutionally inert cobalt complex would make mechanistic studies easier.

My plan is to test the efficiency of the cyclen complex on carefully selected unactivated amides such as DMF or 4-formylmorpholine. Detailed kinetic studies will provide a mechanistic rationale for the observed hydrolysis. The measurement of equilibrium binding constants of amides to the cobalt complex will make it possible to compare the reactivity of this model system with enzymes.

## 2 RESULTS

### 2.1 Kinetics

Cobalt complex promoted hydrolysis of 4-formyl morpholine and DMF were monitored by  $^1\text{H}$  NMR. With the progress of the hydrolysis reaction, the intensities of the signals due to the formyl proton of 4-formyl morpholine decreases with the concomitant increase in formate and morpholine signals (Fig. III.7). The rate constants obtained by fitting data according to a second order kinetic equation ( $R > 0.98$ ) are listed in Table III.1. The  $^1\text{H}$  NMR spectrum obtained by reacting the cyclen complex with formate is identical to that obtained from the reaction mixture during the hydrolysis under the same conditions (Fig.III.8). Hydrolysis of DMF promoted by the cyclen complex was observed but the rate constant could not be obtained due to a signal overlap between the formate and the substrate.

**Table III.1** Observed second order rate constants ( $\text{M}^{-1} \text{sec}^{-1}$ ) for cobalt complexes promoted hydrolysis of 4-formyl morpholine at pD 5.9 and 60 °C.

catalyst	pKa	4-formyl-morpholine
cyclen	5.4 / 7.9	$8.0 \times 10^{-5}$
tetren	5.9	b)
$\text{OH}^-$ a)	.	$1.9 \times 10^{-2}$

a) the second order rate constant for 4-formylmorpholine at 60 °C was obtained from 2nd order rate constant at 25 °C ( $1.4 \times 10\text{M}^{-1}\text{sec}^{-1}$ ) by using the same activation parameters as for DMF hydrolysis. ref: Langlis, S.; Broche, A. *Bull. Soc. Chem. Fr.* 1964, 812.

b) the reaction is too slow to measure the rate constant

The cyclen complex is the most efficient catalyst in hydrolyzing amides, while the tetren complex does not hydrolyze the same substrates to any observable extent under the experimental conditions used.

**Figure III.7**  $^1\text{H}$  NMR spectrum of  $(\text{cyclen})\text{Co(III)(OH)(OH}_2)$  (0.1 M) catalyzed hydrolysis of 4-formyl morpholine (0.03 M) at (a)  $t = 0$ , and (b)  $t = 61.5$  hrs;  $\square$  = benzene (reference 7.2 ppm) and  $\nabla$  = 4-formylmorpholine.

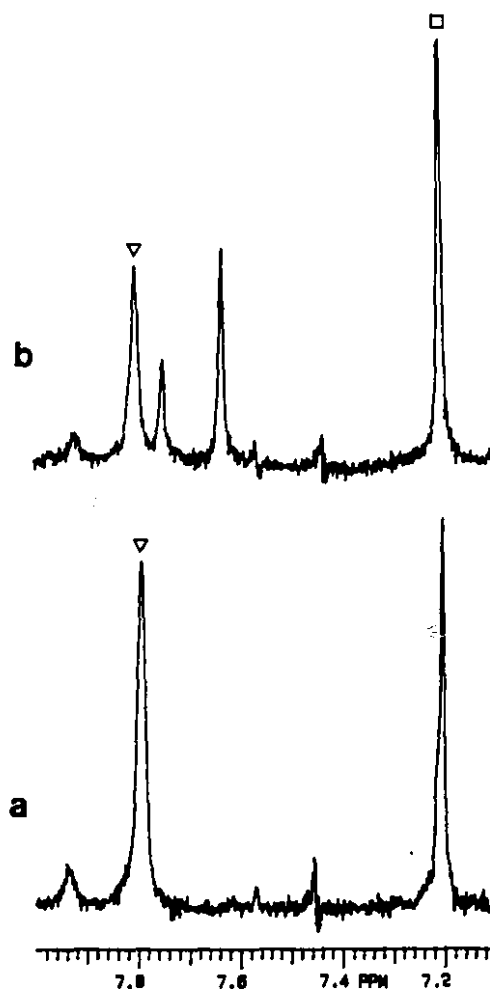
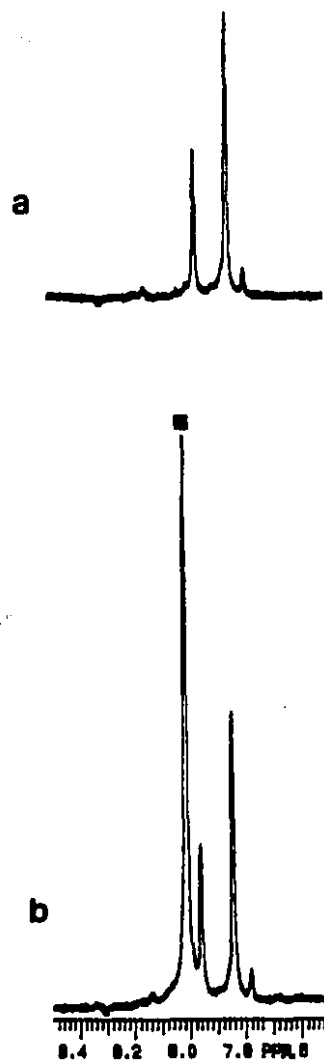


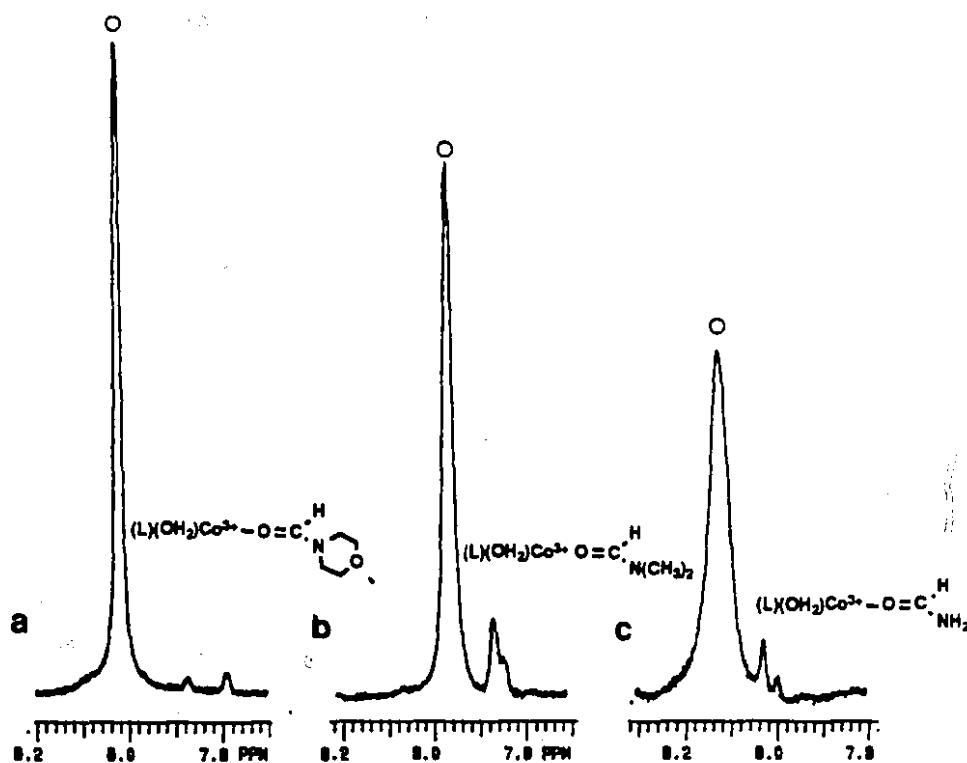
**Figure III.8**  $^1\text{H}$  NMR spectrum of  $(\text{cyclen})\text{Co}(\text{III})(\text{OH})(\text{OH}_2)$  (0.1 M) with a) formate (0.05 M), b) formate (0.05 M) and 4-formyl morpholine (0.05 M) at pD 5.9; ■ = 4-formylmorpholine



## 2.2 Binding of Amides to Cobalt complexes

Binding studies of DMF, 4-formylmorpholine, and formamide to cis-diaqua cobalt complexes have been carried out at pD 2 using  $^1\text{H}$  NMR methods. Under the experimental conditions, the cyclen complex and tmcyclen complex each produces two formyl proton signals upfield-shifted relative to that of the free amide (Fig. III.9). Equilibrium binding constants of amides to both the tmcyclen and the cyclen complexes are in the range of  $0.4$  to  $2 \text{ M}^{-1}$ .

**Figure III.9**  $^1\text{H}$  NMR spectrum of a) (cyclen)Co(III)(OH<sub>2</sub>)<sub>2</sub> and 4-formylmorpholine b) (tmcyclen)Co(III)(OH<sub>2</sub>)<sub>2</sub> and DMF, c) (tmcyclen)Co(III)(OH<sub>2</sub>)<sub>2</sub> and formamide; [Co] 0.1 M, [amide] 0.1 M, at pD 2: O = free amide.



### 3 DISCUSSION

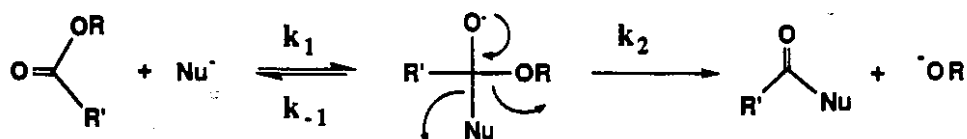
#### 3.1 Structural Requirements for the Catalysts

##### 3.1.1 Model studies based on ester hydrolysis

There has been a great deal of interest in developing artificial enzymes that hydrolyze amides and esters. Most of metallo-esterase and peptidases have been tested on activated esters due to the stability of amides.<sup>25</sup> Esters are more reactive than amides, (second order rate constants for hydroxide-catalyzed hydrolysis of methyl acetate and acetamide are  $1.5 \times 10^{-1} \text{ M}^{-1} \text{ sec}^{-1}$  and  $7.4 \times 10^{-5} \text{ M}^{-1} \text{ sec}^{-1}$ , respectively) so most peptidases hydrolyze esters as well as amides. The mechanism of ester hydrolysis is closely related to peptide hydrolysis since they both involve a formation of tetrahedral intermediate. Often, the knowledge obtained from studies on esters helps to elucidate the catalytic mechanism of peptidases, as in the case of chymotrypsin.<sup>5,25a</sup>

However, the structural requirement of a catalyst for hydrolyzing activated esters might not necessarily be the same as that for hydrolyzing unactivated esters.<sup>26,27,28</sup> Imidazole is only 100 times less reactive than hydroxide in hydrolyzing *p*-nitrophenylacetate, but millions of times less reactive than hydroxide for the hydrolysis of unactivated esters such as methyl trifluoroacetate.<sup>27</sup> The hydrolysis mechanism is shown in Scheme III.4.

Scheme III.4



And  $k^{\text{obs}}$  can be expressed by eq 3.1.

$$k^{\text{obs}} = k_1 k_2 / (k_{-1} + k_2) \quad \dots\dots\dots \text{eq 3.1}$$

The hydrolysis rate depends on the rate constants  $k_{-1}$  and  $k_2$ , which depend on the relative  $\text{pK}_a$  of the nucleophile and the leaving group in the tetrahedral intermediate. When the  $\text{pK}_a$  of the leaving group is lower than, or similar to that of the conjugate acid of the

25 a) Breslow, R. *Pure Appl. Chem.* 1990, 62, 1859. b) Lehn, J. M.; Sirlin, C. *J. Chem. Soc., Chem. Commun.* 1978, 949. c) Cram, D. J.; Lam, P. Y.; Ho, S. P. *J. Am. Chem. Soc.* 1986, 108, 839.

26 Menger, F. M.; Ladika, M. *J. Am. Chem. Soc.* 1987, 109, 3145.

27 Kirsch, J. F.; Jencks, W. P. *J. Am. Chem. Soc.* 1964, 86, 833 and 837.

28 Chin, J.; Zou, X. *J. Am. Chem. Soc.* 1984, 106, 3687.

nucleophile, the reaction proceeds to the product since the formation of a tetrahedral intermediate is the rate limiting step ( $k^{\text{obs}} = k_1$ , where  $k_{-1} \leq k_2$ ). This is the case for the imidazole ( $\text{pK}_a$  of 7) or hydroxide ( $\text{pK}_a$  of 15.5) catalyzed hydrolysis of *p*-nitrophenyl acetate ( $\text{pK}_a$  of *p*-nitrophenol 7.14). When the  $\text{pK}_a$  of the leaving group is higher than that of the nucleophile, the opposite situation occurs since the breakdown of the tetrahedral intermediate to product becomes the rate determining step ( $k^{\text{obs}} = k_1 \times k_2 / k_{-1}$ , where  $k_{-1} > k_2$ ). In the hydrolysis of methyl trifluoroacetate, hydroxide has a comparable  $\text{pK}_a$  to the leaving group alkoxide, so that the reaction can proceed to product, whereas imidazole can not compete with alkoxide and tetrahedral intermediate reverts back to starting material. In this situation, general base catalysis is observed by imidazole.

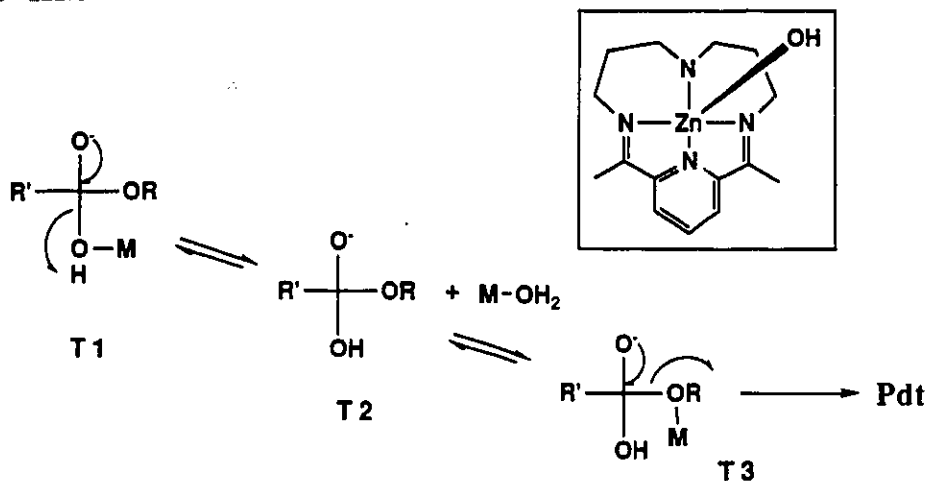
A somewhat different situation arises in metal mediated ester hydrolysis although the same kinetic interpretations can be applied. A simple monoaqua metal complex X (Scheme III.5) is found to be efficient in hydrolyzing methyl trifluoroacetate as well as *p*-nitrophenyl acetate, but not methyl acetate.<sup>28</sup> When a metal ion is involved in the hydrolysis, two types of mechanisms, which are kinetically indistinguishable, are possible. The Lewis acid mechanism can be ruled out based on the reactivity-selectivity principle.<sup>29</sup> According to this, the less reactive the ester, the greater the expected rate acceleration upon coordination to the metal. Since metal coordinated esters are more reactive towards nucleophilic attack than the corresponding free esters, hydroxide should be less selective towards the metal coordinated esters than to the free esters. Experimentally, less rate acceleration was observed for the less reactive esters (e.g. methyl acetate).

The other alternative, the metal hydroxide mechanism, is therefore likely involved in the catalysis. Scheme III.5 shows the tetrahedral intermediates arising from the metal hydroxide mechanism for ester hydrolysis. In the first formed tetrahedral intermediate T1, metal hydroxide ( $\text{pK}_a$  of 8.6) is a better leaving group than the methoxide ( $\text{pK}_a$  of 15), as in the case of imidazole catalyzed hydrolysis of methyl trifluoroacetate. This tetrahedral intermediate will revert back to starting materials unless proton transfer takes place to make the nucleophile a poorer leaving group or alkoxide a better leaving group. For the reaction to proceed to product, the metal has to migrate to the leaving group as shown in T3. This type of migration is possible with metal complexes due to their lability, whereas there is no counterpart in nonmetallic systems such as in imidazole catalyzed hydrolysis reaction. For methyl trifluoroacetate, the life time of T2 is long enough that there is rapid equilibrium between T1 and T3. In T3, the metal bound alkoxide is a better leaving group than the hydroxide and the reaction proceeds to product. However, this metal complex is still not

<sup>29</sup> Lowery, T. H.; Richardson, K. S. In *Mechanism and Theory in Organic Chemistry*; 3rd Ed.; Harper & Row: N. Y. 1987, p 148.

able to hydrolyze methyl acetate. In methyl acetate hydrolysis, the life time of the tetrahedral intermediate T2 is so short that the reaction does not proceed to product. Therefore, the life time of intermediate T2 plays a key role in the hydrolysis.<sup>30</sup>

Scheme III.5



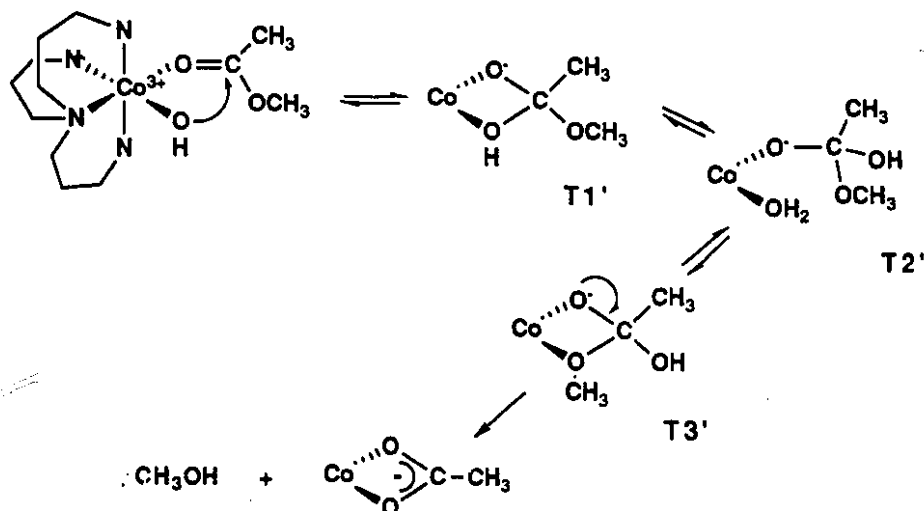
The structural requirements of a catalyst for hydrolyzing activated esters are not necessarily the same as that for hydrolyzing unactivated esters.

One way to hydrolyze unactivated esters is to increase the life time of the tetrahedral intermediate. Recently, it has been shown that the cis diaqua Co(III) and Cu(II) complexes can hydrolyze methyl acetate.<sup>31</sup> The proposed mechanism involves formation of a four-membered acetate intermediate T1'. The difference between the cis diaqua complex and the mono aqua complex is that the metal can coordinate and stabilize anionic oxygens in T1' and facilitate metal migration to form T3'.

30 a) Jencks, W. P. *Acc. Chem. Res.* **1980**, 13, 161. b) Guthrie, J. P. *ibid.* **1983**, 16, 122. c) McClelland, R. A.; Santry, L. J. *ibid.* **1983**, 16, 394.

31 a) Chin, J.; Jubian, V. J. *Chem. Soc., Chem. Commun.* **1989**, 839. b) Chin, J.; Banaszczyk, M. *J. Am. Chem. Soc.* **1989**, 111, 2724.

Scheme III.6



### 3.1.2 Amide hydrolysis

Although valuable information on the metal mediated hydrolysis of amides can be obtained from studies done on esters, there is a need to test catalysts on amide substrates because the structural requirement of a catalyst for hydrolyzing amides might not be the same as that for hydrolyzing esters.

There are several factors that have to be considered in developing catalysts for amide hydrolysis compared to ester hydrolysis.<sup>32</sup> First, the rate determining step of ester hydrolysis involves the relatively facile expulsion of an alkoxide leaving group, whereas amide hydrolysis involves a poor leaving group (NH<sub>2</sub> vs OR), which has to be protonated either prior to, or in concert with C-N bond cleavage. Second, there is a possibility for metal coordination to the amide nitrogen.<sup>33</sup> This interaction retards the hydrolysis reaction since a metal ion is not as good as a proton in activating leaving groups.<sup>34</sup> In the ester hydrolysis, bond cleavage occurs without protonation, so metal coordination to a leaving group alkoxide enhances reactivity towards hydrolysis. Furthermore, subsequent deprotonation of the coordinated amide NH can take place. Once substrates are deprotonated, they are not susceptible to nucleophilic attack by the hydroxide since the amide O-C-N bond is more delocalized than in the free form.<sup>35</sup> This is one reason why no

32 Sayer, L. M. *J. Am. Chem. Soc.* **1986**, 108, 1632. and references therein.

33 Sigel, H.; Martin, R. B. *Chem. Rev.* **1982**, 82, 385.

34 a) Martin, R. B. *J. Am. Chem. Soc.* **1967**, 89, 2501. b) Martin, R. B. *J. Inorg. Nucl. Chem.* **1976**, 38, 511.

35 Hay, R. W.; Basak, A. K.; Pujari, M. P.; Perotti, A. *J. Chem. Soc., Dalton Trans.* **1989**, 197.

further hydrolysis of acetamide to the corresponding acid was observed in acetonitrile hydration. This deprotonation occurs due to the  $pK_a$  lowering effect upon coordination to metal ions, which is greater for trivalent metal ions than it is for divalent metal ions.

Our group achieved free amide hydrolysis by using a cis diaqua copper complex (dpa)Cu(II)(OH<sub>2</sub>)(OH), under rather vigorous conditions.<sup>23</sup> One of my research projects was to study cobalt complex mediated hydrolysis of unactivated amides. We expected at least a 100 fold rate enhancement in the hydrolysis mediated by cobalt complexes, over by copper complexes. This is a quite reasonable expectation since in the model system designed by Groves (Fig. III.6 B)<sup>21g,h</sup>, hydrolysis of a azalactam occurs  $\sim 10^6$  and  $\sim 10^7$  times faster in the presence of cobalt(III) and copper(II), respectively in neutral water. Since the hydrolysis mechanism involves the metal hydroxides as a nucleophile, the reactivity difference is probably resulted from the difference in the basicity of the metal bound water molecules (5.9 vs 7.2).<sup>21g,h,38a</sup> Hence, ca. 10 fold rate enhancement can be obtained according to the metal hydroxide mechanism. In addition, cobalt(III) is a stronger Lewis acid than copper(II). The above two factors would result in a greater rate enhancement over for a Cu(II) complex.

4-Formyl morpholine and DMF were chosen as substrates since they are tertiary amides which do not have dissociable protons, and have moderately low reactivity towards hydrolysis. Primary or secondary amides can not be used for Co(III) complex promoted hydrolysis reactions because they bind to the metal ion tightly following deprotonation of amide NH. The formyl proton signals of the amides and the corresponding product acids make detection of hydrolysis possible by <sup>1</sup>H NMR methods.

### 3.2 Binding of Amides to Cobalt complexes

In order to fully understand the role of metal ions or complexes in amide hydrolysis it is important to know the equilibrium constants for complexation of amides to metal complexes. Although amides coordinated to Co(III) complexes have been synthesized,<sup>36</sup> the equilibrium constants for their formation have not been measured.

Equilibrium complexation of monodentate ligands such as dimethyl phosphate or acetate to cis-diaqua Co(III) complexes has been detected by <sup>31</sup>P NMR methods.

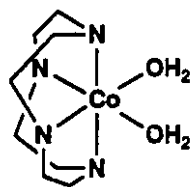
36 a) Angel, R. L.; Fairlie, D. P.; Jackson, W. G. *Inorg. Chem.* 1990, 29, 20. and references therein. b) Balahura, R. J.; Jordan, R. B. *J. Am. Chem. Soc.* 1970, 92, 1533.



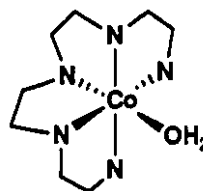
### 3.3 Hydrolysis of Amides promoted by [(cyclen)Co(OH<sub>2</sub>)<sub>2</sub>]<sup>3+</sup>

#### 3.3.1 Mechanism

The observed rate constant for (cyclen)Co(III)(OH)(OH<sub>2</sub>) (0.1M) promoted hydrolysis of 4-formylmorpholine at pD 6 and 60 °C is  $7.97 \times 10^{-5} \text{ M}^{-1} \text{ sec}^{-1}$  which is ca.  $4 \times 10^4$  times faster than that for the free amide under the same conditions (second order hydroxide rate constant  $1.9 \times 10^{-2} \text{ M}^{-1} \text{ sec}^{-1}$  at 60 °C) (Table III.1). In contrast, the monoaqua complex, (tetren)Co(III)(OH<sub>2</sub>) does not catalyze the hydrolysis of 4-formylmorpholine to any observable extent. The diaqua complex (cyclen) is at least two orders of magnitude more reactive than the monoaqua complex (tetren) in hydrolyzing 4-formyl morpholine.



cyclen



a-tetren

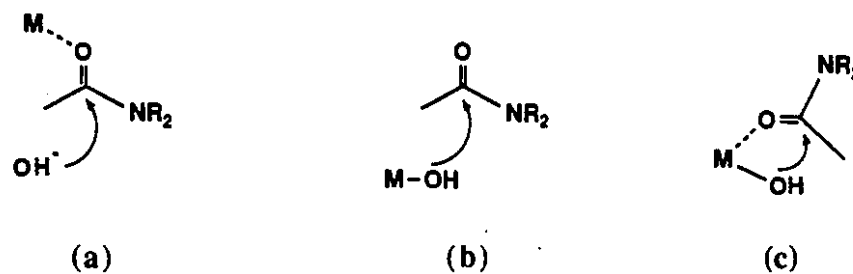
The lower reactivity for the tetren complex can not be due to any steric effect since (cyclen)Co(III)(OH<sub>2</sub>)(OH) and ([15]aneN<sub>5</sub>)Co(III)(OH<sub>2</sub>) are both efficient at hydrolyzing *p*-nitrophenyl acetate.<sup>37</sup> It can not be due to any electronic effect since the pK<sub>a</sub>s of the water molecules coordinated to the tetren and cyclen complexes are almost the same (5.4 vs 5.9). It is assumed that a metal coordinated nucleophile would have a nucleophilicity which broadly parallels its basicity.<sup>38</sup> The maximum rate difference induced from the electronic effect can not exceed 10 ΔpK<sub>a</sub>.

As discussed in section 3.1, there are two possible mechanisms for metal catalyst mediated hydrolysis of amides: Lewis acid and metal hydroxide mechanisms. For monoaqua complexes, only one of these mechanisms can take place, while for cis-diaqua complexes, both mechanisms can be involved at the same time.

37 a) Moore, A. Ph. D. Thesis, McGill University; 1990. b) Hay, R. W.; Bembi, R. *Inorg. Chim. Acta* **1982**, *64*, L179.

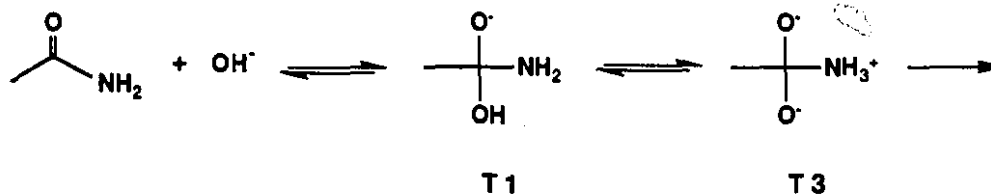
38 a) Buckingham, D. A., in *Biological Aspects of Inorganic Chemistry, Proceedings of the 1976 Symposium*; Addison, A.W. Ed.; Wiley-Interscience: New York, 1977.

Figure III.10



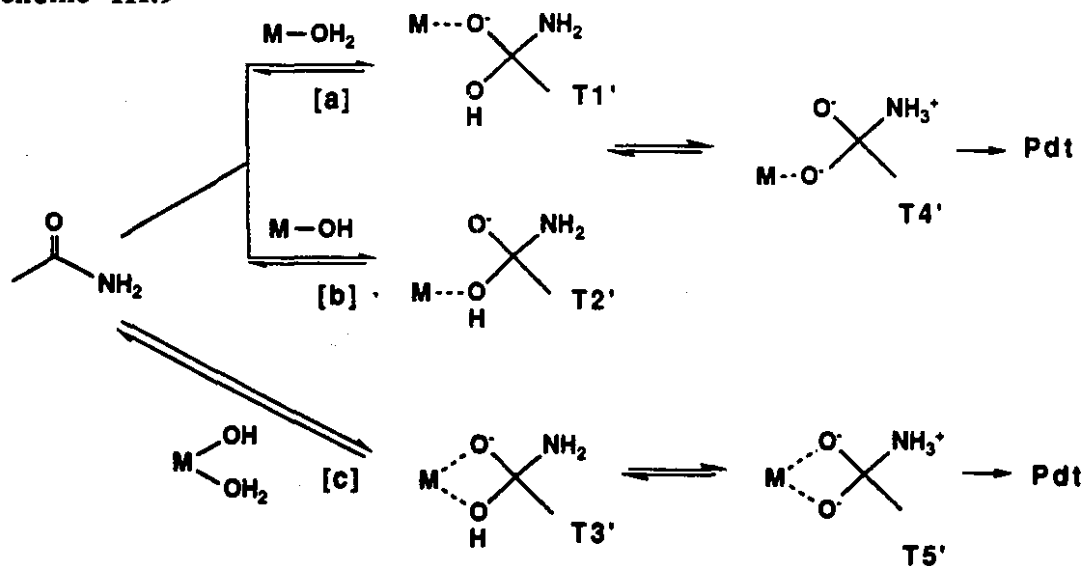
The simplest mechanism that can account for the reactivity difference between the tetren and the cyclen complexes is a bifunctional mechanism. The rate determining step for the hydrolysis of unactivated amides is likely the breakdown of the tetrahedral intermediate prior to, or followed by proton transfer (Scheme III.8). The hydrolysis rate of amides can therefore be accelerated by either stabilizing the tetrahedral intermediate through coordination or facilitating the proton transfer.

Scheme III.8



Scheme III.9 shows the possible tetrahedral intermediates arising from the above three mechanisms.

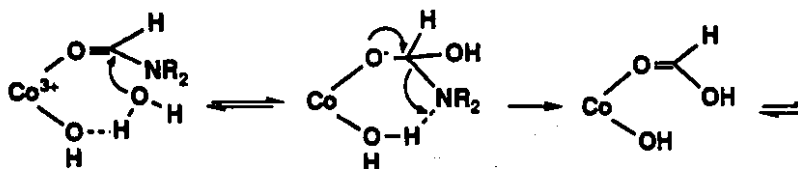
Scheme III.9



According to the experimental results, mechanism (c) predominates over the other two mechanisms. It would be reasonable to compare T4' and T5' instead of T1', T2' and T3' since proton transfer from the tetrahedral intermediate to the dianionic intermediate is rapid and C-N bond cleavage is the rate determining step in the hydrolysis of unactivated amides.<sup>15d</sup> One possible explanation for the difference in their reactivity is based on the difference in nucleophilicity involved in the rate-determining C-N bond cleavage. Breakdown of the tetrahedral intermediate to product can be regarded as a nucleophilic displacement of nitrogen by oxygen lone pairs. A rate for the displacement reaction is directly related to the nucleophilicity of electrons on the oxygens in the tetrahedral intermediates. In this respect, mechanism (b) would predominate over the other two since T2' has free anionic oxygen as a potent nucleophile. This is unlikely since it is known that metal coordination decreases the basicity of ligands significantly without greatly diminishing their nucleophilicity.<sup>32</sup> The best explanation for the different reactivity is better stabilization of the tetrahedral intermediate through chelation (mechanism (c)) over monodentate coordination. The high concentration of tetrahedral intermediate more than compensates for the reduced nucleophilicity of a potent nucleophile (compared to noncoordinated oxygen in mechanism (a) and (b)).

The other possible mechanism involves Lewis acid activation followed by general acid /base catalysis (Scheme III.10) which is difficult to differentiate from mechanism (c). However, the GBC mechanism is unlikely based on the following reasons.

Scheme III.10



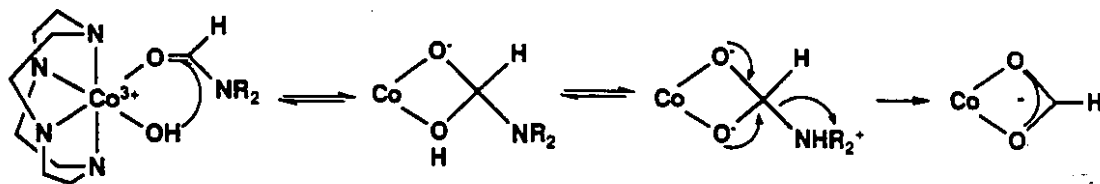
A bifunctional mechanism involving formation of a four-membered ring intermediate has been proposed in the *cis* diaqua cobalt complex mediated hydrolysis of phosphate esters, carboxylic esters, and nitriles.<sup>39</sup> It has also been shown that the amide bond in  $(\text{NH}_3)_5\text{Co(III)(DMF)}^{22}$  and  $([15]\text{janeN}_5)\text{Co(III)(DMF)}^{40}$  is hydrolyzed ca.  $10^2$  to  $10^4$  times more rapidly than free DMF under basic condition. This rate acceleration accounts for the Lewis acid activation. Almost the same rate enhancement can be expected for that in the hydrolysis of 4-formylmorpholine since base catalyzed hydrolysis of 4-formylmorpholine

<sup>39</sup> Chin, J. *Acc. Chem. Res.* 1991, 24,145.

<sup>40</sup> Hay, R. W.; Bembi, R. *Inorg. Chim. Acta* 1982, 64, L199.

is only 4 times slower than that of DMF.\*<sup>41</sup> Of the overall rate enhancement obtained in the cyclen complex promoted hydrolysis of 4-formylmorpholine, ca.  $10^2$  to  $10^4$  fold increase should result from the intramolecular metal hydroxide participation. This rate enhancement is much greater than can be obtained from the GBC mechanism.<sup>42</sup> A bifunctional mechanism, which involves carbonyl activation and intramolecular metal hydroxide participation in stabilizing tetrahedral intermediate by chelation, is most likely to occur in the cyclen complex catalyzed hydrolysis of unactivated amides (Scheme III.11).

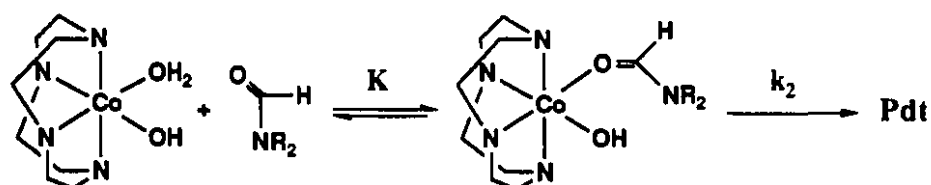
Scheme III.11



### 3.3.2 Reactivity

The mechanism for the cyclen complex promoted hydrolysis of amides is shown in Scheme III.12.

Scheme III.12



Under the reaction conditions used, rapid equilibrium complexation of amides to the cyclen complex is followed by an intramolecular hydroxide attack to form the tetrahedral intermediate which is eventually broken down to the free amine and acid. The complexation of amides to the cyclen complex was monitored by  $^1\text{H}$  NMR at pD 2, free from any hydrolysis and possible catalyst decomposition. The equilibrium binding

\* see the results Table III.1 footnote.

41 a) Guthrie, J. P. *J. Am. Chem. Soc.* 1974, 96, 3608. b) Langlois, S.; Broche, A. *Bull. Soc. Chem. Fr.* 1964, 812.

42 a) Kirby, A. J. *Adv. Phys. Org. Chem.* 1980, 17, 183. b) Jencks, W. P. in *Catalysis in Chemistry and Enzymology*, Dover Ed.; Wiley: New York, 1975.

constant for the aqua-hydroxy form of the complex would be slightly less than that for the diaqua form.

The half-life of the cobalt bound 4-formyl morpholine (35 min) can be calculated from the equilibrium complexation constant of the amide to the cyclen complex ( $0.4 \text{ M}^{-1}$ ) and the second order rate constant for the cyclen complex promoted hydrolysis of the same substrate. The rate constant for the hydroxide catalyzed hydrolysis of 4-formyl morpholine is  $1.4 \times 10^{-3} \text{ M}^{-1} \text{ sec}^{-1}$  at  $25 \text{ }^\circ\text{C}$ . The activation entropy for the hydroxide catalyzed hydrolysis of DMF has been determined to be  $-28.2 \text{ eu}$ .<sup>41b</sup> Assuming the activation entropy for the hydrolysis of 4-formyl morpholine is the same as that for the hydrolysis of DMF, the hydroxide rate for 4-formyl morpholine hydrolysis at  $60 \text{ }^\circ\text{C}$  is  $1.9 \times 10^{-2} \text{ M}^{-1} \text{ sec}^{-1}$ , calculated from the activation parameter. The estimated half-life of the free amide hydrolysis at pH 6 and  $60 \text{ }^\circ\text{C}$  is over 100 years. The cobalt bound 4-formyl morpholine is hydrolyzed ca.  $10^5$  times faster than the free amide in water under the same conditions.\*\*

A typical amide bond in a peptide is known to be hydrolyzed with a half-life of 7 years in water at room temperature,<sup>8</sup> which is about 20 times more reactive than 4-formyl morpholine. Hence, an amide bond in peptides can be cleaved within a few minutes with the cyclen complex since the estimated half-life of 4-formyl morpholine in a solution of the cyclen complex at pH 6 and  $60 \text{ }^\circ\text{C}$  is 35 minutes.

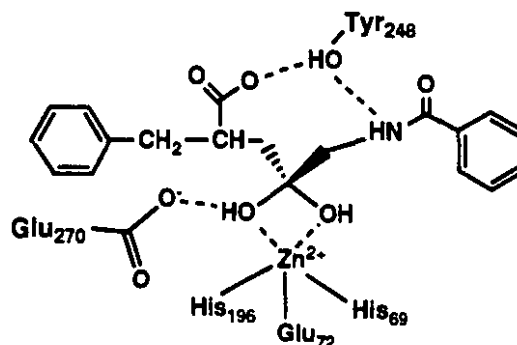
**Comparison to Carboxypeptidase A:** Bovine carboxypeptidase A (CPA) is a metalloexopeptidase of molecular weight 34,472 containing one Zn ion bound to a single polypeptide chain of 307 amino acids.<sup>24,43</sup> Its biological function is the hydrolysis of C-terminal amino acids from polypeptide substrates possessing large, hydrophobic C-terminal side chains such as phenylalanine. There are several different mechanisms proposed for the CPA activity. Concerning the role of metal ions, there are three basic mechanisms possible in CPA catalyzed hydrolysis reaction. In the first mechanism, zinc ion acts as a Lewis acid. The Glu-270 carboxylate can be a nucleophile to give an acyl-enzyme intermediate<sup>44a</sup>, or it behaves as a general base delivering a hydroxide ion to the carbonyl group to form the tetrahedral intermediate. In the second mechanism, the metal bound water molecule is involved as a nucleophile. The Lewis acid mechanism has been tested in model systems<sup>21f</sup> designed by Breslow. The metal hydroxide mechanism also has been

\*\* the acid catalyzed hydrolysis rate can be also calculated from the activation entropy ( $-24.7 \text{ eu}$ ) for the acid catalyzed DMF hydrolysis (ref 43), and the calculated rate constant for formyl morpholine hydrolysis at pH 6 and  $60 \text{ }^\circ\text{C}$  is smaller than that of the base catalyzed hydrolysis of formylmorpholine.

43 Hartsuck, J. A.; Lipscomb, W. N. in *The Enzymes*, 3rd ed.; Boyer, P., Ed.; Academic: New York, 1971; vol 3.  
44 a) Makinen, M. W.; Kuo, L.C.; Dymowski, J. J. *J. Biol. Chem.* 1976, 254, 356. b) Breslow, R.; Wernick, D. L. *Proc. Natl. Acad. Sci. U. S. A.* 1977, 74, 1303.

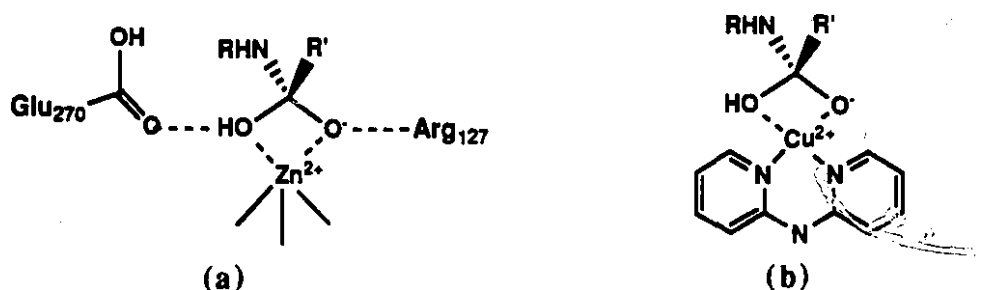
tested in model systems<sup>21g,f</sup> designed by Groves. Both mechanisms appear to give high rate acceleration for amide hydrolysis. However, it is impossible to prove enzyme mechanisms based on the simple model studies. A double activation by the metal ion has been proposed based on the mechanistic studies on metal complex catalyzed amide hydrolysis by Chin et al.<sup>23</sup> The proposed mechanism for unactivated amide hydrolysis involves the above two mechanisms at least concerning the role of metal ions. Buffer catalysis can not be studied due to complexation of the catalyst to the buffer used. Recent success in X-ray crystallography for CPA-substrates structure determinations gives valuable insight in understanding the catalytic mechanism.<sup>24</sup> X-ray structures determined by Christianson and Lipscomb for ketones bound to CPA in their hydrated forms support the bifunctional role of a metal ion even though the structures were used to support the metal hydroxide mechanism.<sup>24</sup> Figure III.11 shows the X-ray structure of 5-benzamido-2-benzyl-4-pentanoic acid hydrate bound to CPA.<sup>45</sup>

Figure III.11



The observed X-ray structures of CPA with gem-diolates, bear the structural and electronic resemblance to the actual proteolytic tetrahedral intermediate (Fig. III.12 a).

Figure III.12



45 Christianson, D. W.; David, P. R.; Lipscomb, W. N. *Proc. Natl. Acad. Sci. U. S. A.* 1987, 84, 1512.

The  $(\text{dpa})\text{Cu}(\text{II})(\text{OH}_2)_2^{23}$  catalyzed hydrolysis of formamides and the CPA catalyzed hydrolysis of peptides both involve the formation of a four-membered ring bidentate metal complex (Fig. III.12).

The cyclen complex can be a better model system in terms of the catalytic efficiency and the possibility for mechanistic studies. It was possible to measure the equilibrium binding constants of amides to the cobalt complex for the first time. The equilibrium binding constants of formamides to the cobalt complex are in the range of 0.4 to 2  $\text{M}^{-1}$ . The kinetics of carboxypeptidase A catalyzed hydrolysis of peptides of more than five amino acids have been studied.<sup>46</sup> The equilibrium constants ( $K_m^{-1}$ ) for binding of the substrates to carboxypeptidase A are in the order of 10 to  $10^2 \text{M}^{-1}$ .<sup>46</sup> It is true that mother nature is ahead in peptidase design. The enzyme bound peptides are hydrolyzed with half-lives of about a few milliseconds<sup>24,46,47</sup> whereas the estimated half-life for the cobalt bound peptide is within a few minutes at 60 °C. Nevertheless, a simple cobalt complex,  $(\text{cyclen})\text{Co}(\text{III})(\text{OH}_2)_2$ , represents the first artificial peptidase for hydrolyzing unactivated amides under mild conditions.

---

46 Abramowitz, N.; Schechter, I.; Berger, A. *Biochem. Biophys. Res. Commun.* 1967, 29, 862.

47 Lipscomb, W. N. *Acc. Chem. Res.* 1970, 3, 81.

**PART IV EXPERIMENTAL (PART I, II, AND III)**

## 1 GENERAL

$^1\text{H}$  NMR,  $^{13}\text{C}$  NMR, and  $^{31}\text{P}$  NMR were taken on Varian XL-200 and 300 spectrometers. Data are reported in parts per million (ppm) downfield from the following references:  $^1\text{H}$  NMR; tetramethylsilane (TMS) in  $\text{CDCl}_3$ , 3-(trimethylsilyl)-1-propane-sulfonic acid (DSS) and t-butyl alcohol (1.22 ppm), in  $\text{D}_2\text{O}$ :  $^{13}\text{C}$  NMR;  $\text{CDCl}_3$  (77.0 ppm), 1,4-dioxane (67.4 ppm in  $\text{D}_2\text{O}$ ),  $\text{CD}_2\text{Cl}_2$  (54.3 ppm):  $^{31}\text{P}$  NMR; trimethylphosphate (TMP) in  $\text{D}_2\text{O}$ .

Kinetic studies were carried out with either a Hewlett-Packard 8451 diode array spectrophotometer equipped with a Lauda RM6 thermostat, or a PYE UNICAM PU88 UV/VIS spectrophotometer equipped with an Accuron SPX 876 S2 Temperature Programme Controller.

Titration of metal complexes was carried out with a Radiometer PHM63 pH meter equipped with a Radiometer RTS822 automatic titrator.

X-ray structures were obtained with a  $\alpha$  Rigaku AF C6S diffractometer with graphite monochromated  $\text{Mo K}\alpha$  radiation at 1.75 KW.

Elemental analyses were performed by Guelph Chemical Laboratories Ltd.

## 2 MATERIALS

The following chemicals were purchased from Sigma-Aldrich Chemical Company and used without further purification: 5'-AMP, c-AMP, 2'-deoxy-c-AMP, ApA, UpU, 2'-deoxyadenosine, adenine, phenylphosphonate, BNPP, tetraethylenepentaamine, and tren.

$^{13}\text{C}$  labelled chemicals,  $\text{CH}_3^*\text{CN}$ ,  $\text{CH}_3^*\text{COONa}$ ,  $\text{H}^*\text{COONa}$  and  $\text{CH}_3^*\text{COCl}$  were purchased from MSD Isotopes and  $\text{BrCH}_2^*\text{CO}_2\text{H}$  and  $\text{Bz}^*\text{OH}$  were purchased from Aldrich Chemical Company. Acetamide  $\text{CH}_3\text{C}^*\text{ONH}_2$  was synthesized from  $\text{CH}_3^*\text{COCl}$  and  $\text{NH}_3$  in pyridine.<sup>1</sup>

Dimethyl phosphate (DMP) (Na salt), methyl phosphate (MP) (Na salt), and BDNPP were provided by Dr. Mariusz Banaszczyk and Dr. Andrew Moore. The following compounds were purified according to the established methods<sup>2</sup>: acetonitrile,

<sup>1</sup> Vogel, A. I. in *A Text of Practical Organic Chemistry*, 4th Ed.; English Language Book Society and Longman; London, 1978, p 516.

<sup>2</sup> Perrin, D. D.; Armarego, W. L. F.; Perrin, D. R. in *Purification of Laboratory Chemicals*; 2nd Ed.; Pergamon Press; 1980.

benzonitrile, trimethylacetonitrile, acrylonitrile, DMF, and 4-formylmorpholine. Tetradentate ligands such as cyclen and trpn were synthesized according to the literature procedures.<sup>3</sup>

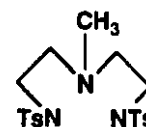
CH<sub>3</sub>CN, doubly distilled water, and MeOH for HPLC were obtained from Fisher Scientific Ltd. HPLC buffer (ammonium phosphate, 0.2 M, pH 5.5) for analysing nucleotides was prepared with HPLC grade NH<sub>4</sub>H<sub>2</sub>PO<sub>4</sub>. The pH of the solution was adjusted with a 40 % ammonium hydroxide solution and was filtered through Millipore 0.45 μm filter paper before use.

### 3 SYNTHESIS

#### 3.1 Synthesis of Tetraamine Ligands

##### N'-methyl-N,N''-bis(toluene-*p*-sulfonyl)diethylentriamine (1)

Compound **1** was synthesized in one step. The literature procedure<sup>4</sup> took 4 reaction steps starting from diethylenetriamine. To a solution of methylamine (2.5 g of 40% water solution, 32 mmol) in acetonitrile (50 mL) was added N-tosylaziridine (12.7 g, 62 mmol)<sup>5</sup>. The mixture was stirred at room temperature for 24 h and evaporated to dryness under reduced pressure. The crude product was recrystallized from methanol to provide 10.6 g (78 %) of **1** as a bright yellow solid: mp 104-106 °C (lit.113-114 °C)<sup>4</sup>; <sup>1</sup>H NMR (200 MHz, CDCl<sub>3</sub>) δ 1.95 (s, 3 H, NCH<sub>3</sub>), 2.34 (t, *J* = 5.7 Hz, 4 H, NCH<sub>2</sub>), 2.42 (s, 6 H, TsCH<sub>3</sub>), 2.94 (t, *J* = 5.7 Hz, 4 H), 7.31 (d, *J* = 8.3 Hz, 4H, ArH), 7.79 (d, *J* = 8.3 Hz, 4 H, ArH); <sup>13</sup>C NMR (75.4 MHz, CDCl<sub>3</sub>) δ 21.48 (TsCH<sub>3</sub>), 41.19, 40.57 (NCH<sub>3</sub>), 107.14, 120.69, 136.7, 143.23.



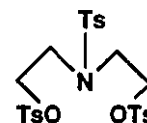
3 a) Richman, J. E.; Atkins, T. J. *J. Am. Chem. Soc.* **1974**, *96*, 2268. b) Chin, J.; Banaszczyk, M.; Jubian, V. *J. Am. Chem. Soc.* **1989**, *111*, 186.

4 Ciampolini, M.; Micheloni, M.; Nardi, N.; Paoletti, P.; Dapporto, P.; Zanobini, F. *J. Chem. Soc., Dalton Trans.* **1984**, 1357.

5 Martin, A. E.; Ford, T. M.; Bulkowski, J. E. *J. Org. Chem.* **1982**, *47*, 412.

**N,O,O'-Tris(toluene-*p*-sulfonyl)bis(2-hydroxyethyl)amine<sup>6</sup> (2)**

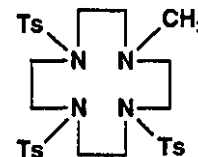
To a solution of diethanolamine (10.5 g, 0.1 mol) and triethylamine (33 g, 3.3 mol) in dichloromethane (500 mL) was added tosylchloride (57.1 g, 3 equiv) over a period of 1 h in an ice bath.



After the addition was complete, the mixture was refluxed for 2 days and evaporated to dryness under reduced pressure. The crude solid material was recrystallized from methanol to give **2** (65 %) as a white solid: mp 73-75 °C; <sup>1</sup>H NMR (200 MHz, CDCl<sub>3</sub>) δ 2.43 (s, 3 H, NCH<sub>3</sub>), 2.46 (s, 6 H, OCH<sub>3</sub>), 3.35 (t, *J* = 6 Hz, 4 H, NCH<sub>2</sub>), 4.11 (t, *J* = 6 Hz, 4 H, OCH<sub>2</sub>), 7.3 (d, *J* = 8.0 Hz, 2H, NTs ArH), 7.36 (d, *J* = 7.94 Hz, 4H, OTs ArH), 7.62 (d, *J* = 8.4 Hz, 2H, NTs ArH), 7.76 (d, *J* = 8.4 Hz, 4H, OTs ArH).

**1-Methyl-4,7,10-tris(toulene-*p*-sulfonyl)-1,4,7,10-tetraazacyclododecane (3)**

To a solution of **1** (9 g, 21.1 mmol) dissolved in dry DMF (500 mL), NaH (1.4 g of 80 % oil dispersion, 2.7 equiv) was added. The solution was heated to 80 °C so that a controlled H<sub>2</sub> evolution took place<sup>7</sup> and then heated to 110 °C for 1 h until H<sub>2</sub> evolution



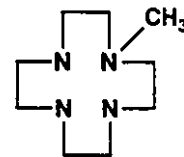
ceased. To the reaction mixture, compound **2** (12.5 g, 21.1 mmol) dissolved in dry DMF (500 mL) was added dropwise over a period of 2 h at 110 °C. The mixture was stirred for an additional 2 h, cooled to room temperature and the residual NaH was decomposed by addition of 10 mL of water. The reaction mixture was filtered, and the solvent was evaporated. The residue was diluted with water and extracted with CHCl<sub>3</sub>. The organic layers were dried over Na<sub>2</sub>SO<sub>4</sub>, and the solvent was evaporated. Crystallization from CHCl<sub>3</sub>-ether provides 8.2 g of **3** (59 %) as a white solid: mp 192-194 °C; <sup>1</sup>H NMR (200 MHz, CDCl<sub>3</sub>) δ 2.17 (s, 3H, NCH<sub>3</sub>), 2.43 (s, 6H, TsCH<sub>3</sub>), 2.46 (s, 3H, TsCH<sub>3</sub>), 2.61 (t, *J* = 4.4 Hz, C2, C12H), 3.0 (t, *J* = 4.3 Hz, C3, C11H), 3.25 (t, *J* = 5.8 Hz, 4H, C5, C9H), 3.51 (t, *J* = 5.8 Hz, 4H, C6, C8H), 7.3 (d, *J* = 8.4 Hz, 4H, N4 and N11ArH), 7.35 (d, *J* = 8.4 Hz, 2H, N7ArH), 7.63 (d, *J* = 8.2 Hz, 4H, N4 and N11ArH), 7.82 (d, *J* = 8.2 Hz, 2H, N7ArH); <sup>13</sup>C NMR (75.4 MHz, CDCl<sub>3</sub>) δ 21.50 and 21.55 (TsCH<sub>3</sub>), 42.49, 45.40, 48.64, 50.13, 51.87, 59.29, 134.83, 136.38, 143.30, 143.51.

<sup>6</sup> Moi, M. K.; Mears, C. F.; DeNardo, S. J. *J. Am. Chem. Soc.* **1988**, *110*, 6266.

<sup>7</sup> Hediger, M.; Kaden, T. A. *Helv. Chim. Acta* **1983**, *66*, 861.

**1-Methyl-1,4,7,10-tetraazacyclododecane (4)**

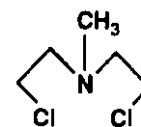
Compound **3** (7.8 g, 11.7 mmol) was detosylated with concentrated sulfuric acid (20 mL) as described previously.<sup>8</sup> The resulting amine sulfate was dissolved in water. The water solution was made alkaline with a 2N NaOH solution and extracted with CHCl<sub>3</sub>.



The organic layers were dried over Na<sub>2</sub>SO<sub>4</sub> and evaporated under reduced pressure. A thick oily residue was solidified upon standing at room temperature to give **4** as a pale yellow solid in a quantitative yield: <sup>13</sup>C NMR (75.4 MHz, CDCl<sub>3</sub>) δ 43.47 (CH<sub>3</sub>), 44.74, 46.30, 48.77, 53.84.

**Bis(2-chloroethyl)methylamine (5)**

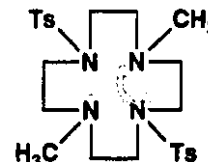
A solution of N-methyldiethanolamine (61.9 g, 0.52 mol) in CHCl<sub>3</sub> (50 mL) was added dropwise over a period of 2 h to a solution of thionyl chloride (86 mL, 1.14 mmol) in CHCl<sub>3</sub> (60 mL) at room temperature.<sup>9</sup> The mixture was refluxed for an additional 1 h cooled to room temperature, and evaporated to dryness. The residue was recrystallized from acetone to give **5** as a hydrochloride salt.



The HCl salt (5 g, 26.4 mmol) was dissolved in a small amount of water, and the water solution was made alkaline with NaOH powder. The solution was extracted with CH<sub>2</sub>Cl<sub>2</sub>, dried over Na<sub>2</sub>SO<sub>4</sub>, and evaporated to produce 4 g (98 %) of **5** as a yellow oil: <sup>1</sup>H NMR (200 MHz, CDCl<sub>3</sub>) δ 2.38 (s, 3H, CH<sub>3</sub>), 2.82 (t, *J* = 6.8 Hz, 4 H, NCH<sub>2</sub>), 3.56 (t, *J* = 6.9 Hz, 4 H, CH<sub>2</sub>Cl).

**1,7-Dimethyl-4,7-bis(toluene-p-sulfonyl)-1,4,7,10-tetraazacyclododecane (6)**

Compound **6** was prepared from **1** and **5** by the method used for the synthesis of **3**. Thus **1** (18 g, 42.3 mmol) and **5** (6 g, 38.7 mmol) gave 6.8 g of **6** (35%) as a white solid after recrystallization from methanol: mp 167-170 °C (lit. 175-177 °C)<sup>4</sup>; <sup>1</sup>H NMR (200



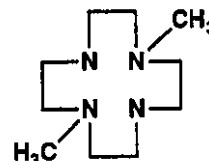
<sup>8</sup> Atkins, J. A.; Richman, J. E.; Eittle, W. F. *Org. Synth.* 1978, 58, 86.

<sup>9</sup> Cammack, T.; Reeves, P. C. *J. Heterocyclic Chem.* 1986, 23, 73.

MHz, CDCl<sub>3</sub>)  $\delta$  2.23 (s, 3 H, NCH<sub>3</sub>), 2.43 (s, 3 H, TsCH<sub>3</sub>), 2.71 (t,  $J$  = 5.3 Hz, 8 H, C2, C12, C6, C8H), 3.19 (t,  $J$  = 5.3 Hz, 8 H, C3, C5, C9, C11H), 7.31 (d,  $J$  = 8.2 Hz, 4H, ArH), 7.68 (d,  $J$  = 8.2 Hz, 4 H, ArH); <sup>13</sup>C NMR (75.4 MHz, CDCl<sub>3</sub>)  $\delta$  21.49 (TsCH<sub>3</sub>), 42.30, 47.55, 57.17, 127.34, 129.68, 135.39, 143.28.

#### 1,7-Dimethyl-1,4,7,10-tetraazacyclododecane (7)

Compound 6 was detosylated using the method<sup>7,8</sup> described for the synthesis of 4 to give 7 (99 %) as a yellow solid: <sup>1</sup>H NMR (200 MHz, CDCl<sub>3</sub>)  $\delta$  1.22 (m, 1H, NH), 2.28 (s, 6H, CH<sub>3</sub>), 2.46 (bs, 8H, R<sub>2</sub>NCH<sub>2</sub>), 2.63 (t,  $J$  = 4.8 Hz, 8H, RHNCH<sub>2</sub>), 3.49 (m, 1H, NH); <sup>13</sup>C NMR (75.4 MHz, CDCl<sub>3</sub>)  $\delta$  43.89 (CH<sub>3</sub>), 44.78, 54.24.



#### 4,7-Dibenzyl-1,10-bis(toluene-*p*-sulfonyl)triethylenetetraamine (8)

Compound 8 was prepared from the *N,N'*-dibenzylethylenediamine and *N*-tosylaziridine as described for the synthesis of 1 in 85 % yield: <sup>1</sup>H NMR (200 MHz, CDCl<sub>3</sub>)  $\delta$  2.39 (s, 4H, C5, C6H), 2.41 (s, 6H, TsCH<sub>3</sub>), 2.46 (t,  $J$  = 5.5 Hz, 4H, C3, C8H), 2.94 (t,  $J$  = 5.5 Hz, 4H, C2, C9H), 5.5 (bs, 2H, NH), 7.15 (m, 10H, Bn), 7.3 (d,  $J$  = 8.0 Hz, 4H, ArH), 7.69 (d,  $J$  = 8.3 Hz, 4H, ArH)

**O,O'-Ditosylethyleneglycol (9)** Compound 9 was prepared according to the known procedure<sup>5</sup>: <sup>1</sup>H NMR (200 MHz, CDCl<sub>3</sub>)  $\delta$  2.46 (s, 6H, TsCH<sub>3</sub>), 4.11 (s, 4H, OCH<sub>2</sub>), 7.34 (d,  $J$  = 8.0 Hz, 4H, ArH), 7.74 (d,  $J$  = 8.1 Hz, 4H, ArH)

#### 1,4-Dibenzyl-7,10-bis(toluene-*p*-sulfonyl)-1,4,7,10-tetraazacyclododecane (10)

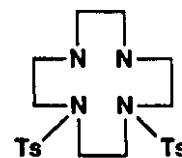
This compound was prepared from 8 (12.05 g, 19 mmol) and 9 (7.1 g, 19.1 mmol) using the method described for the synthesis of 3. The crude product was dissolved in hot benzene and the solution was cooled to 0 °C. The resulting slurry was filtered to remove the starting material 8. The filtrate was then evaporated and



1.5 g of the final product **10** (12 %) was isolated by fractional recrystallization from ethanol:  $^1\text{H}$  NMR (200 MHz,  $\text{CDCl}_3$ )  $\delta$  2.39 (s, 4H, C3H), 2.44 (s, 6H, TsCH<sub>3</sub>), 2.64 (t,  $J = 5.04$  Hz, C5, C12H), 3.24 (t,  $J = 5.04$  Hz, C6, C11H), 3.47 (s, 4H, CH<sub>2</sub>Bn), 3.70 (s, 4H, C8, C9H), 7.19 (bs, 10H, Bn), 7.3 (d,  $J = 8.2$  Hz, 4H, ArH), 7.68 (d,  $J = 8.2$  Hz, 4H, ArH);  $^{13}\text{C}$  NMR ( $\text{CDCl}_3$ , 75.4 MHz)  $\delta$  21.53 (TsCH<sub>3</sub>), 47.58, 49.02, 51.20, 54.81, 59.09, 127.05, 127.36, 128.17, 129.67, 129.51, 135.84, 137.75, 143.09.

### 1,4-Bis(toluene-*p*-sulfonyl)-1,4,7,10-tetraazacyclododecane (11)

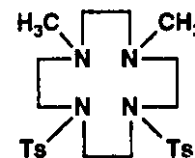
To a solution of **10** (4 g, 6.3 mmol) in acetic acid (60 mL) was added 2 g of 10% Pd-C catalyst.<sup>7,10</sup> The hydrogenolysis was allowed to proceed until no further hydrogen was taken up. The reaction mixture was filtered through celite and evaporated. The crude product



was dissolved in a 1N NaOH solution and extracted with  $\text{CHCl}_3$ . The organic layers were dried over  $\text{Na}_2\text{SO}_4$  and slowly evaporated to give **11** as a yellow solid (98 %):  $^1\text{H}$  NMR (200 MHz,  $\text{CDCl}_3$ )  $\delta$  1.65 (bs, 2H, NH), 2.44 (s, 6H, TsCH<sub>3</sub>), 2.73 (s, 4H, C8, C9H), 2.90 (t,  $J = 5.1$  Hz, 4H, C6, C11H), 3.13 (t,  $J = 5.1$  Hz, 4H, C5, C12H), 3.54 (s, 4H, C2, 3H), 7.35 (d,  $J = 8.3$  Hz, 4H, ArH), 7.73 (d,  $J = 8.3$  Hz, 4H, ArH);  $^{13}\text{C}$  NMR (75.4 MHz,  $\text{CDCl}_3$ )  $\delta$  21.5, 46.83, 48.0, 50.47, 50.59, 127.58, 129.75, 134.25, 143.55.

### 1,4-Dimethyl-7,10-bis(toluene-*p*-sulfonyl)-1,4,7,10-tetraazacyclododecane (12)

To a slurry of **11** (1.5 g, 30 mmol) in water (3 mL) was added formic acid (3.4 mL, 1 equiv) and formaldehyde (2.8 mL, 1 equiv).<sup>11</sup> The reaction mixture was refluxed for 24 h and cooled to 0 °C. The solution was made alkaline with a concentrated NaOH solution to yield



a sticky solid. The crude material was dissolved in 20 mL of hot benzene and was filtered to remove unidentified side product after cooling. The filtrate was evaporated to give 0.8 g (51%) of **12** as a white crystalline solid: mp 144-146 °C;  $^1\text{H}$  NMR (200 MHz,  $\text{CDCl}_3$ )  $\delta$  2.19 (s, 6H, CH<sub>3</sub>), 2.29 (s, 4H, C2, C3H), 2.43 (s, 6H, TsCH<sub>3</sub>), 2.56 (t,  $J = 5.1$  Hz, C5, C12H), 3.14 (t,  $J = 4.5$  Hz, 4H, C6, C11H), 3.58 (s, 4H, C8, C9H), 7.32 (d,  $J =$

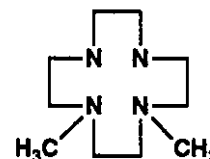
<sup>10</sup> Bergern, R. J.; McGovern, K. A.; Channing, M. A.; Burton, P. S. *J. Org. Chem.* **1980**, *45*, 1589.

<sup>11</sup> Barefield, E. K.; Wagner, F. *Inorg. Chem.* **1973**, *12*, 2435.

7.94 Hz, 4H, ArH), 7.75 (d,  $J = 8.2$  Hz, 4H, ArH);  $^{13}\text{C}$  NMR (75.4 MHz,  $\text{CDCl}_3$ )  $\delta$  21.5, 43.56 (NCH<sub>3</sub>), 49.14, 50.37, 54.97, 127.3, 129.65, 135.82, 143.06.

### 1,4-Dimethyl-1,4,7,10-tetraazacyclododecane (13)

Compound **13** was prepared according to the method described for the synthesis of **4**. A solution of **12** (1.1 g, 2.16 mmol) in concentrated sulfuric acid (2 mL) was stirred for 72 h at 100 °C. The reaction mixture was cooled to 0 °C and dry ethylether was added slowly. After filtration, a sticky solid was dissolved in water. The solution was made alkaline with a 2 N NaOH solution, extracted with  $\text{CHCl}_3$ , and dried over  $\text{Na}_2\text{SO}_4$ . Evaporation gave 0.4 g (93 %) of **13** as a deliquescent solid:  $^1\text{H}$  NMR (200 MHz,  $\text{CDCl}_3$ )  $\delta$  2.29 (s, 6H, CH<sub>3</sub>), 2.41 (s, 4H, C2, C3H), 2.4 to 2.45 (m, 4H, C5, C12H), 2.68 to 2.74 (m, 4H, C6, C11H), 2.75 (s, 4H, C8, C9H);  $^{13}\text{C}$  NMR (75.4 MHz,  $\text{CDCl}_3$ )  $\delta$  43.73 (CH<sub>3</sub>), 45.29, 47.28, 54.0, 55.56.



## 3.2 Synthesis of Co(III) Complexes.

### 3.2.1 Synthesis of [(L)Co(III)CO<sub>3</sub>]ClO<sub>4</sub>

All the cobalt complexes have been synthesized according to literature procedures<sup>12</sup> with minor modifications. A solution of tetraamine ligand (1 mmol) dissolved in 5 to 10 mL of water (for cyclen) or 30 to 50 % aqueous ethanol (for cyclen derivatives) was added to  $\text{Co(II)(ClO}_4)_2 \cdot 6\text{H}_2\text{O}$  (1 equiv) in 5 mL of water, and to this was added  $\text{PbO}_2$  (1.5 equiv) and  $\text{NaHCO}_3$  (1 equiv). The resulting suspension was stirred overnight at room temperature (cyclen) or for 6 h at 50 °C (cyclen derivatives), and the pH of solution was adjusted to ca. 6.5 by adding a dilute  $\text{HClO}_4$  solution. After filtration, it was evaporated to dryness in *vacuo*. The crude residue was triturated with absolute ethanol, and then filtered. The overall yields after recrystallization from water are in the range of 75 to 85 %:  $(\text{cyclen})\text{Co(III)CO}_3 \cdot \text{ClO}_4 \cdot \text{H}_2\text{O}$ <sup>13</sup>;  $^{13}\text{C}$  NMR (75.4 MHz,  $\text{D}_2\text{O}$ ) 167.43 ( $\text{CO}_3$ ), 56.47, 54.02, 50.02, 47.91.

<sup>12</sup> Harris, G. M.; Dasgupta, T. P. *J. Am. Chem. Soc.* 1975, 97, 1733.

<sup>13</sup> X-ray structure; Loehlin, J. H.; Fleisher, E. B. *Acta Cryst.* 1976, B32, 3063.

Anal. Calcd for  $C_9H_{20}ClCoN_4O_7$ : C, 27.67; H, 5.16; N, 14.34; Cl, 9.08. Found: C, 27.43; H, 4.76; N, 14.26; Cl, 8.93; Co, 15.19.

**(monomethylcyclen)Co(III)CO<sub>3</sub>·ClO<sub>4</sub>**: <sup>13</sup>C NMR (75.4 MHz, D<sub>2</sub>O) δ 167.77 (CO<sub>3</sub>), 66.93, 64.14, 56.42, 53.91, 50.35, 49.32, 48.36, 47.8, 45.7(CH<sub>3</sub>).

Anal. Calcd for  $C_{10}H_{22}ClCoN_4O_7$ : C, 29.67; H, 5.48; N, 13.72; Co, 14.56. Found: C, 29.41; H, 5.20; N, 13.72; Co, 14.77.

**(trans-dimethylcyclen)Co(III)CO<sub>3</sub>·ClO<sub>4</sub>**<sup>14</sup>: <sup>13</sup>C NMR (75.4 MHz, D<sub>2</sub>O) δ 168.25 (CO<sub>3</sub>), 66.85, 64.06, 49.14, 48.09, 46.32 (CH<sub>3</sub>).

Anal. Calcd for  $C_{11}H_{24}ClCoN_4O_7$ : C, 31.55; H, 5.77; N, 13.55; Cl, 8.47; Co, 14.07. Found: C, 31.0; H, 5.40; N, 13.64; Cl, 8.61; Co, 14.23.

**(cis-dimethylcyclen)Co(III)CO<sub>3</sub>·ClO<sub>4</sub>**: <sup>13</sup>C NMR (75.4 MHz, D<sub>2</sub>O) δ 167.94 (CO<sub>3</sub>), 66.34, 65.93, 60.16, 59.72, 55.89, 49.92, 48.93, 46.77 and 45.71(CH<sub>3</sub>).

Anal. Calcd for  $C_{11}H_{24}ClCoN_4O_7$ : C, 31.55; H, 5.77; N, 13.55; Cl, 8.47; Co, 14.07. Found: C, 31.13; H, 5.36; N, 13.50; Cl, 8.14; Co, 13.71.

### 3.2.2 Synthesis of Co(III)(L)(OH<sub>2</sub>)<sub>2</sub>·(ClO<sub>4</sub>)<sub>3</sub>

**General methods** : To a solution of Co(III) carbonato complex (1 mmol) in 0.5 mL of water was added dropwise 2.5 mmol of 70% aqueous HClO<sub>4</sub> and the mixture was stirred at room temperature until the CO<sub>2</sub> evolution ceased. The mixture was then stirred under reduced pressure for 0.5 h and was evaporated to dryness in an ice-water bath. The residue was triturated with anhydrous ethylether, filtered, and dried in vacuo over P<sub>2</sub>O<sub>5</sub>. The aqueous solution is often used directly without isolation of the diaqua cobalt complexes:

**(cyclen)Co(III)(OH<sub>2</sub>)<sub>2</sub>(ClO<sub>4</sub>)<sub>3</sub>**: <sup>13</sup>C NMR (75.4 MHz, D<sub>2</sub>O) δ 57.97, 54.6, 50.6, 48.6

**(monomethylcyclen)Co(III)(OH<sub>2</sub>)<sub>2</sub>(ClO<sub>4</sub>)<sub>3</sub>**: <sup>13</sup>C NMR (75.4 MHz, D<sub>2</sub>O) δ 67.64, 64.55, 57.71, 54.26, 50.54, 50.07, 49.73 (CH<sub>3</sub>), 49.07, 48.54

**(trans-dimethylcyclen)Co(III)(OH<sub>2</sub>)<sub>2</sub>(ClO<sub>4</sub>)<sub>3</sub>**: To a finely powdered cobalt carbonato complex (1 mmol) was added dropwise 100 μL of 70% aqueous HClO<sub>4</sub> and the mixture was stirred at room temperature until CO<sub>2</sub> evolution stopped. The mixture was diluted with 1 mL of water and stirred at 50 °C for 1 h. The solution was cooled to room temperature and stirred for an additional 1 h under reduced pressure. The diaqua tmcyclen

<sup>14</sup> X-ray structure; Giusti, J.; Chimichi, S.; Ciampolini, M. *Inorg. Chem. Acta* 1984, 88, 51.

complex can be isolated using the same methods as for the cyclen complex:  $^{13}\text{C}$  NMR (75.4 MHz,  $\text{D}_2\text{O}$ )  $\delta$  67.95, 64.62, 50.93, 50.51, 49.57( $\text{CH}_3$ ).

### 3.2.3 Preparation of (tetren)Co(III)(OH<sub>2</sub>)

Initially prepared as a mixture of  $\alpha$ - and  $\beta$ -(tetren)Co(III)(Cl)(ZnCl<sub>4</sub>)<sub>2</sub>, the complex was converted to a mixture of  $\alpha$ - and  $\beta$ -(tetren)Co(III)Cl(ClO<sub>4</sub>)<sub>2</sub><sup>15</sup> and treated with 1 equiv of base (NaOH) to give  $\alpha$ -(tetren)Co(III)(OH<sub>2</sub>)(Cl)(ClO<sub>4</sub>)<sub>2</sub>. This aqua cobalt complex was used directly without isolation.

$\alpha$ - and  $\beta$ -(tetren)Co(III)Cl(ClO<sub>4</sub>)<sub>2</sub> Anal. Calcd for C<sub>8</sub>H<sub>23</sub>Cl<sub>3</sub>CoN<sub>5</sub>O<sub>13</sub>: C, 19.91; H, 4.8; N, 14.51; Cl, 22.04; Co, 12.21. Found: C, 19.87; H, 5.27; N, 14.47; Cl, 21.91; Co, 12.11.

### 3.3 Synthesis of [(tmcyclen)Co( $\eta^2$ -N,O-benzamide)]<sup>2+</sup> complex

To a solution of cobalt carbonato complex (900 mg, 2.15 m mole) dissolved in 5 mL of water was added 0.5 mL of concentrated perchloric acid. The solution was stirred at room temperature until CO<sub>2</sub> evolution ceased and then stirred for an additional 2 h at 60 °C. The solution was cooled to room temperature and excess CO<sub>2</sub> was removed under reduced pressure. The solution was diluted to 5 mL with water and the pH of the solution was adjusted to 6.5 with a 2 N NaOH solution. To the catalyst solution was added 1 equiv of benzonitrile (219 mg) and the mixture was stirred at room temperature overnight. After filtration, 700 mg of a fine powder was obtained. The crude product was recrystallized from 25 mL of hot water (70 - 80 °C) and washed with 50 % aqueous ethanol, ethanol, and ether yielding 370 mg of a purple multifaceted crystal :

$^{13}\text{C}$  NMR (75.4 MHz,  $\text{CD}_2\text{Cl}_2$ )  $\delta$  185.1(CO), 134.2, 130.9, 129.3, 126.6, 67.3, 64.9, 48.7, 47.9 ( $\text{CH}_3$ ), 47.8 : ref  $\text{CD}_2\text{Cl}_2$  (54.26 ppm).

$^{13}\text{C}$  NMR (75.4 MHz,  $\text{D}_2\text{O}$ )  $\delta$  185.9, 184.6, 134.6, 134.5, 132.1, 131.8, 129.7, 127.2, 127.0, 68.0, 67.5, 64.8, 64.1, 50.6, 49.0, 48.4 ( $\text{CH}_2$ ,  $\text{CH}_3$ ), 48.2, 47.8 ( $\text{CH}_3$ ) : ref: t-BuOH (30.47 and 70.59 ppm).

$^1\text{H}$  NMR (200 MHz,  $\text{CD}_2\text{Cl}_2$ )  $\delta$  1.62 (s, H<sub>2</sub>O), 2.38 (s,  $\text{CH}_3$ ), 2.7 - 3.6 (m, cyclen), 6.17 (bs, NH), 6.77 (bs, NH), 7.5 - 8.0 (m, ArH), 8.7 (bs, NH) : ref  $\text{CH}_2\text{Cl}_2$  (5.24 ppm).

$^1\text{H}$  NMR (200 MHz,  $\text{D}_2\text{O}$ )  $\delta$  2.39 and 2.43 (s,  $\text{CH}_3$ ), 2.7 - 3.45 (m, cyclen  $\text{CH}_2$ ), 7.5 - 8 (m, benzamide) : ref : t-BuOH (1.22 ppm).

15 a) House, D. A.; Garner, C. S. *Inorg. Chem.* 1967, 6, 272. b) Ni, T. L.; Garner, C. S. *ibid.* 1967, 6, 1071.

*Crystal data*  $C_{17}H_{34}CoN_5O_{11}Cl_2$ ,  $M = 614.32$ . Orthorhombic,  $a = 13.130$  (4) Å,  $b = 18.357$  (4) Å,  $c = 10.805$ (1) Å,  $\beta = 55^\circ$ ,  $V = 2604$  (1) Å<sup>3</sup>, space group;  $P2_12_12_1$  (#19),  $Z = 4$ ,  $D_x = 1.567$  g/cm<sup>3</sup>, Purple, multifaceted crystal. Crystal dimensions: 0.300 x 0.200 x 0.500 (mm),  $\mu$ (Mo-K $\alpha$ ) = 9.24 cm<sup>-1</sup>.

*Data Collection and Processing* Rigaku AFC6S diffractometer,  $\omega - 2\theta$  mode with  $\omega$  scan width =  $1.00 + 0.30 \tan \theta$ , scan speed 16.0 deg min<sup>-1</sup>, graphite-monochromated Mo-K $\alpha$  radiation, temperature:  $20 \pm 0.1$  °C; 6424 reflections measured 5996 unique after absorption correction (max. min. transmission factors: 0.89 - 1.00) giving 3014 with  $I > 3.00 \sigma(I)$ . The intensities of three representative reflections remained constant throughout data collection indicating crystal and electronic stability (no decay correction was applied). The data were corrected for Lorentz and polarization effects.

*Structure analysis and refinement* All non-hydrogen atom positions were solved by direct methods<sup>16</sup> using the TEXAN crystallographic software package of Molecular Structure Corporation.<sup>17</sup> All hydrogen atom positions were determined from a Fourier Difference map. All positional and thermal parameters (non-hydrogen atoms: anisotropic; hydrogens; isotropic) and an extinction parameter were refined by full-matrix least squares. Final  $R$  and  $R_w$  were 0.068 and 0.065 for 3014 observed reflections and 281 variable parameters. The weighting scheme  $w = 4 F_o^2 / \sigma^2(F_o^2)$  obtained from counting statistics gave satisfactory agreement analyses. The maximum and minimum peaks on the final difference Fourier map correspond to 0.60 and -0.56 eÅ<sup>-3</sup>, respectively. Neutral atom scattering factors were taken from Cromer and Waber.<sup>18</sup> Anomalous dispersion effects were included in  $F_{calc}$ <sup>19</sup>; the values for  $\Delta f'$  and  $\Delta f''$  were those of Cromer.<sup>20</sup> Two disoriented perchlorate ions were located, as well as two lattice water molecules. The refinement gave  $R$  factor of the syn isomer (see part II section 3.2) of 0.073.

### 3.4 Synthesis of [(trpn)Co(III)( $\eta^2$ -O,O'- $\beta$ -ala)]<sup>3+</sup> complex

16 Gilmore, C. J. *J. Appl. Cryst.* 1984, 17, 42. and Beurskens, P.T. DIRDIF: Direct Methods for Difference Structures—an Automatic Procedure for Phase Extension and Refinement of Difference Structure Factors, Technical Report; Crystallography laboratory, Toernooiveld, 6525 Ed Nijmegen, Netherlands, 1984.

17 TEXAN-TEXRAY Structure Analysis Package, Molecular Structure Corporation, 1985.

18 Cromer, D. T.; Waber, J. T. in *International Tables for X-Ray Crystallography*; The Kynoch Press: Birmingham, 1974, Vol. 4, Table 2.2.A.

19 Ibers, J. A.; Hamilton, W. C. *Acta Crystallogr.* 1964, 17, 781.

20 Cromer, D. T. in *International Tables for X-Ray Crystallography*; The Kynoch Press: Birmingham, 1974, Vol. 4, Table 2.3.1.

To a solution of  $(\text{trpn})\text{Co}(\text{III})(\text{OH}_2)_2\text{ClO}_4$  (1 g, 1.62 mmol) dissolved in 5 mL of water was added  $\beta$ -alanine (144.2 mg, 1 equiv). The pH of the solution was adjusted to 5 using a 1N NaOH or a 1N HClO<sub>4</sub> solutions and stirred for 3 h at room temperature. The volume of the solution was reduced to 1 mL. The precipitate formed was filtered, redissolved in a minimum amount of water and the same volume of a saturated NaClO<sub>4</sub> solution was slowly added. A needle shaped violet crystal was obtained on standing overnight. The ORTEP<sup>21</sup> view of the crystal is shown in Figure IV.1.

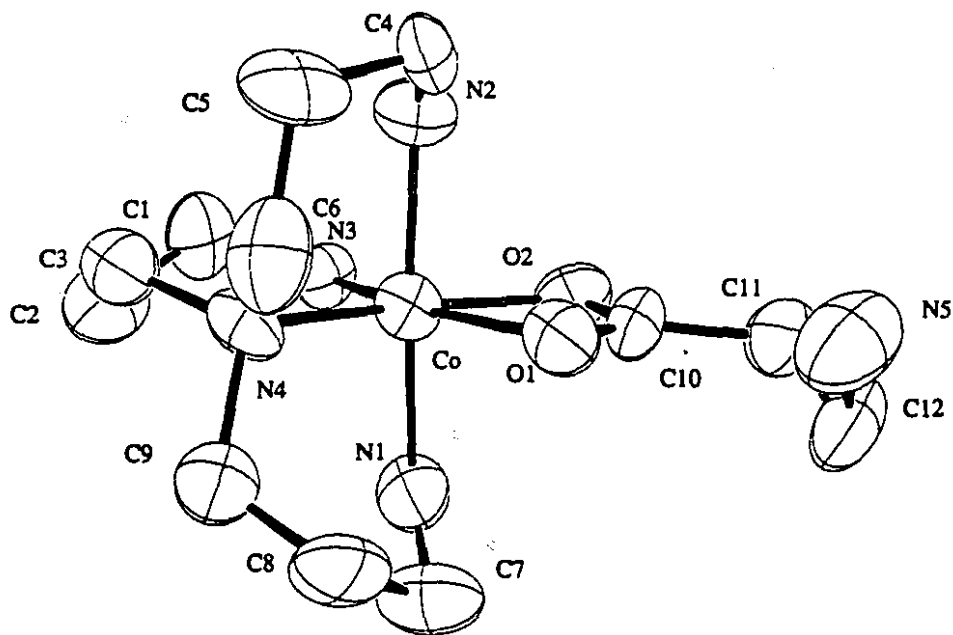
*Crystal data* C<sub>12</sub>H<sub>33</sub>CoN<sub>5</sub>O<sub>15</sub>Cl<sub>3</sub>, M = 652.71. orthorhombic, a = 16.396 (8), b = 19.836 (6), c = 15.059 (1) Å,  $\beta$  = 50°, V = 4898 (4) Å<sup>3</sup>, space group; Pbc<sub>a</sub> (#61), Z = 8, D<sub>x</sub> = 1.770 g/cm<sup>3</sup>, violet needle. Crystal dimensions: 0.450 x 0.200 x 0.280 (mm),  $\mu(\text{Mo-K}\alpha)$  = 11.05 cm<sup>-1</sup>.

*Data Collection and Processing* Rigaku AFC6S diffractometer,  $\omega$  - 2  $\theta$  mode with  $\omega$  scan width = 1.00 + 0.30 tan  $\theta$ , scan speed 16.0 deg min<sup>-1</sup>, graphite-monochromated Mo-K $\alpha$  radiation, temperature: 20 ± 0.1 °C; 4809 reflections measured 1384 unique after absorption correction (max. min. transmission factors: 0.61 - 1.17) giving 1384 with I > 1.00  $\sigma$  (I). The intensities of three representative reflections remained constant throughout data collection indicating crystal and electronic stability (no decay correction was applied). The data were corrected for Lorentz and polarization effects.

*Structure analysis and refinement* All non-hydrogen atom positions were solved by direct methods<sup>16</sup> using the TEXAN crystallographic software package of Molecular Structure Corporation.<sup>17</sup> All hydrogen atom positions were determined from a Fourier Difference map. All positional and thermal parameters (non-hydrogen atoms: anisotropic; hydrogens; isotropic) and an extinction parameter were refined by full-matrix least squares. Final R and R<sub>w</sub> were 0.095 and 0.061 for 1384 observed reflections and 235 variable parameters. The weighting scheme  $w = 4 F_o^2 / \sigma^2 (F_o^2)$  obtained from counting statistics gave satisfactory agreement analyses. The maximum and minimum peaks on the final difference Fourier map correspond to 0.56 and -0.61 eÅ<sup>-3</sup>, respectively. Neutral atom scattering factors were taken from Cromer and Waber.<sup>18</sup> Anomalous dispersion effects were included in F<sub>calc</sub><sup>19</sup>; the values for  $\Delta f'$  and  $\Delta f''$  were those of Cromer.<sup>20</sup>

21 Johnston, C. K. ORTEPII. Report ORNL-5138; Oak Ridge National Libray: Oak Ridge, Tennessee, 1976.

**Figure IV.1** Perspective ORTEP drawing of  $(\text{trpn})\text{Co}(\text{III})(\eta^2\text{-O,O}'\text{-}\beta\text{-ala})(\text{ClO}_4)_3$ . Nonhydrogen atoms are represented by thermal vibration ellipsoids drawn to encompass 50 % of electron density; hydrogen atoms are omitted for clarity.



#### 4. TITRATION

Titration to determine the pKa of the water bound to cobalt complexes were carried out on solutions of cobalt complex (1mM, 5mL) and titrated from pH 3 to 10 using a NaOH solution (0.01 M). Both sodium hydroxide and perchloric acid solutions were prepared from degassed water.

#### 5 KINETICS / BINDING STUDIES

##### 5.1 UV/VIS Spectroscopy

**Hydrolysis of phosphate esters:** Hydrolysis of BDNPP, BNPP, and NPP promoted by cobalt complexes was monitored at 400 nm following the production of the corresponding substituted phenolate. The reactions were carried out under pseudo first order conditions with excess cobalt complex over phosphate esters. The rate constants were obtained by fitting the first 3 half lives of the reaction according to a first order kinetic equation (correlation coefficient > 0.98). In a typical kinetic run, a cuvette was filled with a freshly prepared aqueous solution of 5 mM of cobalt complex (2 mL) that has been adjusted to the desired pH at 25 °C. The hydrolysis reaction was initiated by injecting 0.01 M stock solution of phosphate esters (5 µL). For experiments done at high temperature, the cobalt solution in a cuvette was preequilibrated for 5 min before substrate injection. The pH of the reaction did not change during the course of reaction. An aqueous stock solution was prepared for BNPP and NPP whereas a stock solution in acetonitrile was prepared for BDNPP. The anation reaction was performed in the same way as described above following the formation of bidentate phosphato complex at 550 to 570 nm .

**Equilibrium binding constant of acetonitrile and acetamide to cobalt complexes:** Binding of acetonitrile and acetamide to cobalt complexes was monitored at 460 and 560 nm by following the formation of acetonitrile-cobalt complex adducts and acetamido-cobalt complex, respectively. The equilibrium binding constant was obtained from a plot of the observed pseudo first order rate constant for the approach to the equilibrium vs substrate concentration, where a ratio of slope ( $k_1$ ) over intercept ( $k_{-1}$ ) determines the equilibrium constant  $K$ . In a typical kinetic run, to an aqueous solution of cobalt complex (10 mM) at appropriate pH was injected 20 to 100 equiv of acetonitrile or acetamide (1 M stock solution).

**Hydration of acetonitrile :** Accumulation of the cobalt acetamido complex was monitored at 500 nm (for the cyclen complex) and 600 nm (for the tmcyclen complex). The observed first order rate constants were obtained by fitting the data according to a first order kinetic equation ( $R > 0.99$ ). In a typical kinetic run, 1 to 10 equiv of acetonitrile was injected to a catalyst solution (10 mM) which was preheated to 40 °C and preadjusted to pH 7 with a 1 N NaOH solution.

## 5.2 $^1\text{H}$ NMR and $^{31}\text{P}$ NMR spectroscopy

**Binding of phosphates:** To a solution of  $(\text{L})\text{Co}(\text{III})(\text{OH}_2)_2$  (0.1 M) was added a stock solution of inorganic phosphate (monobasic) or phenyl phosphonate (sodium salt) solution (0.1 M). The pD of the solution was not adjusted after mixing, and the solution was allowed to equilibrate for 1 h. The chemical shifts in  $^{31}\text{P}$  NMR spectrum were recorded with respect to trimethyl phosphate as an external reference.

Equilibrium binding constants for DMP to the cobalt complexes of cyclen and tetren were obtained by directly converting the integration value of each peak to concentration. In a typical experiment, a solution was prepared by adding 0.5 to 1 equiv of DMP to a catalyst solution (0.1 M) at pD 2. The pD of the solution was adjusted again to 2 with an aqueous  $\text{HClO}_4$  solution. Best results were obtained when a 1:1 mixture was allowed to equilibrate for 1 h at room temperature for the cyclen complex and at 60 °C for the tetren complex.

**Hydrolysis of nucleotides:** Hydrolysis of nucleotides such as c-AMP, 2'-deoxy c-AMP, 5'-AMP, ApA, and UpU was monitored by  $^{31}\text{P}$  NMR methods by following the formation of inorganic phosphate-cobalt complexes. The results were plotted as the appearance of the product signal measured in terms of integration relative to the total integration of all the signals. The time for the acquisition of each data point is corrected properly for the time of data collection. The values of  $k^{\text{obs}}$  calculated from the data were reproducible to  $\pm 10\%$  at 50 °C. In a typical kinetic run, 0.1 equiv of a stock solution of phosphate esters was added to a cobalt complex solution (0.1 M) adjusted to the desired pD at 25 °C. The pD of solution was adjusted again. The reaction mixture is placed in a NMR tube, sealed, and heated to 50 °C.

### Hydrolysis of DMP, nitriles and amides

**General methods:** Hydrolysis of DMP, nitriles, and amides are monitored by  $^1\text{H}$  NMR methods. The reaction mixture is placed in a NMR tube, sealed, and heated to the desired

temperature. NMR spectra were recorded at different time intervals. As the reaction proceeds, a decrease in the substrate signal is accompanied by an increase in the product signal. The results were plotted as the appearance of the product signal measured in terms of integration relative to the internal standard *t*-BuOH or 1,4-dioxane.

**Hydrolysis of DMP:** As the reaction proceeds, the intensity of the signal due to methanol increases. The rate constant was obtained by fitting data according to a second order kinetic equation (correlation coefficient > 0.95). In a typical kinetic run, 2.5 equiv of DMP sodium salt was added to a freshly prepared and pD preadjusted catalyst solution (0.2 M) in D<sub>2</sub>O. The solution was adjusted again to the desired pD by using a 1M NaOD or a 70 % DClO<sub>4</sub> solution.

**Hydration of nitriles:** Hydrolysis of acetonitrile, acrylonitrile, trimethylacetoneitrile, benzonitrile was monitored by following the increase in the signals due to the corresponding amides. The observed pseudo first order rate constants were obtained by fitting the data according to a first order kinetic equation (correlation coefficient > 0.98). In a typical kinetic run, nitriles (10 to 50 equiv) were added to a D<sub>2</sub>O solution of catalyst (0.01 M) at appropriate pD.

**Hydrolysis of amides:** Hydrolysis of amides was monitored by following the decrease of signal due to the amide formyl proton or by following the increase due to the formate proton. The rate constant was obtained by fitting data according to a second order kinetic equation (correlation coefficient > 0.98). In a typical kinetic run, an amide (0.3 to 0.5 equiv) was added to a D<sub>2</sub>O solution of catalyst (0.1 M) at pD 6.

### 5.3 <sup>13</sup>C NMR spectroscopy

**Binding of acetate:** A D<sub>2</sub>O solution of Co(III) diaqua complex (0.1 M) was mixed with 0.5 or 1 equiv of a stock solution of <sup>13</sup>C<sub>1</sub> enriched acetate and then allowed to equilibrate for 1 h. The pD of the solution was not adjusted afterwards. The NMR spectra were then recorded relative to 1,4-dioxane as a internal standard.

For binding of carboxylates, a D<sub>2</sub>O solution of Co(III) diaqua complex (0.1 M, 0.2 mL) was mixed with a stock solution of <sup>13</sup>C<sub>1</sub> enriched carboxylates (0.05 M, 0.2 mL) and then allowed to equilibrate for 1 h. The pD of the solution was not adjusted after. The NMR spectra were then recorded relative to 1,4-dioxane as a internal standard.

**Binding of acetonitrile and acetamide:** 1 to 2 equiv of  $^{13}\text{C}_1$  enriched acetonitrile and a stock solution of  $^{13}\text{C}_1$  enriched acetamide (4 M) were added to a solution of Co(III) complex (50 mM) at pD 2 and pD 7, respectively. Spectra were recorded in a certain time period until it reached equilibrium. Best results were obtained when a 1: 1 ratio of catalyst and substrate were allowed to react in  $\text{D}_2\text{O}$ .

#### 5.4 HPLC

**Hydrolysis of 2'-deoxy adenosine and dApA:** The decreases in signal of substrates were followed relative to the area of internal standard (benzyl alcohol or benzene). Data were fit according to a first order kinetic equation ( $R > 0.94$ ). In typical experiments, a solution of catalyst (0.1 M) adjusted to desired pH at 25 °C was mixed with 0.1 equivalent of nucleotides and internal standard. The pH of solution was adjusted again and was placed in 5 to 10 of 1mL ampules, sealed and heated to 80 °C. In a certain time interval, a ampule was taken and chilled in an ice bath. The seal was broken and 5 to 10  $\mu\text{L}$  of the reaction mixture was diluted 10 times with 0.5 M phosphate buffer (pH 5). For each run, 1 $\mu\text{L}$  of above solution was injected on to a  $\text{C}_{18}$  column (5 micron Vydak) and eluted with a 20 to 50 % nonlinear gradient of  $\text{NH}_4\text{H}_2\text{PO}_4$  (0.2 M) and 60 %  $\text{CH}_3\text{OH}$  in water solutions over 45 minutes with a flow rate of 0.7 mL/ min.

## CONTRIBUTION TO KNOWLEDGE

Considerable progress has been made in developing artificial nucleases and proteases that hydrolyze unactivated phosphate esters, amides and nitriles.

### Part I Hydrolysis of Phosphate esters

- 1) A series of cyclic tetradentate amine ligands based on the cyclen structure has been synthesized and the efficiency and the stability of their cis diaqua Co(III) complexes were tested by means of binding properties to anionic ligands such as acetate and phosphates, as well as kinetic studies with BNPP, c-AMP, and ApA.
- 2) Hydrolysis of dimethyl phosphate at neutral pH has been accomplished for the first time using a simple metal complex. (Cyclen)Co(III)(OH<sub>2</sub>)<sub>2</sub> hydrolyzes dimethyl phosphate (DMP) by a bifunctional mechanism involving intramolecular metal hydroxide attack on the coordinated phosphate ester.
- 3) DMP coordinated to the cyclen complex is hydrolyzed 10<sup>10</sup> times faster than the free ester at neutral pH and 60 °C. This reaction provides valuable insight into the mechanistic role of metal ions in ribozyme catalyzed cleavage of DNA.

### Part II Hydration of Nitriles

- 1) (Cyclen)Co(III)(OH<sub>2</sub>)<sub>2</sub> efficiently hydrolyzes nitriles to amides under mild conditions (pD 7, 40 °C) with catalytic turnover.
- 2) The equilibrium binding constants of nitriles to cobalt complexes has been measured for the first time. Equilibrium binding constant of acetonitrile to the cis-diaqua cyclen complex is measured to be 0.6 M<sup>-1</sup> by using UV/VIS and <sup>13</sup>C NMR methods.
- 3) A mechanism for the catalytic hydration of nitriles is proposed based on equilibrium and kinetic studies. The reactivity of the two structurally related cobalt complexes, (tmcyclen)Co(III)(OH<sub>2</sub>)<sub>2</sub> and (cyclen)Co(III)(OH<sub>2</sub>)<sub>2</sub> has been compared, where only the

cyclen complex gives catalytic turnovers. The mechanism involves equilibrium complexation of nitriles to the cobalt complex followed by intramolecular metal hydroxide attack producing a four-membered ring chelated amide intermediate. The rate determining step involves dissociation of the chelated amide from the metal complex to give the free amide. The chelated amide intermediate has been isolated for the first time and its X-ray structure determined.

- 4) The above bifunctional mechanism also leads the regioselective hydration of acrylonitrile to acrylamide without allowing any C=C double bond hydration.

### Part (III) Hydrolysis of Amides

- 1) Hydrolysis of unactivated free amides has been achieved with a simple metal complex (cyclen)Co(III)(OH)<sub>2</sub>. More than 10<sup>5</sup> fold rate enhancement over that of uncatalyzed reaction is obtained in the cyclen complex promoted hydrolysis of 4-formyl morpholine under mild conditions (pD 6, 60 °C).
- 2) Equilibrium binding constants of DMF and formyl morpholine to the Co(III) complexes have been measured using <sup>1</sup>H NMR methods ( $K_{eq} = 0.4$  to  $2 \text{ M}^{-1}$  at 25 °C). This represents the first measurements for the equilibrium constant for binding of amides to metal complexes.
- 3) Base catalyzed hydrolysis mechanism of unactivated amides involves nucleophilic attack of hydroxide on carbonyl carbon producing the tetrahedral intermediate, which is followed by proton transfer and rate determining C-N bond cleavage. The observed rate enhancement by the cyclen complex was ascribed to the catalyst ability to stabilize this tetrahedral intermediate by chelation, thereby increasing its steady state concentration.

As a result of my Ph. D study I have contributed to the following papers:

Chin, J.; Banaszczyk, M.; Jubian, V.; Kim, J. H.; Mrejen, K. *Bioorganic Chemistry Frontiers* (ed), "*Artificial Hydrolytic Metalloenzymes.*" Springer-Verlag: New York, 1990.

Chin, J.; Kim, J. H. "Catalytic Hydration of Acrylonitrile to Acrylamide under Mild Conditions". *Angew. Chem. Int. Ed. Engl.* **1990**, 29, 523.

Chin, J.; Kim, J. H. "Trapping of a Chelated Benzamide: A Key Intermediate in Catalytic Hydration of Nitriles by Double Activation." manuscript in preparation.

Chin, J.; Kim, J. H.; Takasaki, B. "Metal Binding and Hydrolysis of an Unactivated Amide Under Mild Conditions." manuscript in preparation.

Chin, J.; Kim, J. H. "Dimethyl Phosphate Hydrolysis at Neutral pH." manuscript in preparation.

# APPENDIX

## A. X-ray Structure Determination of [(tmcyclen)Co(III)( $\eta^2$ -N,O-benzamide)] (ClO<sub>4</sub>)<sub>2</sub>·2H<sub>2</sub>O

Table A-1 Positional parameters and B(eq) for [(tmcyclen)Co( $\eta^2$ -N,O-benzamide)](ClO<sub>4</sub>)<sub>2</sub>·2H<sub>2</sub>O

atom	x	y	z	B (eq)
Co	0.4166 (1)	0.88141 (7)	0.8553 (1)	2.17 (5)
Cl (1)	0.7304 (3)	0.8870 (2)	0.3380 (3)	6.5 (2)
Cl (2)	0.2740 (3)	0.8302 (2)	0.3992 (3)	5.5 (2)
O (1)	0.2830 (5)	0.9138 (3)	0.9058 (6)	3.5 (3)
O (2)	0.7088 (7)	0.9387 (5)	0.0081 (9)	6.9 (6)
O (3)	-0.0035 (9)	0.7800 (6)	0.393 (1)	10.1 (8)
N (1)	0.4425 (7)	0.9649 (5)	0.7417 (8)	4.1 (5)
N (2)	0.4859 (7)	0.9384 (5)	0.9782 (8)	3.8 (4)
N (3)	0.5308 (7)	0.8361 (5)	0.7768 (8)	4.3 (5)
N (4)	0.4231 (7)	0.7998 (4)	0.9779 (8)	4.0 (4)
N (5)	0.3124 (6)	0.8381 (5)	0.7588 (7)	3.4 (4)
C (1)	0.491 (1)	1.0253 (7)	0.821 (1)	6.2 (8)
C (2)	0.461 (1)	1.0137 (7)	0.954 (1)	5.6 (7)
C (3)	0.4480 (9)	0.9111 (6)	1.102 (1)	4.8 (6)
C (4)	0.468 (1)	0.8306 (7)	1.096 (1)	5.4 (6)
C (5)	0.496 (1)	0.7455 (6)	0.926 (1)	4.7 (6)
C (6)	0.580 (1)	0.7846 (6)	0.861 (1)	5.2 (6)
C (7)	0.592 (1)	0.8896 (7)	0.714 (1)	5.3 (6)
C (8)	0.518 (1)	0.9399 (7)	0.650 (1)	5.8 (7)
C (9)	0.354 (1)	0.9955 (6)	0.677 (1)	5.5 (7)
C (10)	0.327 (1)	0.7610 (7)	1.006 (1)	5.4 (7)
C (11)	0.2432 (8)	0.8761 (6)	0.8190 (8)	3.4 (4)
C (12)	0.1317 (7)	0.8788 (6)	0.7949 (8)	3.4 (4)
C (13)	0.081 (1)	0.8261 (6)	0.727 (1)	4.6 (6)
C (14)	-0.022 (1)	0.8340 (8)	0.706 (1)	5.8 (7)
C (15)	-0.076 (1)	0.887 (1)	0.756 (1)	6.2 (7)
C (16)	-0.027 (1)	0.9402 (7)	0.823 (1)	5.5 (7)
C (17)	0.076 (1)	0.9367 (6)	0.843 (1)	4.9 (6)
H (1)	0.3100	0.8032	0.6938	3.8
H (2)	0.5031	0.8067	0.7121	5.1
H (3)	0.5570	0.9319	0.9727	4.4
H (4)	0.1168	0.7847	0.6950	5.3
H (5)	-0.0563	0.7997	0.6532	6.9
H (6)	-0.1477	0.8895	0.7433	7.3
H (7)	-0.0659	0.9795	0.8554	6.4
H (8)	0.1094	0.9740	0.8899	5.8
H (9)	0.5383	0.8223	1.0974	6.3
H (10)	0.4363	0.8078	1.1656	6.3
H (11)	0.3770	0.9214	1.1131	5.5
H (12)	0.4846	0.9330	1.1691	5.5
H (13)	0.4990	1.0457	1.0065	6.3
H (14)	0.3904	1.0229	0.9653	6.3
H (15)	0.4675	1.0722	0.7931	7.2
H (16)	0.5628	1.0236	0.8122	7.2
H (17)	0.4606	0.7141	0.8685	5.5
H (18)	0.5228	0.7156	0.9906	5.5
H (19)	0.6210	0.8084	0.9193	6.2
H (20)	0.6202	0.7498	0.8158	6.2
H (21)	0.6360	0.8674	0.6531	6.1
H (22)	0.6337	0.9162	0.7702	6.1

B<sub>eq</sub> is the mean of the principal axes of the thermal ellipsoid.

Table A-1 Positional parameters and B(eq) for [(tmcyclen)Co( $\eta^2$ -N,O-benzamide)](ClO<sub>4</sub>)<sub>2</sub> · 2H<sub>2</sub>O (cont).

atom	x	y	z	B(eq)
H(23)	0.5539	0.9815	0.6167	6.7
H(24)	0.4850	0.9155	0.5843	6.7
H(25)	0.2795	0.7933	1.0434	6.2
H(26)	0.3393	0.7212	1.0605	6.2
H(27)	0.2979	0.7424	0.9310	6.2
H(28)	0.3744	1.0352	0.6251	6.3
H(29)	0.3054	1.0132	0.7355	6.3
H(30)	0.3229	0.9591	0.6273	6.3
O(4)	0.737(1)	0.9597(6)	0.281(1)	9.8(2)
O(5)	0.793(1)	0.8905(9)	0.451(1)	9.8(2)
O(6)	0.6265(7)	0.8755(8)	0.375(1)	9.8(2)
O(7)	0.766(1)	0.8340(7)	0.258(1)	9.8(2)
O(12)	0.642(2)	0.850(1)	0.279(3)	9.8
O(13)	0.771(2)	0.932(1)	0.221(2)	9.8
O(14)	0.719(2)	0.924(1)	0.429(2)	9.8
O(15)	0.812(2)	0.829(1)	0.339(3)	9.8
O(8)	0.180(1)	0.831(1)	0.466(2)	10.7(3)
O(9)	0.271(2)	0.784(1)	0.296(1)	10.7(3)
O(10)	0.311(1)	0.9002(6)	0.376(2)	10.7(3)
O(11)	0.351(1)	0.795(1)	0.491(2)	10.7(3)
O(16)	0.238(2)	0.855(1)	0.274(1)	10.7
O(17)	0.376(1)	0.849(1)	0.411(2)	10.7
O(18)	0.210(2)	0.864(1)	0.488(2)	10.7
O(19)	0.260(2)	0.7522(7)	0.401(2)	10.7

Table A-2 U values for [(tmcyclen)Co( $\eta^2$ -N,O-benzamide)](ClO<sub>4</sub>)<sub>2</sub> · 2H<sub>2</sub>O.

atom	U11	U22	U33	U12	U13	U23
Co	0.0405(7)	0.0461(7)	0.0340(6)	0.0040(8)	0.0013(7)	-0.0035(7)
Cl(1)	0.085(2)	0.074(2)	0.089(3)	-0.001(2)	-0.010(2)	-0.011(2)
Cl(2)	0.079(2)	0.073(2)	0.058(2)	0.011(2)	0.012(2)	-0.004(2)
O(1)	0.043(4)	0.053(4)	0.039(4)	0.009(4)	-0.004(3)	-0.006(3)
O(2)	0.082(7)	0.098(7)	0.083(7)	-0.008(6)	-0.013(6)	0.005(6)
O(3)	0.14(1)	0.15(1)	0.097(9)	-0.015(8)	0.022(8)	-0.057(8)
N(1)	0.050(7)	0.058(6)	0.046(5)	-0.002(5)	-0.006(4)	0.004(5)
N(2)	0.054(6)	0.049(6)	0.042(5)	-0.004(5)	0.012(5)	-0.010(4)
N(3)	0.057(6)	0.061(6)	0.045(5)	0.004(5)	0.001(5)	-0.008(5)
N(4)	0.042(5)	0.058(5)	0.053(5)	0.002(5)	0.006(5)	0.004(4)
N(5)	0.047(6)	0.050(5)	0.033(4)	0.011(4)	0.003(4)	-0.013(4)
C(1)	0.10(1)	0.047(7)	0.10(1)	-0.014(7)	0.011(9)	-0.005(7)
C(2)	0.09(1)	0.08(1)	0.045(7)	-0.011(8)	-0.000(7)	-0.027(7)
C(3)	0.07(1)	0.072(8)	0.036(6)	0.011(7)	-0.019(6)	-0.011(5)
C(4)	0.060(8)	0.10(1)	0.047(7)	0.001(8)	0.003(6)	0.007(7)
C(5)	0.067(9)	0.049(7)	0.064(8)	0.005(6)	0.003(7)	-0.000(6)
C(6)	0.060(7)	0.073(7)	0.067(7)	0.019(7)	-0.003(9)	-0.005(7)
C(7)	0.055(7)	0.085(9)	0.062(7)	-0.005(8)	0.021(6)	-0.005(7)
C(8)	0.076(9)	0.10(1)	0.047(7)	-0.027(8)	0.027(8)	0.000(8)
C(9)	0.09(1)	0.061(8)	0.06(1)	0.007(7)	-0.009(7)	0.013(6)
C(10)	0.072(8)	0.09(1)	0.047(7)	-0.008(7)	0.008(6)	0.019(7)
C(11)	0.056(7)	0.040(5)	0.034(5)	0.003(6)	-0.009(5)	-0.002(5)
C(12)	0.034(5)	0.055(6)	0.039(5)	-0.006(6)	-0.004(4)	0.011(6)
C(13)	0.070(8)	0.062(7)	0.043(6)	-0.017(8)	-0.003(7)	-0.000(5)
C(14)	0.052(9)	0.12(1)	0.052(8)	-0.025(8)	-0.009(6)	0.016(8)
C(15)	0.052(8)	0.12(1)	0.061(8)	-0.00(1)	0.008(7)	0.03(1)
C(16)	0.050(8)	0.09(1)	0.07(1)	0.014(7)	0.010(6)	0.011(8)
C(17)	0.062(7)	0.074(7)	0.051(7)	-0.000(7)	-0.007(8)	0.016(6)

Table A-3 Intramolecular Distance Involving the Nonhydrogen Atoms

atom	atom	distance	atom	atom	distance
Co	O(1)	1.930(7)	N(1)	C(9)	1.47(2)
Co	N(1)	1.993(9)	N(2)	C(2)	1.45(2)
Co	N(2)	1.920(9)	N(2)	C(3)	1.52(1)
Co	N(3)	1.913(9)	N(3)	C(6)	1.46(2)
Co	N(4)	2.002(8)	N(3)	C(7)	1.44(2)
Co	N(5)	1.895(8)	N(4)	C(4)	1.51(1)
Co	C(11)	2.31(1)	N(4)	C(5)	1.49(1)
Cl(1)	O(4)	1.47(1)	N(4)	C(10)	1.48(2)
Cl(1)	O(5)	1.47(1)	N(5)	C(11)	1.32(1)
Cl(1)	O(6)	1.44(1)	C(1)	C(2)	1.51(2)
Cl(1)	O(7)	1.38(1)	C(3)	C(4)	1.50(2)
Cl(1)	O(12)	1.49(2)	C(5)	C(6)	1.49(2)
Cl(1)	O(13)	1.60(2)	C(7)	C(8)	1.51(2)
Cl(1)	O(14)	1.21(2)	C(11)	C(12)	1.49(1)
Cl(1)	O(15)	1.52(2)	C(12)	C(13)	1.39(2)
Cl(2)	O(8)	1.43(2)	C(12)	C(17)	1.39(2)
Cl(2)	O(9)	1.39(2)	C(13)	C(14)	1.38(2)
Cl(2)	O(10)	1.40(1)	C(14)	C(15)	1.32(2)
Cl(2)	O(11)	1.55(2)	C(15)	C(16)	1.37(2)
Cl(2)	O(16)	1.51(2)	C(16)	C(17)	1.37(2)
Cl(2)	O(17)	1.40(2)	O(4)	O(13)	0.93(3)
Cl(2)	O(18)	1.42(2)	O(4)	O(14)	1.74(3)
Cl(2)	O(19)	1.44(1)	O(5)	O(14)	1.17(3)
O(1)	C(11)	1.28(1)	O(5)	O(15)	1.68(3)
N(1)	C(1)	1.54(2)	O(6)	O(12)	1.16(3)
N(1)	C(8)	1.48(2)	O(6)	O(14)	1.62(3)
O(7)	O(12)	1.67(3)	O(10)	O(16)	1.68(3)
O(7)	O(15)	1.06(3)	O(10)	O(17)	1.33(2)
O(8)	O(18)	0.77(3)	O(11)	O(17)	1.36(3)
O(9)	O(16)	1.39(3)	O(11)	O(19)	1.72(3)
O(9)	O(19)	1.28(3)			

Table A-4 Intramolecular Bond Angle Involving the Nonhydrogen Atoms

atom	atom	atom	angle	atom	atom	atom	angle
O(1)	Co	N(1)	95.3(3)	O(6)	Cl(1)	O(12)	47(1)
O(1)	Co	N(2)	93.9(3)	O(6)	Cl(1)	O(13)	128(1)
O(1)	Co	N(3)	166.2(3)	O(6)	Cl(1)	O(14)	75(2)
O(1)	Co	N(4)	94.7(3)	O(6)	Cl(1)	O(15)	124(1)
O(1)	Co	N(5)	68.2(3)	O(7)	Cl(1)	O(12)	71(1)
O(1)	Co	C(11)	33.6(3)	O(7)	Cl(1)	O(13)	76(1)
N(1)	Co	N(2)	85.7(4)	O(7)	Cl(1)	O(14)	161(1)
N(1)	Co	N(3)	85.8(4)	O(7)	Cl(1)	O(15)	43(1)
N(1)	Co	N(4)	167.4(4)	O(12)	Cl(1)	O(13)	99(1)
N(1)	Co	N(5)	96.1(4)	O(12)	Cl(1)	O(14)	121(2)
N(1)	Co	C(11)	95.5(4)	O(12)	Cl(1)	O(15)	103(1)
N(2)	Co	N(3)	99.9(4)	O(13)	Cl(1)	O(14)	113(1)
N(2)	Co	N(4)	96.0(4)	O(13)	Cl(1)	O(15)	98(1)
N(2)	Co	N(5)	162.1(4)	O(14)	Cl(1)	O(15)	119(2)
N(2)	Co	C(11)	127.4(4)	O(8)	Cl(2)	O(9)	113(1)
N(3)	Co	N(4)	86.3(4)	O(8)	Cl(2)	O(10)	113(1)
N(3)	Co	N(5)	98.0(4)	O(8)	Cl(2)	O(11)	104(1)
N(3)	Co	C(11)	132.7(4)	O(8)	Cl(2)	O(16)	100(1)
N(4)	Co	N(5)	94.6(4)	O(8)	Cl(2)	O(17)	141(1)
N(4)	Co	C(11)	97.0(4)	O(8)	Cl(2)	O(18)	31(1)
N(5)	Co	C(11)	34.7(3)	O(8)	Cl(2)	O(19)	84(1)
O(4)	Cl(1)	O(5)	105.9(9)	O(9)	Cl(2)	O(10)	115(1)
O(4)	Cl(1)	O(6)	107.8(9)	O(9)	Cl(2)	O(11)	106(1)
O(4)	Cl(1)	O(7)	110.9(8)	O(9)	Cl(2)	O(16)	57(1)
O(4)	Cl(1)	O(12)	106(1)	O(9)	Cl(2)	O(17)	105(1)
O(4)	Cl(1)	O(13)	35(1)	O(9)	Cl(2)	O(18)	142(1)
O(4)	Cl(1)	O(14)	80(1)	O(9)	Cl(2)	O(19)	54(1)
O(4)	Cl(1)	O(15)	127(1)	O(10)	Cl(2)	O(11)	106(1)
O(5)	Cl(1)	O(6)	107.8(8)	O(10)	Cl(2)	O(16)	70(1)
O(5)	Cl(1)	O(7)	110.9(9)	O(10)	Cl(2)	O(17)	57(1)
O(5)	Cl(1)	O(12)	144(1)	O(10)	Cl(2)	O(18)	86(1)
O(5)	Cl(1)	O(13)	116(1)	O(10)	Cl(2)	O(19)	163(1)
O(5)	Cl(1)	O(14)	51(1)	O(11)	Cl(2)	O(16)	155(1)
O(5)	Cl(1)	O(15)	68(1)	O(11)	Cl(2)	O(17)	54(1)
O(6)	Cl(1)	O(7)	113.1(9)	O(11)	Cl(2)	O(18)	98(1)

Table A-4 Intramolecular Bond Angle Involving the Nonhydrogen Atoms. (cont)

atom	atom	atom	angle	atom	atom	atom	angle
O(11)	Cl(2)	O(19)	70(1)	N(1)	C(8)	C(7)	109(1)
O(16)	Cl(2)	O(17)	108(1)	Co	C(11)	O(1)	56.6(5)
O(16)	Cl(2)	O(18)	107(1)	Co	C(11)	N(5)	55.0(5)
O(16)	Cl(2)	O(19)	106(1)	Co	C(11)	C(12)	175.7(8)
O(17)	Cl(2)	O(18)	113(1)	O(1)	C(11)	N(5)	111.5(9)
O(17)	Cl(2)	O(19)	112(1)	O(1)	C(11)	C(12)	120.9(9)
O(18)	Cl(2)	O(19)	111(1)	N(5)	C(11)	C(12)	127.6(9)
Co	O(1)	C(11)	89.9(6)	C(11)	C(12)	C(13)	123(1)
Co	N(1)	C(1)	106.4(7)	C(11)	C(12)	C(17)	118.5(9)
Co	N(1)	C(8)	106.8(7)	C(13)	C(12)	C(17)	118(1)
Co	N(1)	C(9)	116.8(7)	C(12)	C(13)	C(14)	119(1)
C(1)	N(1)	C(8)	108.5(9)	C(13)	C(14)	C(15)	122(1)
C(1)	N(1)	C(9)	108.5(9)	C(14)	C(15)	C(16)	120(1)
C(8)	N(1)	C(9)	109.6(9)	C(15)	C(16)	C(17)	121(1)
Co	N(2)	C(2)	106.7(7)	C(12)	C(17)	C(16)	120(1)
Co	N(2)	C(3)	106.0(6)	Cl(1)	O(4)	O(13)	80(2)
C(2)	N(2)	C(3)	113.8(9)	Cl(1)	O(4)	O(14)	43.1(9)
Co	N(3)	C(6)	110.6(7)	O(13)	O(4)	O(14)	120(2)
Co	N(3)	C(7)	110.7(7)	Cl(1)	O(5)	O(14)	53(1)
C(6)	N(3)	C(7)	119.2(9)	Cl(1)	O(5)	O(15)	57.0(9)
Co	N(4)	C(4)	107.0(7)	O(14)	O(5)	O(15)	110(2)
Co	N(4)	C(5)	106.1(6)	Cl(1)	O(6)	O(12)	69(1)
Co	N(4)	C(10)	117.4(7)	Cl(1)	O(6)	O(14)	46(1)
C(4)	N(4)	C(5)	108.7(9)	O(12)	O(6)	O(14)	114(2)
C(4)	N(4)	C(10)	109.7(9)	Cl(1)	O(7)	O(12)	57(1)
C(5)	N(4)	C(10)	107.6(9)	Cl(1)	O(7)	O(15)	76(1)
Co	N(5)	C(11)	90.3(6)	O(12)	O(7)	O(15)	118(2)
N(1)	C(1)	C(2)	109(1)	Cl(1)	O(12)	O(6)	64(1)
N(2)	C(2)	C(1)	104(1)	Cl(1)	O(12)	O(7)	51.6(8)
N(2)	C(3)	C(4)	103.2(9)	O(6)	O(12)	O(7)	111(2)
N(4)	C(4)	C(3)	110.0(9)	Cl(1)	O(13)	O(4)	65(2)
N(4)	C(5)	C(6)	109.3(9)	Cl(1)	O(14)	O(4)	57(1)
N(3)	C(6)	C(5)	106(1)	Cl(1)	O(14)	O(5)	76(2)
N(3)	C(7)	C(8)	106(1)	Cl(1)	O(14)	O(6)	59(1)

Table A-4 Intramolecular Bond Angle Involving the Nonhydrogen Atoms. (cont)

atom	atom	atom	angle	atom	atom	atom	angle
O(4)	O(14)	O(5)	106(2)	Cl(2)	O(11)	O(17)	57.1(9)
O(4)	O(14)	O(6)	89(1)	Cl(2)	O(11)	O(19)	52.0(7)
O(5)	O(14)	O(6)	113(2)	O(17)	O(11)	O(19)	99(1)
Cl(1)	O(15)	O(5)	54.5(9)	Cl(2)	O(16)	O(9)	57(1)
Cl(1)	O(15)	O(7)	62(1)	Cl(2)	O(16)	O(10)	51.7(8)
O(5)	O(15)	O(7)	116(2)	O(9)	O(16)	O(10)	100(1)
Cl(2)	O(8)	O(18)	73(2)	Cl(2)	O(17)	O(10)	61.5(9)
Cl(2)	O(9)	O(16)	65(1)	Cl(2)	O(17)	O(11)	68(1)
Cl(2)	O(9)	O(19)	65(1)	O(10)	O(17)	O(11)	122(2)
O(16)	O(9)	O(19)	123(2)	Cl(2)	O(18)	O(8)	76(2)
Cl(2)	O(10)	O(16)	57.8(9)	Cl(2)	O(19)	O(9)	61(1)
Cl(2)	O(10)	O(17)	62(1)	Cl(2)	O(19)	O(11)	57.7(9)
O(16)	O(10)	O(17)	102(1)	O(9)	O(19)	O(11)	102(1)

**B. X-ray Structure Determination of  $[(\text{trpn})\text{Co}(\text{III})(\eta^2\text{-O,O-}\beta\text{-ala})](\text{ClO}_4)_3 \cdot \text{H}_2\text{O}$**

Table B-1 Positional parameters and  $B(\text{eq})$  for  $[(\text{trpn})\text{Co}(\eta^2\text{-O,O-}\beta\text{-ala})](\text{ClO}_4)_3 \cdot \text{H}_2\text{O}$

atom	x	y	z	$B(\text{eq})$
Co(1)	0.8606(2)	0.2047(1)	0.6521(2)	3.9(1)
O(1)	0.8682(8)	0.2981(6)	0.6145(8)	4.4(7)
O(2)	0.8634(8)	0.2668(6)	0.7509(8)	4.6(7)
N(1)	0.743(1)	0.2153(9)	0.653(1)	5(1)
N(2)	0.9798(8)	0.1983(8)	0.659(1)	5(1)
N(3)	0.852(1)	0.1280(7)	0.728(1)	3.9(8)
N(4)	0.860(1)	0.1587(8)	0.534(1)	4(1)
N(5)	0.903(1)	0.4404(8)	0.582(1)	7(1)
C(1)	0.871(1)	0.060(1)	0.701(1)	5(1)
C(2)	0.837(1)	0.045(1)	0.607(2)	6(1)
C(3)	0.879(1)	0.086(1)	0.538(2)	6(1)
C(4)	1.025(1)	0.228(1)	0.582(1)	4(1)
C(5)	1.006(1)	0.191(1)	0.498(2)	6(1)
C(6)	0.917(1)	0.194(1)	0.473(1)	6(1)
C(7)	0.702(1)	0.252(1)	0.582(2)	7(2)
C(8)	0.741(1)	0.233(1)	0.491(2)	6(2)
C(9)	0.776(1)	0.166(1)	0.491(1)	6(1)
C(10)	0.866(1)	0.315(1)	0.698(1)	4(1)
C(11)	0.868(1)	0.386(1)	0.724(1)	6(1)
C(12)	0.841(1)	0.435(1)	0.652(2)	6(1)
Cl(1)	0.1070(3)	0.1397(2)	0.2435(4)	5.6(3)
Cl(2)	0.5299(3)	0.1119(2)	0.6082(3)	6.1(2)
Cl(3)	0.1709(3)	0.0805(2)	0.6288(3)	6.4(2)
O(3)	0.4897(7)	0.1665(5)	0.6535(8)	11.7(6)
O(4)	0.5306(7)	0.1250(6)	0.5142(3)	9.9(5)
O(5)	0.4868(7)	0.0500(4)	0.6252(8)	11.3(6)
O(6)	0.134(1)	0.1019(8)	0.317(1)	7.1(3)
O(7)	0.072(1)	0.0972(8)	0.176(1)	7.1(3)
O(8)	0.174(1)	0.177(1)	0.205(1)	7.1(3)
O(9)	0.045(1)	0.1885(9)	0.271(1)	7.1(3)
O(10)	0.1657(8)	0.0216(7)	0.0438(9)	7(1)
O(11)	0.2137(6)	0.0244(4)	0.6676(7)	8.5(5)
O(12)	0.0844(3)	0.0684(6)	0.6324(7)	10.3(5)
O(13)	0.1958(7)	0.0885(5)	0.5376(4)	9.7(5)
O(14)	0.1899(7)	0.1411(4)	0.6774(6)	8.1(5)
O(15)	0.6124(4)	0.1060(6)	0.6400(8)	12.2(6)
O(16)	0.096(3)	0.211(1)	0.258(3)	7.1
O(17)	0.192(2)	0.123(2)	0.248(3)	7.1
O(18)	0.071(3)	0.119(2)	0.164(2)	7.1
O(19)	0.066(3)	0.105(2)	0.319(2)	7.1

$B_{\text{eq}}$  is the mean of the principal axes of the thermal ellipsoid.

Table B-2 U values for  $[(\text{trpn})\text{Co}(\eta^2\text{-O,O-}\beta\text{-ala})](\text{ClO}_4)_3 \cdot \text{H}_2\text{O}$ 

atom	U11	U22	U33	U12	U13	U23
Co(1)	0.049(2)	0.051(2)	0.048(2)	-0.002(2)	0.000(2)	0.002(2)
O(1)	0.052(9)	0.06(1)	0.054(8)	-0.003(9)	-0.001(8)	-0.003(8)
O(2)	0.059(9)	0.062(9)	0.05(1)	0.013(8)	-0.00(1)	0.014(8)
N(1)	0.05(1)	0.08(1)	0.08(1)	-0.00(1)	0.02(1)	-0.03(1)
N(2)	0.04(1)	0.07(1)	0.06(1)	-0.00(1)	0.00(1)	0.01(1)
N(3)	0.05(1)	0.03(1)	0.06(1)	-0.00(1)	0.00(1)	0.012(8)
N(4)	0.05(1)	0.07(1)	0.04(1)	-0.01(1)	-0.02(1)	-0.01(1)
N(5)	0.07(2)	0.08(1)	0.11(2)	0.01(1)	0.03(1)	0.02(1)
C(1)	0.10(2)	0.04(1)	0.06(2)	-0.00(2)	-0.01(2)	0.02(1)
C(2)	0.06(2)	0.06(2)	0.11(2)	-0.01(1)	0.02(1)	0.01(2)
C(3)	0.06(2)	0.06(2)	0.11(2)	0.00(1)	-0.02(1)	-0.01(1)
C(4)	0.06(1)	0.04(1)	0.07(2)	-0.01(1)	-0.00(1)	-0.01(1)
C(5)	0.04(1)	0.08(2)	0.10(2)	-0.02(1)	0.01(1)	0.03(2)
C(6)	0.11(2)	0.07(2)	0.06(2)	-0.01(2)	0.03(2)	-0.01(1)
C(7)	0.06(2)	0.11(2)	0.07(2)	0.02(2)	-0.02(2)	0.02(2)
C(8)	0.07(2)	0.09(2)	0.07(2)	0.02(2)	-0.03(1)	0.01(2)
C(9)	0.07(2)	0.07(2)	0.07(2)	0.01(1)	-0.02(1)	-0.01(1)
C(10)	0.06(2)	0.03(1)	0.07(2)	0.01(1)	-0.01(2)	-0.01(1)
C(11)	0.07(2)	0.07(2)	0.09(2)	0.01(2)	-0.01(1)	-0.03(1)
C(12)	0.07(2)	0.04(1)	0.10(2)	0.01(1)	0.03(2)	0.01(1)
O(10)	0.08(1)	0.09(1)	0.09(1)	0.01(1)	0.01(1)	-0.03(1)
Cl(1)	0.076(4)	0.071(4)	0.068(4)	0.001(4)	-0.005(3)	0.004(4)

Table B-3 Calculated hydrogen parameters and  $B(\text{iso})$  for  $[(\text{trpn})\text{Co}(\eta^2\text{-O,O-}\beta\text{-ala})](\text{ClO}_4)_3 \cdot \text{H}_2\text{O}$ 

	x	y	z	$B(\text{iso})$
H(1)	0.7210	0.1710	0.6533	6.6
H(2)	0.7300	0.2374	0.7068	6.6
H(3)	0.9971	0.2202	0.7114	5.8
H(4)	0.9938	0.1515	0.6623	5.8
H(5)	0.8876	0.1369	0.7767	4.8
H(6)	0.7975	0.1271	0.7481	4.8
H(7)	0.9137	0.3971	0.5590	8.4
H(8)	0.8826	0.4691	0.5369	8.4
H(9)	0.9510	0.4591	0.6068	8.4
H(10)	0.9282	0.0538	0.7000	6.5
H(11)	0.8467	0.0292	0.7410	6.5
H(12)	0.8460	-0.0010	0.5944	7.2
H(13)	0.7811	0.0552	0.6065	7.2
H(14)	0.8649	0.0678	0.4820	6.9
H(15)	0.9361	0.0824	0.5470	6.9
H(16)	0.9116	0.1733	0.4159	7.2
H(17)	0.9012	0.2395	0.4696	7.2
H(18)	1.0213	0.1452	0.5053	7.1
H(19)	1.0369	0.2108	0.4520	7.1
H(20)	1.0093	0.2736	0.5770	5.2
H(21)	1.0815	0.2249	0.5946	5.2
H(22)	0.8334	0.3910	0.7735	7.0
H(23)	0.9226	0.3962	0.7397	7.0
H(24)	0.6467	0.2405	0.5826	7.9
H(25)	0.7094	0.2987	0.5921	7.9
H(26)	0.7803	0.1517	0.4316	7.1
H(27)	0.7394	0.1373	0.5225	7.1
H(28)	0.8330	0.4778	0.6786	6.7
H(29)	0.7915	0.4194	0.6270	6.7
H(30)	0.6985	0.2343	0.4473	7.3
H(31)	0.7815	0.2647	0.4764	7.3
H(32)	0.1414	0.0636	0.0929	7.3
H(33)	0.2010	-0.0163	0.0442	7.3

Hydrogen atom positions calculated assuming C/N-H distance of 1.08 Å.  
 $B(\text{iso})$  is derived from U of the bonded atom plus 0.01.

Table B-4 Intramolecular Distance Involving the Nonhydrogen Atoms

atom	atom	distance	atom	atom	distance
Co(1)	O(1)	1.94(1)	C(11)	C(12)	1.52(3)
Co(1)	O(2)	1.93(1)	Cl(1)	O(16)	1.45(3)
Co(1)	N(1)	1.94(2)	Cl(1)	O(17)	1.43(3)
Co(1)	N(2)	1.96(1)	Cl(1)	O(18)	1.40(4)
Co(1)	N(3)	1.91(1)	Cl(1)	O(19)	1.48(4)
Co(1)	N(4)	2.00(2)	Cl(1)	O(6)	1.40(2)
Co(1)	C(10)	2.30(2)	Cl(1)	O(7)	1.44(2)
O(1)	C(10)	1.30(2)	Cl(1)	O(8)	1.45(2)
O(2)	C(10)	1.25(2)	Cl(1)	O(9)	1.46(2)
N(1)	C(7)	1.45(3)	Cl(2)	O(3)	1.44(1)
N(2)	C(4)	1.49(3)	Cl(2)	O(4)	1.440(7)
N(3)	C(1)	1.45(2)	Cl(2)	O(5)	1.44(1)
N(4)	C(3)	1.48(3)	Cl(2)	O(15)	1.440(8)
N(4)	C(6)	1.49(3)	Cl(3)	O(11)	1.44(1)
N(4)	C(9)	1.53(3)	Cl(3)	O(12)	1.440(7)
N(5)	C(12)	1.46(3)	Cl(3)	O(13)	1.440(8)
C(1)	C(2)	1.54(3)	Cl(3)	O(14)	1.440(9)
C(2)	C(3)	1.49(3)	O(16)	O(8)	1.65(5)
C(4)	C(5)	1.49(3)	O(16)	O(9)	0.98(5)
C(5)	C(6)	1.51(3)	O(17)	O(6)	1.47(5)
C(7)	C(8)	1.56(3)	O(17)	O(8)	1.29(5)
C(8)	C(9)	1.45(3)	O(18)	O(7)	0.47(4)
C(10)	C(11)	1.45(3)	O(19)	O(6)	1.11(5)

Table B-5 Intramolecular Bond Angle Involving the Nonhydrogen Atoms

atom	atom	atom	angle	atom	atom	atom	angle
O(16)	Cl(1)	O(6)	117(2)	O(3)	Cl(2)	O(5)	109.5(7)
O(16)	Cl(1)	O(7)	129(2)	O(3)	Cl(2)	O(15)	109.5(7)
O(16)	Cl(1)	O(8)	69(2)	O(4)	Cl(2)	O(5)	109.4(8)
O(16)	Cl(1)	O(9)	39(2)	O(4)	Cl(2)	O(15)	109.4(7)
O(17)	Cl(1)	O(18)	112(3)	O(5)	Cl(2)	O(15)	109.4(7)
O(17)	Cl(1)	O(19)	108(3)	O(11)	Cl(3)	O(12)	109.5(6)
O(17)	Cl(1)	O(6)	63(2)	O(11)	Cl(3)	O(13)	109.5(6)
O(17)	Cl(1)	O(7)	107(2)	O(11)	Cl(3)	O(14)	109.5(6)
O(17)	Cl(1)	O(8)	53(2)	O(12)	Cl(3)	O(13)	109.4(7)
O(17)	Cl(1)	O(9)	144(2)	O(12)	Cl(3)	O(14)	109.4(7)
O(18)	Cl(1)	O(19)	109(2)	O(13)	Cl(3)	O(14)	109.4(6)
O(18)	Cl(1)	O(6)	130(2)	Cl(1)	O(16)	O(8)	56(1)
O(18)	Cl(1)	O(7)	19(2)	Cl(1)	O(16)	O(9)	71(2)
O(18)	Cl(1)	O(8)	97(2)	O(8)	O(16)	O(9)	125(3)
O(18)	Cl(1)	O(9)	98(2)	Cl(1)	O(17)	O(6)	58(1)
O(19)	Cl(1)	O(6)	45(2)	Cl(1)	O(17)	O(8)	64(2)
O(19)	Cl(1)	O(7)	95(2)	O(6)	O(17)	O(8)	117(3)
O(19)	Cl(1)	O(8)	152(2)	Cl(1)	O(18)	O(7)	85(5)
O(19)	Cl(1)	O(9)	77(2)	Cl(1)	O(19)	O(6)	64(2)
O(6)	Cl(1)	O(7)	112(1)	Cl(1)	O(6)	O(17)	60(2)
O(6)	Cl(1)	O(8)	111(1)	Cl(1)	O(6)	O(19)	71(2)
O(6)	Cl(1)	O(9)	110(1)	O(17)	O(6)	O(19)	130(3)
O(7)	Cl(1)	O(8)	109(1)	Cl(1)	O(7)	O(18)	76(5)
O(7)	Cl(1)	O(9)	108(1)	Cl(1)	O(8)	O(16)	55(1)
O(8)	Cl(1)	O(9)	107(1)	Cl(1)	O(8)	O(17)	63(2)
O(3)	Cl(2)	O(4)	109.5(7)	O(16)	O(8)	O(17)	106(2)
O(1)	Co(1)	O(2)	67.3(5)	Co(1)	N(4)	C(3)	114(1)
O(1)	Co(1)	N(1)	87.8(6)	Co(1)	N(4)	C(6)	109(1)
O(1)	Co(1)	N(2)	90.8(6)	Co(1)	N(4)	C(9)	110(1)
O(1)	Co(1)	N(3)	160.1(6)	C(3)	N(4)	C(6)	111(2)
O(1)	Co(1)	N(4)	100.2(6)	C(3)	N(4)	C(9)	107(2)
O(1)	Co(1)	C(10)	34.3(6)	C(6)	N(4)	C(9)	105(1)
O(2)	Co(1)	N(1)	87.2(6)	N(3)	C(1)	C(2)	111(2)
O(2)	Co(1)	N(2)	88.8(6)	C(1)	C(2)	C(3)	112(2)
O(2)	Co(1)	N(3)	92.8(6)	N(4)	C(3)	C(2)	118(2)

Table B-5 Intramolecular Bond Angle Involving the Nonhydrogen Atoms. (cont)

atom	atom	atom	angle	atom	atom	atom	angle
O(2)	Co(1)	N(4)	167.5(6)	N(2)	C(4)	C(5)	111(2)
O(2)	Co(1)	C(10)	33.0(6)	C(4)	C(5)	C(6)	113(2)
N(1)	Co(1)	N(2)	175.9(7)	N(4)	C(6)	C(5)	115(2)
N(1)	Co(1)	N(3)	90.8(7)	N(1)	C(7)	C(8)	110(2)
N(1)	Co(1)	N(4)	92.7(7)	C(7)	C(8)	C(9)	112(2)
N(1)	Co(1)	C(10)	86.1(8)	N(4)	C(9)	C(8)	116(2)
N(2)	Co(1)	N(3)	69.3(7)	Co(1)	C(10)	O(1)	57.5(9)
N(2)	Co(1)	N(4)	91.3(7)	Co(1)	C(10)	O(2)	57.0(9)
N(2)	Co(1)	C(10)	90.6(7)	Co(1)	C(10)	C(11)	178(2)
N(3)	Co(1)	N(4)	99.7(6)	O(1)	C(10)	O(2)	114(2)
N(3)	Co(1)	C(10)	125.8(7)	O(1)	C(10)	C(11)	121(2)
N(4)	Co(1)	C(10)	134.5(7)	O(2)	C(10)	C(11)	125(2)
Co(1)	O(1)	C(10)	88(1)	C(10)	C(11)	C(12)	114(2)
Co(1)	O(2)	C(10)	90(1)	N(5)	C(12)	C(11)	111(2)
Co(1)	N(1)	C(7)	120(1)	O(16)	Cl(1)	O(17)	110(3)
Co(1)	N(2)	C(4)	115(1)	O(16)	Cl(1)	O(18)	111(3)
Co(1)	N(3)	C(1)	124(1)	O(16)	Cl(1)	O(19)	107(2)
Cl(1)	O(9)	O(16)	70(2)				